Australian Government

Land & Water Australia

final report

knowledge for managing Australian landscapes

Modelling Microbial Utilisation of Macrophyte Organic Matter Inputs to Rivers under Different Flow Condition

Patricia Margaret Bowen

Published by: Land & Water Australia

Product Code: PN30302

Postal address: GPO Box 2182, Canberra ACT 2601

Office Location: Level 1, The Phoenix
86-88 Northbourne Ave, Braddon ACT

Telephone: 02 6263 6000

Facsimile: 02 6263 6099

Email Land&WaterAustralia@lwa.gov.au

Internet: lwa.gov.au

Disclaimer

The information contained in this publication is intended for general use, to assist public knowledge and discussion and to help improve the sustainable management of land, water and vegetation. It includes general statements based on scientific research. Readers are advised and need to be aware that this information may be incomplete or unsuitable for use in specific situations. Before taking any action or decision based on the information in this publication, readers should seek expert professional, scientific and technical advice and form their own view of the applicability and correctness of the information.

To the extent permitted by law, the Commonwealth of Australia, Land & Water Australia (including its employees and consultants), and the authors of this publication do not assume liability of any kind whatsoever resulting from any person's use or reliance upon the content of this publication.

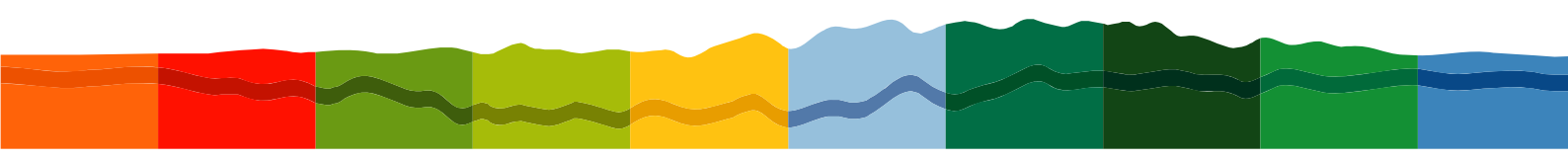

Modelling Microbial Utilisation of Macrophyte Organic Matter Inputs to Rivers under Different Flow Conditions

Patricia Margaret Bowen
B. Sc. (Hons)

Institute for Applied Ecology,
University of Canberra, ACT, 2601

Murray-Darling Freshwater Research Centre
University Drive, Wodonga, VIC, 3689

A thesis submitted in accordance with assessment requirements for
the Doctor of Philosophy Degree of
the University of Canberra.

March, 2006

"…macrophytes often constitute a major fraction of the organic matter produced in freshwater wetlands and littoral zones of lakes (Wetzel and Howe, 1999) … the fate of vascular plant detritus represents an important component in understanding energy flow and nutrient cycling within [aquatic] ecosystems." (Kuehn et al. 1999)

Abstract

The timing and composition of organic matter (OM) inputs to rivers are important as carbon plays a major role in river functioning. Management of Australian rivers since European settlement has altered inputs of organic matter to these systems. Heterotrophic microbes play a critical role in the transformation of OM in rivers, allowing transfer of carbon to other biota. Alteration to the proportions of OM from different sources affects microbial functioning due to differences in OM composition. Macrophytes can represent important sources of carbon to rivers, however their inputs and in-stream processing are poorly understood. The aim of my study was to examine inputs and microbial processing of macrophyte OM in Australian lowland rivers under different flows.

Distributions of dominant macrophytes (*Typha orientalis, Phragmites australis, Vallisneria gigantea* and *Persicaria prostrata*) were mapped in three lowland river reaches in south eastern Australia. Integration with flow data in a GIS allowed the determination of macrophyte inundation patterns under different flows. Resource allocation (biomass and nutrients), live and dead shoot densities and litter production were monitored in the field over 18 months. DOM release from different macrophyte tissues was examined in the laboratory and leachate composition was assessed using nutrient and spectral analyses. Responses of riverine microbial communities to different OM sources were assessed from substrate-induced respiration and enzyme activity experiments and field measurements of respiration and enzymatic responses to varied OM inputs. Finally, all data were integrated into a model of microbial responses to macrophyte OM inputs induced by different flows.

Large populations of macrophytes occurred at all three sites, at bed level, on in-channel benches and on banks. Bank slope, channel heterogeneity and the vertical distribution of macrophyte beds all affected macrophyte inundation patterns. Substantial differences in biomass allocation, nutrient dynamics and litter composition were observed among different plant growth forms and over time. While leaves represented the major shoot component in litter for all species, stems and reproductive structures were also important in some species. Aside from the litter pool, translocation to rhizomes represented a major sink for annual production in emergent plants.

Patterns of shoot density and litter production over time varied among species, providing a source of variation for particulate, and hence dissolved OM inputs upon inundation. The majority of DOM release from POM occurred within 24 hours of inundation. Growth form, tissue type (blade, stem, etc.) and status (live or dead) affected rates, quantities and composition of DOM release, with implications for microbial utilisation. Both overall activity and patterns of carbon utilisation in riverine microbes changed in response to altered OM inputs. Patterns of microbial carbon use were shown to be specific to the carbon source which induced them.

Modelling showed that flow regulation had a major impact on OM inputs and microbial metabolism, through the effects of flow variability on macrophyte vertical distributions, macrophyte bed inundation and dilution. Positive relationships between discharge, DOM inputs and microbial metabolism were observed at the most highly regulated site (drought < current < historic < flood). While a similar pattern occurred at the less regulated site in terms of total loading, dilution effects resulted in a reversal of this trend on a reach volume basis. Microbial metabolism and DOM inputs were restricted to summer/autumn under regulated flows compared to a greater emphasis on winter/spring inputs and microbial activity under unregulated flows. Continual OM inputs during winter with pulsed inputs in spring under natural flows probably benefit larger, slow-growing macro-invertebrates. River regulation promotes pulsed macrophyte OM inputs during spring/summer, potentially favouring riverine microbial and zooplankton production, although at lower levels due to the overall reduction in OM inputs.

The predictive model of macrophyte OM inputs and microbial responses developed throughout this thesis represents a major step forward in our understanding of macrophyte-microbe interactions and our ability to manage our river systems. This work has shown that flow manipulation can be used to influence macrophyte organic matter inputs to rivers and microbial responses, affecting whole stream metabolism and food web interactions.

Certificate of Authorship of Thesis

Except where clearly acknowledged in footnotes, quotations and the bibliography, I certify that I am the sole author of the thesis submitted today entitled “Modelling microbial utilisation of macrophyte organic matter inputs to rivers under different flow conditions”.

I further certify that to the best of my knowledge the thesis contains no material previously published or written by another person except where due reference is made in the text of the thesis.

The material in the thesis has not been the basis of an award of any other degree or diploma except where due reference is made in the text of the thesis.
The thesis complies with University requirements for a thesis as set out in
http://www.canberra.edu.au/research/policies/goldbook/appendices

……
Signature of Candidate

.....
Signature of chair of the supervisory panel

Date: ……..

Acknowledgements

I would like to thank my supervisors, Gavin Rees from the Murray-Darling Freshwater Research Centre and David Williams from the University of Canberra, for all your support and assistance through what has been a trying time for us all. You have both been great role models and mentors while pushing me to perform at my best. Funding for my project and stipend was provided by Land and Water Australia and the Co-operative Research Centre for Freshwater Ecology. Thanks for your support and encouragement to develop myself personally and professionally.

Thanks to everyone at the MDFRC, UC, CRCFE, MDBC, MWWG and Monash, La Trobe and Charles Sturt Universities and all the other friends and family scattered throughout Australia, the world and cyber-space who provided discussion, inspiration, data, field assistance, broad shoulders, laughs, cups of tea and wine as required. It's been a long slog and you all helped a great deal. Thanks especially to the studes (Meeney-moo, Perryman, Suzie-Ann and Jessie-Bear), my local vet/ plant waterer/ pasta cooker Rhonda Sinclair and the Queen Switch-Bitch, Rosie-Posie.

And finally thanks to Ben, Jack, Adara and the rest of the gang. I wish that I'd had more time to spend with you all (especially Ben ☺), and while I was a bit of a nutter at times your encouragement and love really did see me through to the end. Your passion for science has re-inspired my flagging interest and reminded me that nature really is pretty damn cool.

Tanks heaps, luv yez all.

Contents

List of Tables

List of Figures

Chapter 1. Supply and breakdown of macrophyte organic matter in rivers.

Macrophytes are important components of aquatic ecosystems as a source of primary production, in nutrient and water cycling, sediment stabilisation, flow modification, for their habitat value and in the supply of detrital material. Unlike terrestrial systems where higher plant carbon often passes through the food web directly via primary and secondary consumers, the paucity of direct herbivory in aquatic systems (Polunin, 1984; Mann, 1988), means that the major pathway for macrophyte carbon is through the microbial loop (Findlay et al., 1986; Moran et al., 1988; Meyer, 1994). This chapter reviews current scientific understanding of the supply of macrophyte carbon to aquatic systems and its utilisation by micro-organisms.

1.1 Macrophyte Growth and Litter Drop Patterns

Rates, standing stocks and annual quantities of primary production by macrophytes have been well studied in a range of aquatic habitats for over 80 years (e.g. Rickett, 1922). Aquatic plants are often the dominant contributors to primary production in wetland and littoral habitats (Wetzel, 1990; Gessner et al., 1996) and also lotic systems of a range of sizes (Fisher and Carpenter, 1976; Gawne et al., 2002). Indeed, emergent macrophyte communities represent some of the most productive systems in the world (Westlake 1963; Wetzel 1990; Wetzel and Howe, 1999).

However, less is known about macrophyte growth cycles, timing of important phenological events and litter production. Many species exhibit high productivity in spring/summer (Rogers and Breen, 1980; Hill, 1987; Karunaratne et al., 2004) with peak above-ground biomass from late spring to late autumn (Mason and Bryant, 1975; Kvet et al., 1969; Hocking, 1989; Kuehn and Suberkropp, 1998a; Rolletschek et al., 1999). Depending on the species and local conditions, plants may then enter a period of dormancy or translocate resources to storage structures and undergo senescence of above-ground biomass (Dickerman and Wetzel, 1985; Madsen, 1991; Pergent et al., 1997; Klimes et al., 1999; Soetaert et al., 2004). Plants within the former group (e.g. *Vallisneria gigantea, Juncus effusus*) tend to produce new leaves,

and hence discard old leaves as litter, continuously throughout the year, although with some seasonal rate variation (Blanch et al., 1998; Bouchard et al., 1998; Kuehn and Suberkropp, 1998a; Bouchard and Lefeuvre, 2000). In contrast, strong seasonality of litter production is associated with plants in the latter group (e.g. *Typha* spp., *Phragmites australis*) (Roberts and Ganf, 1986; Asaeda et al., 2002), although different shoot components may be shed over different time scales (Gessner, 2000; Kominkova et al., 2000).

Recently, effort has been expended into developing compartmental models of macrophyte production, which describe apportioning of plant production into different biomass components, some of which include estimates of litter production (Allirand and Gosse, 1995; Asaeda et al., 2000; Asaeda and Karunaratne, 2000; Asaeda et al., 2002; Asaeda et al., 2005). Variation in habit, growth and senescence cycles and litter production patterns will all affect inputs of organic matter from macrophytes to their associated water body.

1.2 Macrophyte OM Inputs to Aquatic Systems

While macrophyte organic matter can be utilised by some components of both the aquatic and terrestrial ecosystems (e.g. herbivory by macro-invertebrates, birds and mammals) and also undergoes aerial decomposition (the sole form of decomposition for some species where dead material is not abscised – e.g. Newell, 2001a), the majority of decomposition processing occurs in the aquatic phase after standing biomass or litter is inundated.

Littoral aquatic plants can contribute considerable amounts of detritus to lakes (Howard-Williams and Lenton, 1975) and small streams (Fisher and Carpenter, 1976). Inputs to large rivers are often thought to be negligible due to the relatively small biomass of macrophytes compared to reach volume (Vannote et al., 1980). While no work has been done to directly quantify inputs of macrophyte OM to rivers, estimates from nett above-ground primary production (NAPP) indicate that macrophytes can represent a major carbon source even in rivers where the ratio of plant biomass to discharge is small (Findlay and Sinsabaugh, 1999; Gawne et al., 2002). The contribution from even small populations of macrophytes may be very important to lowland rivers in Australia. Historically, floodplains and riparian vegetation provided large quantities of carbon to the main channel of lowland rivers (Robertson et al., 1999). Anthropogenic modification has reduced interactions of lowland rivers with their floodplains and land clearing has reduced riparian inputs (Robertson et al., 1999). Thus, remnant macrophyte populations may represent the only source of higher plant carbon for many lowland rivers.

Carbon inputs from macrophytes may be in the form of particulate organic matter (POM) – leaves, stems, flowers, etc. – or dissolved organic matter (DOM). Particulate organic matter inputs from macrophytes are represented by standing stems, leaves, flowers, etc. which become

inundated, or litter abscised from shoots either directly into the water column or retained within the bed until inundation occurs through water level changes, wind action or run-off. POM is often categorised into different size fractions in respect of perceived relationships between size (or surface area to volume ratio) and microbial processing rates (Sinsabaugh et al., 1994b; Jackson et al., 1995). Dissolved organic matter is released from macrophyte POM to enter the water column upon inundation or through leaching by rainfall.

1.2.1 Particulate Inputs

Entry of particulate material to rivers may occur via a number of pathways. Litter may detach directly into the water column (e.g. submerged or inundated emergent plants) (Ibarra-Obando et al., 1997; Bouchard and Lefeuvre, 2000) or be retained in the bed (Kuehn et al., 1999) to undergo lateral transportation along banks induced by wind action or runoff (Boschker and Cappenberg, 1998). Variation in water level has a major influence on reducing standing dead material in macrophyte beds, and hence causing POM inputs to associated water bodies (Christian et al., 1990; Findlay et al., 1990; Lee, 1990; Newell et al., 1995; Kuehn and Suberkropp, 1998a; Wetzel and Howe, 1999). Other factors affecting macrophyte POM inputs (from both live and dead tissues) include the action of herbivores, shredding invertebrates, nesting birds or large fauna accessing the water (Newell, 1993; Newell & Barlocher, 1993).

There has been very little work done to directly quantify particulate inputs from macrophytes to water bodies. In systems where flushing of macrophyte beds by flows occurs, inputs of particulate organic matter have been estimated from NAPP (Bouchard and Lefeuvre, 2000; Gawne et al., submitted). Given the numerous possible pathways for primary production (storage structures, respiration, leaching, etc.) (e.g. Asaeda and Karunaratne, 2000) and range of factors influencing inputs of POM to water bodies, more accurate methods of quantifying inputs and estimates of inputs for a range of systems are required.

1.2.2 Dissolved Inputs

Dissolved carbon from aquatic plants can enter aquatic ecosystems through the excretion of photosynthate or leaching of particulate material once immersed (Wetzel, 1969); Wetzel and Manny, 1972a; Wetzel and Manny, 1972b; Findlay et al., 1986). Rates of photosynthate excretion of approximately 4% of net production have been estimated for aquatic macrophytes (Wetzel and Manny, 1972b). Leaching of DOM from macrophyte POM has received quite a lot of research attention, although the definition of what constitutes dissolved fractions varies somewhat between workers (for example, material that passes through 0.2 to 1.0 µm pore size) (e.g. Findlay et al., 1986; Mann and Wetzel, 1996; Kominkova et al., 2000).

The fastest rates of DOM release from macrophyte POM occur within the first 24 – 48 hours of inundation (Otsuki and Wetzel, 1974; Harrison and Mann, 1975; Godshalk and Wetzel, 1978a; O'Connell et al., 2000). DOM derived from this initial leaching phase is comprised mainly of low molecular weight compounds (under 10 000 Da) (Mann and Wetzel, 1996).

DOM release from macrophyte tissues varies with the plant's growth cycle – for untreated samples, senescent tissues release 5 to 25 times the DOM of equivalent green tissues[1] where substantial aerial decomposition and leaching by rainfall have not occurred (Mann and Wetzel, 1996). Differences in rates and quantities of DOM released from different tissue types (e.g. leaves greater than stems – Kominkova et al., 2000) and plant growth forms (Godshalk and Wetzel, 1978a; Anesio et al., 2000; Esselmont and Maher, unpub.) have also been observed.

Some attempts have been made at estimating dissolved inputs from aquatic plants in the field by measuring DOC in water samples around vegetated areas (e.g. Findlay et al., 1998). However, the rapid uptake of labile fractions of DOM by aquatic microbes means that the carbon observed in the water column at any time has low bio-availability and so only a subset of total DOM is captured in instantaneous field sampling. In order to accurately estimate inputs of DOM from macrophytes to aquatic systems, data from controlled laboratory leaching experiments on material which has not undergone unnatural pre-treatments should be scaled to the reach/wetland scale using macrophyte distribution, standing biomass and water exchange data.

1.3 Processing of Macrophyte OM

Although some grazing of standing live macrophyte tissues by birds and terrestrial mammals occurs (Naiman and Rogers, 1997; Brookshire et al., 2002; van Geest et al., 2003), and substantial quantities of detritus is ingested by invertebrates (Flint and Goldman, 1975; Pip and Stewart, 1976; Kornijow, 1996; Kneib et al., 1997; Graca et al., 2000; Bohman and Tranvik, 2001; Silliman and Zieman, 2001), the majority of macrophyte carbon is processed via the microbial loop (Azam et al., 1983; Findlay et al., 1986; Moran et al., 1988; Meyer, 1994). This involves the actions of both fungi and bacteria, with different relative contributions of these two main groups to processing depending on OM composition, particle size (Findlay et al., 2002) and degree of biological and physical pre-treatment, water and oxygen availability and location in the system (sediment, water column, etc).

Fungi play an important role in the aerial decomposition of emergent macrophytes (Newell and Fallon, 1991; Newell et al., 1995, Barlocher and Biddiscombe, 1996, Kuehn and Suberkropp, 1998a; Kuehn et al., 1999). However, microbial community structure changes dramatically upon

[1] Most work on DOM release from macrophyte POM to date has involved pre-treatment of the plant tissues in a manner unlikely to occur under natural conditions (e.g. freezing, high temperature drying, grinding). While often this is for logistical reasons, it makes it difficult to extrapolate results to real-world situations. Many authors simply ignore this fact, a few make mention of these considerations (e.g. Mann and Wetzel, 1996), but even fewer conduct trials to determine the effect of their pre-treatment (Harrison and Mann, 1975; Godshalk and Wetzel, 1978a).

inundation, with bacteria generally dominating aquatic decomposition (Benner et al., 1984; Mann, 1991; Robertson et al., 1999; Kominkova et al., 2000; Kuehn et al., 2000). Higher rates of POM breakdown generally occur under aerobic than anaerobic conditions (Godshalk and Wetzel, 1978b), although lower oxygen concentrations in sediments does not cause slower rates of microbial processing than in the water column (Godshalk and Wetzel, 1978b; Jackson et al., 1995; Emery and Perry, 1996; Picek et al., 2000). The source of sediment OM does affect processing rates and microbial community composition, however, with systems based on planktonic detritus composed equally of bacteria and fungi whereas macrophyte detritus loading increases the proportion of microbial productivity due to fungi (Sinsabaugh and Findlay, 1995). Physical and biological pre-treatment of organic matter affects the succession of decomposers – generally the fungal-dominated community present on coarser particles gives way to bacteria as decomposition progresses and particle size decreases (Gessner and Chauvet, 1994; Jackson et al., 1995; Meyer et al., 1988, Kominkova et al., 2000), although some workers report the opposite trend (Kuehn et al., 1999).

Some of the more common methods used to assess microbial biomass and productivity are summarised in Table 1.1. See Boulton and Boon (1991) for a detailed review of methods used to measure POM breakdown in aquatic systems, including limitations of different methods. As with experiments on DOM release from POM, unnatural pre-treatment of samples (Godshalk and Wetzel, 1978b; Moran and Hodson, 1989; Sinsabaugh et al., 1994b; Jackson et al., 1995) often confounds interpretation of OM processing data (Newell, 1993; Kominkova et al., 2000). The effects of pre-treatment appear to be most significant within the first 24-48 hours and become less important over long time periods (eg. Harrison and Mann, 1975; Godshalk and Wetzel, 1978a; Briggs et al., 1985).

Work on cycling of carbon from macrophytes via the microbial loop has tended to be done at one of two scales: either looking at large-scale decomposition of coarse particulate organic matter over weeks to years (including the influence of invertebrates) and from the perspective of the microbes utilising (generally) DOM over hours to days.

1.3.1 Particulate OM Breakdown

Utilisation of macrophyte particulate matter by other components of the aquatic system is a function of the material's physical and chemical properties, which depend on its state when decomposition commences (Godshalk and Wetzel, 1978b; Melillo et al., 1984; Moran and Hodson, 1989; Gallardo and Merino, 1993; Gessner and Chauvet, 1994). OM quality, or bio-availability, varies with plant growth form, stage in the growth cycle and tissue type (Moran and Hodson, 1989; Gessner, 2000).

Table 1.1 Summary of methods used to assess microbial biomass and productivity

Method	Group*	Example Refs
Measurements of activity (either rates or capacity to perform certain functions)		
POM mass loss using litter bags	Both	Bocock and Gilbert 1957; Briggs et al. 1985; Kuehn and Suberkropp 1998a; Kominkova et al. 2000; Gessner 2000; Godshalk and Wetzel 1978b; Sinsabaugh et al. 1994b; Moran and Hodson 1989
POM mass loss using litter packs	Both	Newell and Fallon 1989; Barlocher and Biddiscombe 1996
POM mass loss of standing biomass	Both	Kuehn and Suberkropp 1998a; Kuehn et al. 1999
Enzymatic decomposition modelling	Both	Sinsabaugh et al. 1992; Sinsabaugh et al. 1994a; 1994b; Sinsabaugh and Linkins 1993; Moorhead and Sinsabaugh 2000; Jackson et al. 1995
Enzyme activities	F or B	Hoppe 1983; Sinsabaugh and Linkins 1988; Chrost 1990; Scholz and Boon 1993; Sinsabaugh and Findlay 1995; Findlay et al. 1998; Wehr et al. 1999
Incorporation of tritiated thymidine	B	Moran and Hodson 1989; Findlay et al. 1998
Respiration rates (O_2 consumption or CO_2 production)	F or B	Kominkova et al. 2000; Kuehn et al. 1999; Picek et al. 2000
Methane production	B	Picek et al. 2000
Nitrification, denitrification	B	Picek et al. 2000
Fatty acid ester analyses	F	Mallory and Sayler 1984
Incorporation of [^{14}C] acetate into ergosterol	F	Gessner and Newell 1997
Substrate utilisation (e.g. Biolog® plates)	F or B	Wehr et al. 1999, Amy et al. 1992, Bochner 1989, Bossio and Skow 1998, Garland and Mills 1991, Konopka et al. 1998, Smalla et al. 1998
Measurements of standing stocks		
Ergosterol concentration	F	Wehr et al. 1999
Cell counts	F or B	Porter and Feig 1980; Jones and Simon 1975; Wehr et al. 1999; Moran and Hodson 1989
Molecular analysis of community structure	F or B	Mills and Wassel 1980; Giovannoni et al. 1990; Olsen et al. 1986; Stahl et al. 1985

* Fungi (F) or bacteria (B); (Both) where these are indistinguishable.

A lot of work has been done on plant breakdown in aquatic systems, mostly at the broad scale of mass loss from leaf packs over weeks to years (See Tables 1.2 and 1.3). Most studies have focused on the decomposition of leaves (e.g. Briggs et al., 1985; Moran and Hodson, 1989; Kuehn and Suberkropp, 1998a), although some workers have examined other above-ground biomass partitions (Gessner, 2000; Kominkova et al., 2000). Very little is known about breakdown of macrophyte roots and rhizomes (Wrubleski et al., 1997).

The majority of work has been done in lentic systems (lakes, wetlands, ponds, marshes) (e.g. Mason and Bryant, 1975; Briggs et al., 1985; Hietz, 1992; Kuehn et al., 1999; Gessner, 2000), with very little focus on rivers and creeks (Palumbo et al., 1987; Findlay and Arsuffi, 1989; Battle and Mihuc, 2000) (Table 1.2, 1.3). This major knowledge gap is due to the assumption that macrophyte inputs to lotic systems are insignificant (Thorp and DeLong, 1994; Delong and Thorp, 2006). As well as being untrue in many systems (see Section 1.2), water flow in lentic systems may well enhance OM breakdown, due to increased supply of oxygen, nutrients and re-suspension and transportation of POM within the water column (Sinsabaugh et al., 1994b; Picek et al., 2000).

Table 1.2 Summary of percentage weight loss of different aquatic plants during decomposition

Species	Mass loss	Duration	Location	References
Carex walteriana	37-46%			Davis and van der Valk 1978, Newell et al. 1995
Distichilis spicata	60%	365 d	salt marsh	de la Cruz 1975
Erianthus giganteus	25-32%		wetland	Kuehn et al. 1999
Juncus effusus	50%	730 d	wetland	Kuehn and Suberkropp 1998a
Juncus effusus	83-100%	154 d	lake	Moran and Hodson 1989
Juncus roemerianus	40%	365 d	salt marsh	de la Cruz and Gabriel 1974
Juncus tracyi	34%	?	pond	Hodkinson 1975
Nuphar variegatum	60-90%	180 d	lab	Godshalk and Wetzel 1978b
Panicum hemotomon	84-100%	154 d	lake	Moran and Hodson 1989
Phragmites australis	75%	365 d	lake	Mason and Bryant 1975
Phragmites australis			lake	Gessner 2000
leaves	80%	240 d		
sheaths	80%	240 d		
stems	80%	720 d		
Potamogeton diversifolius	57%	100 d	pond	Wohler et al. 1975
Scirpus acutus	20-40%	180 d	lab	Godshalk and Wetzel 1978b
Scirpus americanus	60%	365 d	salt marsh	de la Cruz 1975
Spartina cynosuroides	60%	365 d	salt marsh	de la Cruz 1975
Typha latifolia	45%	365 d	lake	Mason and Bryant 1975
Typha latifolia	100%	154 d	lake	Moran and Hodson 1989
Typha latifolia	55%	210 d		Barlocher and Biddiscombe 1996
Vallisneria spiralis	30%	1 d	lake	Briggs et al. 1985
	95%	30 d		

Macrophyte tissue breakdown in or on sediments (Godshalk and Wetzel, 1978b; Jackson et al., 1995; Emery and Perry, 1996; Picek et al., 2000) is usually faster than in the water column (Briggs et al., 1985; Moran and Hodson, 1989) which is usually more rapid than aerial decomposition (Newell, 1993; Newell et al., 1995; Barlocher and Biddiscombe, 1996; Kuehn & Suberkropp, 1998a; 1998b; Kuehn et al., 1998; 1999; Barlocher, 1999; Gessner, 2000, Kominkova et al., 2000).

Macrophyte decomposition rate has been linked to growth form (a plant's characteristic physical structure – e.g. free-floating, rooted with floating leaves, rosette-forming) (Godshalk and Wetzel, 1978a; 1978b; Moran and Hodson, 1989) and explained by the fibre content of the different species (Polisini and Boyd, 1972). Submerged plant tissues decompose the most rapidly (Petersen and Cummins, 1974; Bastardo, 1979; Howard-Williams and Davies, 1979; Rogers and Breen, 1982; Briggs et al., 1985). Plants with a floating-leaved habit decompose more rapidly than emergent macrophytes (Godshalk and Wetzel, 1978b). Similarly, shoot components with limited structural constituents, such as leaves, induce higher rates of microbial metabolism than those with high proportions, such as stems (Gessner, 2000; Kominkova et al., 2000). Microbial production on POM is also affected by temperature (Godshalk and Wetzel, 1978b; Moran and Hodson, 1989; Kuehn et al., 1999) and oxygen availability (Picek et al., 2000).

Table 1.3. Summary of decay rate coefficients (k) for different aquatic plants

Species	k	Duration	Location	Ref
Nuphar variegatum	0.016-0.085	180 d	lab	Godshalk and Wetzel, 1978b
Myriophyllum sp.	0.006-0.037	180 d	lab	Godshalk and Wetzel, 1978b
Najas flexilis	0.007-0.028	180 d	lab	Godshalk and Wetzel, 1978b
Scirpus subterminalis	0.002-0.017	180 d	lab	Godshalk and Wetzel, 1978b
Scirpus acutus	0.002-0.011	180 d	lab	Godshalk and Wetzel, 1978b
Phragmites australis	0.008-0.027	86 d	lake	Kominkova et al., 2000
Phragmites australis				
leaves	0.0045	240 d	lake	Gessner, 2000
sheaths	0.0051	240 d		
stems	0.0015	740 d		
Phragmites australis	0.0029-0.0036		lake	Mason and Bryant, 1975
Phragmites australis	0.0011		lake	Polunin, 1982
Phragmites australis	0.0028		lake	Lee, 1990
Phragmites australis	0.0018-0.0021		lake	Andersen, 1978
Vallisneria spiralis	0.1429	60 d	lake	calculated from data in Briggs et al., 1985
Juncus effusus (aerial)	0.0010	730 d	wetland	Kuehn and Suberkropp, 1998a
Typha latifolia	0.05 – 0.20		wetland	Jackson et al., 1995
Typha spp.	0.08 – 0.15			Davis and van der Valk 1978, Cahoon and Stevenson 1986, Findlay et al. 1990, Mason and Bryant 1975

Many researchers have emphasised the need for a more integrated approach to the study of macrophyte OM breakdown, incorporating patterns of senescence, transferral between the aerial and aquatic phases, decomposition within each phase and the condition (particle size, composition, degree of biological and physical pre-treatment) of the material at the commencement of each decompositional stage (e.g. Newell, 1993; Barlocher, 1997; Gessner, 2000).

1.3.2 Dissolved OM Utilisation

The responses of microbes to carbon and nutrients has been studied extensively in laboratory cultures using artificial substrates (e.g. Amblard et al., 1998), however much less work has been done on microbial utilisation of POM and DOM from environmental sources, especially *in situ* assessments. Where microbial responses to macrophyte organic matter have been assessed, temperature and oxygen availability are often cited as important drivers of activity (e.g. Godshalk and Wetzel, 1978a; Kuehn et al., 1999; Picek et al., 2000). While attempts have been made to link the activity of aquatic microbes to carbon concentration, a common relationship in soil microbial science, it seems that rates of loading are more important to aquatic microbial communities than total carbon content (Findlay et al., 1998: Findlay and Sinsabaugh, 1999). However, this may actually be a reflection of the rapidity with which any labile fractions of DOM are removed by microbes from the total dissolved carbon pool, with any instantaneous sampling of TOC probably consisting primarily of refractive material (see Section 1.2.2).

Of the many factors affecting microbial responses to organic matter (including water temperature, particle size, microbial population size and composition), the bio-availability of a given substrate, based on the energetic efficiency of assimilation of its constituent compounds (Mann and Wetzel, 1996; Sun et al., 1997), is particularly important (Mann and Wetzel, 1996; Pinney et al., 1999; Stepanauskas et al., 2000). For example, the low bioavailability of humic substances (Tranvik, 1988; Leff and Meyer, 1991; Hessen, 1992), which decompose 10 to 100 times more slowly than nitrogen-rich materials, relates to their large amorphous poly-phenolic structure, which cannot pass directly into microbial cells, forcing microbes to produce a suite of enzymes to break them down fully (Godshalk and Wetzel, 1978a). Methods used to assess OM bio-availability are summarised in Table 1.4.

Table 1.4 Summary of methods used to assess bio-availability of organic matter

Type of analysis	Parameters	References
Proportion structural compounds	Lignin / cellulose content	Moran and Hodson 1989; Sinsabaugh and Linkins 1990
Chemical composition	compound types present, molecular size, solubility	Meyer et al. 1987; Sun et al. 1996; McCarthy et al. 1997; Hopkinson et al. 1998; Findlay and Sinsabaugh, 1999; Sinsabaugh and Linkins 1990
Elemental composition	Nutrient contents and ratios	Polisini and Boyd, 1972; Hodkinson 1975; Godshalk & Wetzel 1978b; Polunin 1982; Moran and Hodson 1989; Sinsabaugh and Linkins 1990; Sinsabaugh et al., 1993; Gessner and Chauvet 1994 ; Gessner 2000; Kominkova et al. 2000
Spectral qualities	UV absorbance, fluorescence	Levesque 1972; Godshalk & Wetzel 1978a ;Findlay et al. 1998
Enzymatic	ratios of oxidative to hydrolytic enzyme activities	Sinsabaugh and Findlay 1995

In general, the highest rates of leachate DOC utilisation occur in the first 24 hours of incubation (Wetzel and Manny, 1972a; Findlay et al., 1986; Mann and Wetzel, 1996). At this time leachates contain a fraction of rapidly-utilisable (labile) DOC (Mann and Wetzel, 1996). After these compounds are consumed, microbes switch to other, more refractive compounds. Patterns of bacterial production can vary over the time course of the incubation, often showing secondary peaks or higher final rates (Mann and Wetzel, 1996), possibly due to microbes altering their metabolism to utilise alternate carbon compounds as preferred ones are used up (Suberkropp et al., 1976; Godshalk & Wetzel, 1978a; Wilson et al., 1986 Moran et al., 1989).

Bacterial growth efficiencies (ratio of biomass produced to substrate assimilated) on macrophyte leachates range from 10% to greater than 90%, with a median of around 50% for freshwater species (Billen et al., 1980; Robinson et al., 1982; Linley and Newell, 1984; Bauerfeind, 1985; Findlay et al., 1986; Meyer et al., 1987; Mann and Wetzel, 1996). While lower than BGE reported on algal exudates (30 – 80%, median of 60%), these values are higher

than those measured for transported organic matter in rivers (around 30%) or terrestrial leaf leachates (10 – 20%) (Meyer et al., 1987; del Giorgio and Cole, 1998). BGE varies across different macrophyte growth forms, with submerged macrophyte leachates inducing similar responses as algal extracts, which are higher than those induced by floating-leaved plants, with emergent macrophytes having the lowest values (Findlay et al., 1986; 1992; Mann and Wetzel, 1996; Linley and Newell, 1984; Meyer et al., 1987; Godshalk and Wetzel, 1978a).

In other instances, rates of microbial activity remain steady with additions of different carbon sources, but a shift in metabolic function occurs (as evidenced by changes to enzyme activities) (Findlay et al., 1998). The substantial temporal variation in response to each type of DOC in this study indicates temporal variation in the composition of the OM, possibly linked to plant growth cycles, however little work has been done on this topic, except to report higher microbial activities on leachates derived from senescing rather than green tissues (Mann and Wetzel, 1996) where heavy rainfall has not removed the most bio-available compounds.

Obviously the uptake and utilisation of dissolved organic matter by aquatic microbes involves a complex series of processes which need closer investigation including experiments using untreated environmental carbon sources to enable scaling of microbial responses to the river reach/landscape scale and determine flow-on effects at the ecosystem level.

1.4 Ecosystem Level Effects

Macrophyte OM inputs and microbial metabolism can affect stream functioning at an ecosystem level through their contribution to food webs, effects on dissolved gas availability and competitive or complementary interactions with other biota.

1.4.1 Trophic Links

Some macrophyte organic matter enters aquatic and terrestrial food webs through direct herbivory by macro-invertebrates, water birds, terrestrial insects or mammalian herbivores (Flint and Goldman, 1975; Pip and Stewart, 1976; Naiman and Rogers, 1997; Kneib et al., 1997; Graca et al., 2000; Bohman and Tranvik, 2001; Silliman and Zieman, 2001; Brookshire et al., 2002; van Geest et al., 2003). However, the vast bulk of material is processed via the microbial loop (Azam et al., 1983; Findlay et al., 1986; Moran et al., 1988; Meyer, 1994).

During processing by heterotrophic microbes, OM is either converted to microbial biomass or respired as CO_2. For freshwater macrophyte OM, bacterial growth efficiencies are highly variable but generally between 30 and 50% (see section 1.3.2), so while 50 – 70% of the plant material assimilated by microbes is respired, a large proportion is incorporated into microbial biomass and thence transferred to higher trophic levels. Protozoan grazing is responsible for the removal of vast quantities of bacterial biomass from aquatic systems (Wright & Coffin, 1984; Riemann, 1985;

Servais et al., 1985; Findlay et al., 1986; Hulot et al., 2001; Hahn and Höfle, 2001; Menon et al., 2003). Protozoa are in turn consumed by zooplankton and micro-invertebrates (Gilbert, 1989; Pace and Funke, 1991), providing the link between the macrophyte-bacterial complex and the rest of the aquatic food web (Williamson, 1983; Wickham, 1995; David et al., 2006).

Thus, microbes represent a link between a generally unavailable organic carbon source (aquatic plant OM) and higher trophic levels. The action of the microbial loop means that food chains in aquatic systems consist of many more trophic levels than traditionally conceptualised (Fenchel, 1988; Pomeroy and Wiebe, 1988; Chrost, 1992). Different theoretical models of food webs in large rivers attribute varying levels of importance to the contributions of carbon sources such as phytoplankton, macrophytes and riparian vegetation to higher trophic levels (Junk et al., 1989; Vannote et al., 1980; Thorp and Delong, 1994). While some work on food-webs in large rivers demonstrates contributions of higher plant carbon to diets of higher trophic levels or stresses the importance of the microbial loop to carbon passage to higher trophic levels (Suren and Lake, 1989; Korinjow et al., 1995; Gawne et al., in prep.; also reviewed in Carpenter and Lodge, 1986), others found that riparian and aquatic plants were not supporting higher trophic levels either directly (Bunn et al., 2003) or via the microbial loop, which was concluded to be an almost closed cycle (Thorp et al., 1998; Thorp and Delong, 2002; Delong and Thorp, 2006).

However, interpretation of data from food web studies which track composition changes in tissue constituents through trophic levels (such as stable isotope research) is confounded by the lack of information on the degree of transformation of organic and inorganic compounds as they pass through the microbial loop. The isotopic discrimination which occurs in higher trophic levels (and which underlies the use of stable isotopes to identify trophic level) would be expected to also occur in microbes. If so, then each cycle through the loop could change the isotopic signature the equivalent of a trophic level addition. Obviously, understanding the effect of the microbial loop on compositional changes in OM, such as isotopic modification, is critical to understanding aquatic food webs and the role of different organic matter sources.

1.4.2 Biotic Interactions

The aquatic microbial community can have a profound effect on whole-stream metabolism and aquatic food webs through their interactions with algae. Although microbes can utilise organic carbon sources unavailable to algae, these groups actively compete for other nutrients (Chrost, 1992). Indeed, where bacteria are not carbon limited, they usually out-compete algae for inorganic nutrients, to the extent of limiting algal production and population size (Pengerud et al., 1987; Rothaupt, 1992; Blomqvist et al., 2001; Hulot et al., 2001). Similarly, where top-down control of phytoplankton populations occurs, bacterial dominance (and hence heterotrophy) can occur despite low organic carbon loadings (Findlay et al., 1998).

In other instances, components of the microbial loop (bacteria, protozoa, heterotrophic nanoflagellates and microflagellates) play a role in increasing the availability of carbon and nutrients to algae, oxidizing organic material and releasing CO_2, PO_4, NH_4, SO_4 and other inorganics that are required for algal production (Chrost, 1992). Indeed the apportioning by microbes of organic carbon metabolism into assimilation or catalysis (Findlay et al., 1986) becomes critically important in systems where algal communities are carbon-limited.

Thus, the supply and metabolism of dissolved organic matter, and hence the microbial loop, represents a major regulatory mechanism of nutrient balances and energy flow in aquatic systems (Findlay and Sinsabaugh, 1999) which can profoundly influence food webs and shift net ecosystem metabolism between autotrophy and heterotrophy (Kemp et al., 1997).

1.5 Concluding Remarks

This review presents an overview of current scientific understanding regarding the supply of macrophyte carbon to aquatic systems and its utilisation by micro-organisms.

While macrophytes are highly productive and some aspects of their productivity are well understood, it is less clear how variation in habit, growth and senescence cycles and litter production patterns may affect inputs of organic matter from macrophytes to their associated water body. Given the changes to carbon loading to rivers caused by previous catchment and river management practices in Australia, remnant macrophyte populations may represent the only source of higher plant carbon for many lowland systems.

One of the major factors affecting inputs from macrophytes is variation to water levels. Flow manipulation is an emerging tool for managing aquatic ecosystems, however very little is known about the links between flow and ecology, including how flow variability affects inputs of OM from macrophyte beds to rivers. Some data are available on what happens when macrophyte OM is inundated, although for a limited range of tissue types and species. Release of DOM from inundated macrophyte OM is fastest within the first day or so, and composed of highly bio-available compounds. Variation in both release rates and bio-availability are based on the composition of plant tissue inundated (proportion structural compounds, nutrient contents and ratios, etc.), external nutrient supplies, temperature, oxygen availability and tissue pre-treatment. In order to accurately estimate inputs of DOM from macrophytes to aquatic systems, data from controlled laboratory leaching experiments on material which has not undergone unnatural pre-treatments should be scaled using macrophyte distribution, standing biomass and water exchange data.

Broad-scale *in situ* tissue decomposition studies and small-scale laboratory experiments have been used to examine microbial processing of macrophyte OM in relation to growth form, substrate type and composition, temperature and nutrient and oxygen availability. Studies that fill the gap between these scales or integrate across them to follow the entire decomposition process have not been performed, however. Macrophyte OM inputs and microbial metabolism can affect stream functioning at an ecosystem level through their contribution to food webs and competitive or complementary interactions with other biota. The supply and metabolism of dissolved organic matter, and hence the microbial loop, represents a major regulatory mechanism of nutrient balances and energy flow in aquatic ecosystems.

1.5.1 Thesis Justification

Given the importance of macrophytes to Australian lowland rivers, especially in light of changes to carbon loading since European settlement, the limited data availabile on their longitudinal distributions along rivers and vertical ranges within channels (although see Blanch et al., 1999b; Walker et al., 1994) presents obstacles in linking the ecosystem functions the plants perform to the rest of the system. In combination with data on flow variability, macrophyte distribution data would allow the prediction of macrophyte inundation responses at the reach-scale, hence enabling the determination of their ecological significance.

Within riverine macrophyte communities, resource allocation has implications for the photosynthetic and reproductive capacity of individual shoots, plant populations and the associated ecosystem. While some aspects of resource allocation have received substantial research attention, reproductive mass losses, detailed allocation changes during senescence and litter production dynamics are rarely quantified or even estimated.

A better understanding of resource allocation and pools and fluxes of macrophyte POM in rivers would clarify the link between macrophyte production and the rest of the system. Seasonal variation in above-ground biomass has been observed for many aquatic plants, however this is often not quantified or differentiated into live and dead biomass. Similarly, litter production in macrophytes is rarely monitored and measurements of standing litter crop are scarce. Inundation of macrophytes in rivers by changing water levels releases DOM into the water column, fuelling microbial production. Understanding of DOM release from macrophyte POM is currently limited by a lack of research effort and consistency of methods. Information on leachate bio-availability provides a link to microbial utilisation, and hence to the rest of the system. However, most data are not directly applicable to estimation of DOM release from POM in the field, making it difficult to extrapolate DOM release processes and potential microbial utilisation to the reach scale.

Heterotrophic microbes play a critical role in aquatic ecosystems in the transformation of DOM into microbial biomass or inorganic carbon, allowing cycling of carbon to other riverine biota. Alterations to the proportions of organic matter supplied from different sources affect microbial functioning due to differences in the composition of the material. While bio-availability varies with growth form, tissue type and tissue status, data on the coverage of species and tissue types is sparse and methodological issues make extrapolation to reach scales difficult.

Microbial responses of importance to ecosystem functioning include oxygen consumption (potential for "black-water" events), competition with algae for inorganic nutrients (possible attenuation of algal blooms), food supply to higher trophic levels and the provision of inorganic carbon to the water column for autotroph production. As well as being important for improving our understanding of these interactions, knowledge about microbial functioning is critical for predicting system responses to management interventions.

In summary, the major knowledge gaps identified in this review regarding macrophyte-microbial interactions in lowland rivers are:

- Macrophyte distributions, elevation ranges and linking of known inundation responses to inundation patterns under different hydrographs.
- Resource allocation dynamics, including detailed changes during senescence and reproductive mass losses.
- Changes to standing biomass and litter production on a sub-seasonal time-scale.
- Processes affecting inputs of POM to rivers (e.g. inundation by variable flows, wind and rain action, faunal activity).
- Rates of release and composition of DOM leached from a range of green and senescent tissues from macrophyte species with different growth forms.
- Responses of riverine microbial communities to macrophyte OM inputs at spatial scales intermediate to, or spanning those currently studied (microcosm or reach).
- The quantification of OM inputs from macrophytes to rivers at the reach scale, and microbial responses to these.

The aim of my study was to examine inputs and microbial processing of macrophyte OM in Australian lowland rivers under different flows, by addressing each of the knowledge gaps listed above, and to ultimately incorporate my data into a predictive model to provide a decision support tool for the management of river flows. My approach was to integrate small- and large-scale measurements of macrophyte OM production, input and decomposition by scaling results of lab experiments to the reach and ecosystem-response scale using field monitoring of macrophytes and microbes.

1.5.2 Thesis Outline

Each of the knowledge gaps identified above is addressed throughout this thesis as outlined below.

Chapter 2 describes population sizes and distributions of dominant macrophyte species in three Australian lowland rivers. Flow regimes specific to each river are integrated into a GIS containing three-dimensional channel and vegetation maps to determine patterns of macrophyte inundation at each site under different hydrographs.

Chapter 3 describes an extensive field sampling program where I measured shoot compositional changes throughout the plants' growth cycles to determine changes to resource allocation (biomass and nutrient) during senescence and determine the shoot components contributing to litter production over a 1-2 year time scale.

In Chapter 4, functions describing litter production and standing biomass changes over time developed from monitoring macrophyte populations in the field are presented. Inputs of macrophyte POM to rivers under different flows are quantified, by incorporating data from Chapters 2 and 3 with the litter and standing biomass functions.

Rates and composition of DOM released from a range of shoot biomass components are presented in Chapter 5. The bio-availability of different leachates is described, providing a link to microbial metabolism, and hence to the rest of the system.

Chapter 6 describes the responses of riverine microbial communities to different carbon inputs likely to dominate under different flow regimes, including macrophyte OM. This chapter highlights how flow manipulation could be used by managers to affect microbial functioning.

Finally, all data are integrated into a single model of microbial responses to macrophyte OM inputs induced by different flows in Chapter 7. The implications of different flow regimes for macrophyte inputs, and hence microbial functioning, are discussed.

As well as addressing the major knowledge gaps highlighted in this review, my research contributes to the knowledge base to assist in management decisions regarding river flow releases. This thesis presents an integrated, predictive model of reach-scale microbial responses to inundation of macrophytes in lowland rivers and outlines potential ecosystem effects arising from projected macrophyte decomposition.

Chapter 2. Hydrological modelling of macrophyte inundation in some south eastern Australian lowland rivers.

2.1 Introduction

Macrophytes perform many roles in aquatic systems. Their high productivity (Keefe, 1972; Westlake, 1975; Roberts and Ganf, 1986; Wetzel, 1990; Wetzel and Howe, 1999) represents a major source of organic matter in wetlands (Howard-Williams and Lenton, 1975) and some streams and rivers (Thorp and de Long, 1994; Gawne et al., submitted). While primarily processed through the microbial loop (Gawne et al., in prep; Findlay et al., 1986; Moran et al., 1989), macrophyte organic matter is also grazed by macro-invertebrates, fish, birds and mammals (Suren and Lake, 1989; Lodge, 1991; Newman, 1991; Jacobsen and Sand-Jensen, 1992; Johnson et al., 1998). Sediment aeration, stabilisation and localised flow modification are associated with rooted aquatic plants, while nutrient and water cycling functions are performed by all growth forms (Haslam, 1978). Macrophyte beds provide habitat for fish (Weaver et al., 1997; Pusey et al., 1993; Pusey et al., 1998), birds (Parkinson et al., 2002; Poulin et al., 2002; Leslie, 2001) and macro- and micro-invertebrates (Hawking and Smith, 1997; Lillie and Budd, 1992; Lombardo, 1997; Cyr and Downing, 1988; Taniguchi et al., 2003), and also often support abundant and diverse epiphytic growth (Haslam, 1978; Cattaneo et al., 1998).

While no extensive mapping of macrophyte distributions has been attempted for south-eastern Australia, it is generally acknowledged that plant abundance and diversity are greater in floodplain wetlands than the channels of large rivers, a situation which may have been exacerbated since European settlement (Roberts and Sainty, 1996; Roberts, 2000). However, dense stands of aquatic vegetation do occur in many streams and rivers in this region, and include species such as *Phragmites australis*, *Typha* spp., *Cyperus* spp., *Myriophyllum* spp., *Juncus* spp., *Eleocharis* spp., *Ludwigia peploides*, *Rumex* spp., *Persicaria* spp., *Vallisneria gigantea*, *Sagittaria* spp., *Potamogeton* spp. and *Bolboschoenus* spp. (Sainty and Jacobs, 1981; 1994; Roberts and Sainty, 1996; Roberts and Ganf, 1986; Walker et al., 1995; Blanch et al., 1999).

The rivers in south-eastern Australia form part of the Murray-Darling Basin (MDB), a primarily dry-land catchment of over 1 million km^2 with a median annual discharge of 8500 GL (Blanch et al., 1999). The MDB has been extensively cleared and supports 40% of Australian agricultural production (Crabb, 1997). Prior to European settlement the rivers and streams in southeastern Australia were subjected to highly variable flows (Walker, 1992; Walker and Thoms, 1993; Boulton and Brock, 1999), comparable to the most variable rivers in the world (Puckeridge et al., 1998; Olden and Poff, 2003). However, regulation of nearly all of the large rivers in south-eastern Australia has considerably diminished flow variability (Walker and Thoms, 1993; Hillman, 1995; Maheshwari et al., 1995; Poff et al., 1997; Puckeridge et al., 1998).

The variability remaining in these rivers is generally still sufficient to cause various degrees of inundation and exposure of riverine macrophyte beds throughout the year (Blanch et al., 1999b; Walker et al., 1994; Roberts and Ganf, 1986). Inundation has been shown to affect productivity of both emergent and submerged macrophytes (Blanch et al., 1998; Blanch et al., 1999a; Crawford and Braendle, 1996; Froend and McComb, 1994; Keefe, 1972; Kirkman and Sharitz, 1993; van den Brink et al., 1995). Habitat components considered important in terrestrial ecosystems, such as patch size, connectivity and habitat quality (Hart and Horwitz, 1991; Denno and Roderick, 1991; Murcia, 1995; Major et al., 2003; Fleishman et al., 2002; Franken and Hik, 2004; Fred and Brommer, 2003) have also been shown to affect community structure and stability in aquatic systems (Weaver et al., 1997; Cyr and Downing, 1988; Heck and Crowder, 1991; Tonn and Magnuson, 1982; Douglas and Lake, 1994; Lillie and Budd, 1992). Habitat features of macrophyte beds may be affected by inundation and exposure. Primary grazing roles might be expected to switch between terrestrial fauna and in-stream herbivores depending upon the degree of immersion. Finally, inundation of riverine vegetation is probably the primary pathway for input of its organic matter to lowland river channels.

No data are available on changes to habitat features of macrophyte beds, access by grazers or OM inputs caused by flow variability. While data do exist on changes to productivity under different flows for a limited number of species, this work has not been linked back to macrophyte distributions in lowland rivers and their inundation patterns**.** This study aimed to examine the distributions of in-channel macrophytes in three lowland river reaches in south-eastern Australia and determine patterns of inundation caused by within-channel flows. Models generated predict macrophyte inundation patterns under different flow scenarios. These data will provide the first step in the overall aim of this thesis of predicting inputs to lowland rivers of OM from macrophytes under different flow conditions.

2.2 Methods

2.2.1 Plant Species

Four plant species which are common in south-eastern Australian aquatic systems and which cover a range of growth forms were selected for study. These were *Typha orientalis* C. Presl, *Phragmites australis* (Cav.) Trin. ex Steudel, *Persicaria prostrata* (R.Br.) Sojak and *Vallisneria gigantea* Graebn. Plant names follow the Flora of NSW (1990). The first two of these are emergent plants with different modes of growth. *Persicaria* is a low-growing hydrophyte occurring in areas which are generally inundated only during very high flows but have high soil moisture content and *Vallisneria* is a submerged species. Unless otherwise stated, the use of the generic name only is taken to refer to these species throughout.

2.2.2 Study Sites

Three study sites were selected on lowland rivers in south-eastern Australia. Selection was based on the presence of at least one of the species of interest in reasonable abundance, with an attempt made to choose rivers with different flow regimes. Study sites were visited on nine occasions over 18 months from May 2001 to December 2002.

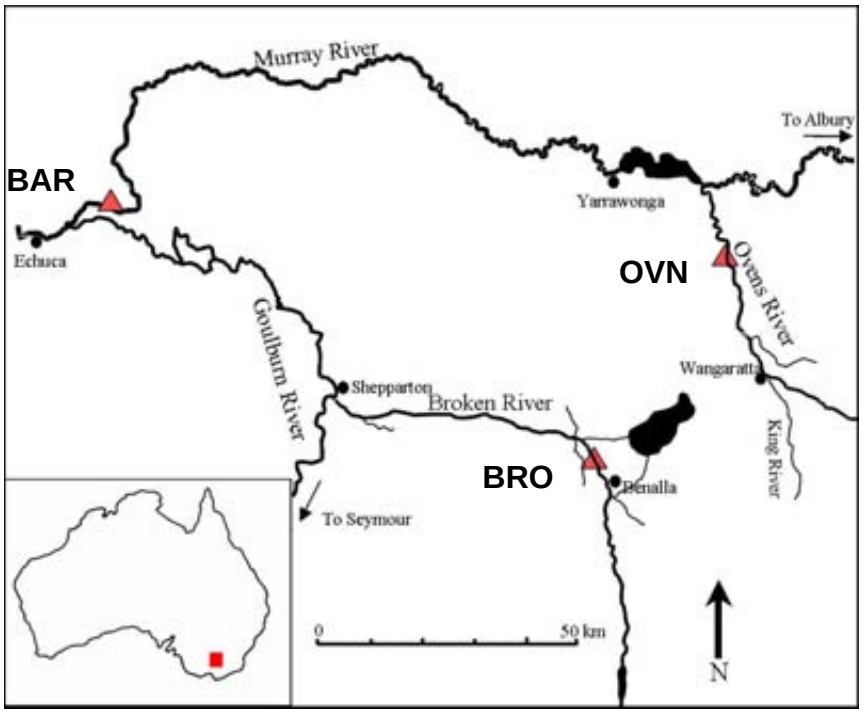

Figure 2.1. Location of field sites. 'BAR' is the site on the Murray River the in Barmah-Millewa forest. 'BRO' is the site on the Broken River. 'OVN' is the site on the Ovens River.

2.2.2.1 Murray River

The Murray River field site ('BAR') was a 3 km lowland reach of the Murray River in the Barmah-Millewa forest (35° 49' 33" S, 145° 05' 35') (Figures 2.1 and 2.2). Here the river flows through relatively intact floodplain forest dominated by River Red Gums (*Eucalyptus camaldulensis*) managed for forestry with grazing as a secondary land-use. As such, the site differs from many lowland river reaches in the region, which have generally experienced substantial clearing of native vegetation for intensive cropping or grazing. However, the study site's vegetation was representative of the river section passing through this iconic floodplain forest, and the flow patterns were similar to those in the majority of regulated rivers in the region. The river bed has numerous sand bars and benches of sand, silt and mud, which are exposed at low water levels. Most of the benches support beds of macrophytes, including *Phragmites australis*, *Typha orientalis*, *Juncus ingens*, *Cyperus exaltatus*, *Persicaria hydropiper*, *Troglochin procerum* and other annual forbs and sedges.

2.2.2.2 Broken River

The site on the Broken River ('BRO') was a 1 km reach located 5 km north of Benalla (Figures 2.1 and 2.3). Typically for lowland rivers in the region, the riparian zone at the study site has been cleared for grazing on both sides of this regulated river, and is dominated by pasture grasses with individual mature River Red Gums occurring intermittently along the river's edge. Silver wattle (*Acacia dealbata*), Weeping and Crack willows (*Salix babylonica* and *S. fragilis*) and other introduced tree species comprise the sparse lower and middle riparian canopies. *Phragmites australis* occurs in patches along the banks and forms a dense colony on a large island at the downstream end of the study reach. Numerous small beds of *Vallisneria gigantea* occur within the river channel at bed level. Sediment in the river is primarily sand overlaying heavy clay and large woody debris (LWD) is common. Water quality is generally poor with high turbidity and nutrient levels.

2.2.2.3 Ovens River

The third field site was a 1 km reach of the Ovens River between Wangaratta and the confluence with the Murray River, near the township of Peechelba, which was representative of the lowland section of this river ('OVN') (Figures 2.1 and 2.4). Meander migration and cut-offs have created many anabranches and billabongs, which fill directly from the main channel or by overbank flow during floods. The river banks are very steep and bed composition at this site is mostly clay, sand and silt. The Ovens River is one of the last unregulated rivers in south-east Australia and has been declared a Heritage River under the Victorian Heritage Rivers Act 1992.

Figure 2.2. Macrophyte beds at BAR. (Photo B. Gawne)

Figure 2.3. Photo of Broken River study site showing patches of fringing macrophytes. (Photo B. Gawne)

River Red Gum forms a relatively dense riparian overstorey at this site, with patches of Silver Wattle and River Bottlebrush (*Callistemon sieberi*) occurring intermittently. The dense riparian ground layer is comprised mainly of herbaceous species and the introduced canary grass (*Phalaris aquatica*) is widespread. While diverse communities of submerged and emergent macrophytes occur throughout floodplain billabongs, aquatic vegetation on lower banks and in-channel benches at this site is dominated by a single species, *Persicaria prostrata*. Considerable quantities of large woody debris occur within the river channel.

Figure 2.4. Photo of OVN showing steep banks and dense beds of *Persicaria*.(Photo B. Gawne)

2.2.3 Macrophyte Distributions

A differential GPS and laser surveyor (Criterion Instruments) were used to survey within-channel benches and both banks at each site (joint data with CRCFE project A200). The locations and areas of macrophyte beds along the entire length of each study reach were recorded, as were their elevations relative to the river channel. Digital LIDAR images of the floodplain surrounding each river reach were obtained from the Murray-Darling Basin Commission. Data were combined into a Geographic Information System (GIS) for each site using ESRI ArcGIS software version 8.3.

2.2.4 Hydrology

Hydrological data for the three sites were obtained from Thiess Environmental Services. Gauging stations used for BAR and OVN were 409215 and 403241, respectively. As there was no gauging station associated with the field site on the Broken River, discharge at this site was determined by calculation (flow at site 404203A less known extractions between the gauging station and field site). The rating curve from the nearest gauging station with channel morphology most similar to the study site was used for BRO (404222).

2.2.5 Modelling

Flow data for each site were incorporated into the respective GIS to allow three-dimensional modelling of channel water depth for different discharge values. For a range of discharges (and hence water depths within the channel) from base flows to over-bank flows, macrophyte inundation curves were determined for each species. During this modelling, it was

assumed that the water surface was flat over the area of interest, which was reasonable given the scale of the study (advice provided by MDBC GIS personnel). Inundation curves described the area of macrophyte bed inundated and the mean depth of water overlying beds for a given discharge at each site. This modelling enabled prediction of macrophyte inundation under different flow scenarios, namely, present (current) conditions, flows prior to river regulation (historic), during flood years and during droughts. These scenarios were selected as being important to current debate over effects of environmental flows on components of aquatic ecosystems. Hydrographs representing each scenario were calculated from flow data provided by Thiess Environmental Services as outlined in Table 2.1.

Table 2.1 Hydrographs used in modelling scenarios were obtained from averaging over these years.

Site	Current	Historic	Drought	Flood
BAR	1998-2003	1914-1926	1915, 1919, 1923, 1997, 1998, 2001, 2002	1917, 1918, 1924
BRO	1991-2003	1916-1926	1938, 1940, 1943, 2002	1917,
OVN	1990-2003	1915-1926	1902, 1914, 1938, 1940, 1944, 1994, 2002	1917, 1974, 1981, 1993, 1996, 1998

2.3 Results

2.3.1 Macrophyte Distributions

2.3.1.1 Typha

While some *Typha orientalis* occurred on the bank at BAR, the majority was found on in-stream benches (13,500 m^2 within the 3 km reach) (Figure 2.5; Table 2.2). *Typha* occurred in four beds of relatively similar size, with the largest bed having an area of 4,700 m^2. *Typha*'s vertical distribution extended from 95.6 to 99.4 m elevation (3.8 m range).

2.3.1.2 Phragmites

At BAR *Phragmites australis* covered approximately 13,600 m^2, which was distributed among four beds, ranging in size from 300 – 5,400 m^2 (Figure 2.5; Table 2.2). The densest stands of *Phragmites* at this site occurred on benches within the river channel with sparser growth occurring extensively throughout the floodplain, however floodplain distribution was not mapped for this study. The vertical extent of *Phragmites* distribution on benches at Barmah was similar to *Typha*, commencing at 95.8 m elevation and extending to 99.6 m.

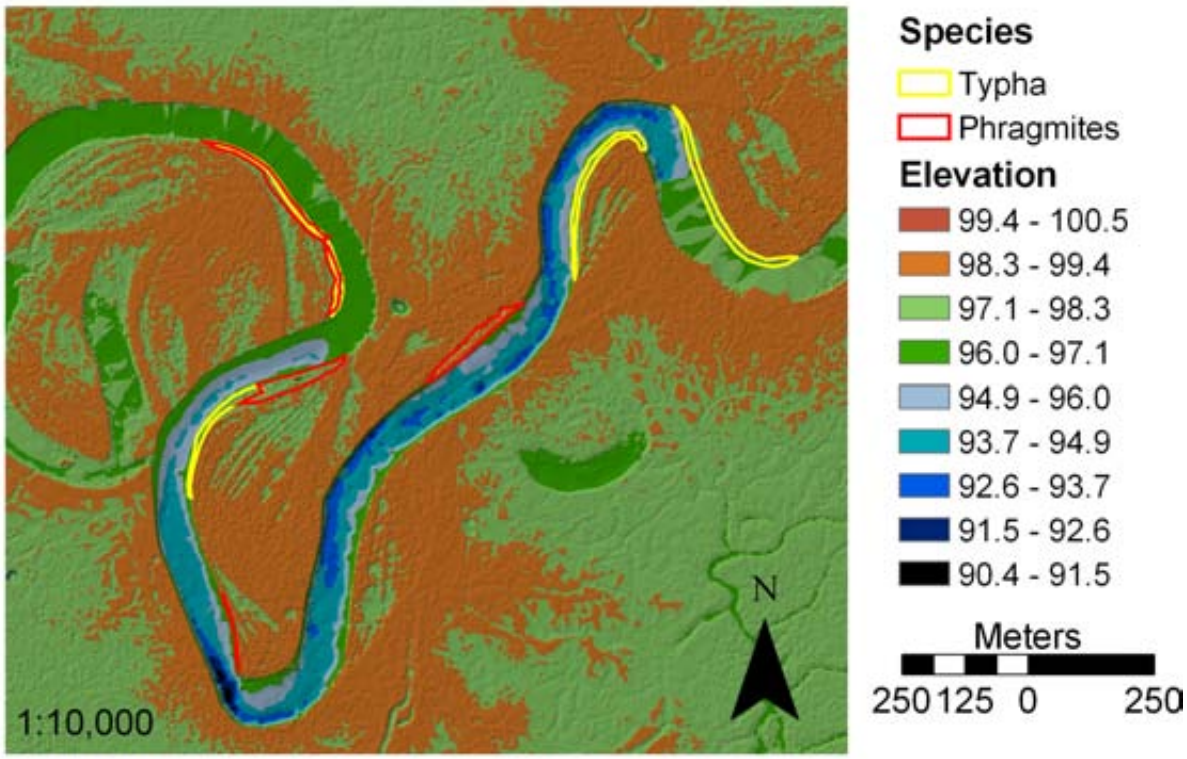

Figure 2.5. GIS map of the Barmah field site showing the locations of *Typha* (yellow bordered regions) and *Phragmites* (red bordered regions) beds. One of the benches used in later assessments of shoot density and litter production (Bench 'B') is marked. The river channel shown is only partly mapped (unmapped sections on either end of the study reach are shaded light and dark green).

Table 2.2 Summary of macrophyte distribution parameters at each site.

		No.	Bed Area (m^2)			Mean	Elevation (m)		
Species	**Site**	**Beds**	**Min**	**Max**	**Total**	**Edge:Area**	**Min**	**Max**	**Range**
Typha	BAR	4	2,690	4,750	13,500	0.21	95.6	99.4	3.8
Phragmites	BAR	4	320	5,450	13,600	0.32	95.8	99.2	3.4
Phragmites	BRO	7	0.74	240	310	3.00	115.3	118.7	3.4
Vallisneria	BRO	7	30	120	480	0.62	115.4	117.2	1.8
Persicaria	OVN	12	177	1,550	6,500	0.47	127.8	130.6	2.8

At the Broken River site, *Phragmites* occurred in seven beds totalling 310 m^2 (ranging from 0.74 – 237 m^2) (Figure 2.6; Table 2.2). The vertical distribution of *Phragmites* at BRO was similar to BAR, covering 3.4 m elevation. At the Broken River site, *Phragmites* distribution was limited to the river channel, to which cattle from neighbouring properties had access at times. The shapes of *Phragmites* beds at BAR and BRO represented extremes of patch type, with mean perimeter to area ratios of beds at BAR of 0.32 (ranging from 0.11 – 0.88) compared to 3.00 (ranging from 0.27 – 5.64) for the long, narrow fringing beds at BRO.

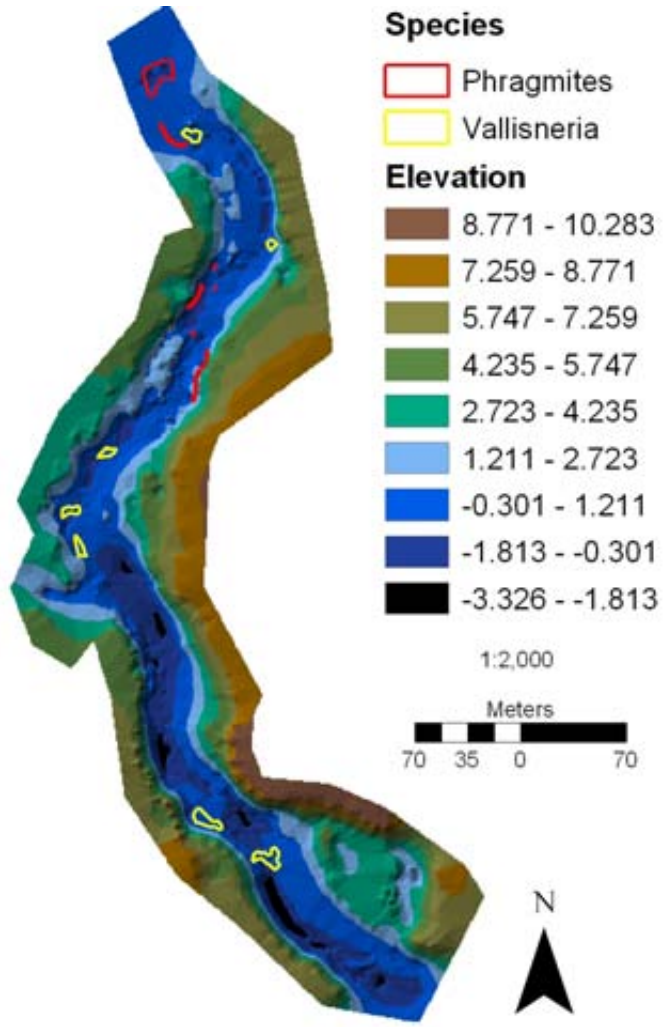

Figure 2.6. GIS map of the Broken River field site showing locations of *Vallisneria* (yellow bordered regions) and *Phragmites* (red bordered regions) beds.

2.3.1.3 Vallisneria

Vallisneria gigantea was present at BRO in seven beds totalling 480 m^2, with bed size ranging from 30 – 123 m^2 (Figure 2.6; Table 2.2). The vertical distribution of *Vallisneria* extended over 1.88 m, while the ratio of perimeter to area averaged across patches was 0.62. All *Vallisneria* beds were associated with the presence of at least one snag, and occurred mostly on the outsides of bends in the channel (i.e. in areas of high current speed).

2.3.1.4 Persicaria

Persicaria prostrata grew extensively at OVN, covering 6,200 m^2 of the 1 km reach (Figure 2.7; Table 2.2). This species formed dense, essentially continuous bands on both banks from the mean low water mark over 2.8 m vertical elevation. *Persicaria prostrata* also occurred at BAR and BRO, however not in sufficient abundance to warrant mapping at these sites. Other species of *Persicaria* (*P. decipiens*, *P. hydropiper*) occurred at all three sites at different times throughout the year in small, but variable, quantities.

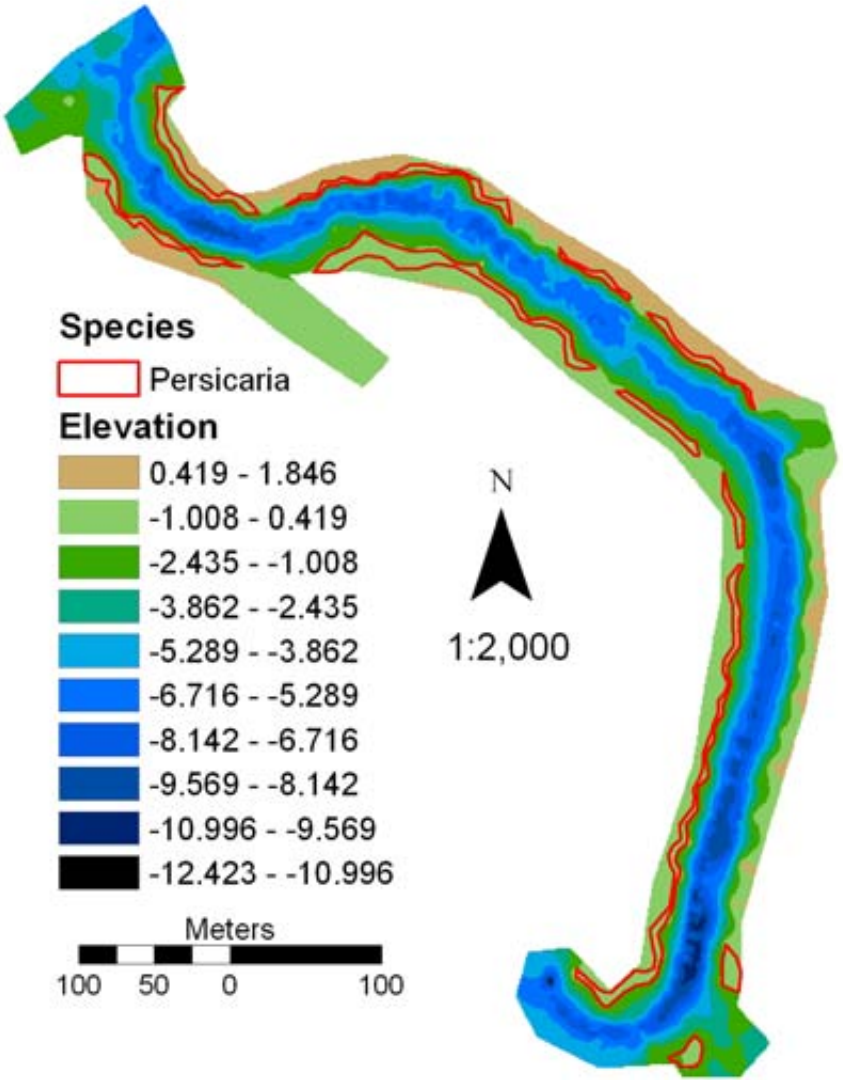

Figure 2.7. GIS map of the Ovens River field site showing locations of *Persicaria* (red bordered regions) beds.

2.3.2 Hydrology

Comparison of data summaries for daily discharge over 4 years (01/01/1999 – 31/12/2002) demonstrates the different flow regime occurring at each site (Figure 2.8). The Murray River at BAR had the highest mean daily discharge over these four years (7300 ML/d), with data point dispersal generally following a Poisson distribution. BRO flows were the lowest of the three sites, with a mean daily discharge of 190 ML/d. Mean daily discharge for the Ovens River site over this time was 3200 ML/d, with a highly skewed distribution of data points towards high flows: the 95th percentile for OVN was higher even than that at BAR despite the much lower mean and median discharge values at OVN.

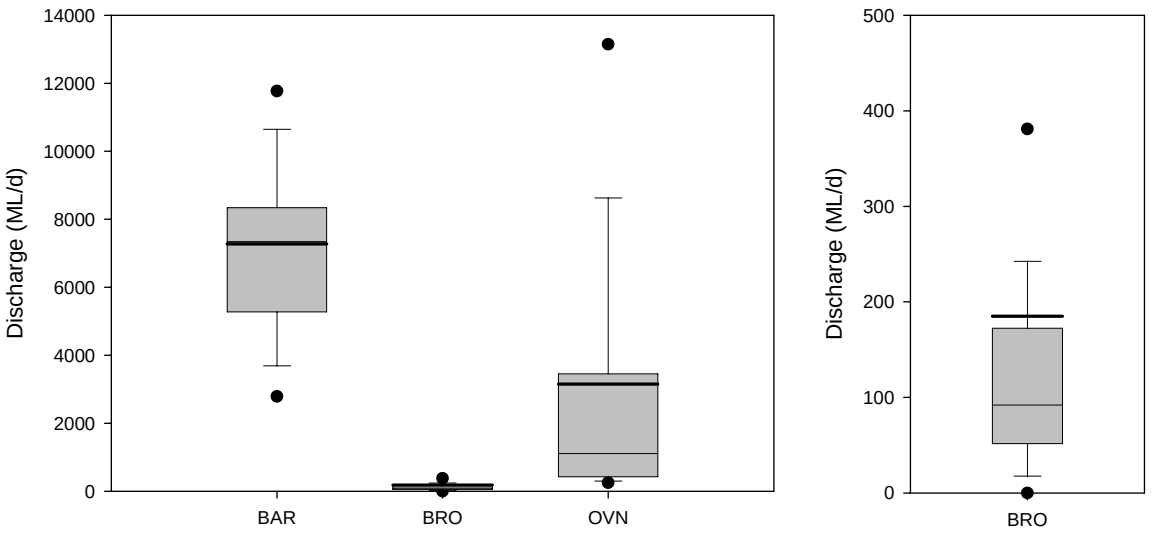

Figure 2.8. Box plots of flow data from each site during the study, with the 'BRO' site also shown separately. Box perimeters bound the 25th and 75th percentile with the 50th percentile (median) marked as a thin line within each box. The thick line in each box represents the mean daily discharge for that site. Whiskers bound the 10th and 90th percentiles and points mark the 5th and 95th percentile.

Regulation of the Murray River for irrigation has resulted in high and relatively steady flows occurring at this site from spring through to mid autumn (Figure 2.9). Levels of variability at BAR are highest from May to January, peaking in October. The maximum discharge recorded from 1998 – 2003 was 23,000 ML/d, while the minimum was 2,000 ML/d.

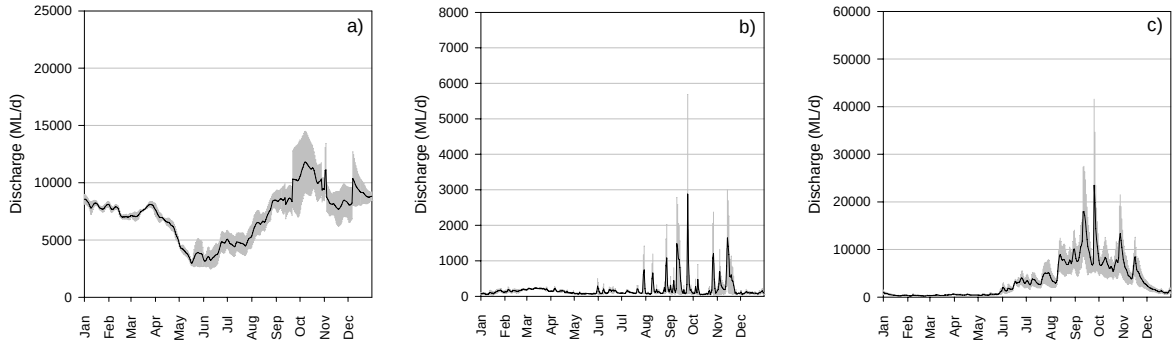

Figure 2.9. Current annual hydrographs of the study sites: a) Murray River at Barmah, b) Broken River at Benalla and c) Ovens River at Peechelba. Black line represents mean discharge calculated over 1998 – 2003 with standard error bars shown in grey.

While the Broken River is also regulated, the study reach is not used to transport irrigation flow releases so no repeated pattern of high, steady discharge occurs at this site (Figure 2.9). Flashy peaks occur from late winter until the start of summer, and while the majority of these peaks are below BAR's mean daily discharge of 7,300 ML/d, large floods do sometimes occur (e.g. 14,000 ML/d in late September, 1998). Daily discharge at this site approaches zero on a regular basis.

The Ovens River is effectively unregulated and so demonstrates a relatively natural discharge pattern (Figure 2.9). Base flows occur throughout summer and autumn (mean discharge of 630 ML/d ranging from 3 to 5,200 ML/d). Discharge increases gradually over winter and flashy peaks occur throughout spring (mean discharge during this period of 6,100 ML/d ranging from 260 to 96,000 ML/d).

For all three sites, the highest flow variability occurred during winter and spring. At BRO and OVN this coincided with periods of highest discharge, with stable, low flows occurring over summer and autumn. Thus, flow at these sites can be broadly classified into four categories:

A. low discharge with low variability (occurs in summer and autumn at BRO and OVN),
B. low discharge with high variability (occurs in winter at BAR),
C. high discharge with high variability (winter and spring – BRO and OVN; spring only – BAR), and
D. high discharge with low variability (occurs at BAR only, in summer and autumn – caused by irrigation flow releases).

To compare flow variability across sites, the coefficient of variation for the period of interest was calculated from daily discharge data. Intra- and inter-annual coefficients of variation were averaged across all data points to produce a single estimate of flow variability within and across years for each site (Table 2.3). Overall, BRO and OVN had greater variability within years than between years, whereas at BAR this trend was reversed. While mean inter-annual CV values for BRO and OVN were similar (0.77 and 0.69, respectively), at BAR this variability metric was halved (0.38). Mean intra-annual variability was also lowest at Barmah, with a mean CV of 0.27 compared to 2.12 at BRO and 1.26 at OVN.

Table 2.3 Flow variability at each site for different time periods assessed using coefficient of variation of the mean calculated from daily discharge data. Means (range).

Time Period	BAR	BRO	OVN
Intra-annual	0.27 (0.02 – 0.71)	2.12 (0.69 – 4.33)	1.26 (1.08 – 1.54)
Inter-annual	0.38 (0.29 – 0.51)	0.77 (0.03 – 2.18)	0.69 (0.19 – 1.72)

Intra-seasonal, inter-seasonal, intra-monthly and inter-monthly variability metrics were calculated separately for each year and then plotted by year (Figure 2.10). The co-efficient of variation of flow at BAR was always lower than at the other two sites. BRO demonstrated the highest degree of variability in CV over the time period assessed. For intra-seasonal and intra-monthly variability, the sites generally ranked BRO > OVN > BAR. However, OVN generally ranked higher than BRO for variability between seasons and months, with BAR again having the

lowest CV values. Although the data only cover 4 years, BRO seems to be following a pattern of alternating troughs and peaks for inter-seasonal and inter-monthly variability, commencing with a trough in 1999. This site displayed a large decrease in 2001 for all measures of CV. Patterns of changes to CV over time at BAR for all time groupings appear to mimic those at OVN somewhat.

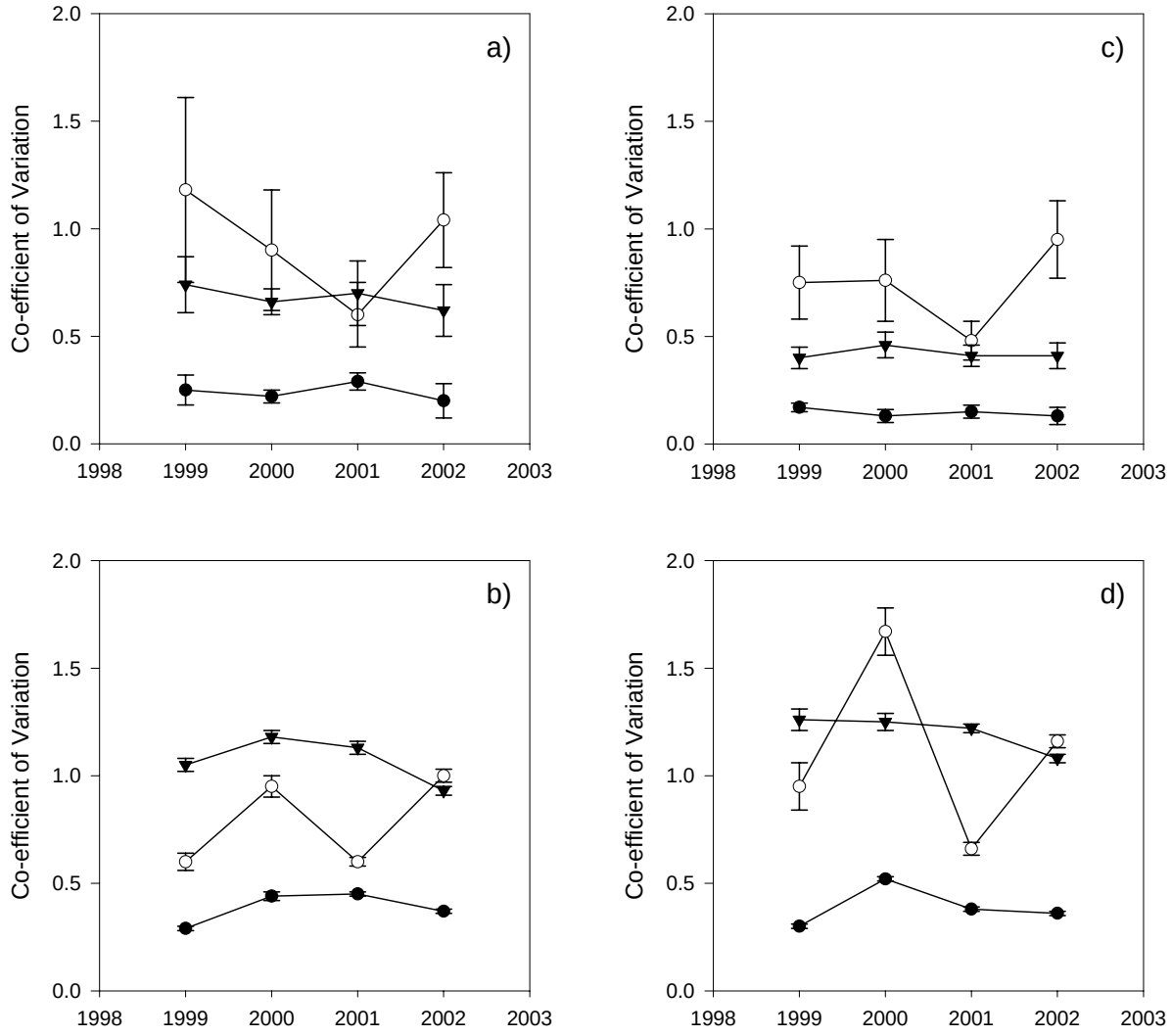

Figure 2.10. Flow variability at the different sites over 1998 – 2003 assessed using coefficient of variation (means ± standard error bars) (● BAR; ○ BRO; ▼ OVN) : a) Intra-seasonal variability; b) Inter-seasonal variability; c) Intra-monthly variability ; d) Inter-monthly variability.

2.3.3 Inundation Functions

Functions describing areas and depths of inundation of macrophyte beds at each site under different discharges were determined (Figures 2.11 – 2.15; all $R^2 > 0.98$, all $p < 0.0001$, n = 23 – 117; Table 2.4).

Table 2.4 Summary of inundation curve equations for each species.

Eqn	Function	Parameters				
1	*Typha Area Inundated (m^2)*	x_0	*a*	*b*		
	$y = \frac{a}{1+\exp^{(-x-x_0)}/b}$	11321	13569	1721		
	R^2 = 0.99; F = 7168; p < 0.0001; n = 23	<0.0001	<0.0001	<0.0001		
2	*Typha Depth Inundated (m)*	*a*	*b*			
	$y = a \cdot \exp^{(b \cdot x)}$	0.0929	0.000137			
	R^2 = 0.98, p < 0.0001, F = 1249, n = 23	<0.0001	<0.0001			
3	*Phragmites Area Inundated (BAR) (m^2)*	x_0	*a*	*b*		
	$y = \frac{a}{1+\exp^{(-x-x_0)}/b}$	12589	13625	1463		
	R^2 = 0.99; F = 36468; p < 0.0001; n = 23	<0.0001	<0.0001	<0.0001		
4	*Phragmites Depth Inundated (BAR) (m)*	x_0	*a*	*b*	*c*	y_0
	y=IF(x-x_0>0, IF(x>6000, y_0+b*x+c*x^2, a*LN(ABS(x-x_0))), 0)	2049	0.0228	-0.00012	7.448e-9	0.6483
	R^2 = 0.99; F = 1230; p < 0.0001; n = 23	<0.0001	<0.0001	<0.0001	<0.0001	<0.0001
5	*Phragmites Area Inundated (BRO) (m^2)*	x_0	*a*	*b*		
	y = IF(x-x_0>0, a*(1-exp(-b*(x-x_0))),0)	4.12	295.21	0.0508		
	R^2 = 0.98, p < 0.0001, F = 2503, n = 85	<0.0001	<0.0001	<0.0001		
6	*Phragmites Depth Inundated (BRO) (m)*	*a*	*b*			
	y = a.x^b	0.0419	0.5175			
	R^2 = 0.99, p < 0.0001, F = 160055, n = 85	<0.0001	<0.0001			
7	*Vallisneria Area Inundated (m^2)*	x_0	*a*	*b*		
	$y = \frac{a}{1+\exp^{(-x-x_0)}/b}$	61.80	477.78	14.26		
	R^2 = 0.99, p < 0.0001, F = 66421, n = 117	<0.0001	<0.0001	<0.0001		
8	*Vallisneria Depth Inundated (m)*	x_0	*a*	*b*	*c*	y_0
	y = IF(x-x_0>1, IF(x-x_0>60, y_0+b*x^c, a*LN(ABS(x-x_0))), 0)	4.74	0.0372	0.0246	0.5878	-0.2249
	R^2 = 0.99, p < 0.0001, F = 25848, n = 106	<0.0001	<0.0001	<0.0001	<0.0001	<0.0001
9	*Persicaria Area Inundated (m^2)*	x_0	*a*	*b*		
	y=IF(x-x_0>0, a*(1-exp(-b*(x-x_0))),0)	3210	6483	0.0004		
	R^2 = 0.99, p < 0.0001, F = 19859, n = 31	<0.0001	<0.0001	<0.0001		
10	*Persicaria Depth Inundated (m)*	x_0	x_1	*a*	y_0	
	y=IF(x-x_0>0, IF(x-x_0-x_1>0, y_0+b*LN(ABS(x-x_0+x_1)), 0.1), 0)	1385	2980	0.9734	-8.377	
	R^2 = 0.99; p < 0.0001, F = 3,970, n = 31	<0.0001	<0.0001	<0.0001	<0.0001	

2.3.3.1 Typha

Inundation of the benches supporting *Typha* at BAR commenced at a discharge of 3450 ML/d, equivalent to a gauge height of 1.6 m at the Barmah gauge, with 0.25 m^2 of bed area inundated at this water level (Figure 2.11). Fifty percent of the total bed area was inundated at a discharge of 11,000 ML/d, but because of the morphology of the in-channel benches, flood-runners and the channel itself, total *Typha* bed area inundation occurred only after floodplain inundation had commenced, at a discharge of 22,000 ML/d.

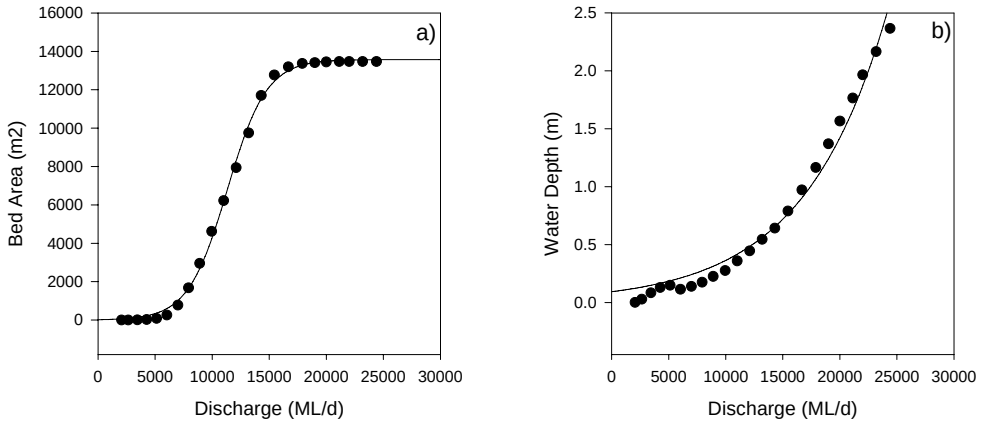

Figure 2.11. Inundation of *Typha* at BAR: a) bed area inundated at different discharges; b) mean water depth over macrophyte beds at different discharges. Points are modelled data and lines are fitted curves.

2.3.3.2 Phragmites

Inundation curves for *Phragmites* at BAR were quite similar to those for *Typha*, due to the similar bed areas and vertical distributions of these species (Figure 2.12). Inundation of *Phragmites* beds at Barmah commenced at a gauge height of 1.4 m and discharge of 2650 ML/d, with an average of 8 cm of water overlying beds (Figure 2.12). Total bed immersion again occurred after banks had been breached, at a discharge of 22,000 ML/d.

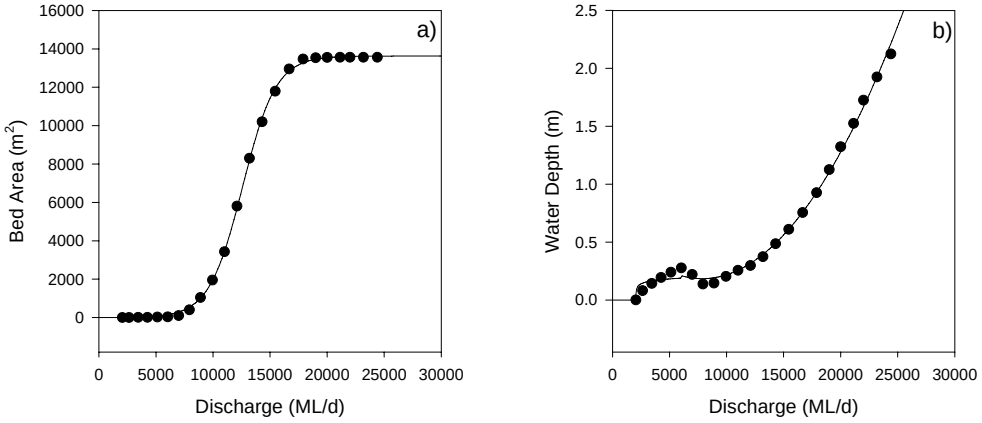

Figure 2.12. Inundation of *Phragmites* at BAR: a) bed area inundated at different discharges; b) mean water depth over beds at different discharges. Points are modelled data and lines are fitted curves.

Inundation curves for *Phragmites* at BRO were quite different to those at BAR. Bed area inundated rose exponentially to a maximum after breaching an initial discharge threshold of 5.5 ML/d (Figure 2.13 a). Above this discharge, the rate of inundation initially increased much more rapidly than at BAR but then slowed and required a relatively high discharge (3000 ML/d) to fully inundate the beds, although 95% of the total bed area was inundated at a discharge of 100 ML/d (Figure 2.13 a). In contrast to patterns of bed area inundation, the relationship between water depth overlying *Phragmites* beds at BRO followed a power curve rather than an exponential curve as at BAR (Figure 2.13 b).

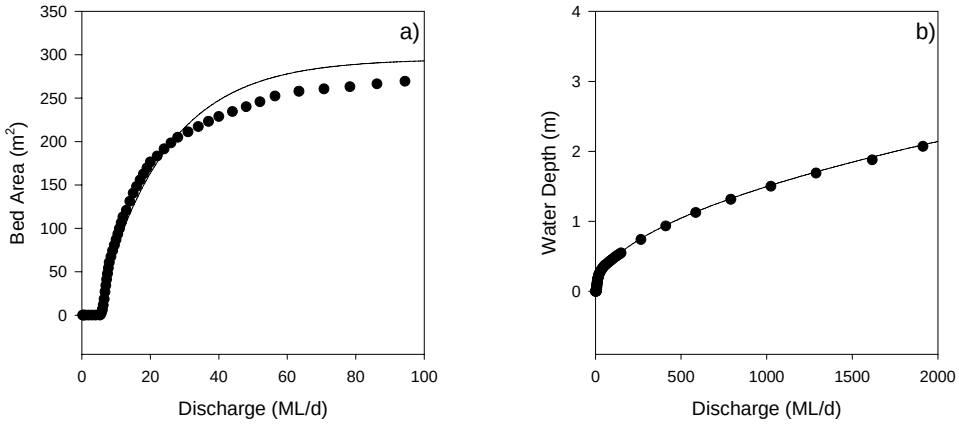

Figure 2.13. Inundation of *Phragmites* at BRO: a) bed area inundated at different discharges; b) mean water depth over beds at different discharges. Points are modelled data and lines are fitted curves.

2.3.3.3 Vallisneria

Inundation modelling of *Vallisneria* revealed total bed area immersion at a discharge of 975 ML/d, although the inundation curve started to plateau at approximately 150 ML/d (Figure 2.14 a). Bed immersion commenced at 6.8 ML/d. Water depth over beds required the development of an equation with different rates of change in water depth for specific ranges of discharge, to accommodate initial small changes in depths over beds which were considered important (Figure 2.14 b).

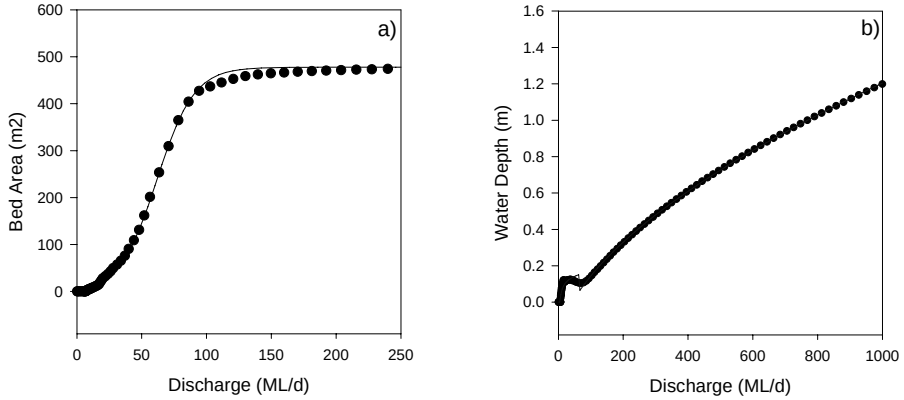

Figure 2.14. Inundation of *Vallisneria* at BRO: a) bed area inundated at different discharges; b) mean water depth over beds at different discharges. Points are modelled data and lines are fitted curves.

2.3.3.4 Persicaria

Functions describing *Persicaria* inundation patterns at the Ovens River site had high initial discharge thresholds due to the higher elevation at which this species grows at this site (Figure 2.15). Inundation of *Persicaria* commenced at 1,600 ML/d (10 cm water depths over beds) and plateaued at 22,000 ML/d.

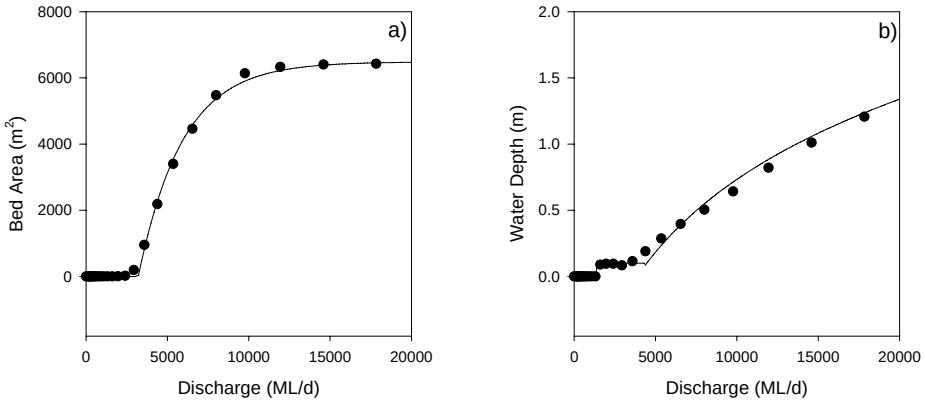

Figure 2.15. Inundation of *Persicaria* at OVN: a) bed area inundated at different discharges; b) mean water depth over beds at different discharges. Points are modelled data and lines are fitted curves.

2.3.4 Hydrological Modelling

Hydrographs representing different flow regimes (current flows, historical flows, drought conditions and floods) were utilised to model macrophyte inundation under different scenarios (Figures 2.16 – 2.35, Table 2.5). Modelling used current macrophyte distributions and channel morphology, although these could well change if a particular flow regime was maintained for many years. Under most of the scenarios, Type A flows (low discharges with low variability) predominated during the summer/autumn period, although Type B flows (low discharges with high variability) occurred at BAR historically at this time of year (Table 2.5). While Type C

flows (high discharges with high variability) occurred in winter/spring under most flow scenarios, Type B flows occurred during droughts at BRO and OVN. The only instance of Type D flows (high discharge with low variability), which are currently associated with irrigation releases at BAR during summer/autumn, occurred at BAR under the historic flow scenario (Table 2.5).

Table 2.5 Summary of flow conditions under the modelled flow scenarios.

Site	Scenario	Summer/Autumn			Winter/Spring		
		Discharge (ML/d)	Variability	Flow Type	Discharge (ML/d)	Variability	Flow Type
BAR	Current	High (12000)	Low	D	Low (3000)	High	B
	Historic	Low (4500)	High	B	High (13000)	Low	D
	Drought	Low (0)	Low	A	High (10000)	High	C
	Flood	Low (7000)	Low	A	High (16000)	High	C
BRO	Current	Low (50)	Low	A	3000	High	C
	Historic	Low (50)	Low	A	High (4500)	High	C
	Drought	Low (0)	Low	A	Low (350)	High	B
	Flood	Low (0)	Low	A	High (26000)	High	C
OVN	Current	Low (250)	Low	A	21000	High	C
	Historic	Low (500)	Low	A	High (16000)	High	C
	Drought	Low (200)	Low	A	Low (2800)	High	B
	Flood	Low (750)	Low	A	High (46000)	High	C

Until very recently, floodplain inundation almost never occurred at BAR or BRO under management for summer irrigation (flooding thresholds of 12,000 and 8,000 ML/d, respectively). In contrast, the Ovens River site still experiences flooding on 78 days in the year, with flashy peaks occurring from late July, and persistent floodplain inundation from early August to late November (flooding threshold of 6,930 ML/d). While the Broken River site was not flooded under modelled historic flows, the BAR site would have been flooded on 68 days in the year, from late August to late October. Historically, persistent floodplain inundation would have occurred from early June to late October at OVN. Under modelled drought conditions, none of the study sites would have flooded, whereas all sites experienced flooding under the floods scenario – with either peaky (BRO) or persistent (BAR and OVN) floodplain inundation from early June to mid-November (30, 116 and 159 days inundated, respectively).

2.3.4.1 Current Flow Regimes

Macrophyte inundation curves were applied to the mean annual hydrograph from the last 5 – 10 years for each site to determine areas and depths of macrophyte inundation in an 'average' year under current flow management (Table 2.6). Under the current flow regime, *Typha* beds at BAR were never fully exposed (minimum bed area covered is 105 m^2) (Figure 2.16), but only about half of the entire bed area (13,500 m^2) of *Typha* was ever inundated (for 9 days). Mean water depth over the beds ranged from 14 to 47 cm, with a mean of 26 cm.

Table 2.6 Summary of macrophyte inundation modelling under current flow conditions.

Species	Fully exposed (# days)	Min Bed area wetted (m^2)	Fully inundated (# days)	Max bed area wetted (m^2)	Water depth min (m)	Water Depth max (m)	Water depth mean (m)
Typha	0	105	0	7740	0.14	0.47	0.26
Phragmites (BAR)	0	20	0	5040	0.16	0.27	0.18
Phragmites (BRO)	0	266	197	310	0.29	2.58	0.58
Vallisneria	0	98	134	480	0.06	2.43	0.28
Persicaria	216	0	1	6500	0.00	0.44**	0.20

** = maximum water depth overlying beds before banks are breached and overbank flows occur

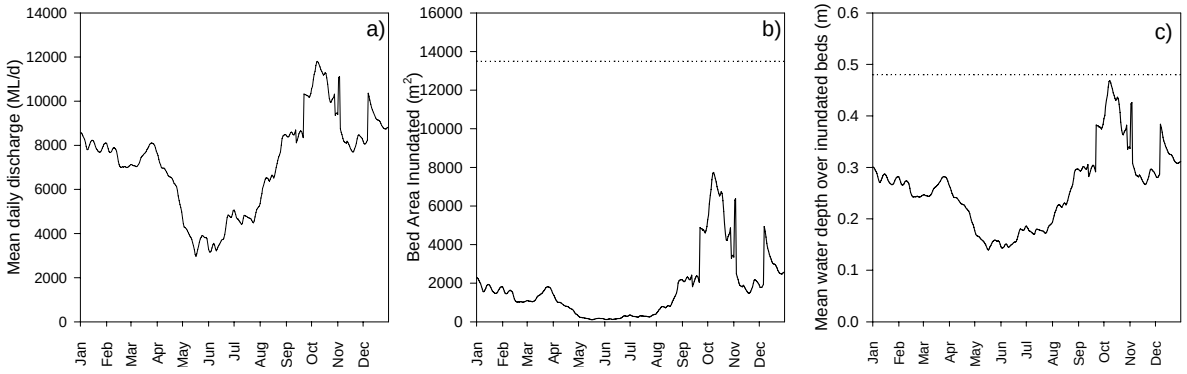

Figure 2.16. Modelled macrophyte inundation under current flow conditions – *Typha* at BAR: a) mean daily discharge; b) bed area inundated (dotted line indicates total bed area); c) mean water depth over inundated macrophyte beds (dotted line indicates maximum depth prediction limit prior to overbank flows).

At BAR, patterns of *Phragmites* inundation under current flows were quite similar to those for *Typha* (Figure 2.17). Nearly two-thirds of the total bed area was exposed for the entire year. In contrast, the majority of *Phragmites* beds at BRO were constantly inundated in this scenario (Figure 2.18). The minimum water depth over *Phragmites* beds was 16 cm at BAR and 29 cm at BRO. At times *Phragmites* beds at BRO were covered by as much as 2.58 m of water compared to a maximum mean water depth of just 0.27 m at BAR.

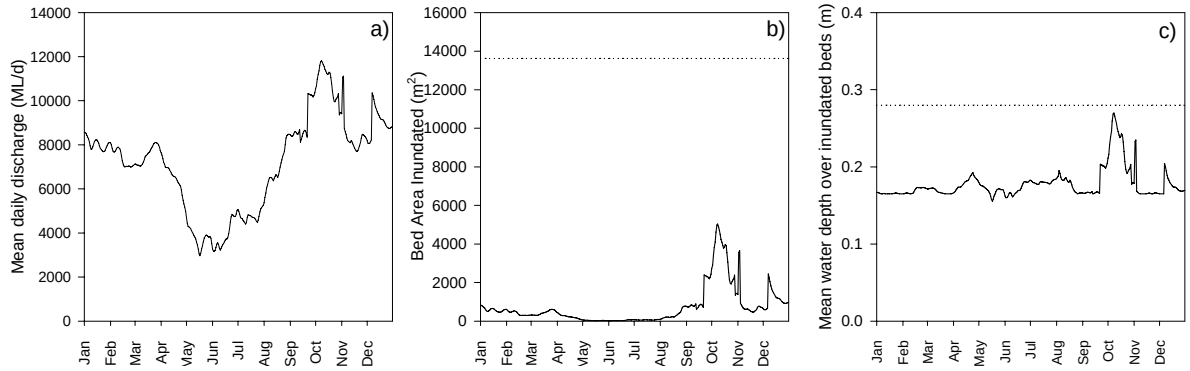

Figure 2.17. Modelled macrophyte inundation under current flow conditions – *Phragmites* at BAR: a) mean daily discharge; b) bed area inundated (dotted line indicates total bed area); c) mean water depth over inundated macrophyte beds (dotted line indicates maximum depth prediction limit prior to overbank flows).

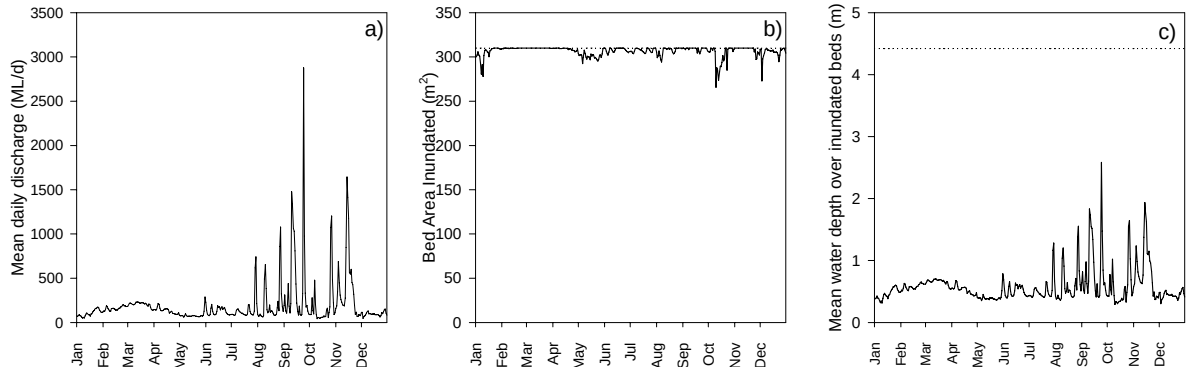

Figure 2.18. Modelled macrophyte inundation under current flow conditions – *Phragmites* at BRO: a) mean daily discharge; b) bed area inundated (dotted line indicates total bed area); c) mean water depth over inundated macrophyte beds (dotted line indicates maximum depth prediction limit prior to overbank flows).

As with *Phragmites*, much of the *Vallisneria* bed area at BRO was inundated for extended periods under current management. Water depth over the beds ranged from 0.06 – 2.43 m, however for 90% of the time water depth was less than 0.5 m (Figure 2.19).

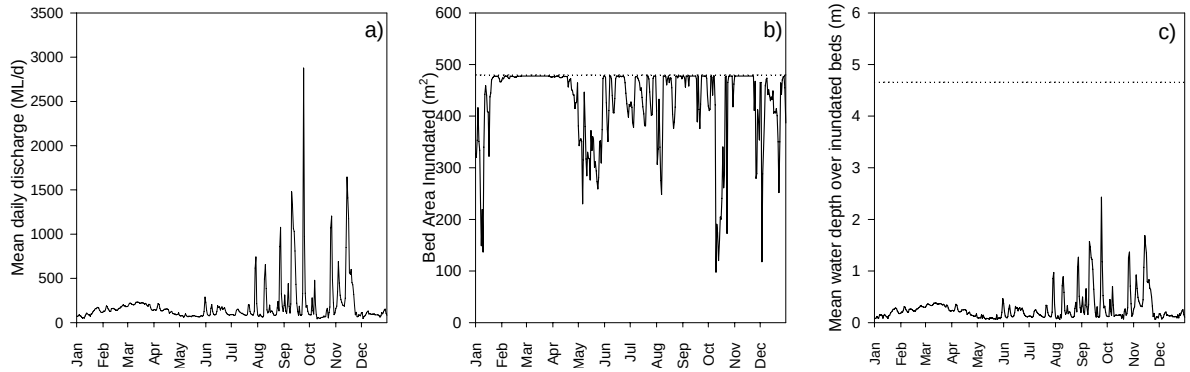

Figure 2.19. Modelled macrophyte inundation under current flow conditions – *Vallisneria* at BRO: a) mean daily discharge; b) bed area inundated (dotted line indicates total bed area); c) mean water depth over inundated macrophyte beds (dotted line indicates maximum depth prediction limit prior to overbank flows).

The tendency for annual flooding at the Ovens River site means that substantial bed inundation still occurs in most years (over 90% of the total bed area was wetted for 54 days in the year under modelled current flows) (Figure 2.20 a). The major period of inundation extended from early August to late November and contrasted with the absence of substantial macrophyte inundation at the heavily regulated BAR site under current flows. Due to floodplain inundation, the maximum water depth over *Persicaria* beds under this scenario was not able to be predicted, however it would have been at least 0.44 m (Figure 2.20 b).

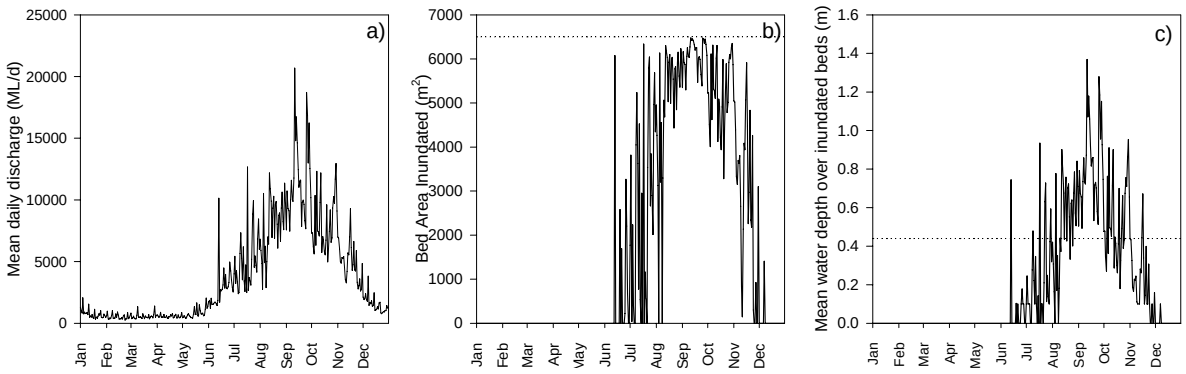

Figure 2.20. Modelled macrophyte inundation under current flow conditions – *Persicaria* at OVN: a) mean daily discharge; b) bed area inundated (dotted line indicates total bed area); c) mean water depth over inundated macrophyte beds (dotted line indicates maximum depth prediction limit prior to overbank flows).

2.3.4.2 Historical Flow Regimes

Modelling of flow conditions prior to river regulation at the Murray River site resulted in immersion of over half the total *Typha* bed area from late July to early November (Figure 2.21; Table 2.7), an inundation period of 102 days compared to 9 days under current flow management. Water depth over the beds was at least 0.44 m during this time. Complete exposure of *Typha* beds at this site did not occur in this scenario – there was always at least 0.17 m water overlying a small proportion of the total bed area (240 m^2).

Table 2.7 Summary of macrophyte inundation modelling under historic flow conditions.

Species	Fully exposed (# days)	Min Bed area wetted (m^2)	Fully inundated (# days)	Max bed area wetted (m^2)	Water depth min (m)	Water Depth max (m)	Water depth mean (m)
Typha	0	240	0	9480	0.17	0.48**	0.33
Phragmites (BAR)	0	50	0	7230	0.16	0.28**	0.21
Phragmites (BRO)	0	200	254	310	0.22	3.22	1.3
Vallisneria	0	32	236	480	0.06	3.18	1.05
Persicaria	163	0	0	6500	0.00	0.44**	0.34

** = maximum water depth overlying beds before banks are breached and overbank flows occur

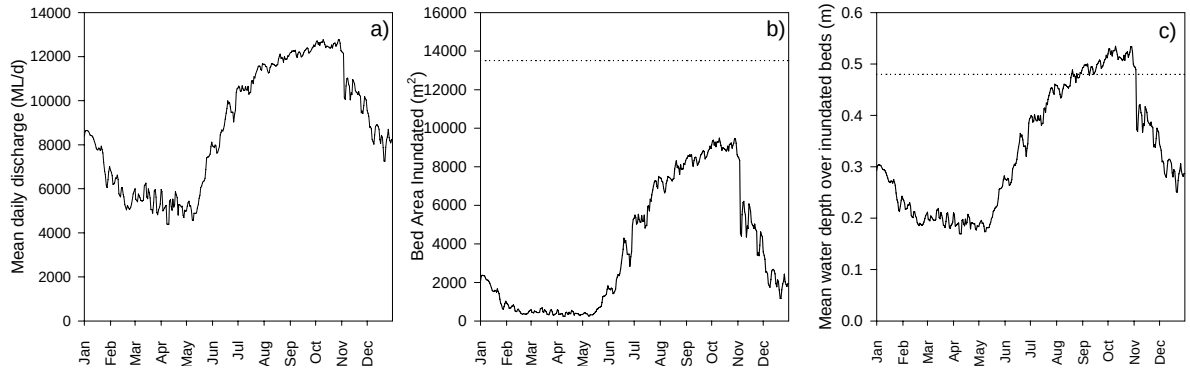

Figure 2.21. Modelled macrophyte inundation under historical flow conditions – *Typha* at BAR: a) mean daily discharge; b) bed area inundated (dotted line indicates total bed area); c) mean water depth over inundated macrophyte beds (dotted line indicates maximum depth prediction limit prior to overbank flows).

Again, the pattern for *Phragmites* at BAR was similar to that for *Typha*, with a greater period of substantial bed area inundation compared to current flows (50% of total bed area wetted for 14 days in the year compared to 0 days under current flows) and some bed area always immersed even during the low flow period (0.16 m water depth over 50 m^2 of macrophyte bed) (Figure 2.22).

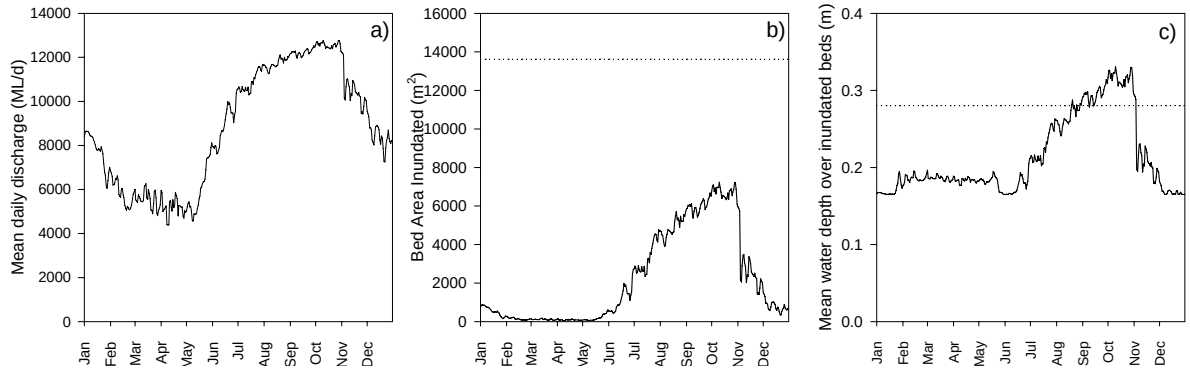

Figure 2.22. Modelled macrophyte inundation under historical flow conditions– *Phragmites* at BAR: a) mean daily discharge; b) bed area inundated (dotted line indicates total bed area); c) mean water depth over inundated macrophyte beds (dotted line indicates maximum depth prediction limit prior to overbank flows).

Historically, *Phragmites* beds at BRO would have been totally inundated for much of the year, with no periods of total bed exposure (Figure 2.23 a; Table 2.7). Similarly, complete immersion of *Vallisneria* beds at BRO would have occurred over 8 months of the year under this scenario (Figure 2.23 a; Table 2.7). While variable flows in summer would have caused repeated wetting and drying of many *Vallisneria* beds, a minimum bed area of 32 m^2 was always inundated, and at least 50% of the total bed area was inundated for 326 days in the year (Figure 2.24 a). The high flow period at BRO historically was also a period of high variability. Water depths over both *Phragmites* and *Vallisneria* beds varied by as much as 2 m over a few days (Figures 2.23 b and 2.24 b).

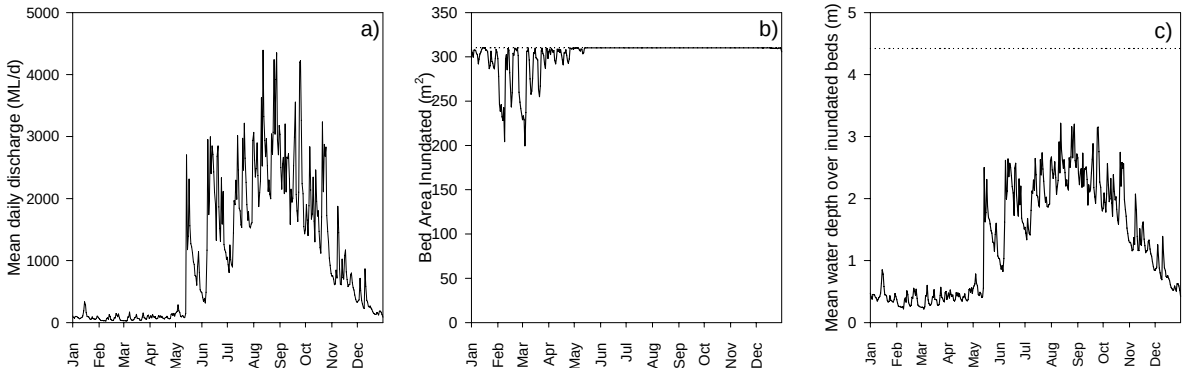

Figure 2.23. Modelled macrophyte inundation under historical flow conditions – *Phragmites* at BRO: a) mean daily discharge; b) bed area inundated (dotted line indicates total bed area); c) mean water depth over inundated macrophyte beds (dotted line indicates maximum depth prediction limit prior overbank flows).

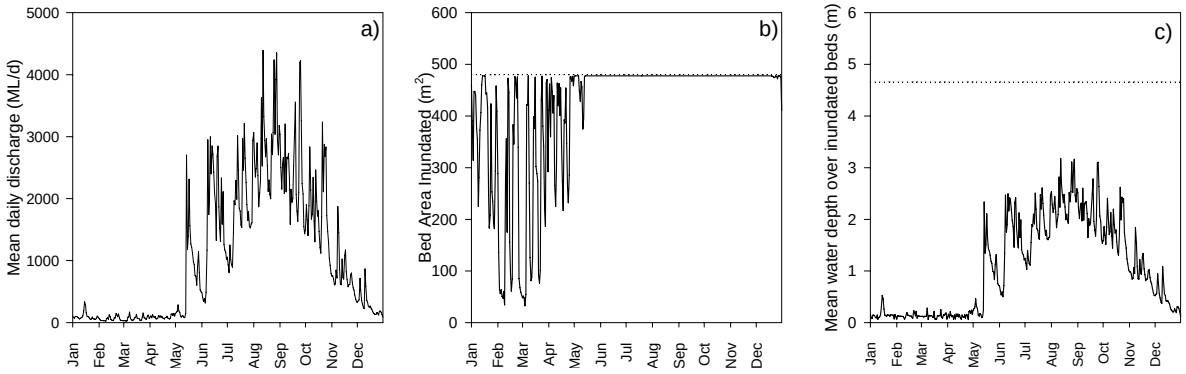

Figure 2.24. Modelled macrophyte inundation under historical flow conditions – *Vallisneria* at BRO: a) mean daily discharge; b) bed area inundated (dotted line indicates total bed area); c) mean water depth over inundated macrophyte beds (dotted line indicates maximum depth prediction limit prior to overbank flows).

Because of the limited degree of regulation of the Ovens River, historical flow conditions would not have been that dissimilar to current, although peak flow would have occurred slightly earlier in the year. The frequency of total bed exposure (163 days in the year) was lower, and the period of substantial bed inundation (> 90% of total bed area wetted for 114 days in the year) was much higher under this scenario than under current flow conditions (Figure 2.25, Table 2.7). Floodplain inundation would have occurred at the Ovens River site under this scenario.

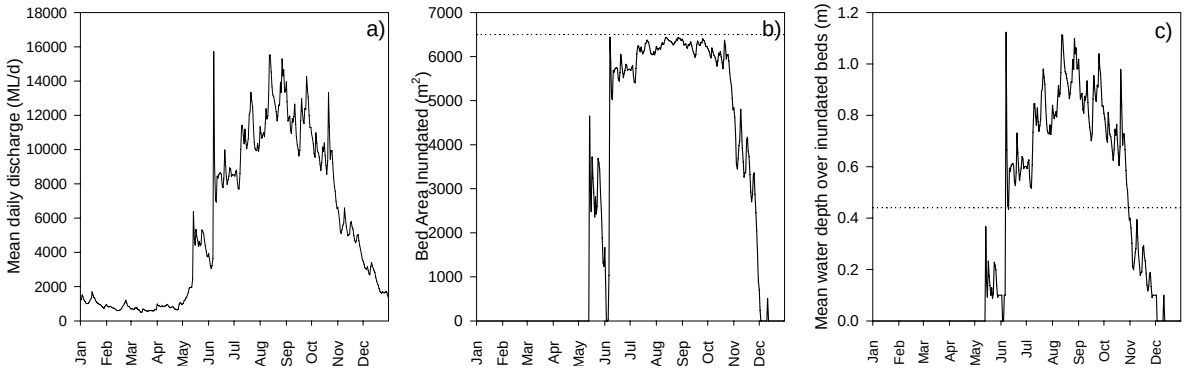

Figure 2.25. Modelled macrophyte inundation under historical flow conditions – *Persicaria* at OVN: a) mean daily discharge; b) bed area inundated (dotted line indicates total bed area); c) mean water depth over inundated macrophyte beds (dotted line indicates maximum depth prediction limit prior to overbank flows).

2.3.4.3 Drought Conditions

Simulated drought conditions resulted in total exposure of all macrophyte beds at all sites for at least 49 days in the year, except for *Typha* at BAR (Figures 2.26 – 2.30; Table 2.8).

Table 2.8 Summary of macrophyte inundation modelling under drought conditions.

Species	Fully exposed (# days)	Min Bed area wetted (m^2)	Fully inundated (# days)	Max bed area wetted (m^2)	Water depth min (m)	Water Depth max (m)	Water depth mean (m)
Typha	0	20	0	4550	0.09	0.37	0.21
Phragmites (BAR)	126	0	0	2160	0.00	0.20	0.11
Phragmites (BRO)	49	0	0	309	0	0.84	0.23
Vallisneria	55	0	10	480	0.00	0.51	0.09
Persicaria	365	0	0	0	0.00	0.00	0.00

At BAR, only one-third of the total *Typha* bed area, and 15% of total *Phragmites* bed area, was ever inundated under drought conditions, with maximum water depths overlying beds of 37 and 20 cm, respectively (Figures 2.26 and 2.27). While some *Typha* bed area was always inundated under this scenario (20 m^2), the vast majority was exposed from early January to mid May (< 100 m^2 inundated) (Figure 2.26). *Phragmites* beds at BAR were totally exposed for 126 days in the year.

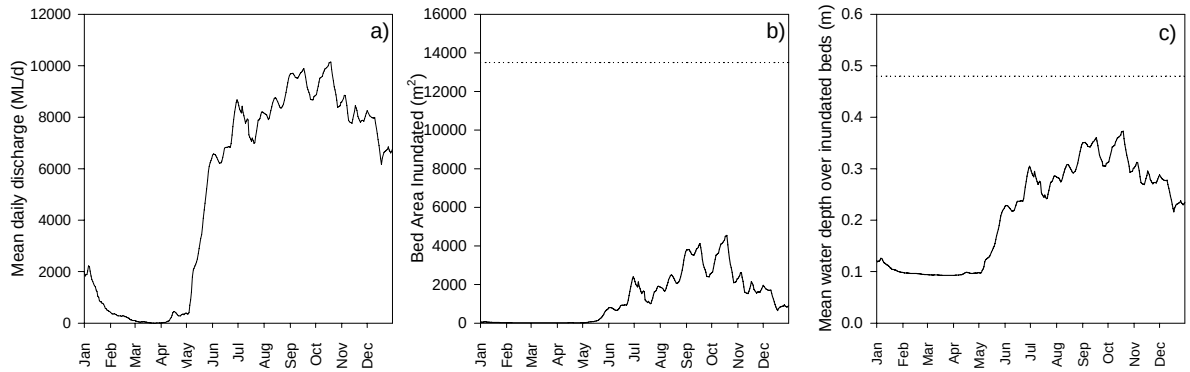

Figure 2.26. Modelled macrophyte inundation under drought conditions – *Typha* at BAR: a) mean daily discharge; b) bed area inundated (dotted line indicates total bed area); c) mean water depth over inundated macrophyte beds (dotted line indicates maximum depth prediction limit prior to overbank flows).

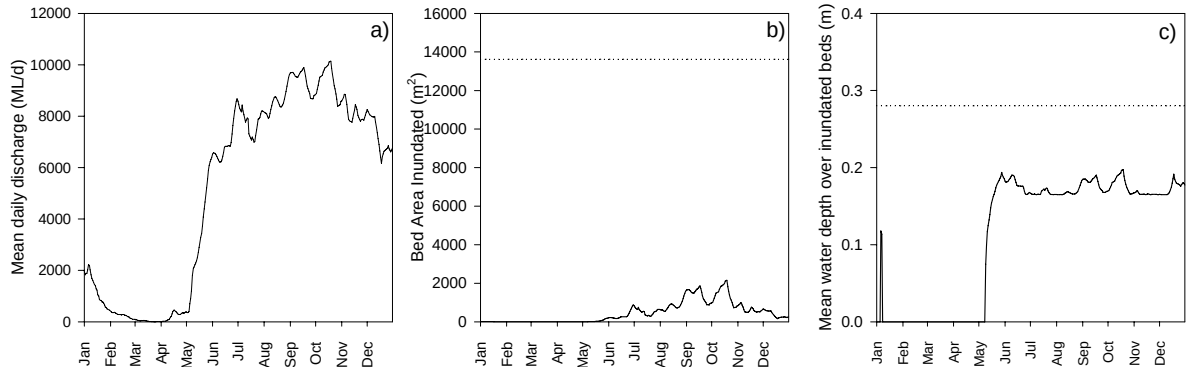

Figure 2.27. Modelled macrophyte inundation under drought conditions – *Phragmites* at BAR: a) mean daily discharge; b) bed area inundated (dotted line indicates total bed area); c) mean water depth over inundated macrophyte beds (dotted line indicates maximum depth prediction limit prior to overbank flows).

Total inundation of macrophyte beds occurred only at BRO, with *Vallisneria* beds fully inundated for 10 days (Figure 2.29). Both *Phragmites* and *Vallisneria* at BRO experienced complete exposure on numerous occasions under this scenario– 49 days for *Phragmites* and 55 days for *Vallisneria* (Table 2.8). While flows at BRO under this scenario were again quite variable, the greatest short-term change in depth was limited to 30 cm, with maximum depths overlying *Phragmites* and *Vallisneria* beds of 84 and 51 cm, respectively (Figures 2.28 and 2.29). *Persicaria* beds at the Ovens River site were totally exposed for the entire year under this flow scenario (Figure 2.30; Table 2.8).

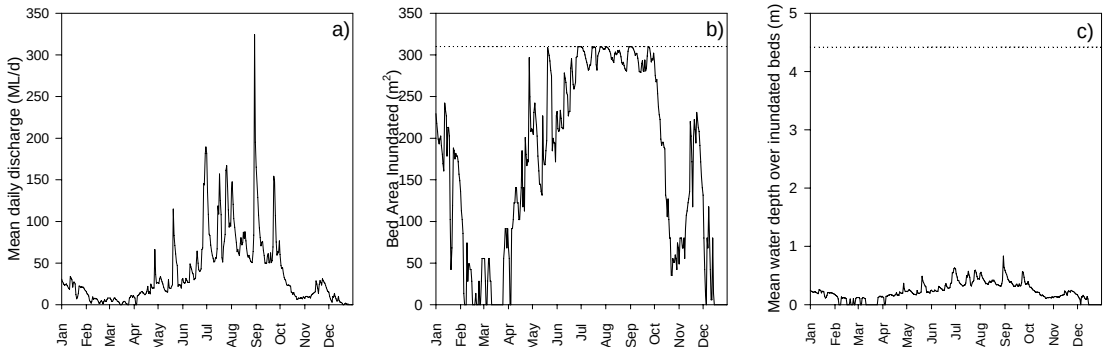

Figure 2.28. Modelled macrophyte inundation under drought conditions – *Phragmites* at BRO: a) mean daily discharge; b) bed area inundated (dotted line indicates total bed area); c) mean water depth over inundated macrophyte beds (dotted line indicates maximum depth prediction limit prior to overbank flows).

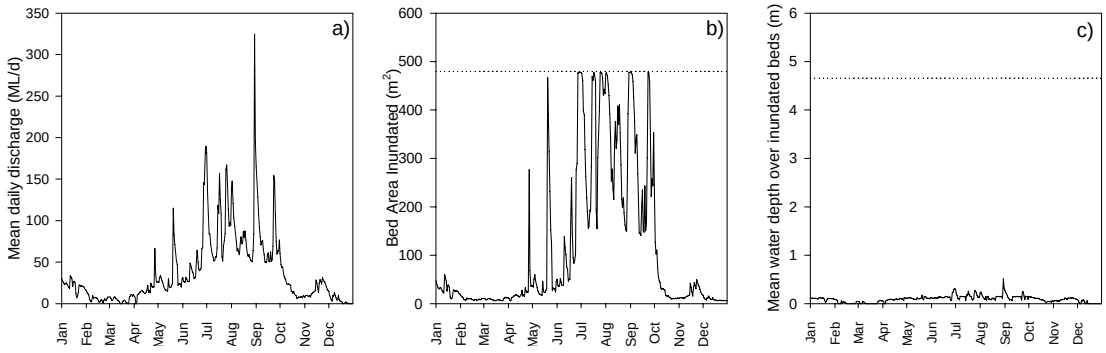

Figure 2.29. Modelled macrophyte inundation under drought conditions – *Vallisneria* at BRO: a) mean daily discharge; b) bed area inundated (dotted line indicates total bed area); c) mean water depth over inundated macrophyte beds (dotted line indicates maximum depth prediction limit prior to overbank flows).

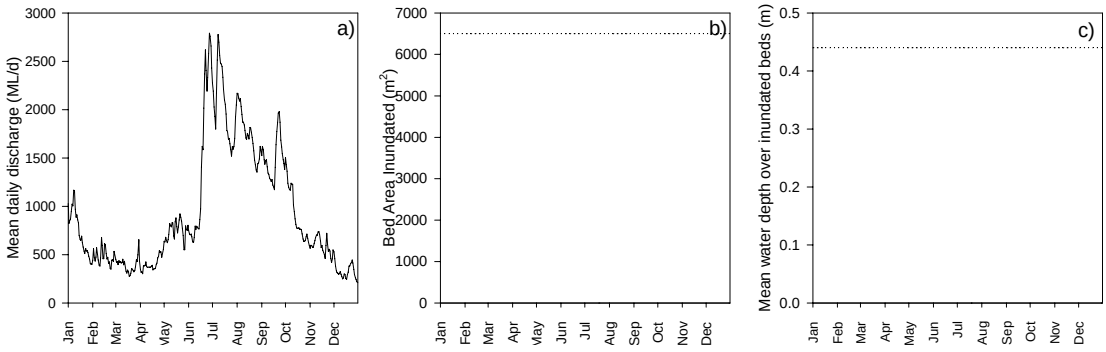

Figure 2.30. Modelled macrophyte inundation under drought conditions – *Persicaria* at OVN: a) mean daily discharge; b) bed area inundated (dotted line indicates total bed area); c) mean water depth over inundated macrophyte beds (dotted line indicates maximum depth prediction limit prior to overbank flows).

2.3.4.4 Floods

During flood years at BAR, *Typha* beds would never have been fully exposed, with at least 20 m^2 of bed area inundated at all times (Figure 2.31; Table 2.9). While flows during an "average" flood year were still too low to fully inundate all *Typha* beds, more than half of the total bed area would have been inundated on 183 days in the year. *Phragmites* beds at BAR were never fully inundated or exposed under this scenario, although over half of the total bed area was wetted on 73 days in the year (Figure 2.32). Predictions of maximum water depths over inundated *Typha* and *Phragmites* beds at BAR were limited, due to floodplain inundation, to being at least 0.48 and 0.28 m, respectively (Table 2.9).

Table 2.9 Summary of macrophyte inundation modelling under flood conditions.

Species	Fully exposed (# days)	Min Bed area wetted (m^2)	Fully inundated (# days)	Max bed area wetted (m^2)	Water depth min (m)	Water Depth max (m)	Water depth mean (m)
Typha	0	20	0	12580	0.09	0.48b	0.43
Phragmites (BAR)	0	0	0	12170	0.00	0.28b	0.25
Phragmites (BRO)	24	0	258	310	0	4.42b	1.89
Vallisneria	31	0	249	480	0.00	4.66b	1.80
Persicaria	163	0	0	6500	0.00	0.44b	0.52

** = maximum water depth overlying beds before banks are breached and overbank flows occur

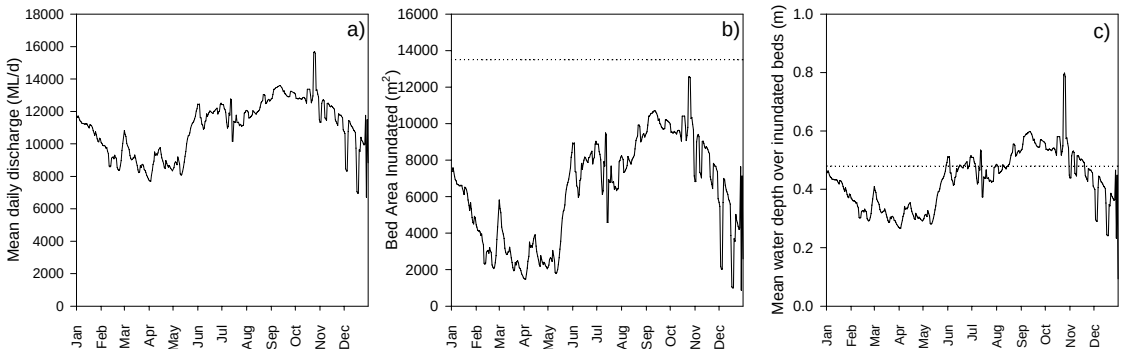

Figure 2.31. Modelled macrophyte inundation during floods – *Typha* at BAR: a) mean daily discharge; b) bed area inundated (dotted line indicates total bed area); c) mean water depth over inundated macrophyte beds (dotted line indicates maximum depth prediction limit prior to overbank flows).

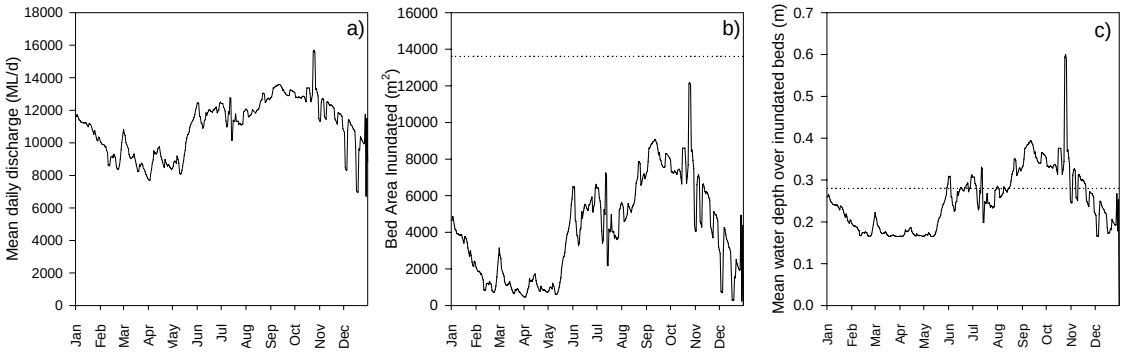

Figure 2.32. Modelled macrophyte inundation during floods – *Phragmites* at BAR: a) mean daily discharge; b) bed area inundated (dotted line indicates total bed area); c) mean water depth over inundated macrophyte beds (dotted line indicates maximum depth prediction limit prior to overbank flows).

Phragmites and *Vallisneria* beds at BRO experienced similar degrees of total exposure (24 and 31 days, respectively) and total inundation (258 and 249 days, respectively) under the flood scenario (Figures 2.33 and 2.34; Table 2.9). The channel shape and vertical distributions of these species at this site resulted in great depths of water overlying beds during floods – over 4 m prior to flows breaching the banks. During an "average" flood year at the Ovens River site, *Persicaria* beds would be fully exposed for 163 days (Figure 2.35; Table 2.9). While complete bed inundation did not occur under this scenario, 90% of the total bed area was wetted for 145 days in the year.

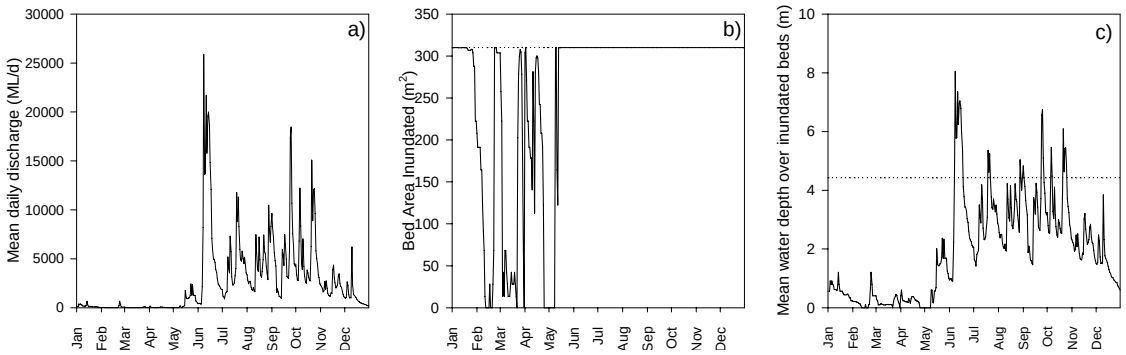

Figure 2.33. Modelled macrophyte inundation during floods – *Phragmites* at BRO: a) mean daily discharge; b) bed area inundated (dotted line indicates total bed area); c) mean water depth over inundated macrophyte beds (dotted line indicates maximum depth prediction limit prior to overbank flows).

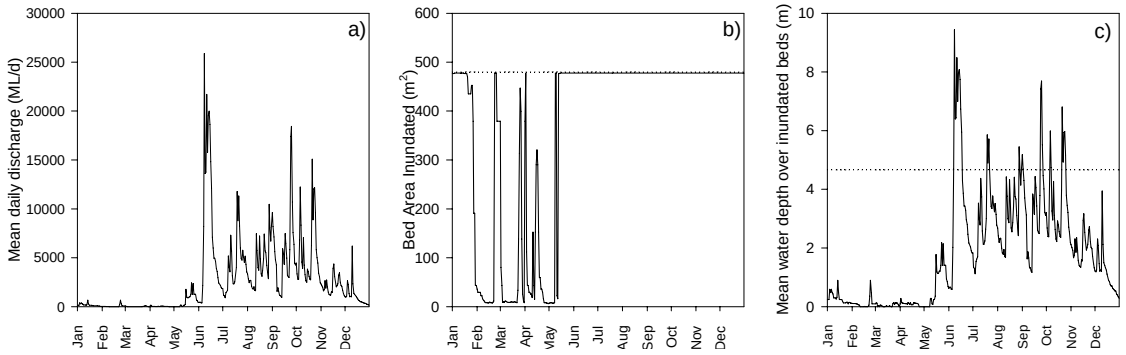

Figure 2.34. Modelled macrophyte inundation during floods – *Vallisneria* at BRO: a) mean daily discharge; b) bed area inundated (dotted line indicates total bed area); c) mean water depth over inundated macrophyte beds (dotted line indicates maximum depth prediction limit prior to overbank flows).

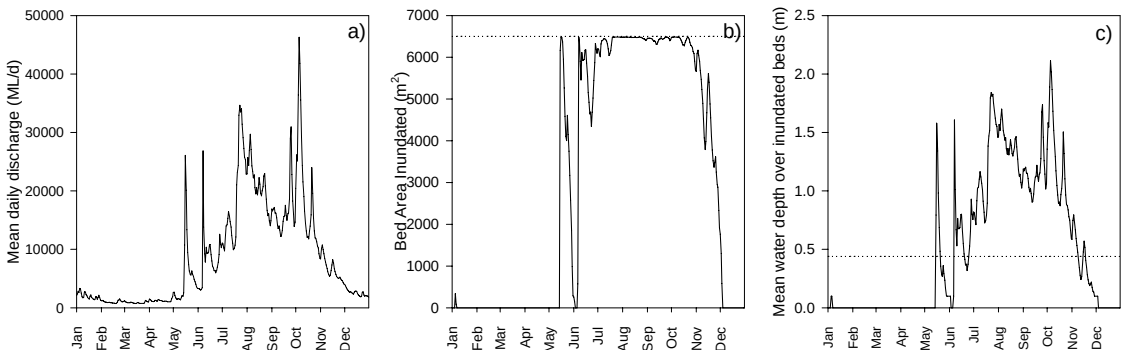

Figure 2.35. Modelled macrophyte inundation during floods – *Persicaria* at OVN: a) mean daily discharge; b) bed area inundated (dotted line indicates total bed area); c) mean water depth over inundated macrophyte beds (dotted line indicates maximum depth prediction limit prior to overbank flows).

2.4 Discussion

This chapter provides the first step in the overall aim of this thesis of predicting inputs to lowland rivers of OM from macrophytes under different flow conditions. The development of quantitative models of macrophyte inundation at different lowland river sites required the incorporation of macrophyte distribution data into three-dimensional river GIS models, the estimation of functions to describe inundation at different gauge heights and the application of these to flow data for different scenarios.

Phragmites australis is one of the most commonly occurring and abundant emergent macrophytes in south-eastern Australian lowland rivers and streams (Roberts and Marston, 2000). The populations at BAR and BRO represent low to medium sizes in the range of in-stream abundance that have been observed for this species (Roberts, 2000). Adjacent land use influenced distributions of this species at the different sites. At BAR, where the riparian zone is an intact floodplain forest with limited grazing, *Phragmites* occurred on the floodplain as well as on in-channel benches. In contrast, cleared pasture adjacent to the Broken River site and frequent access to the river channel by cattle has resulted in limited growth of this palatable species within the river channel and its complete absence on the floodplain. The occurrence of *Phragmites* in narrow patches at BRO, with greater edge to area ratios, would have implications for their use as habitat, given than habitat patch size and shape are known to be important to terrestrial fauna (Denno and Roderick, 1991; Fleishman et al., 2002; Franken and Hik, 2004; Fred and Brommer, 2003), fish (Weaver et al., 1997; Heck and Crowder, 1991; Tonn and Magnuson, 1982) and macro- and micro-invertebrates (Cyr and Downing, 1988; Taniguchi et al., 2003; Douglas and Lake, 1994).

In south-eastern Australia, species of *Typha* are common in wetlands, smaller creeks (Roberts and Ganf, 1986) and to a limited degree in larger lowland rivers (Walker et al., 1994). The extensive beds of *Phragmites* and *Typha* at BAR were likely linked to the presence and morphology of the in-channel benches. The vertical distribution range of *Typha* observed at Barmah (3.8 m) was much greater than that reported in the literature (2 m for wetlands in Western Australia (WA), Froend and McComb, 1994; 0.5 m for lower Murray, Walker et al., 1994). For the WA wetlands this may relate to sediment type and hence water-holding capacity at the different sites. The sandy sediments in the WA wetlands would be unable to retain moisture for very long once exposed as wetland water levels drop, resulting in a narrow band of area habitable by emergent aquatic plants centred on the mean low water mark. In contrast, the heavy clays at BAR retain moisture for extended periods once wetted, allowing emergent plants to colonise and survive in an extensive area above the mean low water level of the river. A combination of factors, including flow variability, sediment type and water quality may be

responsible for the reduced vertical distribution of *Typha* in the lower Murray weir pools observed by Walker et al. (1994). The occurrence of *Typha* in the lower pool area immediately above each weir (zone of minimal stage variability e.g. less than 10 cm) implicates water stability as being of prime importance.

It is interesting that in-channel vegetation at OVN was limited to *Persicaria prostrata*, given that many other creeks in this catchment support dense stands of macrophytes such as *Phragmites australis*, *Juncus exaltatus* and *Cyperus* spp., and adjacent billabongs have diverse aquatic plant populations (pers. obs.). While the steep banks and flashy flows at OVN might be expected to limit plant growth, many of the species listed above grow in streams with similar channel morphology and flow regimes (Roberts and Marston, 2000). Indeed, populations of *Phragmites australis* and *Cyperus* spp. occur in the upper reaches of the Ovens River itself (pers. obs.). Anecdotal evidence suggests that both *Vallisneria gigantea* and *Phragmites australis* occurred in lowland reaches of the Ovens River, including my study site, within the last 50 years (J. Hawking, pers. comm.). Given that the Ovens River is often used as a reference or 'natural' river in assessments of river condition, it would be of interest to determine the factors affecting macrophyte distribution in this system (e.g. land-use activities higher in the catchment).

Vallisneria may once have been distributed abundantly throughout lowland rivers of the Murray-Darling Basin, but population decline since the 1970's has resulted in its loss from many river reaches (Roberts, 2001; Roberts and Sainty, 1996; Walker et al., 1994). As noted in other studies (e.g. Sinclair Knight Mertz, 2001; Rea et al., 2002), *Vallisneria* beds at BRO occurred in areas of high current speed. The association of beds with large woody debris at this site is not common in other rivers, however, and may relate to the sediment composition at BRO. The loose sand overlying clay is easily scoured by high flows where it is not protected by LWD or vegetation. Thus, LWD provides areas of stable sediment for colonisation by *Vallisneria*.

Examining the flow regimes of the three sites, BAR had the highest mean discharge but the lowest variability and the least skewed distribution of flow data. This reflects the high degree of regulation of the lowland Murray River, with management aims of controlled high flows for much of the year for irrigation while minimising water 'loss' and potential public liability claims due to flooding. Although the Broken River is not managed to the same degree as the Murray, flood mitigation efforts result in high flow peaks which are very flashy whereas the Ovens River often has extended periods of flooding. Regulation has resulted in alterations of the types of flow events which occur in the Murray River and their timing, including the loss of extreme flow events, such as floods and droughts, and replacement of the natural low flow period in summer/ autumn with an extended period of artificially elevated and highly stable flows (Hillman, 1995; Walker and Thoms, 1993).

Although many metrics are available for characterising flow variability in rivers (Poff et al., 1997; Puckeridge et al., 1998; Olden and Poff, 2003) these are often complex or require multiple parameters to describe the hydrograph. For our broad comparison of variability at the three sites, the coefficient of variation of the mean was selected as a simple but informative metric which was relatable to other published studies (Boulton and Brock, 1999). Assessments of the coefficient of variation of flow at the different sites revealed, as might be expected, that BAR had the lowest variability for all temporal comparisons. A telling comparison is the inter-annual versus intra-annual mean CV for the three sites. While within-year variability was two or more times the between-year variability at BRO and OVN (due to strong seasonal variation as discussed below), at BAR these values were very similar, with the inter-annual CV slightly higher (although still less than half those of BRO and OVN). The lack of seasonality of flows at BAR may have implications for fauna which use seasonal flow variation as life-cycle cues (Hawking and Smith, 1997). The Ovens River is a tributary of the Murray, and contributes 14% of the average total flow of the Murray-Darling Basin while comprising only 6% of its total catchment area (Dept. Water Resources, 1989). The Ovens River is also largely responsible for variability in Murray River flows. This highlights the importance of maintaining the Ovens as an unregulated river, both for its own ecological value and for its contributions to other systems.

Pronounced seasonality occurred at OVN (inter-seasonal CV > intra-seasonal and inter-monthly CV > intra-monthly) but was not obvious at BRO, although inter-monthly CV was higher than intra-monthly. The cycling of flow variability at BRO from 1999 – 2002 was matched by changes in mean daily discharge for all years except 2002, where mean daily discharge decreased substantially with a concurrent increase in variability. This coincided with an ongoing drought which peaked in 2002. It is unclear why variability increased over this period as it might be expected that a drought would extend the period of Type A flows (stable, low flows), resulting in lower variability for that year.

Complete immersion of macrophyte beds generally occurred quite rapidly after discharges wetting 90% of bed area were reached, except for *Phragmites* at BRO. The elevation of one bed at this site was higher than the commence-to-flow heights of several flood-runners, in-channel benches and billabongs, which substantially increased the volume of water required to inundate the total *Phragmites* area. *Vallisneria* beds at this site were all below the elevations of these channel features and so the inundation curve for this species flattened off relatively quickly. Area inundation curves for *Typha* and *Phragmites* at BAR were similar because both species occur on benches at similar elevations and experience the same flow regime. The rate of increase of inundated macrophyte bed area at OVN was higher than at the other sites due to the very steeply sloping banks on which *Persicaria* grows.

Curves fit to data on water depth overlying macrophyte beds also depended on a combination of channel shape and vertical extent of macrophyte distribution at each site. Steeply sloping banks produced a very rapid initial increase in water depth over beds (hence the logarithmic curve for *Persicaria* at OVN), while more gently sloping banks or the presence of in-channel benches and flood-runners resulted in less rapid, or even inconsequential, initial increases in depth (i.e. *Phragmites* at BRO and both species at BAR). The tail of the curve was shaped by the vertical dispersal of macrophytes at the site, the degree of bank slope over which the majority of the beds occurred and any channel features which constrained or released water from the main channel. At BAR, the combination of gentle slopes on the bench floors and steep slopes on the outer channel banks produced depth inundation curves with slow initial rates of macrophyte inundation as the benches filled, followed by rapid water depth increases while the outer channel banks constrained water on the benches. Once the bank lip was breached and floodplain inundation commenced (above a discharge of 12,000 ML/d), the curve would be expected to plateau out very quickly. Floodplain mapping data were insufficient to determine flooding depth once water reached the floodplain. A limitation of inundation modelling for all three sites is that predictions of water depth overlying macrophyte beds extrapolated from relationships with in-channel flow will be over-estimates once flooding commences. The degree of over-estimation will be minimal at BRO and OVN but extreme for BAR. In acknowledgement of this limitation, predictions of water depths overlying macrophyte beds have been limited to within-channel discharges (less than 12,000 ML/d for BAR, 8,000 ML/d for BRO and 6,930 ML/d for OVN). Where water depth overlying macrophyte beds was modelled during periods of floodplain inundation, values reported are the maxima for in-channel inundation, with the acknowledgement that these are under-estimates.

Under current flows, macrophyte beds at BAR were never fully exposed nor inundated, although the area of beds inundated was at times very small (less than 1% of total bed area). *Typha* beds were inundated by 14 to 47 cm of water throughout the year, which is well within their inundation depth limits (Blanch et al., 1999) and comparable to field observations of immersion of this genus (Froend and McComb, 1994; van den Brink, 1995). At BRO, *Phragmites* beds were also partially inundated for most of the year, however water depths overlying these beds were always greater than at BAR. Depths of inundation ranged from 0.10 – 0.27 m at BAR and 0.29 – 2.58 m at BRO, which *Phragmites* easily tolerates (Blanch et al., 1999).

Modelling of current flow conditions at the Ovens River site revealed substantial *Persicaria* bed immersion during flashy flows from mid June to late October. Indeed, floodplain inundation at this site occurred from early August until late November; hence predictions of water depth overlying *Periscaria* beds for this period have been restricted to the maximum

possible inundation depth for within-channel flows of 0.44 m. *Persicaria prostrata* can tolerate water depths of 20 – 60 cm for up to 71 days in a year, and in fact appears to prefer inundation to this degree for at least 5 days each year (Blanch et al., 1999). In the present study, *Persicaria* beds were inundated with over 20 cm of water for 113 days under the scenario for current flows, which probably affect the lower limit of its vertical distribution at this site.

The depth distribution of *Vallisneria* is limited more by light availability than gas exchange, so inundation tolerances depend upon light attenuation in the water column. This species has been shown to survive inundation depths up to 145 cm for three months in water with turbidity similar to that of the Broken River site (Blanch et al., 1998). The majority of *Vallisneria* bed area at BRO was continuously inundated under modelled current flow conditions (mean water depth of 28 cm). *Vallisneria* prefers to be inundated at all times, with 20 – 60 cm of water overlying beds (Blanch et al., 1999), so current flow conditions at BRO suit this species.

Interesting results emerged when patterns of macrophyte inundation under current flow regimes were compared to those produced under different flow scenarios. Prior to river regulation, macrophytes at BAR would have experienced substantial bed area immersion (one-third to one-half of the total bed area) for over 4 months, compared to less than 10 days under current flows. Floodplain inundation occurred under this scenario, limiting depth predictions to a maximum of 0.48 m for *Typha* and 0.28 m for *Phragmites*. As with the current flow regime, total exposure of macrophyte beds at BAR did not occur. Drought conditions caused the exposure of substantial areas of *Typha* and *Phragmites* beds at BAR (over 90% of total bed area exposed for over 7 months), limited inundation during the wet part of the year and no floodplain inundation. In contrast, large-scale and persistent macrophyte inundation occurred under the flood scenario at BAR.

Macrophyte inundation at BRO under historic flows was quite similar to under current management, although inundation depths and periods of total bed immersion would have been greater, and minimum bed areas inundated during low flows would have been less under flows prior to river regulation. The major differences in macrophyte inundation patterns observed at BRO under the different flow scenarios were between current conditions and droughts or floods. Under both of these scenarios, macrophyte beds were totally exposed for 1-2 months of the year. During drought years, minimal areas of macrophyte beds were inundated throughout the rest of the year, whereas total immersion of all beds occurred for extended periods under the flood scenario. An added impact on *Phragmites* at this site under drought conditions would be the increased grazing pressure, pugging, etc. from cattle due to easier access. Given that *Vallisneria* has very limited tolerance to desiccation (Blanch et al., 1999), the extended exposure of beds at BRO during drought years would also have significant impacts on this species.

While some degree of *Persicaria* bed exposure occurred under all scenarios assessed at OVN, the extent of bed exposure under current flows was more similar to conditions experienced during droughts than during floods or historically. Floodplain inundation occurred under all scenarios except drought, with high flows also causing extended periods of substantial bed area immersion. However, the timing of inundation was quite different under the different scenarios. Currently, beds are immersed more or less constantly from early August to early December, whereas historically this would have occurred up to 2 months earlier. The consequences of substantial changes to inundation timing would be that inundation of rich nutrient sources such as macrophyte beds and floodplains during periods of high temperature (summer and autumn) would result in rapid rates of leaching of dissolved organic matter from inundated areas, very high aquatic microbial production and hence low dissolved oxygen levels (i.e. a black-water event). Currently when the Ovens River site floods during winter/ spring, black-water events usually do not occur (R. Cook, pers. comm.).

2.5 Conclusion

This chapter demonstrates a method of estimating inundation of in-channel macrophytes in lowland rivers that is applicable to any site. The study provided detailed descriptions of distributions of four species of macrophytes in three lowland river reaches in south-eastern Australia, and developed inundation curves to determine patterns of inundation caused by within-channel flows. The range of flow scenarios modelled demonstrate how known macrophyte inundation responses can be linked to inundation patterns under different hydrographs. This work breaks new ground in directly linking hydrology and ecology, allowing the prediction of macrophyte inundation responses at the reach-scale and hence enabling the determination of their ecological significance. These data provide the first step in the overall aim of this thesis of predicting inputs to lowland rivers of OM from macrophytes under different flow conditions.

Chapter 3. Biomass allocation and tissue nutrient composition of macrophytes from some south eastern Australian lowland rivers.

3.1 Introduction

Aquatic plants have a high degree of morphological plasticity (Dennison and Alberte, 1982; Sand-Jensen et al., 1992; Abal et al., 1994; Perez et al., 1994; de Kroon and Hutchings, 1995), varying resource allocation to different shoot components according to environmental conditions and phenology (Coops and van den Brink, 1996; Clevering and Hundscheid, 1998; Vretare et al, 2001; Crossley et al., 2002; Garbey et al., 2004). The allocation of biomass to different shoot partitions has implications for the photosynthetic and reproductive capacity of a particular macrophyte shoot, the population as a whole, and the associated ecosystem. For example, resources may be allocated to maximise photosynthetic capacity in some years or some shoots in a single year at the expense of lateral extension of rhizomes to expand a given macrophyte patch, by investing more resources into above ground photosynthetic tissues than below-ground structures. Where conditions are not favourable for colonisation or recruitment of genets, heavy investment in storage structures rather than sexual reproduction may occur, reducing population genetic diversity and potential dispersal to new areas. Both sexual and vegetative reproduction may be reduced during frequent physical disturbance, with resources channelled instead into reinforcing support structures to allow existing shoots to survive but limit their reproductive capacity and contribution to storage structures to boost emergence of shoots in the following season.

Distribution of shoot biomass between above and below-ground structures varies with growth form. The ratio of above to below ground biomass in emergent species ranges from 0.5-1.7 in *Phragmites*, 0.6-3.4 in *Typha* and 0.8-4.7 in members of the family Cyperaceae, but is usually less than 1.5 in emergent plants (Blanch et al., 1999; Soetaert et al., 2004; Asaeda and Karunaratne, 2000; Mauchamp et al., 2001; Miao and Sklar, 1998; Kercher and Zedler, 2004;

Shaver and Melillo, 1984; Li et al., 2004). In submerged macrophytes, this ratio depends on whether a storage structure is produced as well as growth form. Rosette-forming species (e.g. *Vallisneria*), have above to below ground biomass ratios higher than 1.5, and ranging up to 13.3 (Xie et al., 2005; Madsen, 1991; Madsen and Cedergreen, 2002; Barat-Segretain, 2001). In stalked forms (e.g. *Myriophyllum*, *Potamogeton*, some *Ruppia*), the ratio ranges from 0.8-2.3 (Madsen, 1991; Barat-Segretain, 2001). In the few species of mudflat hydrophyte (e.g. *Lobelia*, *Elatine*, *Persicaria*) studied, biomass is generally distributed evenly between above and below ground parts (Madsen, 1991).

Shoot biomass partitioning is also dependent upon growth form, with emergent stalked species (such as *Phragmites*) allocating 70-80% of their above-ground biomass to stems, 20-25% to leaves and 3-5% to flowers (Sakurai et al, 1985; Hocking, 1989a; Asaeda and Karunaratne, 2000; Soetaert et al., 2004). Emergent macrophytes which only produce stem-like structures for reproduction (e.g. *Typha*) have highly variable patterns of above-ground vegetative biomass allocation – 44-85% leaves and 15-45% shoot bases (sheaths) (Shaver and Melillo, 1984; Miao and Sklar, 1998; Weisner and Miao, 2004). Rosette-forming emergent species (e.g. Cyperaceae) commit 75-85% of above-ground biomass to leaves and 15-25% to shoot bases (Miao and Sklar, 1998; Weisner and Miao, 2004). The above-ground biomass of submerged rosette-forming macrophytes is primarily comprised of leaves (88-100% - Madsen and Cedergreen, 2002; Xie et al., 2005). While stalked submerged species also allocate most biomass to leaves (45-98%), stalks are also important biomass components (4-30%) (Barrat-Segretain, 2001; Madsen and Cedergreen, 2002). No data on resource allocation in mudflat hydrophytes have been reported.

Variation in resource allocation to different shoot components has been associated with water depth/availability (Mauchamp et al., 2001; Vretare et al., 2001; Kercher and Zedler, 2004; Li et al., 2004; Weisner and Miao, 2004), nutrient status (Shaver and Melillo, 1984; Miao and Sklar, 1998; Madsen and Cedergreen, 2002), salinity (Soetaert et al., 2004) sediment type (Xie et al., 2005), and physical damage (grazing, cutting, wave action, flood scouring, etc.) (Coops and Van der Velde, 1996; Barrat-Segretain, 2001; Asaeda et al., 2003).

Plant phenology (and in particular, reproduction, resource translocation to storage structures and senescence), litter production, leaching of standing shoots and aerial decomposition contribute to changes in shoot biomass allocation and nutrient composition over time. Of these, resource translocation and gross changes during senescence have received the greatest research attention (Shaver and Melillo, 1984; Hocking, 1989a; Hietz, 1992; Boar, 1996; Gessner et al., 1996; Gessner, 2001; Newell, 2001; Asaeda et al., 2002; van den Wyngaert et al., 2003; Soetaert et al., 2004). Resource translocation to over-wintering or storage structures has been studied mostly in emergent species. Asaeda and Karunaratne (2000) estimated that 26% of

shoot biomass was translocated to below ground structures in *Phragmites*, with preferential allocation to young rhizomes (Karunaratne et al., 2004), although different genetic clones are known to have differential translocation dynamics (Rolletschek et al., 1999). *Typha* rhizomes recover up to 65% of shoot nitrogen (Hocking, 1989; Gessner, 2001; Soetaert et al., 2004). Reductions in above-ground biomass during autumn have been reported in cold climates for species of *Vallisneria* which produce over-wintering structures (Dawes and Lawrence, 1989; Kurtz et al., 2003). Translocated compounds include starch, glucose, sucrose, fructose, amino acids (mainly asparagine, alanine and glutamine) (Kohl et al., 1998; Klimes et al., 1999; Rolletschek et al., 1999).

Some work on mass loss from and changes to the composition of standing dead shoots (including aerial decomposition) has been performed, with increased interest in the last 10 years. Where aerial decomposition has been examined, mass generally decreases or remains stable (Hietz, 1992; Newell, 1993; Barlocher and Biddiscombe, 1996; Newell et al., 1996; Kuehn and Suberkropp, 1998; Gessner, 2001), however varying trends have been reported for nutrient dynamics (Boyd, 1970; Davis and Van der Valk, 1978; Polunin, 1984; Webster and Benfield, 1986; Kuehn et al., 1998b; Gessner, 2001; Newell, 2001b; Welsch and Yavitt, 2003). Often methodological reasons are cited for discrepancies in nutrient trends (e.g. absorption of nutrients from contact of litter with sediments, pre-treatment of OM, use of tissues removed from plants prior to the completion of translocation) (Gessner, 2001; Welsch and Yavitt, 2003). However, species and site differences (such as nutrient status, microbial community structure and activity, sediment type, water quality, flow, rainfall and acts of God) probably also play a role.

While reproductive structures on some macrophyte species are small and their loss would make insignificant changes to overall shoot mass (e.g. *Vallisneria*, *Phragmites*) (Soetaert et al., 2004), others represent a substantial resource investment, much of which is lost when seeds are shed (e.g. *Typha*). Leaching of standing emergent and mudflat macrophyte shoots may occur during periods of rainfall or inundation, although emergent species might be expected to have developed adaptations to minimise mass and nutrient losses in this manner from live shoots, given their preference for partial submergence (Walker et al., 1994). Litter decomposition has been studied for many macrophyte species (e.g. Hietz, 1992; Miao and Sklar, 1998; Gessner, 2000; Gessner, 2001; Asaeda et al., 2002; Welsch and Yavitt, 2003; Dinka et al., 2004; Goncalves et al., 2004; Xie et al., 2004), however, timing, rates of production and composition of macrophyte litter have received little to no research attention (Hocking, 1989; Blanch et al., 1998; Asaeda et al., 2002; Soetaert et al., 2004).

A component of studying allocation dynamics in plants is the examination of nutrient contents and fluxes to and from different tissue types. Determination of nutrient composition of macrophyte OM from litter decomposition studies and assessments of tissue nutrients throughout growing seasons have generated a reasonably good understanding of nutrient dynamics in macrophytes, although the range of tissues and species covered is quite small (Shaver and Melillo, 1984; Madsen, 1991; Boar, 1996; Kohl et al., 1998; Miao and Sklar, 1998; Gessner, 2001; Soetaert et al., 2004Xie et al., 2005). As with other plant types, carbon content is often associated with the degree of structural strengthening of tissues, with nitrogen and phosphorus related to environmental nutrient concentrations, stressors and physico-chemical attributes, and phase in the growth season (Boar, 1996; Miao and Sklar, 1998; Xie et al., 2005). Carbon to nitrogen and C:P ratios of plant OM have been linked to breakdown rates (Kaushik and Hynes, 1971; Godshalk and Wetzel, 1978; Carpenter and Adams, 1979; Elwood et al., 1981; Gessner et al., 1996), and so are often used as indicators of bio-availability, although other factors, such as active resistance to leaching and the presence of chemical inhibitors, can play a role in limiting the transfer and usefulness of OM to the rest of the system (Webster and Benfield, 1986).

In summary, some aspects of biomass allocation in macrophytes are well studied (e.g. above-below ground ratios, allocation to different shoot components by different species and translocation to storage structures) and others have received some research attention (aerial decomposition, gross changes during senescence). However, reproductive mass losses, detailed allocation changes during senescence, leaching of standing biomass and litter production dynamics are not always quantified or even estimated. Also, the composition and fluxes of nutrients between different tissue types is important in understanding shoot allocation dynamics and potential transfer to the rest of the system. However, the range of tissue types and species studied to date is limited, with most studies considering leaf blades and sometimes stems. This study aimed to fill some of these knowledge gaps, by providing in-depth data tracking changes in biomass allocation and nutrient composition of macrophyte shoots throughout the plant growth cycle, including determination of shoot components important to litter production over 1-2 years. The data could then contribute to the development of a model of macrophyte OM inputs to rivers.

3.2 Methods

3.2.1 Study Sites

Typha orientalis, *Phragmites australis*, *Persicaria prostrata* and *Vallisneria gigantea* were studied at lowland reaches (BAR, BRO and OVN) of three rivers (Murray, Broken and Ovens) in southeastern Australia from May 2001 to December 2002 (described in Chapter 2).

3.2.2 Shoot Biomass Partitioning

Measurement of shoot biomass allocation was limited to above-ground biomass, both for simplification (given the limited resources of the project), and as above-ground biomass was considered to be the major potential source of macrophyte organic matter to rivers. The selection of shoot biomass partitions used in this study were based on the growth form, inundation patterns and litter production of each species, with guidance from other studies where available (Boar, 1996; Gessner et al., 1996; Miao and Sklar, 1998; Gessner, 2000; Hietz, 1992; and c.f. Asaeda et al., 2003; Dinka et al., 2004; van den Wyngaert et al., 2003; Soetaert et al., 2004; Weisner and Miao, 2004).

The greatest effort went into partitioning the emergent macrophytes (*Typha* and *Phragmites*) because substantially different structures were apparent for different shoot components (and so different nutrient composition, leaching rates and bio-availability might be expected). Also, emergent plants often experience partial immersion, with only a subset of biomass partitions inundated, and litter production involves different proportions of each biomass partition (pers. obs.). The biomass partitions selected for these species were leaf blades, leaf sheaths, stems (referring to pedicels on reproductive *Typha* shoots and upright, leaf-bearing stalks for *Phragmites*) and reproductive tissues.

The much shorter shoots of the low-growing, hydrophytic *Persicaria prostrata* tend to either be fully immersed or fully exposed, depending on water levels (pers. obs). The prostrate habit of this plant also causes difficulties in differentiating stems from stoloniferous runners. Reproductive tissues on *Persicaria* shoots represent a very small proportion of above-ground biomass. Litter produced by this species consists of dead leaves (attached to stems) which shatter into fine particles when disturbed, making measurement of litter production rates exceedingly difficult. Thus, partitioning of above-ground biomass and litter production measurements were not attempted for this species, rather, analyses were performed on whole shoots.

While leaf blades of the submerged *Vallisneria gigantea* can be very long, the sheathing bases of leaves are usually short and would either be inundated or exposed concurrently with blades. Therefore, these tissue types were not differentiated in this study, with blades and sheaths grouped into the one biomass partition (leaves) (c.f. Xie et al., 2005). Litter from *Vallisneria* beds is comprised primarily of leaves, with only small proportions of reproductive tissues present (pers. obs.). Thus, the greatest focus for this species was on leaves, however stolons and reproductive biomass were also assessed where available.

3.2.2.1 Phragmites & Typha

In May 2001, three 1 m^2 plots were marked off with stakes and flagging tape for *Typha* at BAR and *Phragmites* at both BAR and BRO. In each plot, current season shoots were marked with uniquely numbered sheep ear tags attached loosely using plastic-coated wire. On each field trip 3 - 5 of these shoots were randomly selected for destructive harvesting. Harvested shoots were washed and partitioned into dead blades, live blades, dead sheaths, live sheaths, stems and reproductive tissues. Samples were dried at 60 ^{o}C in a Thermoline D120 dehydrating oven to a constant weight. Dry weights were obtained for each partition of each shoot. Dried samples were also used to obtain dry weight conversion factors for lineal lengths of live and dead stems and mean dry weights per leaf.

3.2.2.2 Vallisneria

The growth form of *Vallisneria* is such that as components senesce, the damaged tissue is easily broken and removed from the shoot by water action (pers. obs.). Material which appears senescent but which is still attached to the shoot is generally still actively growing and green beneath biofilms which give the appearance of dead tissue (pers. obs; Titus and Pagano, 2002). Thus, any shoots (and their biomass components) found still attached were considered to be live tissue for this study. Intact dead shoots were not observed during the study period, so no data are available on mean mass or composition of *Vallisneria* dead shoots. Senescent material (mainly leaves) trapped within the canopy of *Vallisneria* beds, on snags or entrained in stream flows was classified as dead material for this study.

On each sampling trip to BRO, 10 – 15 live *Vallisneria* shoots were harvested from beds and placed into individual paper bags for drying and weighing as outlined above. Dry weights were obtained for all above-ground biomass, however the numbers of stolons and/or flowers attached to each shoot were noted to enable back-calculation of masses for the different partitions (leaves, stolons and reproductive structures) of live tissues.

3.2.2.3 Persicaria

On each sampling trip to OVN, all shoots within three quadrats (0.09 – 1 m^2) were counted, harvested and placed in paper bags for drying and weighing as outlined above. Total dry mass for each harvested quadrat were obtained, and shoot number used to determine dry weight per shoot. Above-ground biomass was also calculated on an areal basis.

3.2.3 Litter Partitioning

For the purpose of quantitatively modelling litter input under different flow scenarios, the shoot components contributing substantially to litter production over a 1-2 year time scale were determined for each species. For *Typha* and *Phragmites*, the proportions of initial masses of

each shoot biomass component which was lost over 12 months (from the tagged shoots described above) were calculated by fitting exponential decay curves to plots of component masses (expressed as a percent of initial mass). Predictions from fitted curves were compared to the biomass partitions found in standing litter collected from 1 m^2 quadrats at BAR and BRO in August, 2002 (samples were dried and processed for dry weights as outlined above). While different rates of litter production might be expected for emergent plants when inundated versus when exposed, low water levels throughout the study period (due to on-going drought) meant that only data on litter production from un-inundated tissues were obtained. For *Vallisneria*, the composition of material trapped in the canopy of *Vallisneria* beds (the equivalent of standing litter for this species) was determined. Particulate organic matter was collected in 1 mm mesh nets from *Vallisneria* beds at BRO on 18/05/01 by flushing water through and gently agitating the canopy within a 0.25 m^2 quadrat for 2 minutes. Material collected in the net was examined and the presence of different *Vallisneria* shoot components noted, before samples were dried and processed for dry weights as described previously. *Vallisneria* litter assessments were compared to turnover rates for different biomass components of this species obtained from the literature. Standing litter was not observed in *Persicaria* beds at any time over the course of this study, negating the need to include litter as an important OM pool for this species.

3.2.4 Tissue Nutrients

For all species studied, plant samples from shoot partitioning which had not been previously inundated were retained for assessment of tissue carbon, nitrogen and phosphorus content. Dried samples were roughly chopped into 2 – 100 mm^2 pieces using scissors or secateurs and ground using a coffee grinder and/or a Cyclone Sample Mill (UDY Corporation, Colorado, USA). Ground samples were stored in paper soil bags until processing. Total carbon content was measured using an adaptation of APHA Total Organic Carbon Method 5310C (Eaton et al., 1995) (Model 1010 Total Organic Carbon Analyser, O.I. Analytical, Texas). Total nitrogen and total phosphorus were measured on a Lachat Instruments QuickChem 8000 Flow Injection Analyser following persulphate digestion (Hosomi & Sudo, 1986).

3.2.5 Statistical Analyses

One-way and two-way analyses of variance (ANOVA) were performed using Systat version 10. Sigmaplot 2001 for Windows version 7.101was used for plotting graphs, curve-fitting and ANOVA of fitted functions.

3.3 Results

3.3.1 Shoot Biomass Allocation

3.3.1.1 Phragmites

Significant differences were observed in *Phragmites* total shoot dry masses with respect to collection site and shoot status (live or dead) (Figure 3.1, Table 3.1). Live shoots were heavier than dead shoots at both sites ($p < 0.001$, $F = 20.403$, $n = 63$), however this relationship was not statistically significant for BRO. *Phragmites* shoots at the Broken river site were generally smaller (with significantly lower mean dry masses) than their counterparts at BAR (LIVE: $p < 0.001$, $F = 27.856$, $n = 32$; DEAD: $p < 0.001$, $F = 14.908$, $n = 96$).

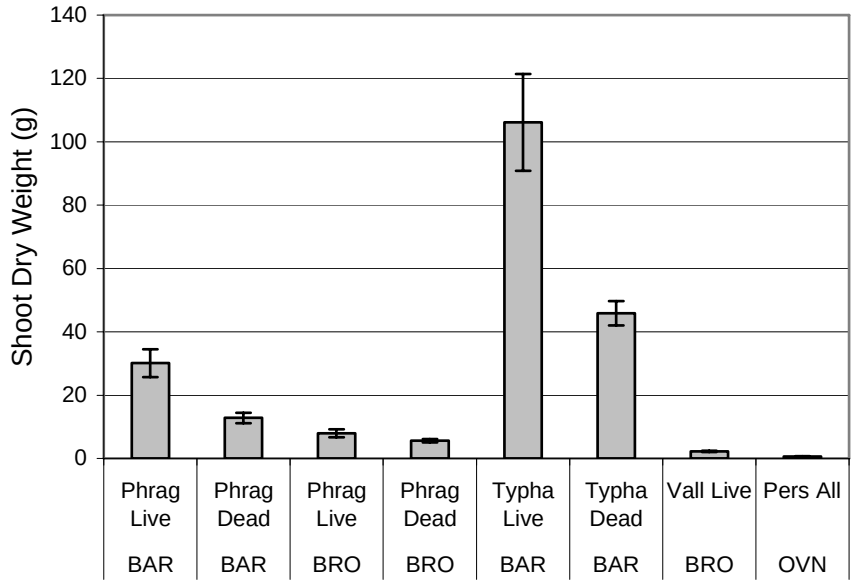

Figure 3.1. Comparison of shoot dry weights for different macrophyte species from each site (means ± standard error). Species abbreviations: Phrag = *Phragmites*; Vall = *Vallisneria*; Pers = *Persicaria*.

Differences in shoot masses from different sites were associated with proportional reductions in masses of all shoot components: the total biomasses of each shoot component on BRO *Phragmites* shoots were ⅓ to ½ those at BAR (Figures 3.2 & 3.3). Rather than relating to differences in quantities of component units produced per shoot, site differences in total component masses were due to reductions in size of shoot partition units (i.e. the mass of an individual blade or sheath from BRO *Phragmites* shoots was generally ½ that of shoots from BAR). For example, the mean dry masses per live blade and sheath from a BRO shoot were 0.26 g and 0.13 g, respectively, compared to 0.59 g and 0.27 g at BAR (all $p < 0.05$, $F > 6.38$, $n > 21$) (Table 3.1).

Table 3.1. Masses of different tissue types (means ± standard error with sample size in parentheses).

Tissue Type	Typha	Phragmites (BAR)	Phragmites (BRO)	Persicaria	Vallisneria
Blade Dead	3.22 ± 0.22 (44)	0.39 ± 0.07 (35)	0.15 ± 0.02 (40)	na	0.21 ± 0.04 (8)
Blade Live	6.93 ± 0.46 (13)	0.59 ± 0.08 (15)	0.26 ± 0.07 (15)	na	0.24 ± 0.02 (91)
Sheath Dead	1.85 ± 0.13 (44)	0.27 ± 0.02 (61)	0.10 ± 0.01 (65)	na	na
Sheath Live	3.85 ± 0.47 (12)	0.27 ± 0.03 (15)	0.13 ± 0.04 (6)	na	na
Stem Dead	28.60 ± 2.01 (7)	9.39 ± 1.30 (48)	3.89 ± 0.35 (50)	na	na
Stem Live	51.49 ± na (2)	14.52 ± 2.38 (15)	4.16 ± 0.66 (15)	na	na
Flower Dead	2.6 ± na (1)				
Flower Live	47.5 ± 13.8 (2)				
Shoot Dead (incl repro)	45.88 ± 3.81 (44)	12.78 ± 1.66 (48)	5.87 ± 0.55 (50)	na	na
Vegetative shoot	41.65 ± 3.84 (37)				
Reproductive shoot	68.28 ± 9.47 (7)				
Shoot Live (all)	106.14 ± 15.33 (15)	30.10 ± 4.39 (15)	7.73 ± 1.48 (15)	0.64 ± 0.07 (5)	2.25 ± 0.21 (91)
Vegetative shoot	93.57 ± 14.30 (13)				
Reproductive shoot	187.88 ± na (2)				

Slight reductions in stem biomass observed during the study (Figures 3.2 & 3.3) were due to breakage of standing stems, with numbers of nodes per shoot gradually decreasing over time (data not shown). However, these differences were not statistically significant over the time period examined. No significant differences were observed in mass per dead blade or sheath over time at BRO (Figure 3.5, mean dry weights per biomass component are reported in Table 3.1). However, there were large initial decreases in dry mass per dead blade and dead sheath at BAR (BLADE: $p < 0.001$, $F = 27.049$, $n = 34$; SHEATH: $p < 0.001$, $F = 17.736$, $n = 62$), which then remained constant over the following months (Figure 3.4). The model of macrophyte litter input to streams developed did not have the capacity to include different masses for litter components of different age at the time of writing, so dry weights per dead blade and sheath were averaged over the entire BAR data set for later modelling, producing values of 0.39 g and 0.27 g, respectively (Table 3.1).

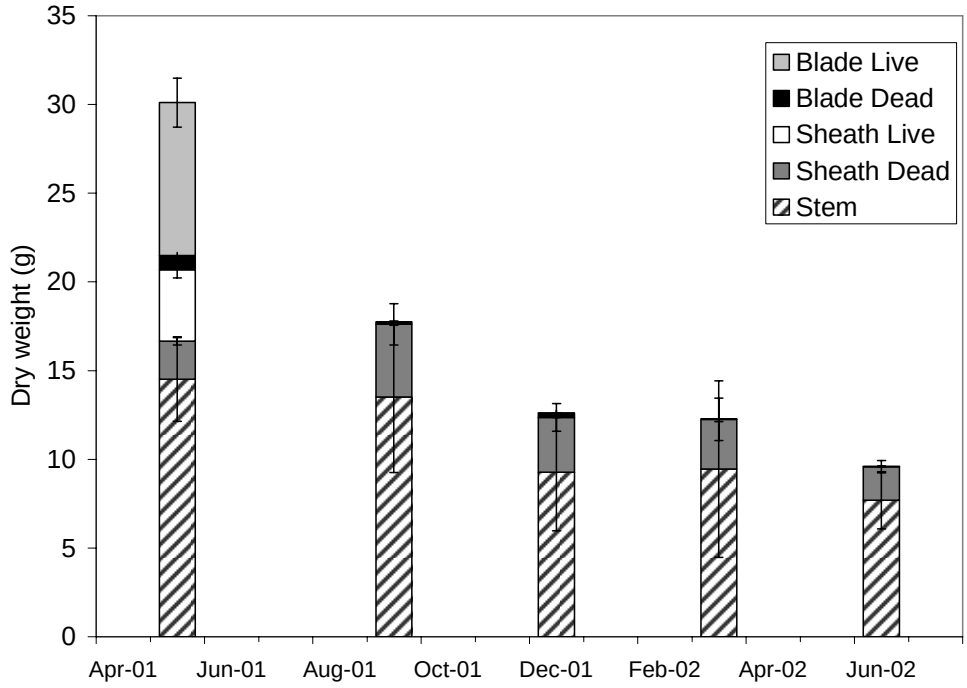

Figure 3.2. Changes to masses of *Phragmites* shoot partitions over time from BAR (means ± standard error).

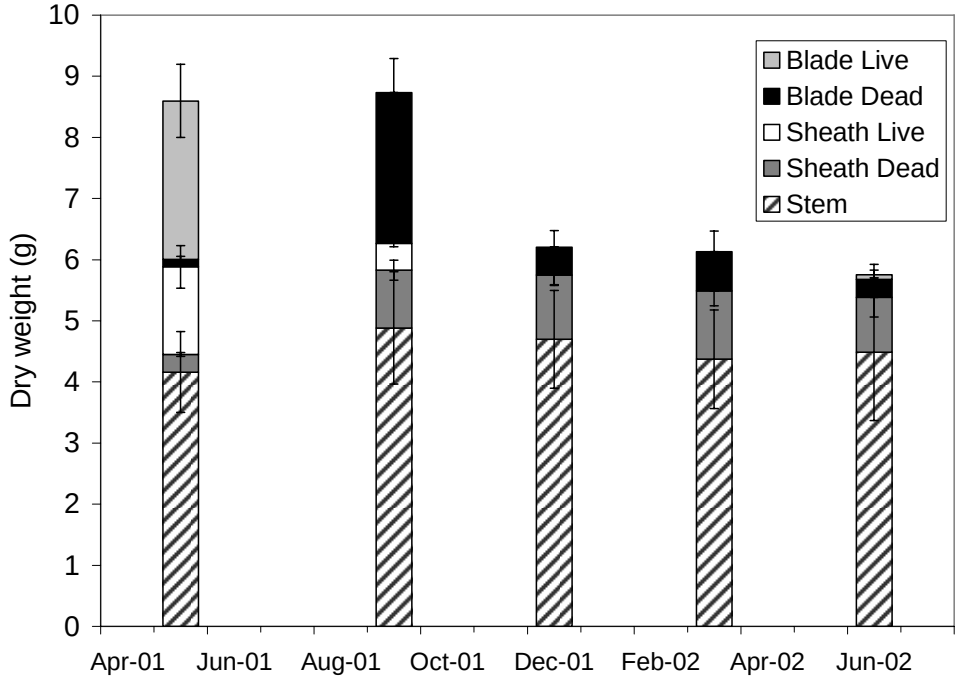

Figure 3.3. Changes to masses of *Phragmites* shoot partitions over time from BRO (means ± standard error).

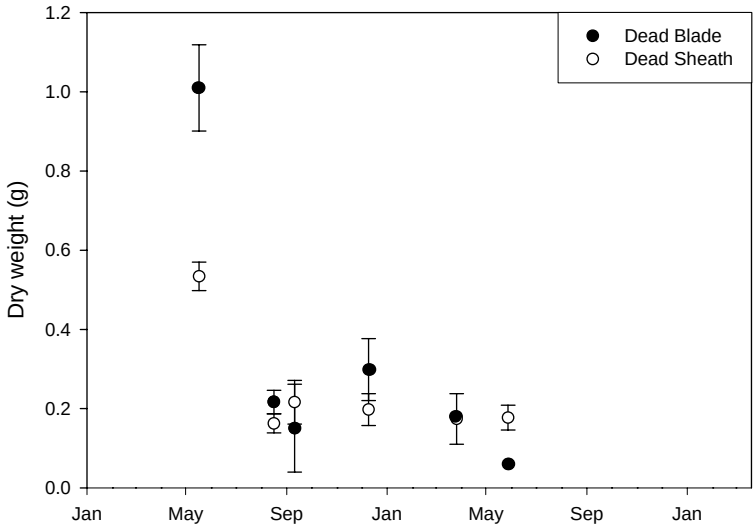

Figure 3.4. Changes to masses of individual dead blades and sheaths from *Phragmites* at BAR over time (means ± standard error).

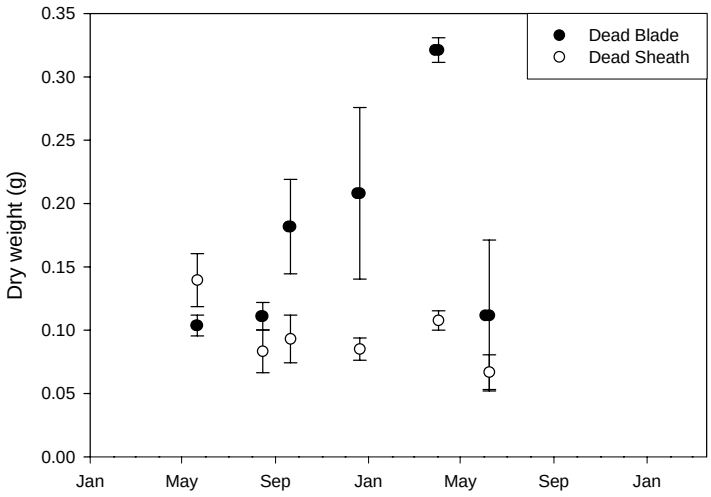

Figure 3.5.Changes to masses of individual dead blades and sheaths from *Phragmites* at BRO over time (means ± standard error).

Shoot status (live or dead) was a greater contributor to differences in shoot composition than site (two-way ANOVA on each shoot component: all $p < 0.01$; $F > 7.60$, $n = 60$), so site data were pooled for comparisons of live and dead shoot composition. Up to 52% of live *Phragmites* shoot biomass was comprised of stems, with live blades (30%) and live sheaths (10%) making up most of the remainder (Table 3.2). Reproductive structures, dead blades and dead sheaths contributed less than 10% of live shoot biomass in *Phragmites*. Stems (73%) and dead sheaths (22%) formed the majority of dead shoot biomass, with very little change in dead shoot composition between December 2001 and June 2002.

Table 3.2. Percentage composition of live and dead emergent macrophyte shoots (means ± standard error of the mean with sample size in parentheses).

Tissue Type	Phragmites Live	Phragmites Dead	Typha Live	Typha Dead
Blade Dead	2.14 ± 0.45 (30)	4.42 ± 0.76 (74)	28.01 ± 4.10 (15)	52.93 ± 2.85 (44)
Blade Live	29.56 ± 1.85 (30)	0.05 ± 0.05 (74)	27.42 ± 5.32 (15)	0.04 ± 0.04 (44)
Sheath Dead	6.21 ± 0.47 (30)	22.20 ± 0.79 (74)	23.21 ± 2.89 (15)	37.94 ± 1.47 (44)
Sheath Live	9.30 ± 1.19 (30)	0	14.40 ± 2.99 (15)	0
Stem	51.52 ± 1.78 (30)	73.02 ± 1.07 (74)	3.66 ± 2.50 (15)	7.25 ± 2.68 (44)
Flower	1.26 ± 0.50 (30)	0.31 ± 0.13 (74)	3.30 ± 2.27 (15)	1.84 ± 0.78 (44)

3.3.1.2 Typha

Mean masses for whole *Typha* shoots were significantly greater than those of *Phragmites* from both BAR and BRO (LIVE: $p < 0.0001$, $F = 34.22$, $n = 47$; DEAD: $p < 0.0001$, $F = 82.01$, $n = 140$) (Figure 3.1, Table 3.1 – averages include masses of both vegetative and reproductive shoots). Live, vegetative *Typha* shoots collected in May 2001 were comprised of 32% live blades, 29% dead blades, 17% live sheaths and 23% dead sheaths, with a mean shoot mass of 93.57 g (± 14.30) (Table 3.3, Figure 3.6). Senescence produced a significant change in vegetative shoot composition (all $p < 0.0001$, $F > 20$, $n = 60$) and overall shoot dry mass ($p < 0.0001$, $F = 24.18$, $n = 50$), which remained relatively constant over the next 9 months (shoot mass of 41.65 g ± 3.84 comprised of 60% dead blades and 40% dead sheaths) (Table 3.3, Figure 3.6).

Table 3.3. Percentage composition of vegetative and reproductive *Typha* shoots (means ± standard error of the mean with sample size in parentheses).

Tissue Type	Typha Live (vegetative)	Typha Dead (vegetative)	Typha Live (reproductive)	Typha Dead (reproductive)
Blade Dead	28.60 ± 4.73 (13)	60.11 ± 1.49 (37)	0	14.99 ± 3.13 (7)
Blade Live	31.63 ± 5.20 (13)	0.04 ± 0.04 (37)	24.21 ± 0.59 (2)	0
Sheath Dead	23.15 ± 3.34 (13)	39.85 ± 1.49 (37)	0	27.85 ± 2.54 (7)
Sheath Live	16.62 ± 3.01 (13)	0	23.56 ± 2.19 (2)	0
Stem	0	0	27.46 ± 0.34 (2)	45.57 ± 5.79 (7)
Flower	0	0	24.77 ± 3.12 (2)	11.58 ± 2.99 (7)

Live and dead *Typha* shoots bearing reproductive structures were substantially heavier than their vegetative counterparts, with mean shoot masses of 187.88 g (n = 2) and 68.28 g (± 9.47), respectively (Table 3.1). Differences in shoot masses of live and dead reproductive shoots were coupled with changes in shoot composition: live shoot biomass was evenly distributed between live blades, live sheaths, stems and flowers whereas dead shoots were comprised of 15% dead blades, 28% dead sheaths, 45% stems and 12% flowers. Low numbers of reproductive shoots occurring in field plots, and hence small sample sizes, meant that analyses of variance did not have sufficient power to demonstrate the statistical significance of differences in biomass and shoot composition.

Where stems and flowers were present (on reproductive *Typha* shoots only), there were initial decreases in biomass of these components associated with senescence (Figure 3.7). For stems, this change did not appear to be due to material entering the litter pool, as no reductions in stem height were observed and mass remained stable over the following year.

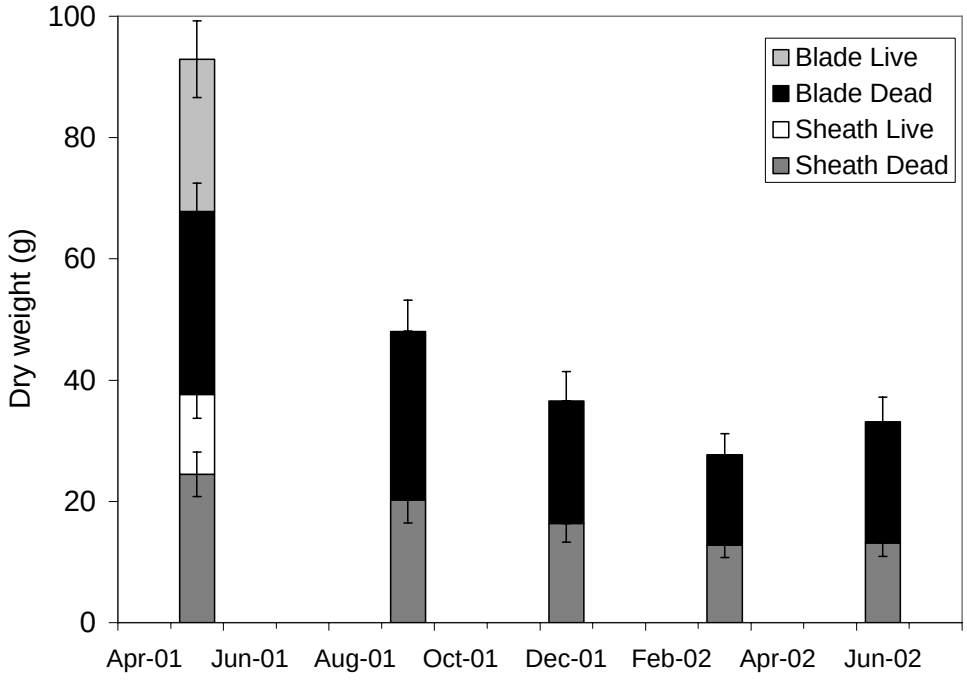

Figure 3.6. Changes to masses of *Typha* shoot partitions over time at the BAR site (vegetative shoots; means ± standard error).

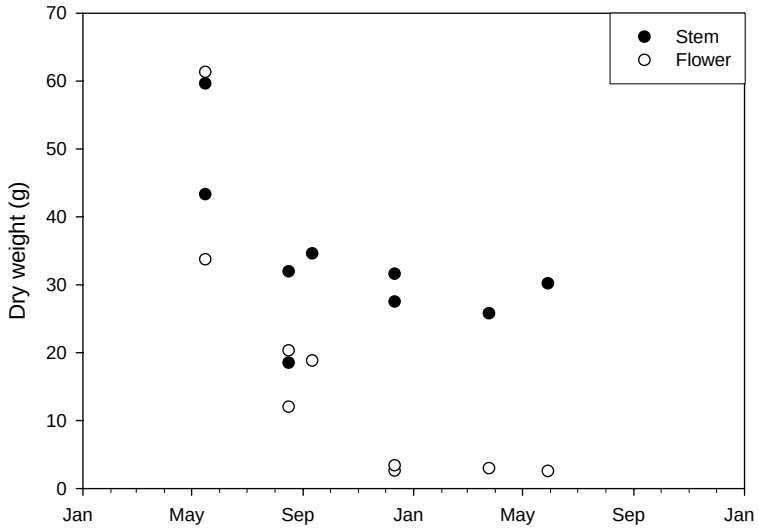

Figure 3.7. Changes to stem and flower biomass per *Typha* shoot over time (individual data points). Note that at the first time-point (May 2001), shoots were still alive.

In contrast, flower biomass did continue to decline after the initial decrease (Figure 3.7), coincident with seed maturation and dehiscence, indicating that flowers may contribute to the litter pool. As with comparisons of total shoot biomass from live and dead reproductive shoots, small sample sizes precluded statistical analyses of differences in stem and flower biomass based on shoot status or time. However, in order to develop a model that predicts input estimates from live and dead *Typha* stems and flowers, mean masses for these tissue types were calculated, despite the inability to confirm the statistical significance of differences using the current data set. The mean dry masses of live and dead *Typha* stems were 51.49 g (n = 2) and 28.60 g (± 2.01), respectively (Table 3.1). Masses of live and dead flowers were based on initial and final flower masses (i.e. 47.5 and 2.6 g, respectively (Table 3.1).

While some temporal variation in mean dead blade and sheath masses was observed for *Typha* (Figure 3.8), these differences were not statistically significant, and mean dry weights of 3.22 g for dead blades and 1.85 g for dead sheaths were used for later modelling. Mean mass per live *Typha* blade and sheath were calculated as being 6.93 g and 3.85 g, respectively (Table 3.1).

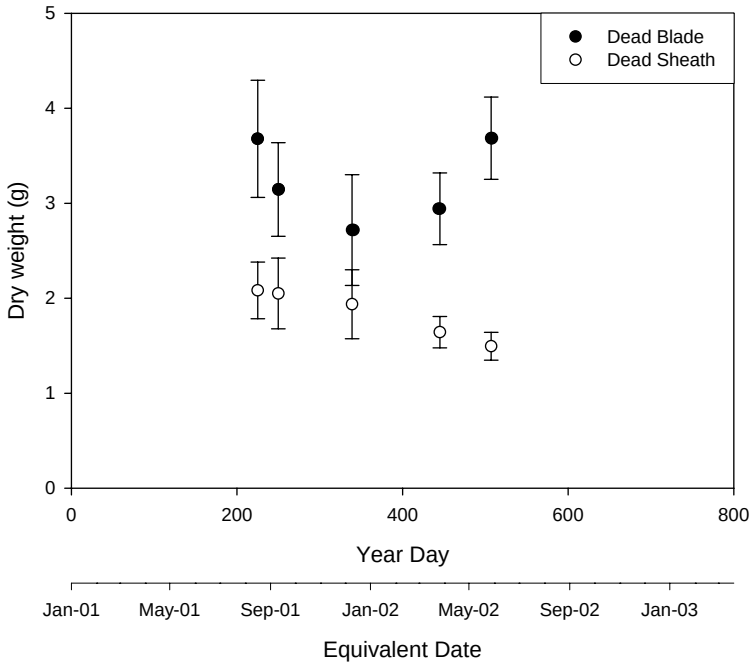

Figure 3.8. Changes to masses of individual dead blades and sheaths from *Typha* over time (means ± standard error).

3.3.1.3 Vallisneria

Mean shoot mass of live *Vallisneria* shoots was significantly smaller than live and dead shoots of *Typha* and *Phragmites* from both sites (Figure 3.1; Table 3.1; $p < 0.0001$, $F = 94.42$, $n = 278$). The determination of shoot biomass composition was attempted by back-calculation of mass per shoot component (i.e. determine mass per leaf from shoots with no stolons or flowers and then use this value in other calculations). However, mass per leaf calculated in this manner was found to be highly variable, because not only did leaf number per shoot change over time but so did leaf length (Figure 3.9). In fact, some seasonality was apparent in both of these parameters, with numerous, shorter leaves occurring in summer and fewer, longer leaves present from winter to spring. Therefore, leaf number on its own was not a good indicator of the total quantity of leaf tissue present.

Instead, the lineal length of leaf tissue per shoot was estimated by multiplying the number of leaves per shoot by ½ the maximum leaf length for that shoot (a rough approximation of median leaf length). Plotting lineal leaf length against shoot dry weight produced an almost 1:1 relationship (Figure 3.10) ($R^2 = 0.74$, $p < 0.0001$, $F = 253.89$, $n = 91$).

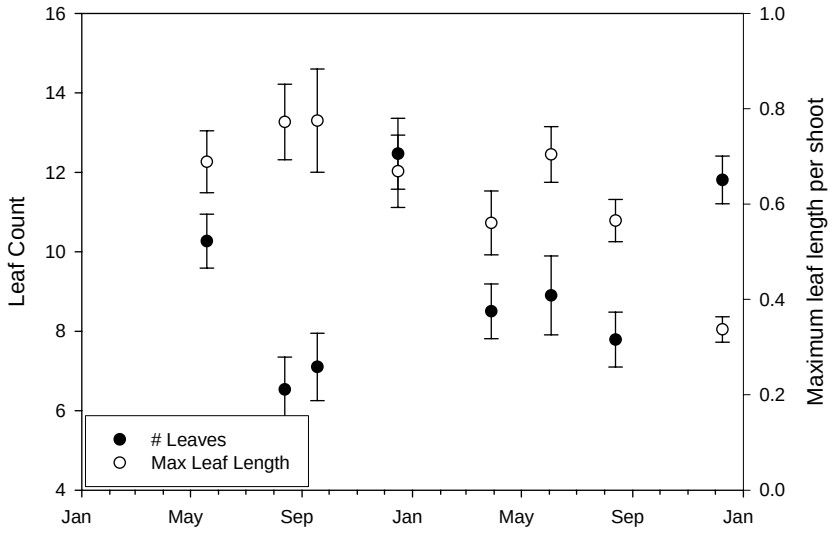

Figure 3.9. Changes to leaf number and maximum leaf length per *Vallisneria* shoot over time (means ± standard error).

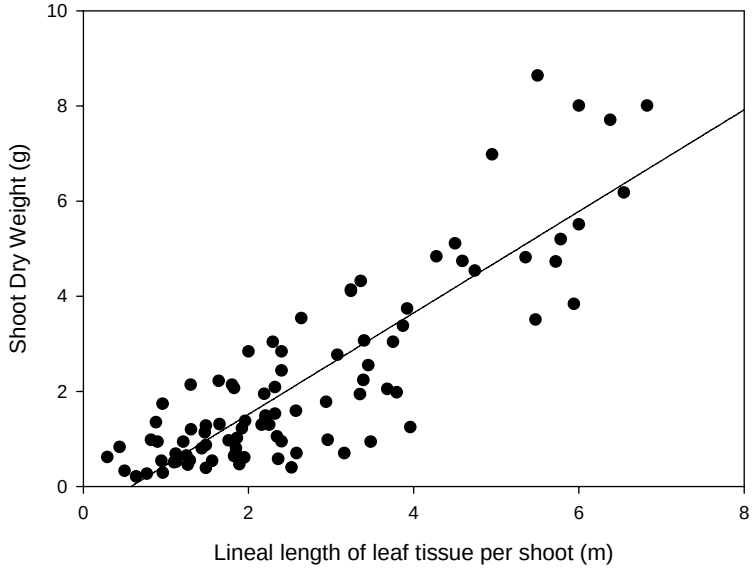

Figure 3.10. Relationship between quantity of leaf tissue per shoot and shoot dry weight for *Vallisneria* (points are raw data, line is fitted linear regression).

Although the number of flowers per shoot also varied over time (with some seasonality apparent, as might be expected) (Figure 3.11) and shoots with higher numbers of flowers were slightly heavier than shoots without (for the same lineal leaf length) (Figure 3.12), inclusion of number of flowers did not improve the curve fit of shoot component quantity versus shoot dry weight ($R^2 = 0.72$, $p < 0.0001$, $F = 83.28$, $n = 66$). Thus, leaf tissue on *Vallisneria* shoots was almost entirely responsible for the weight of that shoot (94% of shoot biomass), with other shoot components (stolons and flowers) contributing little to total shoot biomass. Therefore, no further attempt was made to partition *Vallisneria* shoot biomass. Averaging across the entire data set of harvested shoots, mean mass per live *Vallisneria* leaf was 0.24 g and the mean mass per dead leaf in standing litter was 0.21 g (Table 3.1).

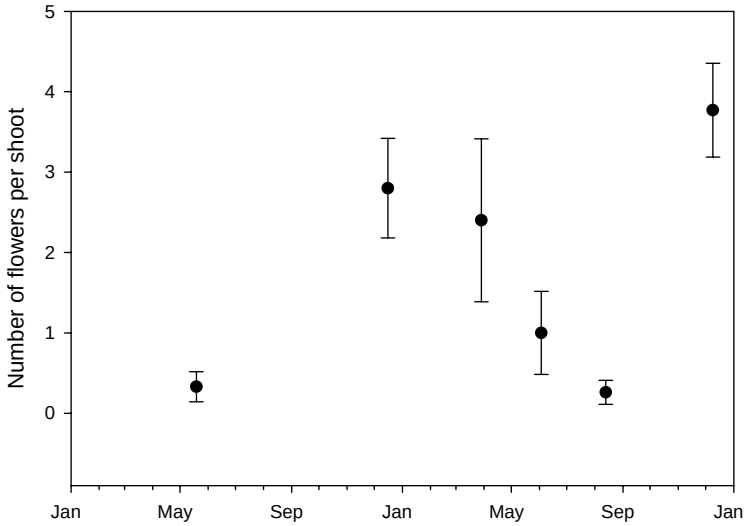

Figure 3.11. Changes to numbers of flowers per *Vallisneria* shoot over time (means ± standard error).

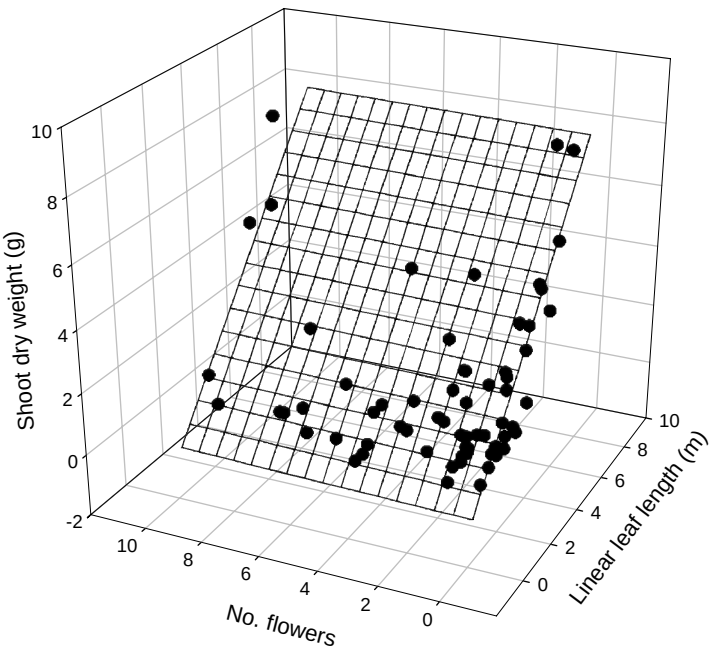

Figure 3.12. Relationship between linear leaf length, number of flowers & shoot dry weight for *Vallisneria*. For a given linear leaf length, shoots with more flowers were slightly heavier than those with few flowers.

3.3.1.4 Persicaria

Persicaria shoots were the smallest of all species studied, with a mean dry mass of 0.64 g per shoot (Figure 3.1, Table 3.1; $p < 0.0001$, $F = 82.86$, $n = 283$). No attempt was made to partition this biomass or monitor changes over time. Later modelling of OM inputs from this species utilised mean areal biomass, calculated as 297.30 g/m^2.

3.3.2 Litter Partitioning

3.3.2.1 Phragmites

Estimates of shoot component masses shed from standing shoots were based on pooled data from BRO and BAR for *Phragmites*. Mass losses over time for different biomass components were converted to percent of initial component mass (Figure 3.13). Exponential decay curves fit to this data allowed prediction of proportional losses of different biomass components over time (BLADES: $R^2 = 0.91$, $p < 0.0001$, $F = 89.57$, $n = 10$; SHEATHS: $R^2 = 0.90$, $p < 0.0001$, $F = 74.23$, $n = 9$; STEMS: $R^2 = 0.70$, $p < 0.005$, $F = 19.63$, $n = 9$) (Table 3.4).

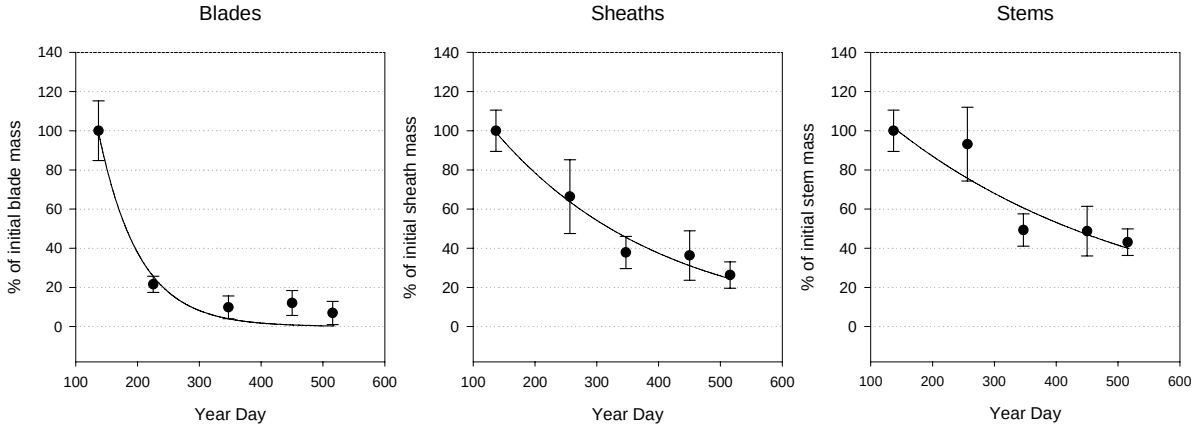

Figure 3.13. Proportions of initial *Phragmites* shoot component masses remaining on shoots over time (pooled site data) (points are means ± standard error, lines are fitted functions).

Table 3.4. Percentages of different macrophyte biomass components lost from shoots over 1 year.

Tissue Type	Phragmites ++	Typha ++	Vallisneria *
Blade	99.6%	83.4%	100%
Sheath	74.1%	78.7%	na
Stem	58.4%	0%	na
Flower	Id	92.2%	id

++ based on exponential curves fit to % initial biomass component data lost over time
* based on estimated turnover times calculated from Blanch et al., 1998
na = not applicable; id = insufficient data

For *Phragmites*, 58% of the initial stem biomass was lost from standing shoots to the litter pool over 12 months, compared to 99% for blades and 74% for sheaths (Table 3.4). Insufficient data were available to assess other biomass components. Using known initial masses of the different tissue types, the mass ratios in litter were predicted to comprise 31% blades, 21% sheaths and 48% stems. Comparisons of these predictions to measurements of standing litter in *Phragmites* beds revealed substantial differences, with *Phragmites* litter from August 2002 comprising 80% blades, 11% sheaths and 5% stems (with some minimal representation of reproductive structures) (Table 3.5). Reasons for this discrepancy are considered in the discussion section of this chapter.

Table 3.5. Litter composition for different species (means ± standard error of the mean with sample size in parentheses).

Tissue Type	Typha	Phragmites	Vallisneria *
Collection Date	Aug 2002	Aug 2002	May 2001
Blades	81% ± 4.9% (3)	80% ± 3.1% (6)	100%
Sheaths	14% ± 3.9% (3)	11% ± 1.6% (6)	0
Stems	2% ± 1.6% (3)	5% ± 1.7% (6)	0
Flowers	0	0% ± 0.04% (6)	0
Rhizomes/roots	0	0	0
Other	3% ± 1.5% (3)	4% ± 1.0% (6)	Biofilm

* based on examinations of standing litter collected in the field for the presence of different shoot components – no measurements of mass ratios were performed for this species

3.3.2.2 Typha

After 12 months, an average of 40 g of *Typha* blade biomass per shoot had been shed, compared to 25 g of sheath material (Figure 3.6). Stem mass per shoot (where present) was relatively stable after senescence (August onwards), whereas flower mass decreased (Figure 3.7). Insufficient data were available to assess other biomass components. When plotted as percent of initial mass for each component versus time (Figure 3.14), exponential decay curves provided good fit to the blade and sheath data (BLADES: $R^2 = 0.97$, $p < 0.005$, $F = 132.70$, $n = 5$; SHEATHS: $R^2 = 0.88$, $p < 0.05$, $F = 30.16$, $n = 5$). Curve fit for flowers was less robust ($R^2 = 0.81$, $p < 0.1$, $F = 18.61$, $n = 5$), while changes to proportional stem mass over time were not significantly different from zero (Figure 3.14)

Curves allowed prediction of degree of contribution to the litter pool of each biomass component, with 83% of initial blade biomass, 79% of initial sheath biomass and 92% of initial flower biomass lost from shoots to the litter pool over 1 year; stems making little if any contribution over this time (Table 3.4). The contribution of flowers to the litter pool would be in the form of seed and frass, and may be difficult to detect in litter collections.

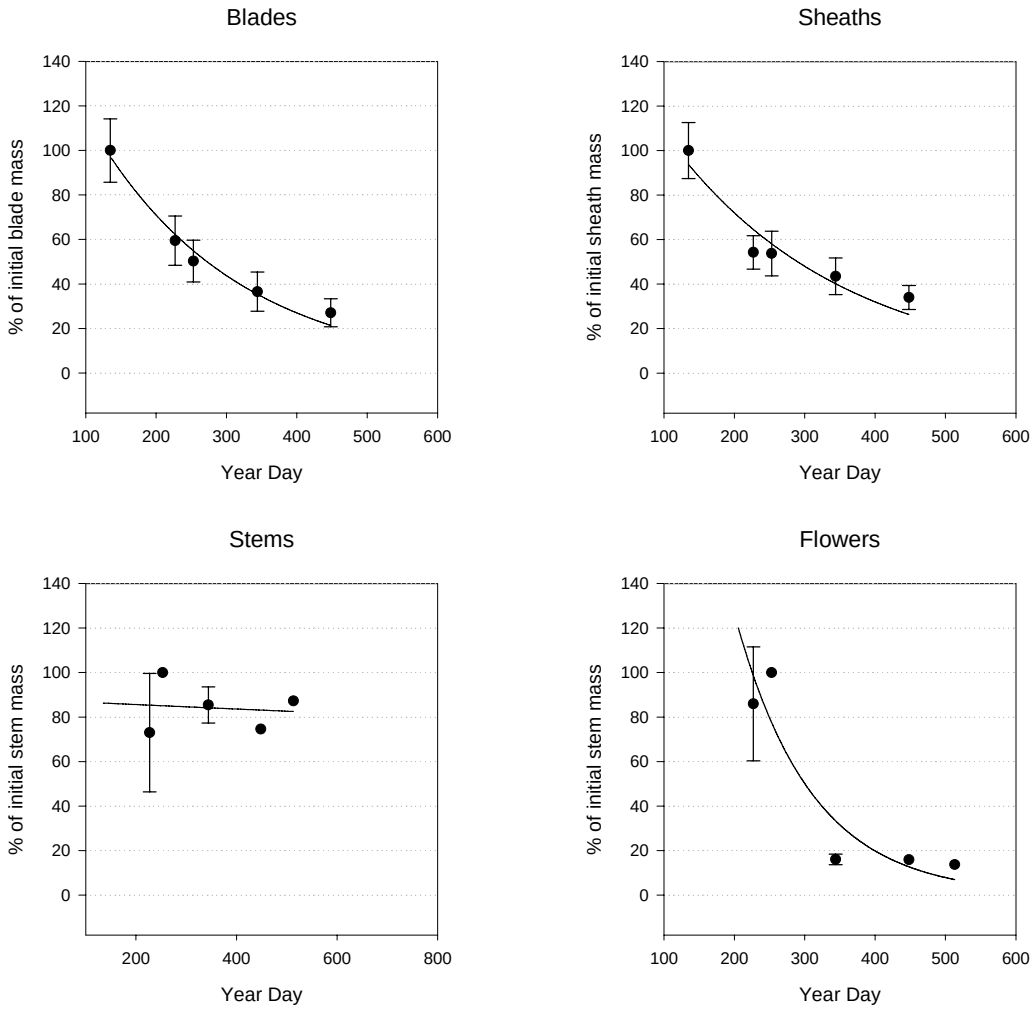

Figure 3.14. Proportions of initial *Typha* shoot component masses remaining on shoots over time (points are means ± standard error, lines are fitted functions).

Assuming the ratios of input to the litter of the other components, and using known initial masses of tissue, the predicted mass ratios of components in litter were 61% blades, 39% sheaths and 0% stems. Again, measured mass ratios of different shoot components in collected litter were quite different to those predicted, comprising 81% blades, 14% sheaths and 2% stems (Table 3.5). The predicted and actual estimates of litter composition did agree, however, that blades and sheaths comprise the vast majority of litter in this species, and that *Typha* stem biomass does not contribute substantially to litter accumulation over 12 months (and more likely 2 – 3 years). While reproductive structures may contribute substantially to the litter pool (15 g per reproductive shoot), reproductive density during the current project did not allow the accumulation of enough data to enable modelling of this component. Therefore, later work modelling litter accumulation in this species focused on blades and sheaths and did not include stems or flowers.

3.3.2.3 Vallisneria

A leaf turnover rate for *Vallisneria* applicable to the study site of 0.037 blades/shoot/d was obtained from the literature (Blanch et al., 1998). Given the mean number of leaves per shoot observed in this study (9.58), leaf replacement would occur every 28 days, and hence total shoot turnover (and hence loss to the litter pool) every 260 days. Thus, 100% of initial shoot leaf mass would easily be shed in the 12 month window of interest to this study (Table 3.4). The presence of different shoot components was noted from collections of material trapped in the canopy of *Vallisneria* beds. Of the three shoot components recognised in this study for this species, only leaves were present in *Vallisneria* litter in collections made in May 2001 (Table 3.5). Biofilm, which grows with increasing density on aging *Vallisneria* leaves, was also noted within *Vallisneria* litter collections.

3.3.3 Tissue Nutrients

3.3.3.1 Phragmites

Percent tissue carbon and phosphorus contents of dead *Phragmites* blades were significantly lower than those of live blades (Table 3.6 and 3.7; CARBON: $p < 0.05$, $F = 10.53$, $n = 9$; PHOSPHORUS: $p < 0.01$, $F = 15.87$, $n = 9$). While the mean nitrogen content of dead *Phragmites* blades was lower than live blades, this difference was not statistically significant (Table 3.8; $p = 0.08$, $F = 4.15$; $n = 9$).

Table 3.6. Carbon composition (%C) of different tissue types (means ± standard error of the mean with sample size in parentheses).

Tissue Type	Typha	Phragmites	Persicaria	Vallisneria
Blade Dead	40.58 ± 2.44 (9)	34.26 ± 1.21 (6)	nd	nd
Blade Live	45.29 ± 0.42 (3)	41.92 ± 2.39 (3)	nd	27.96 ± 1.38 (9)
Sheath Dead	42.06 ± 2.26 (9)	37.11 ± 1.80 (9)	nd	nd
Sheath Live	43.33 ± 1.96 (3)	34.33 ± 3.92 (3)	nd	nd
Stem Dead	46.25 ± 1.05 (6)	32.98 ± 3.65 (6)	nd	nd
Stem Live	38.17 ± 7.12 (3)	28.83 ± 2.53 (3)	nd	nd
Shoot Dead	41.67	33.96	42.50 ± 2.78 (3)	na
Shoot Live	42.91	33.84	39.67 ± 5.34 (3)	27.96 ± 1.38 (9)

nd = no data; na = not applicable

Table 3.7. Phosphorus composition (%P) of different tissue types (means ± standard error of the mean with sample size in parentheses).

Tissue Type	Typha	Phragmites	Persicaria	Vallisneria
Blade Dead	0.099 ± 0.016 (9)	0.066 ± 0.006 (6)	nd	nd
Blade Live	0.260 ± 0.058 (3)	0.188 ± 0.045 (3)	nd	0.261 ± 0.022 (9)
Sheath Dead	0.046 ± 0.007 (9)	0.039 ± 0.006 (9)	nd	nd
Sheath Live	0.043 ± 0.001 (3)	0.112 ± 0.008 (3)	nd	nd
Stem Dead	0.238 ± 0.028 (6)	0.023 ± 0.004 (6)	nd	nd
Stem Live	0.563 ± 0.087 (3)	0.072 ± 0.004 (3)	nd	nd
Shoot Dead	0.092	0.028	0.133 ± 0.013 (3)	na
Shoot Live	0.155	0.108	0.253 ± 0.020 (3)	0.261 ± 0.022 (9)

nd = no data; na = not applicable

Table 3.8. Nitrogen composition (%N) of different tissue types (means ± standard error of the mean with sample size in parentheses).

Tissue Type	Typha	Phragmites	Persicaria	Vallisneria
Blade Dead	0.092 ± 0.043 (9)	0.645 ± 0.149 (6)	nd	0.099 ± 0.023 (9)
Blade Live	0.493 ± 0.236 (3)	1.333 ± 0.393 (3)	nd	0.280 ± 0.053 (9)
Sheath Dead	0.219 ± 0.029 (9)	0.531 ± 0.037 (9)	nd	nd
Sheath Live	0.150 ± 0.026 (3)	0.667 ± 0.033 (3)	nd	nd
Stem Dead	0.282 ± 0.119 (6)	0.176 ± 0.030 (6)	nd	nd
Stem Live	0.830 ± 0.329 (3)	0.382 ± 0.053 (3)	nd	nd
Shoot Dead	0.158	0.259	0.045 ± 0.018 (3)	na
Shoot Live	0.291	0.704	0.430 ± 0.015 (3)	0.280 ± 0.053 (9)

nd = no data; na = not applicable

Over the course of 12 months, no change in percent carbon composition of dead blades was observed, whereas N% significantly decreased ($p < 0.001$, $F = 98.06$, $n = 6$) and percent phosphorus significantly increased ($p < 0.0001$, $F = 624.10$, $n = 6$) (Figure 3.15).

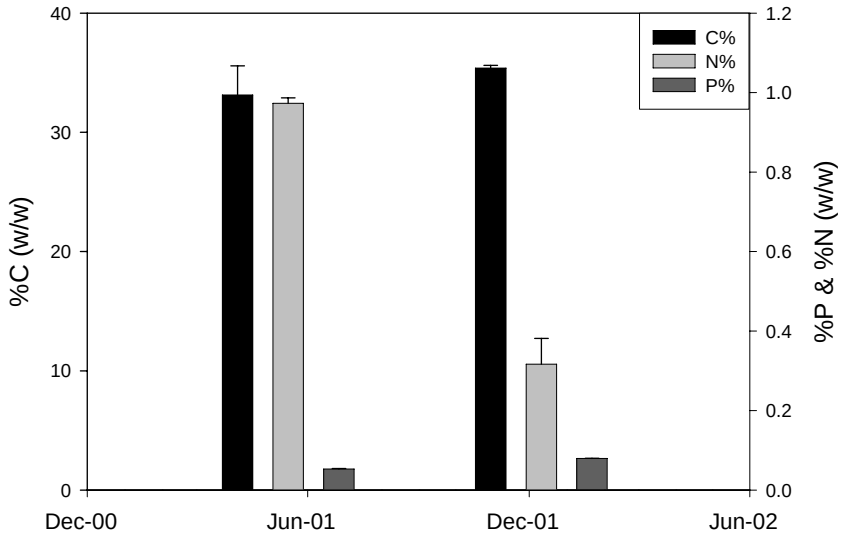

Figure 3.15. Variation in tissue nutrient composition of dead *Phragmites* blades over 12 months (means ± standard error). No dead blades were attached to shoots by May 02, and hence no nutrient data was able to be obtained.

While %P was higher in live *Phragmites* sheaths than dead ($p < 0.0005$, $F = 35.75$, $n = 12$), there were no significant differences in %C or %N (Table 3.6, 3.7 & 3.8). No significant changes to the %C, %N or %P content of dead sheaths occurred over time (Figure 3.16).

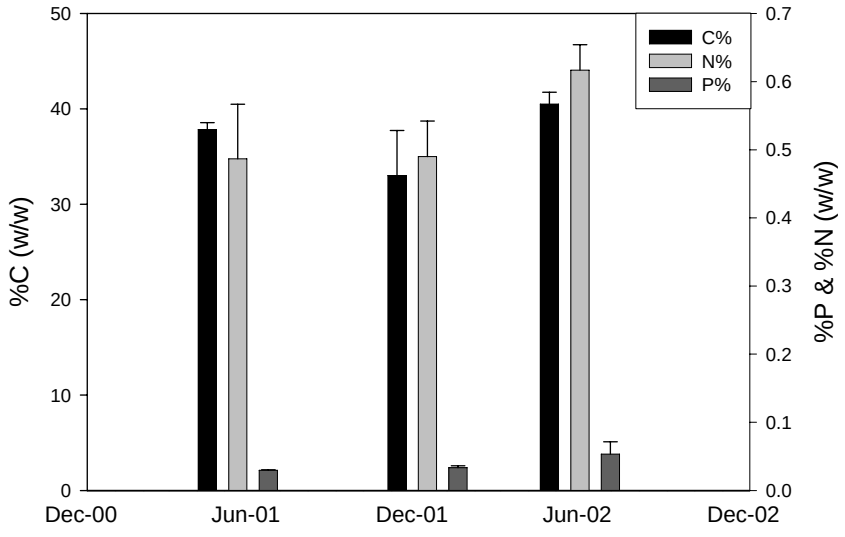

Figure 3.16. Changes to tissue nutrient composition of dead *Phragmites* sheaths over 12 months (± s.e.).

Both nitrogen and phosphorus content were higher in live *Phragmites* stems than dead (NITROGEN: $p < 0.05$, $F = 10.40$, $n = 9$; PHOSPHORUS: $p < 0.0005$, $F = 54.58$, $n = 9$; Tables 3.7 and 3.8), whereas carbon content was not significantly different (Table 3.6). Concentrations of all three nutrients in dead stems were stable over the time period assessed (Figure 3.17).

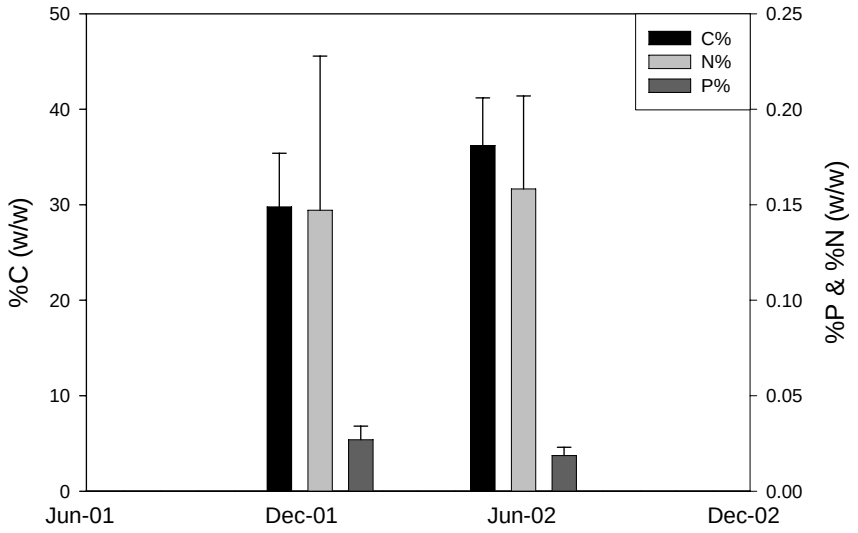

Figure 3.17. Changes to tissue nutrient composition of dead *Phragmites* stems over 12 months (means ± s.e.). No dead stems were present in May 01 on which to perform analyses of tissue nutrient composition.

Carbon to nitrogen and carbon to phosphorus ratios of different *Phragmites* tissues varied considerably, driven mostly by changes in N and P content while C was relatively similar (Table 3.9). Dead tissues always had higher C:N, C:P and N:P ratios than their live counterparts. Dead stems had the highest C:N ratio (188:1) whereas live blades had the lowest (31:1). Dead stems had high C:P (1,445:1) compared to live blades (223:1) and live sheaths (307:1). Nitrogen to phosphorus ratios ranged from 5.3 in live stems to 13.7 in dead sheaths (Table 3.9).

The nutrient composition of whole *Phragmites* shoots was estimated by combining biomass composition data for live and dead shoots with nutrient content data for each biomass partition (using stem nutrient values for flowers). Live *Phragmites* shoots were thus estimated to be comprised of 33.8 % C, 0.7 % N and 0.1 % P. Dead shoots had similar C (33.96%) but lower N (0.26%) and P (0.03%) (Tables 3.6, 3.7 and 3.8). The C:N:P ratios of live and dead shoots were 313:7:1 and 1,200:9:1, respectively (Table 3.9)

Table 3.9. Nutrient ratios of different macrophyte tissue types.

Species	Tissue	C:N	C:P	N:P	C:N:P
Phragmites	Blade Live	31	223	7.079	223:7:1
Phragmites	Blade Dead	53	518	9.748	518:10:1
Phragmites	Sheath Live	52	307	5.952	307:6:1
Phragmites	Sheath Dead	70	956	13.677	956:14:1
Phragmites	Stem Live	76	399	5.276	400:5:1
Phragmites	Stem Dead	188	1,445	6.689	1,445:7:1
Phragmites	Shoot Live	48	313	6.516	313:7:1
Phragmites	Shoot Dead	131	1,197	9.128	1,200:9:1
Typha	Blade Live	92	174	1.897	174:0:1
Typha	Blade Dead	440	409	0.930	409:1:1
Typha	Sheath Live	289	1,016	3.516	1,016:4:1
Typha	Sheath Dead	192	923	4.805	923:5:1
Typha	Stem Live	46	68	1.473	68:1:1
Typha	Stem Dead	164	194	1.182	194:1:1
Typha	Shoot Live	148	277	1.879	277:2:1
Typha	Shoot Dead	265	455	1.721	455:2:1
Vallisneria	Blade Live	100	107	1.074	107:1:1
Persicaria	Shoot Live	92	157	1.697	157:2:1
Persicaria	Shoot Dead	944	319	0.338	319:0:1
Redfield					**106:16:1**

3.3.3.2 Typha

Despite an apparent decrease in nitrogen and phosphorus content of dead *Typha* blades over the study period (Figure 3.18), significant differences in percent carbon, nitrogen or phosphorus were not detectable over 12 months. Therefore, sample replicates for dead blades were pooled to obtain overall means for tissue nutrients. Mean carbon contents of live and dead *Typha* blades were similar (45 and 41 %C, respectively), while dead blades had just under half the phosphorus content (0.10 %P) and one fifth of the nitrogen content (0.09% N) of live blades (0.26 %P and 0.49% N) (PHOSPHORUS: $p < 0.005$, $F = 14.91$, $n = 12$; NITROGEN: $p < 0.05$, $F = 6.29$, $n = 12$) (Table 3.6, 3.7). The carbon contents of *Typha* blades were similar to those of *Phragmites* blades, and while phosphorus was slightly higher in *Typha* blades than their counterparts in *Phragmites*, these differences were not statistically significant. Absolute nitrogen concentrations in live blades were similar in *Typha* and *Phragmites*, however dead *Phragmites* blades had seven times the nitrogen of dead *Typha* blades ($p < 0.005$, $F = 15.63$, $n = 15$).

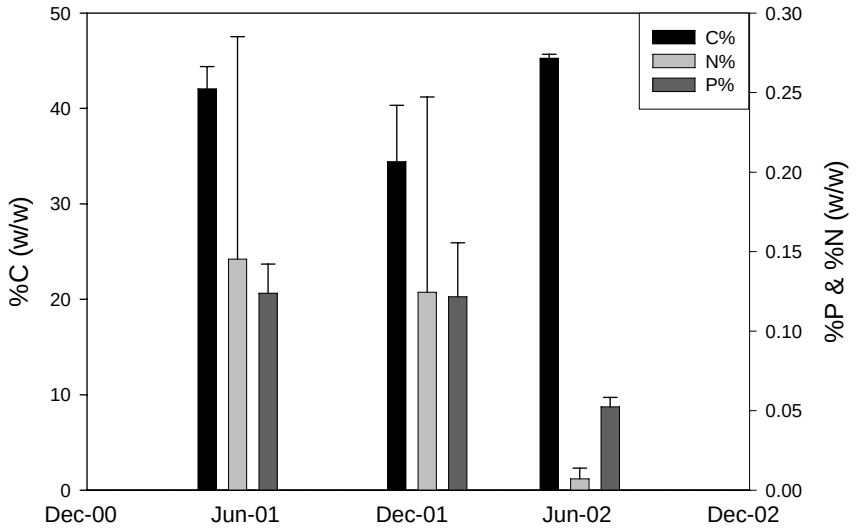

Figure 3.18. Variation in tissue nutrient composition of dead *Typha* blades over 12 months (means ± standard error).

The carbon and phosphorus contents of dead *Typha* sheaths did not change over time, and there were no significant differences in these nutrients between live and dead sheaths (Figure 3.19; Tables 3.6, 3.7 and 3.8). Despite a significant increase in nitrogen content of standing dead sheaths over time ($p < 0.05$, $F = 6.29$, $n = 9$), no significant differences were detected between %N of live and dead *Typha* sheaths at any time during the 12 months they were assessed (Table 3.8). Concentrations of nitrogen and phosphorus in live *Typha* sheaths were 3-4 times lower than in *Phragmites* tissues (NITROGEN: $p < 0.0005$, $F = 150.16$, $n = 6$; PHOSPHORUS: $p < 0.005$, $F = 73.45$, $n = 6$). Dead sheaths from *Typha* had lower nitrogen contents than from *Phragmites* ($p < 0.0001$, $F = 44.60$, $n = 18$), however phosphorus contents were about the same.

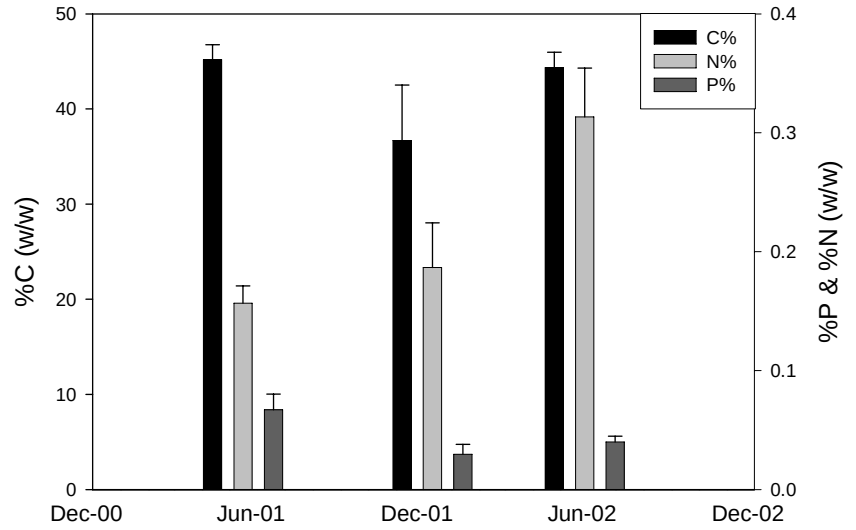

Figure 3.19. Variation in tissue nutrient composition of dead *Typha* sheaths over 12 months (means ± standard error).

No significant differences were observed in carbon or nitrogen concentrations between live and dead *Typha* stems, or in these nutrients or phosphorus content in dead stems over time (Figure 3.20; Tables 3.6 and 3.8). However %P of live *Typha* stems was twice that of dead stems ($p < 0.005$, $F = 21.14$, $n = 9$) (Table 3.7). Despite apparently higher nitrogen content in live and dead *Typha* stems than *Phragmites*, no significant differences were detected. However, phosphorus contents of *Typha* stems were 8 – 10 times those of *Phragmites* (DEAD: $p < 0.0001$, $F = 56.62$, $n = 12$; LIVE: $p < 0.005$, $F = 31.46$, $n = 6$).

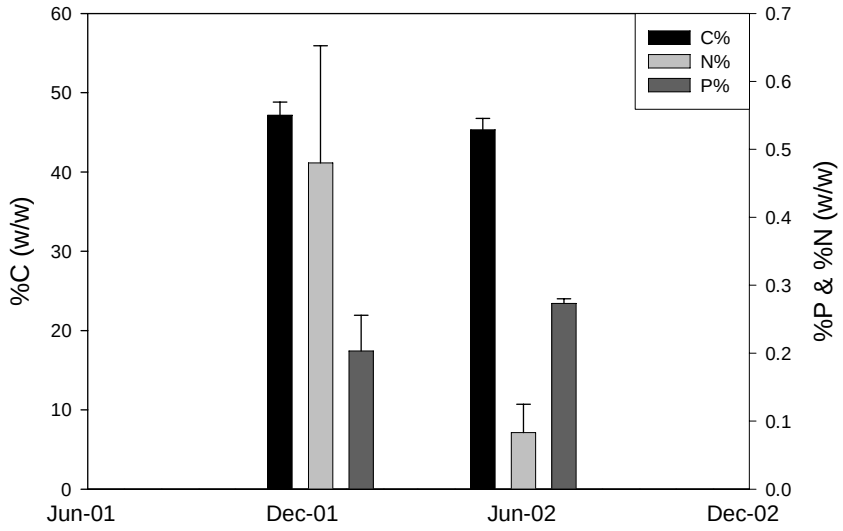

Figure 3.20. Variation in tissue nutrient composition of dead *Typha* stems over 12 months (means ± standard error). No dead stems were present in May 01 on which to perform analyses of tissue nutrient composition.

Similar to *Phragmites*, nutrient ratios in different *Typha* tissue types were dependent upon changes to nitrogen and phosphorus concentrations associated with senescence. The highest *Typha* C:N ratio, in live blades (91,804:1), was three times the *Phragmites* maximum, which also occurred in live blades (Table 3.9). The lowest C:N ratio observed in *Typha* (46:1) was associated with one of the tissue types exhibiting low a C:N ratio in *Phragmites*, live stems (76:1). Live stems also had the lowest C:P ratio of all *Typha* tissue types (68:1), with high C:P occurring in live sheaths (1,016:1). Several *Typha* tissue types exhibited very low N:P ratios – live and dead blades were below one and live and dead stems were below 1.5 (Table 3.9).

Whole *Typha* shoot nutrient compositions were estimated as 42.9 % C, 0.2 % N, 0.2 % P for live shoots and 41.2 % C, 0.2 % N, 0.1 % P for dead shoots (Tables 3.6, 3.7 and 3.8). Thus, live *Typha* shoots have similar carbon and nitrogen contents as dead shoots but higher phosphorus content. This produced marked effects on the C:N:P ratio of the different shoot types; the ratio for live shoots was 277:1:1 whereas it was 455:2:1 for dead shoots (Table 3.9).

3.3.3.3 Vallisneria

The nitrogen and phosphorus contents of live *Vallisneria* blades did not change significantly over the course of the study (Figure 3.21). However, carbon content significantly increased from May 2001 to December 2001 ($p < 0.05$, $F = 9.78$, $n = 6$), then remained stable until May 2002 (Figure 3.21). Compared to live blades from the emergent plant species (*Typha* and *Phragmites*), *Vallisneria* blades had significantly lower carbon content (PHRAGMITES: $p < 0.0005$, $F = 25.63$, $n = 12$; TYPHA: $p < 0.0001$, $F = 48.97$, $n = 12$), and significantly higher nitrogen content (PHRAGMITES: $p < 0.05$, $F = 8.61$, $n = 12$; TYPHA: $p < 0.05$, $F = 8.67$, $n = 12$) (Tables 3.6, 3.7 and 3.8). The phosphorus content of live *Vallisneria* blades was not significantly different to those of *Typha* or *Phragmites*. Given that live blades comprise the vast majority of live shoot biomass for *Vallisneria*, nutrient composition of blades was used as a surrogate for shoots in comparisons to other species. The nitrogen content of live *Vallisneria* shoots was similar to that of live *Phragmites* shoots, and higher than that of *Typha*. *Vallisneria* shoots had higher phosphorus content and lower carbon content than either *Typha* or *Phragmites* (Tables 3.6, 3.7 and 3.8). The C:N:P ratio of live *Vallisneria* blades (and hence, shoots) was 107:1:1 (Table 3.9).

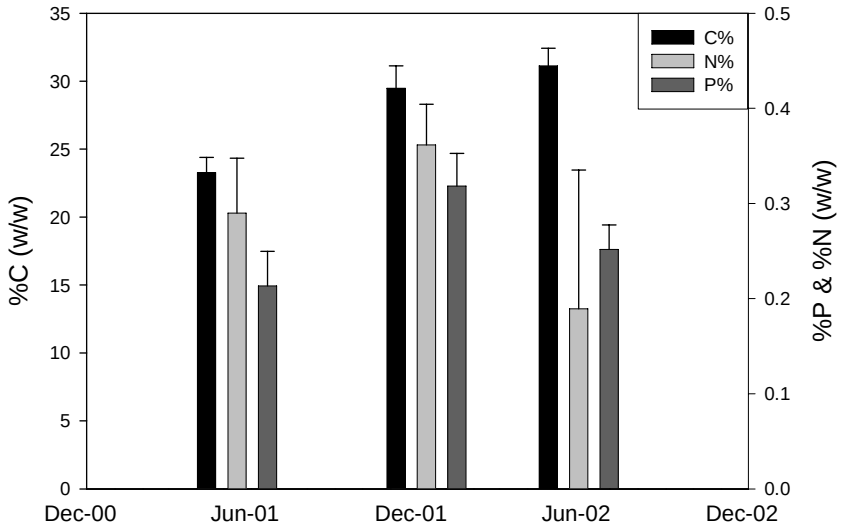

Figure 3.21. Variation in tissue nutrient composition of live *Vallisneria* blades over 12 months (means ± standard error).

3.3.3.4 Persicaria

The nutrient composition of whole *Persicaria* shoots was assessed, rather than individual biomass partitions. No significant differences were detected in carbon content of live and dead shoots (Table 3.6). The nitrogen and phosphorus contents of live shoots were significantly higher than dead shoots (tenfold and doubled differences, respectively) (NITROGEN: $p < 0.0001$, F

= 260.20, n = 6; PHOSPHORUS: $p < 0.01$, $F = 24.45$, n = 6) (Tables 3.7 and 3.8). Although not tested statistically as shoot nutrient compositions for other species were estimated, live *Persicaria* shoots had the highest nitrogen content of all species assessed, and the second highest phosphorus content (after *Vallisneria*) (Tables 3.7 and 3.8). While the phosphorus content of dead *Persicaria* shoots was the highest of all species assessed, the nitrogen content was the lowest (Table 3.9). Nutrient ratios (C:N:P) for live and dead *Persicaria* shoots were 157:1.6:1 and 319:0.3:1, respectively (Table 3.9).

3.4 Discussion

This chapter describes the structural and nutrient composition of shoots of some macrophyte species common to south-eastern Australian lowland rivers. Comparisons were made between species, between shoots of different status (live and dead) and over time.

Substantial differences observed in total shoot masses between the different species were related to plant growth form, with emergent species having greater biomass than the submerged species or mudflat hydrophyte. This pattern supports previously described studies (e.g. Roberts and Ganf, 1986; Weisner and Miao, 2004; Xie et al., 2005). Within-species differences in shoot biomass of the two emergent species were also observed. *Phragmites* shoots at BRO were lighter than those at BAR, with proportionally smaller shoot components. *Phragmites* shoots at BRO exhibited evidence of regular disturbance which caused damage to stems (possibly grazing by cattle or breakage by sand slugs). Damage of this kind induces the production of additional stems from nodes below the damaged area in this species (Haslam, 1969; Coops, 1996; Asaeda et al., 2003; van den Wyngaert et al., 2003), resulting in the smaller, multi-stemmed shoots observed at BRO compared to the undisturbed site (BAR). Shoot and shoot component masses and nutrient composition data from plants at BAR were used for later modelling of *Phragmites* OM inputs, as it was thought that these shoots better represented the shoot type that would occur in future management scenarios (where management strategies will probably include fencing off waterways from livestock).

Disturbances may also have affected reproductive allocation of *Typha* during the study period. The production of reproductive shoots at BAR during the study period was substantially lower than in previous years (Williams, unpub. data) or at other sites (Roberts and Ganf, 1986). The ongoing drought during the study period may have been responsible for this phenomenon, with increased grazing pressure and trampling by fauna compounding stress caused by less frequent inundation. *Typha* OM inputs modelled in later chapters may thus underestimate the contribution to litter from *Typha* stems because of the low numbers of stems encountered during this project's sampling.

Aquatic plants can display substantial morphological plasticity, and water depth and nutrient availability are known to stimulate variation in the proportions of biomass allocated to above- and below-ground structures, and even to different above-ground parts of aquatic plants (Grace, 1989; Squires and Van der Valk, 1992; Coops et al., 1996; Miao and Sklar, 1998; Vretare et al., 2001; Weisner and Miao, 2004). Despite this known variability, shoot compositions observed in this study were similar to those reported elsewhere for *Phragmites* (Gessner et al., 1996), *Typha* (Miao and Sklar, 1998; Weisner and Miao, 2004) and *Vallisneria* (Xie et al., 2005).

Major changes in shoot composition occurred during senescence of *Phragmites* shoots. Mass loss of whole shoots during senescence was lower in this study (24-58%) than comparisons of dead shoot mass to maximum above-ground biomass elsewhere (74% - Hocking, 1989a), probably because live shoot masses were not determined during peak biomass period in this study. While 50% of above-ground shoot biomass was stems in live *Phragmites* shoots, which is lower than reported elsewhere (Sakurai et al, 1985; Hocking, 1989a; Asaeda and Karunaratne, 2000; Soetaert et al., 2004), the vast majority of dead shoot biomass was comprised of stem tissue (73%). The proportion of shoot biomass comprised of sheath tissue remained fairly constant during senescence, with a transition from the live to dead pool occurring, and dead sheaths generally remaining attached to the stems (as per Gessner et al., 1996). The major change in *Phragmites* shoot biomass allocation during senescence was in the proportion of blade tissue – 32% of live shoots were comprised of blades (similar to literature values - Sakurai et al, 1985; Hocking, 1989a; Asaeda and Karunaratne, 2000; Soetaert et al., 2004), compared to 4% in dead shoots. In my study, this was due to both a reduction in mass per leaf blade and the rapid loss of the majority of blades to the litter pool. Other work on *Phragmites* reported similar blade mass losses during senescence (20-30%), but with little associated litter production (Gessner, 2001). This may be related to the size and level of disturbance of *Phragmites* beds studied – Gessner worked in large beds in a lake whereas the present study examined fringing reeds along a large river. Physical disturbance by wind, flow, fauna, etc. would affect a far greater proportion of plants within fringing versus large reed beds, causing the fragile leaf blades to break off more easily.

Changes to shoot composition upon senescence were less dramatic in *Typha*. Similar total proportions of blade and sheath tissues occurred in live and dead shoots, with values similar to those reported in the literature (Shaver and Melillo, 1984; Miao and Sklar, 1998; Weisner and Miao, 2004). Thus, each *Typha* shoot retained its total complement of blades and sheaths for a longer period than *Phragmites*. Large differences were apparent in the proportions of stem and flower between live and dead reproductive shoots, with substantial losses of *Typha* stem and

flower biomass upon senescence. Although not explicitly quantified in this study, no obvious changes in *Typha* stem height were observed over the course of the study as in *Phragmites*, and stem mass stabilised when these shoots were fully dead. This indicates that stem mass losses were probably not due to direct transfer to the litter pool of stem tissues. The initial loss of *Typha* stem biomass may be related to the translocation of stem resources either to reproductive tissues or to the rhizome in preparation for over-wintering (Hocking, 1989; Boar, 1996; Gessner, 2001; Soetaert et al., 2004; Weisner and Miao, 2004). Retention of standing dead stems in *Typha* until major disturbance has been reported elsewhere (Welsch and Yavitt, 2003). Alternatively, stems (which are the last tissue type to complete senescence) may exist in a metabolically stressed condition for periods of weeks during senescence, with respiration requirements continuing but no on-going photosynthetic production. Thus, respiration of biomass during senescence may account for some stem mass loss in this species.

While several biomass partitions were identified for *Vallisneria* shoots (leaves, stolons, flowers), and some seasonality was apparent in their occurrence and morphology, leaves comprised the vast majority of shoot biomass for live *Vallisneria* shoots in this study (c.f. Madsen and Cedergreen, 2002; Xie et al., 2005). As previously described, this phenomenon may be related to the environmental conditions experienced by plants at the study site, where water depths were never extreme during the study period (max depth of 0.96 m) but turbidity was often quite high (mean of 70 NTU) (Gigney, pers. comm.).

Although usually not quantified in the literature, the shoot components considered important contributors to litter can be deduced from the tissues selected for use in studies of litter decomposition. Most studies of *Phragmites* assume that blades are the major contributor to litter, although stems (sometimes with sheaths attached) have also been considered (Hietz, 1992; Gessner et al., 1996; Gessner, 2000; Gessner, 2001; Asaeda et al., 2002; Dinka et al., 2004; Soetaert et al., 2004). Similar shoot components were found to be important to *Phragmites* litter production in this study. For *Typha* and *Vallisneria*, litter studies generally focus on blade tissues (Ennabili et al., 1998; Miao and Sklar, 1998; Welsch and Yavitt, 2003; Goncalves et al., 2004; Xie et al., 2004). In contrast, the current study found that sheaths and flowers may also make substantial contributions to litter production in *Typha*.

Using the biomass allocation data for *Phragmites* and *Typha* obtained in the present study, conceptual models of changes to shoot composition during senescence and litter production were developed for these species (Figure 3.22, 3.23). Rapid and comprehensive senescence of blades and sheaths (transition from the live to dead pool) is followed by either rapid (*Phragmites*) or gradual (*Typha*) loss of the majority of blade tissue. Sheath tissue is then shed gradually in both species, although *Phragmites* tends to retain sheath tissue to a greater

degree than *Typha*. Sheath loss in *Phragmites* is usually associated with stem breakage (evidenced by a decrease in number of nodes per stem – data not shown). Shoot "stumps", comprised of dead sheath bases in *Typha* and dead stems in *Phragmites*, can remain standing in macrophyte beds for several years (Hocking et al., 1983; Polunin, 1984; Coops, 1996; Asaeda et al., 2002; Dinka et al., 2004).

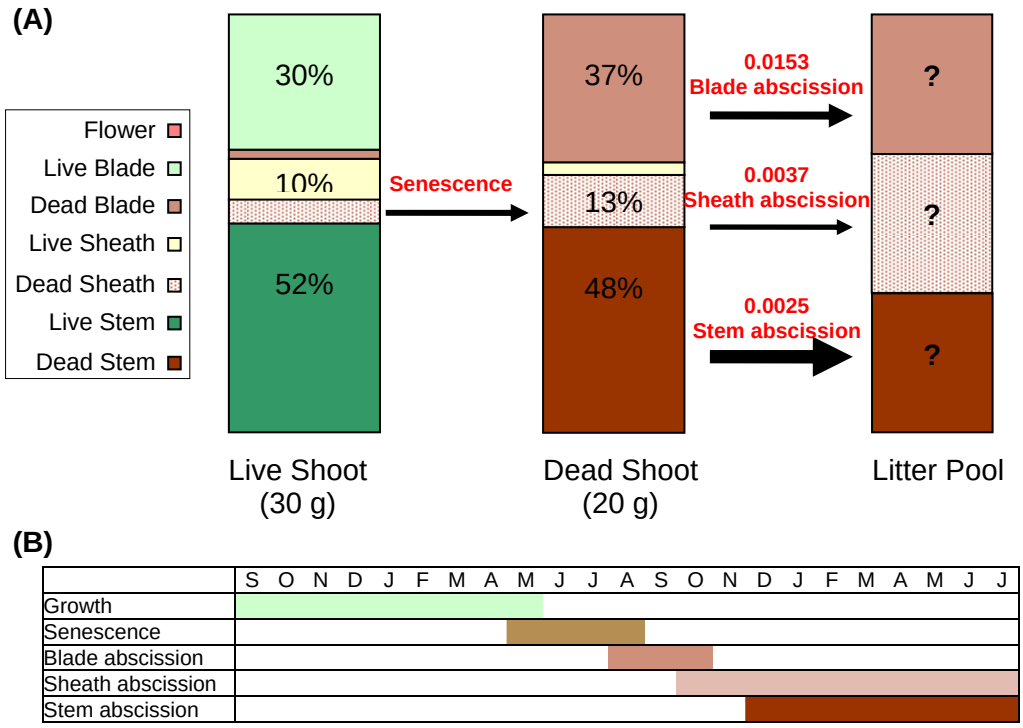

Figure 3.22. Model of biomass allocation and transformation in a single cohort of *Phragmites* shoots: A) pools and processes; B) timing of processes. Pools are represented by boxes and processes by labelled arrows; arrow width is indicative of process magnitude and values show rate coefficients from exponential decay curves. Shoot components contributing less than 10% to total shoot biomass are not shown. Dead shoot composition prior to abscission of any shoot components was estimated from measured values.

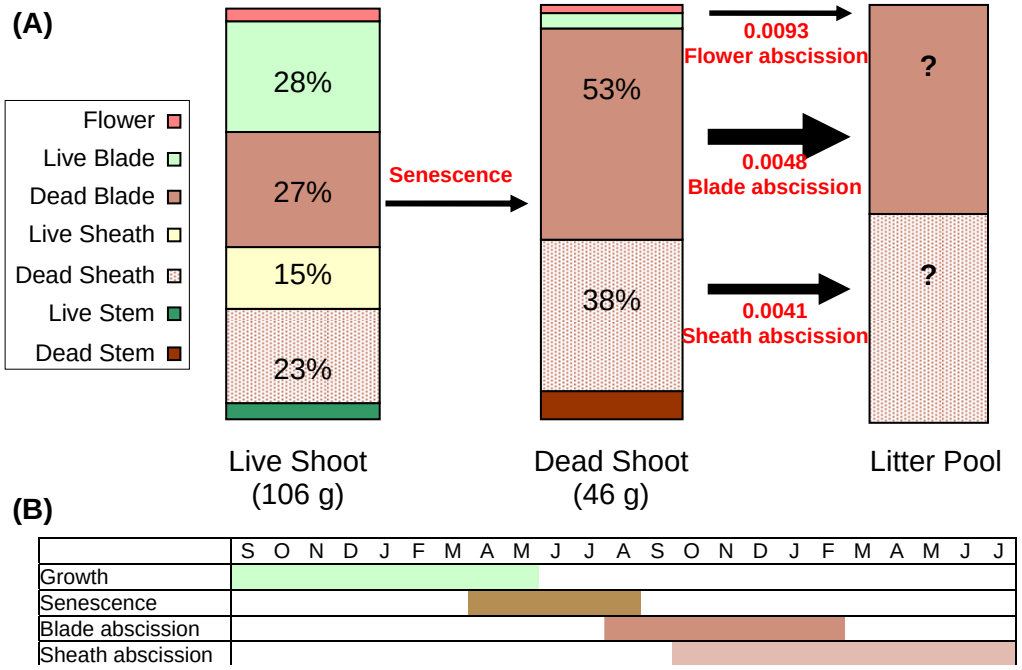

Figure 3.23. Model of biomass allocation and transformation in a single cohort of *Typha* shoots: A) pools and processes; B) timing of processes. Pools are represented by boxes and processes by labelled arrows; arrow width is indicative of process magnitude and values show rate coefficients from exponential decay curves. Shoot components contributing less than 10% to total shoot biomass are not shown. Dead shoot composition prior to abscission of any shoot components was estimated from measured values.

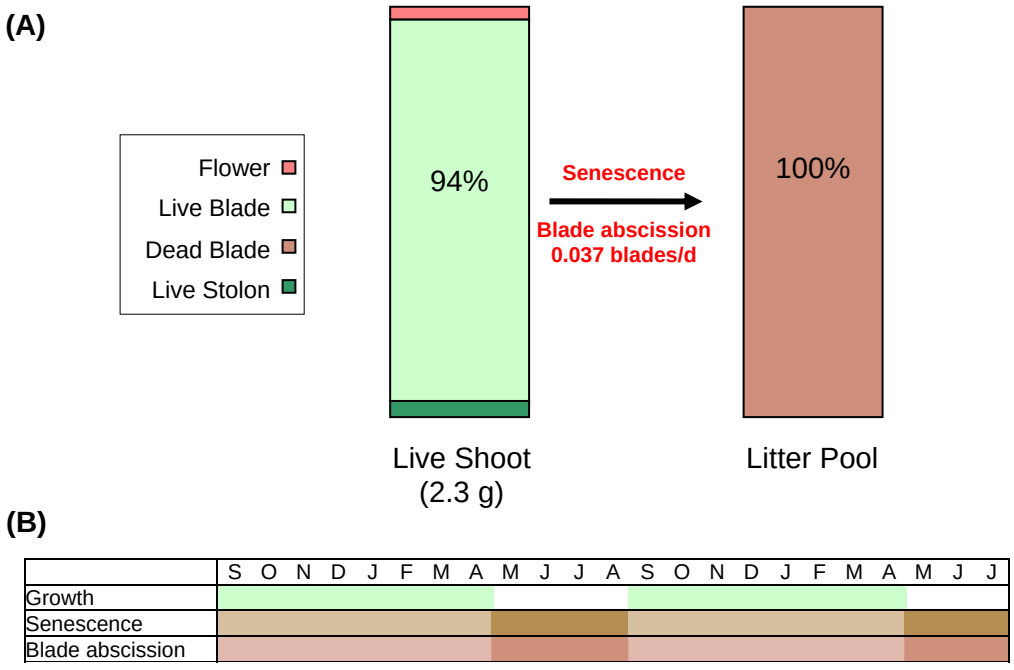

Figure 3.24. Model of biomass allocation and transformation in *Vallisneria* shoots: A) pools and processes; B) timing of processes. Pools are represented by boxes and black text while processes by red text and arrows – arrow width is indicative of process magnitude. No values are shown for shoot components contributing less than 10% to total shoot biomass.

A conceptual model of senescence and litter production was also developed for *Vallisneria* (Figure 3.24). Standing dead biomass generally does not occur in this species; rather, organic matter passes directly from live, attached biomass to the litter pool. Senescence and abscission of litter components (mostly leaf blades) occur throughout the year, peaking in winter.

Measured mass ratios of shoot components in collected *Phragmites*, *Typha* and *Vallisneria* litter were quite different to predictions based on proportional losses from shoots over time. This may reflect the timing of the collection in relation to plant growth and litter production cycles, variable decomposition rates or flow-related displacement of litter elsewhere in the system (although a brief field experiment examining litter movement and export from macrophyte beds suggested that components underestimated in litter predictions were less subject to displacement than other tissues). Litter production and accumulation in macrophytes are obviously complex processes which cannot be easily predicted by simple models, and this study demonstrates the need for more work in this area (see Chapter 4).

The nutrient composition of shoots and their components is an important aspect of understanding shoot dynamics and litter production. Differences in carbon content of whole shoots were related to the degree of structural strengthening associated with the different growth forms, with the lowest values in the submerged *Vallisneria* and highest in the somewhat woody mudflat hydrophyte, *Persicaria*. The link between structural strengthening and carbon content is a common phenomenon in plant nutrient studies. Live and dead *Persicaria* shoots represented the extremes of nitrogen content observed in this study, with other live shoots generally higher in the order of nitrogen content ranking. *Vallisneria* shoots had the highest phosphorus concentration, and again live shoots generally tended to have higher P than dead shoots.

Several studies have reported changes in nutrient content of live macrophyte tissues throughout the growth season (e.g. Boar, 1996; Shaver and Melillo, 1984; Kohl et al., 1998; Madsen, 1991; Xie et al., 2005), although these differences are quite small at times. In contrast, studies on aerial decomposition and leaching by rainfall of standing dead macrophyte OM indicate that substantial changes to tissue nutrient composition can occur in these circumstances (e.g. Hietz, 1992; Kuehn and Suberkropp, 1998; Kuehn et al., 1999; Gessner, 2001; Newell, 2001; Welsch and Yavitt, 2003). Therefore, live tissues were not analysed for temporal variation in nutrient composition in this study but dead tissues were.

Nutrients in live tissues are thought to be translocated to storage structures during senescence (Gessner, 2001; Soetaert et al., 2004). Studies have demonstrated substantial differences between N and P content of live and dead macrophyte tissues (Shaver and Melillo, 1984; Hietz, 1992; Boar, 1996; Gessner, 2001; van den Wyngaert et al., 2003). With the exception of *Typha* sheaths, the phosphorus contents of all tissue types assessed in this study

were two to three times higher in live tissues than in dead. Nitrogen contents of dead tissues were either similar to their live counterparts (*Phragmites* and *Typha* sheaths) or two to four times lower than their live counterparts (although dead *Persicaria* shoots had one tenth of the nitrogen of live *Persicaria* shoots).

Nutrient composition values for species in the current study were generally similar to, although often at the lower end of, ranges reported in the literature (Table 3.10), although it should be noted that there were large gaps in the data available for some tissue types and species. The low levels of nutrients, and particularly nitrogen, in macrophyte tissues in the current study may be due to trophic status of the study sites or timing of sampling. Relationships have been found between macrophyte tissue N content and the concentration of nitrogen in surrounding waters and sediments (Boar, 1996; Miao and Sklar, 1998; Xie et al., 2005). It might be expected for plants at BAR to have N values at the low end of published ranges, given that this site has low nitrogen concentrations in the water column and surrounding sediments (Gigney, pers. comm.). However specimens from BRO also had low tissue nitrogen concentrations, despite medium levels in the water column at this site (Gigney, pers. comm.).

A possible explanation for the low N content of live *Typha* and *Phragmites* blades in this study is that the plants had already translocated the majority of N to rhizomes by the time that sampling of live tissues took place, given that macrophyte N content is known to vary throughout the growth season (Boar, 1996), with rhizomes recovering up to 65% of shoot N (Hocking, 1989; Gessner, 2001; Soetaert et al., 2004). The nitrogen content of *Vallisneria* blades was also quite low in this study compared to other work (Xie et al., 2004; Xie et al., 2005). For live blades, this may relate to the nutrient status of the study sites, while time of collection (and hence degree of prior leaching and microbial uptake of tissue N) may also be affecting dead *Vallisneria* N content.

Nitrogen availability is often suggested as a limiting factor for breakdown rates of particulate organic matter (POM) (Kaushik and Hynes, 1971; Carpenter and Adams, 1979; Godshalk and Wetzel, 1978b), and C:N ratio is often used as an indicator of OM bio-availability (Gessner et al., 1996). While some studies support a similar situation for phosphorus (Kaushik and Hynes, 1971; Elwood et al., 1981), others have not found this link (Carpenter and Adams, 1979; Howarth and Fisher, 1976). Carbon to nitrogen ratios determined for macrophyte tissues in this study were generally higher than those reported elsewhere, although the range of tissue types described in the literature is limited and mostly comprise dead samples (Polunin, 1982; Hietz, 1992; Gessner, 2000; Xie et al., 2004). In contrast, C:P values presented in this chapter were generally comparable to, but often much lower than, literature values (Hietz, 1992; Gessner, 2000; Xie et al., 2004).

Table 3.10. Nutrient composition ranges of macrophyte shoots from the present study compared to literature values.

	Live			Dead			
Species	%C	%N	%P	%C	%N	%P	Source
Phragmites	29 – 42	0.4 – 1.3	0.07 – 0.19	33 – 34	0.1 – 0.7	0.02 – 0.07	this study
	46	1.0 – 4.0	0.09 – 0.50	40 – 46	0.1 – 1.3	0.03 – 0.15	2, 3, 4, 6, 7, 8, 10
Typha	46	0.2 – 0.5	0.04 – 0.56	41	0.1 – 0.3	0.05 – 0.24	this study
	n.d.	0.5 – 4.7	0.04 – 0.55	40 – 45	0.2 – 1.5	0.06 – 0.30	1, 4, 5, 9, 11
Vallisneria	28	0.3	0.26	n.d.	0.1	n.d.	this study
	n.d.	3.8 – 5.8	0.27 – 0.50	33	4.3	0.42	12, 13
Persicaria	40	0.43	0.25	43	0.05	0.13	this study
	n.d.	n.d.	n.d.	n.d.	n.d.	n.d.	no lit vals

1 Shaver and Melillo, 1984
2 Hietz, 1992
3 Boar, 1996
4 Ennabili et al., 1998
5 Miao and Sklar, 1998
6 Hocking, 1989
7 Gesssner, 2001
8 van den Wyngaert et al., 2003
9 Welsch and Yavitt, 2003
10 Dinka et al., 2004
11 Goncalves et al., 2004
12 Xie et al., 2004
13 Xie et al., 2005
n.d. = no data

Given the relatively similar carbon contents of the tissues studied, it has been assumed that higher proportions of N and P in tissues are indicative of higher bio-availability. Tissues assessed in this study which ranked highly for N content were live and dead *Phragmites* blades, live *Typha* stems, live and dead *Phragmites* sheaths, live *Typha* blades and live *Persicaria* shoots. Live *Typha* stems also ranked highly for phosphorus content, as did live *Vallisneria* blades, live *Typha* blades, dead *Typha* stems and live *Persicaria* shoots. Of those components comprising the majority of litter, only dead *Phragmites* blades ranked highly for either N or P, although dead *Vallisneria* blades may have high N and P content immediately after being shed. Thus, the majority of litter components are possibly less bio-available than some of the standing biomass (e.g. live *Typha* stems and *Persicaria* shoots), although other factors may limit the transfer and usefulness of standing live biomass to the rest of the system (e.g. active resistance to leaching and presence of chemical inhibitors) (Webster and Benfield, 1986).

Many studies have demonstrated decomposition processes occurring in standing dead plant material (mainly emergent species) prior to inundation (Boyd, 1970; Davis and Van der Valk, 1978; Bruquetas de Zozaya and Neiff, 1991; Hietz, 1992; Newell, 1993; Halupa and Howes, 1995; Barlocher and Biddiscombe, 1996; Newell et al., 1996; Samiaji and Barlocher, 1996; Kuehn and Suberkropp, 1998a; Kuehn and Suberkropp, 1998b; Kuehn et al., 1999; Gessner, 2001; Newell, 2001; Welsch and Yavitt, 2003). In this study, most of the biomass partitions monitored did not exhibit mass losses or changes to nutrient composition over time in the standing dead position (the exception being live blades in *Typha* and *Phragmites*). Thus, most tissues showed little evidence of leaching or aerial decomposition over 12 months. Reasons for this discrepancy include:

1. the processes were occurring at a rate too slow to detect using the selected methods,
2. high variability within the populations required more sampling to enable detection,
3. the processes were occurring, but other factors confounded detection.

The restricted timeline for this project meant that initial power analyses to determine the degree of replication required to detect changes over time were not performed, so it is impossible to determine if number 2 applies or not. Given that the study occurred in the middle of a drought, the lack of rainfall during the study period could certainly have reduced any leaching which might normally occur to levels below detection limits (number 1). Number 3 could also have played a role – e.g. colonisation by decomposing organisms such as fungi may have incorporated compounds taken up from plant tissues, so mass loss and nutrient changes could not be detected, although fungal respiration of plant biomass should still have caused tissue mass loss.

3.5 Conclusion

Resource allocation in aquatic plants has implications for individual shoots, plant populations and the associated ecosystem. While some aspects of resource allocation, including nutrient dynamics, have received substantial research attention, reproductive mass losses, detailed allocation changes during senescence, leaching of standing biomass and litter production dynamics are not always quantified or even estimated.

This chapter fills some of these knowledge gaps, by presenting in-depth data tracking changes in biomass allocation and nutrient composition of some macrophyte species common to south eastern Australian lowland rivers throughout their growth cycles, including determination of shoot components important to litter production over 1-2 years. Substantial differences in biomass allocation and nutrient dynamics were observed between different plant growth forms and during senescence. Growth form also had major effects on litter composition. Across all the species assessed, few shoot components showed signs of aerial decomposition over a 1-2 year time period.

As well as adding to our understanding of resource allocation dynamics in aquatic plants, the data described in this chapter allowed the development of conceptual models of biomass allocation, senescence and litter production for emergent and submerged macrophytes for use in models of macrophyte OM inputs to rivers developed in later chapters.

Chapter 4. Modelling pools and fluxes of macrophyte particulate organic matter in some south eastern Australian lowland rivers.

4.1 Introduction

Organic matter (OM) in lowland rivers can be derived from a range of sources including phytoplankton, attached algae, riparian vegetation, material transported from upstream, floodplain interaction and submerged and emergent macrophytes (Minshall et al., 1992; Thorp and deLong, 1994; Robertson et al., 1999; Gawne et al., submitted). Current management practices have changed flow patterns, diminished interactions between rivers and their floodplains, altered riparian and in-stream vegetation and removed significant quantities of wood from our rivers (Robertson et al., 1999). These have all changed the quantities, composition and timing of inputs of organic matter to our river systems.

The high productivity of macrophytes (Westlake, 1963; Keefe, 1972; Westlake, 1975; Roberts and Ganf, 1986; Wetzel, 1990; Wetzel and Howe, 1999) can represent a potentially important source of carbon for aquatic systems, even in rivers where the ratio of plant biomass to discharge is small (Gawne et al., submitted; Fisher and Carpenter, 1976). Macrophyte production is utilised by higher trophic levels (Gawne et al., in prep.), often via the microbial loop (Findlay et al,. 1986; Moran et al., 1988; Meyer et al., 1994). Fungal communities play a major role in aerial decomposition of exposed senescent plant tissues (Gessner, 2001; Newell, 2001; Welsch and Yavitt, 2003) and also have a role in aquatic decomposition (Bergbauer et al., 1992; Kuehn et al., 1999; 2000; Barlocher and Biddiscombe, 1996; Baldy et al., 1995; Weyers and Suberkropp, 1996; O'Connell et al., 2000), however bacteria are the major decomposers of inundated material (Moran and Hodson, 1989; Kominkova et al., 2000).

While some inputs of macrophyte tissue occur due to the action of wind, run-off, grazers, nesting birds or large fauna accessing the water (Newell, 1993; Newell and Barlocher, 1993), the majority of POM inputs are due to changing water levels caused, in rivers, by flow variation.

Patterns of flow in most south eastern Australian lowland rivers are determined by a combination of dam releases and tributary inputs associated with rainfall and snow melt events (AWRC, 1987). Flow variability results in varying degrees of inundation and exposure of riverine macrophyte beds throughout the year (Blanch et al., 1999b; Walker et al., 1994; Roberts and Ganf, 1986; also see macrophyte inundation modelling in Chapter 2 of this thesis), affecting inputs of particulate organic matter.

Macrophyte inputs of particulate organic matter (POM) undergo leaching to release dissolved material (DOM). Particulate inputs of above-ground biomass are comprised of standing live and dead shoots and leaf litter, which may drop directly into the water column or accumulate on the sediment surface or canopy within the macrophyte bed. Seasonal variation in above-ground biomass has been observed for many aquatic plants (Dawes and Lawrence, 1989; Kurtz et al., 2003), with light availability and temperature often cited as major drivers of shoot morphology or density changes (Blanch et al., 1998; Kurtz et al., 2003). Other factors affecting the quantity of standing live and dead macrophyte biomass in Australian lowland rivers include grazing by water rats, cattle and kangaroos; damage by water birds, burrowing animals, stock accessing water courses; tree-fall; scouring; and aerial decomposition (Newell, 1993; Newell and Barlocher, 1993). The production of leaf litter by macrophytes is associated with leaf turnover in aquatic plant species with continual leaf production and seasonal senescence patterns in plants with annual growth cycles (West and Larkum, 1979; Wahbeh, 1984; Dennison and Alberte, 1986; Christian et al., 1990; Olesen and Sand-Jensen, 1994; Newell et al., 1995; Kuehn and Suberkropp, 1998). Litter production in macrophytes is usually not monitored (Carr et al., 1997), although some studies note fragmentation of dead shoots as a cause of shoot mass loss (Welsch and Yavitt, 2003) or calculate leaf turnover rates (Blanch et al., 1998). Measurements of standing litter crop are scarce (Roberts and Ganf, 1986; Atkinson and Cairns, 2001). Some estimates of litter production are available from mass-balance models which partition annual macrophyte production into a range of potential sinks (Asaeda and Karunaratne, 2000; Asaeda et al., 2002; Soetaert et al., 2004). By not including estimates of litter production or standing stocks, the numerous studies of macrophyte litter decomposition (e.g. Davis and van der Valk, 1978; Briggs, et al., 1985; Hietz, 1992; Gessner, 2000; Titus and Pagano, 2002) fail to place their decay rates into an ecosystem perspective.

In order to understand the links between macrophyte production and other ecosystem processes and determine the relative importance of macrophyte OM to the rest of the system, a better understanding is needed of pools and fluxes of macrophyte POM in rivers. This includes changes to standing biomass and litter production over time and the quantification of POM inputs (inundation) due to flow variation.

This study aimed to advance our understanding of litter production and variation in standing biomass over time, and perform one of the first attempts at direct quantification of macrophyte POM inputs to rivers. Quantitative models developed from assessments of litter production and shoot density changes over time were used to predict the effects of flow regime on the quantity, composition and timing of organic matter inputs from macrophyte beds to lowland river channels.

4.2 Methods

4.2.1 Study Sites

Typha orientalis, Phragmites australis, *Persicaria prostrata* and *Vallisneria gigantea* were studied at lowland reaches (BAR, BRO and OVN) of three rivers (Murray, Broken and Ovens) in south eastern Australia from May 2001 – December 2002 (described in Chapter 2).

4.2.2 Modelling Approach

In order to estimate the quantity of macrophyte organic matter available for input into a river channel, mathematical functions were required to describe the standing organic matter pool (standing shoot biomass) expected at a given time and the quantity of litter produced/ accumulated between two specified time points. The different growth forms of the species chosen for study meant that different approaches were required for measuring each growth form. The large, distinct standing shoots of *Typha* and *Phragmites* with clear differentiation of live and dead tissue allow easy quantification of shoot density. Also, shoot components are readily identifiable in their litter. Conceptual models of above-ground standing OM and litter pools for *Typha, Phragmites* and *Vallisneria* (Figure 3.22 – 3.24) illustrate the processes requiring description in order to develop a mathematical model for these species.

The more complex ramifying habit of *Persicaria prostrata,* with intertwining upright shoots which may become prostrate and produce additional uprights or even roots, makes identification of individual shoots impossible. Additionally, stems bearing only dead leaves may in fact be viable and re-shoot at any time. Thus, no attempts were made to model changes in shoot density or differentiate live and dead standing biomass. This growth form, plus the size and fragility of dead tissues, made measurement of tissue loss from shoots and litter accumulation impractical. For *Persicaria*, modelling OM available for input was limited to assessments of standing biomass susceptible to inundation and hence release of DOM, most likely resulting in under-estimates of organic matter inputs from this species.

Organic matter cycling and transformation in the submerged *Vallisneria* is quite different from emergent species (Figure 4.2). Shoots are comprised mainly of live tissue, with leaf blades forming the vast majority of above-ground biomass (see Chapter 3). As blades senesce, they

accumulate biofilm and floc. Fragmentation of dead blades and disturbance of floc release POM directly into the water column (assuming that plants are submerged most of the time), although blade material may also accumulate as litter in beds by being trapped in the canopy.

Parameters required to construct mathematical models of OM available for input, including macrophyte bed areas, shoot densities, and rates of senescence and loss of biomass components, were measured in the field over 18 months. Some components have been described in earlier chapters, others are described below.

4.2.3 Shoot Densities

For *Phragmites* and *Typha*, numbers of live and dead shoots within macrophyte beds were counted in three to fifteen randomly selected quadrats per site per trip and scaled to obtain shoot densities per square metre. Quadrat size selection (0.0225 – 1 m^2) was based on a rough visual assessment of density in order that fewer than fifty shoots were counted per quadrat to reduce operator error. Shoots were classified as dead if over 50% of the above-ground biomass was visibly chlorotic. Because *Vallisneria* shoots are rarely totally dead (except when exposed for extended periods, which did not occur to any substantial degree during this study and so wasn't quantified), total shoot density was assessed for this species. *Vallisneria* shoot density at BRO was assessed in three to twelve quadrats (0.0225 – 0.25 m^2) distributed randomly throughout beds on each sampling occasion. Again, quadrat size selection was guided by the objective of limiting shoot counts to fifty per quadrat. Assessments of *Persicaria* shoot density (assessed as the number of upright stems bearing only leaves) and biomass were obtained at the Ovens River site in May and August, 2001.

4.2.4 Shoot Composition and Litter Production

Changes to shoot composition over time were used to examine shoot senescence and rates of loss of biomass components considered important contributors to litter over a 1-2 year time scale. For *Typha* and *Phragmites*, substantial losses from shoots of blade and sheath material occur within this time frame, whereas stems contribute little to the litter pool over this period (Chapter 3). Thus, blade and sheath tissues were the focus of shoot monitoring for these species. However, the contribution of dead standing emergent plant stems older than 2 years to the litter pool were estimated. For *Vallisneria*, shoot monitoring focused on blades, the only shoot component contributing to litter in this species over a 1-2 year time period (Chapter 3).

Field plots (1 m^2) were established in *Typha* and *Phragmites* beds at BAR and BRO at the beginning of the study and all current season shoots contained within were tagged for sequential harvests for biomass assessments (Chapter 3). Additional current season shoots were randomly selected from within each plot at the start of the study and labelled with a different

numbering system for non-destructive monitoring of shoot senescence and litter production. Numbers of live and dead blades and sheaths on the tagged shoots were monitored over the following 18 months, with shoot components classified as dead if over 50% of their surface area was visibly chlorotic or dead.

The contributions of old (>2 years) standing dead stems to litter of the emergent species were estimated from a combination of my stem mass loss data and field observations of timing of stem fragmentation, and literature estimates of the timing of stem breakage. Sequential harvests provided a fairly complete data set for stem mass losses for *Phragmites* over time (Chapter 3; Figure 3.13), with data from Asaeda et al. (2002) incorporated to produce a curve of stem loss rate over time (stem loss period limited to two years and the curve shape restricted so that the area under the curve equalled mean mass of dead stem tissue per *Phragmites* shoot at BAR). The data set for *Typha* was less complete, due to the limited number of stems produced during the course of the study. Curves for stem loss rate over time for this species were estimated by assuming that the total mass of dead stem tissue entered the litter pool within a two year period, after initially losing 25% of their mass to aerial decomposition (Welsch and Yavitt, 2003). The curve shape was restricted so that the area under the curve equalled the mean mass of dead stem tissue per *Typha* shoot at BAR, and timed so that stem loss commenced as dead shoot density began to decline.

Changes to shoot structure of *Vallisneria* over time were monitored at BRO by harvesting 10 – 30 randomly-selected shoots from within submerged beds on each trip. Total number of leaf blades was recorded for each shoot, which were then retained for biomass assessments (Chapter 3). Seasonal changes in blade numbers per shoot were converted into blade loss data by subtracting March, May, August and September data from December data for each year (assuming that peak canopy density occurs in December and using subsequent year data as replicate cohorts). Assessment of direct loss of *Vallisneria* blades to the water column was attempted in May 2001 by deploying drift nets (250 – 1000 µm mesh) downstream of beds for 4 – 12 hours, with the intention of examining collected material for discernable blade fragments. However, this method proved unsuitable and in future it is recommended that assessments of litter production in this species utilise short-term leaf-tagging methods.

4.2.5 Standing Litter

Standing litter was collected from exposed *Typha* and *Phragmites* beds at BAR and BRO in August 2002 (0.0625 – 1 m^2 quadrats) for comparison with predictions of litter accumulation derived from modelling. Although 3 replicate samples were collected for each species/site combination, some samples were subsequently lost, producing sample sizes less than three for some collections. Thus, statistical analyses of differences between litter standing stocks in

inundated and exposed beds were not possible. The equivalent of standing litter in *Vallisneria* beds is OM (such as blade fragments and biofilm/floc) trapped in the canopy which is easily released by variations in current speed or physical disturbance. *Vallisneria* standing litter was quantified at BRO in May 2001 by flushing beds with large volumes of water (pumped from upstream of beds) and collecting entrained POM in drift nets (1000 µm mesh). Collected material was dried to a constant weight at 60 ^{o}C in a Thermoline D120 dehydrating oven and weighed.

4.2.6 Model Development and Application

Standing OM available for input into the channel was calculated by multiplying shoot densities by the bed area in the reach for each species (total number of shoots in the reach). The quantity of standing OM inundated under different flow scenarios was calculated by multiplying shoot densities by the inundated bed area determined from macrophyte inundation curves developed in Chapter 2 (number of inundated shoots in the reach).

Litter production rates were generated by multiplying rates of loss of different litter components by their mean mass and the density of dead shoots. For *Typha*, approximately one in five shoots produced stems during the study, so dead shoot density was amended by a factor of 0.2 in calculating litter production from stems. Where more than one biomass component contributed to litter (e.g. blades and sheaths), production rates for each were summed to obtain a total litter production rate ($g/m^2/d$). To calculate litter accumulation in beds of emergent macrophytes between two time points, litter production rates were calculated for the total area of exposed bed for each day. These were sequentially summed, subtracting any litter losses due to bed inundation on the preceding day. For *Vallisneria*, changes to mean numbers of blades per shoot over time were used, in conjunction with literature values for leaf turnover rates, to estimate litter production rates. All litter was assumed to be retained in the canopy unless discharge increased, causing an estimated 50% reduction[3] in the standing litter pool.

4.2.7 Statistical Analyses

Single-factor analyses of variance (ANOVA) were used to ensure there were no differences between different field plots which allowed pooling of all replicates for final analyses. Sigmaplot for Windows version 8.0 was used to perform Fourier analyses, for plotting graphs, curve-fitting and ANOVA of fitted functions. Programming for modelling changes to standing OM and litter pools,

[3] Initial trials were conducted to determine quantities of OM flushed from *Vallisneria* beds during rising limbs (using a water pump to increase flow through the beds and catching OM in drift nets deployed downstream). While only a few trials were conducted and factors such as flow velocity, shoot density and bed area seemed to affect OM retention, a rough estimate of 50% loss with flushing was determined to be sufficient for the degree of sensitivity required.

litter production, accumulation and inputs was performed in Microsoft Excel using Visual Basic for Applications.

4.3 Results

4.3.1 Shoot Densities

4.3.1.1 Typha

Annual cycles of seasonal change in live and dead shoot densities were observed over the study period for *Typha* at BAR (Figure 4.1). Live shoot density peaked in December at 16 shoots/m^2 whereas the maximum dead shoot density occurred in August at 25 shoots/m^2. Because the data were cyclic, sine curves were fitted to model changes to shoot density over time. Curve fitting used Fourier analysis to derive functions predicting numbers of live and dead shoots per square metre for a given day of the year (Figure 4.1). The functions for *Typha* live (R^2 = 0.62, F =7.62, $p < 0.01$, n =13) and dead (R^2 = 0.63, F = 6.46, $p < 0.01$, n = 14) shoot density changes over time are shown in Table 4.1 (Eqns 1 and 2).

Modelled *Typha* live shoot density never fell below 8 shoots/m^2 (nadir in early April) (Figure 4.1). Early season shoots produced in Apr/May remained dormant over winter, with the main period of growth commencing in September and peak biomass occurring in late November, producing an initial early pulse in both live and dead shoot densities followed by the major peak later in the year. The maximum rate of senescence of live shoots was approximately equal to the production rate, whereas the maximum rate of increase of dead shoot density was 2-3 times as fast. Major losses of live shoots occurred between November and March (4 months); over this time the rate of increase of dead shoots was about half the rate of loss of live shoots. From March to June there was a very rapid increase in the number of dead shoots, concurrent with the first "shoulder" on the live shoot density curve. Minimum dead shoot density of 6 shoots/m^2 occurred in November.

4.3.1.2 Phragmites

Seasonal changes in live and dead shoot densities were observed for both the Broken and Murray River sites. *Phragmites* live shoot density maxima at Barmah was 142 shoots/m^2 in mid May 2001 compared with 158 shoots/m^2 on 3/6/02 for BRO, with troughs occurring in August/September. Data were averaged across the two sites for plotting and curve-fitting (Figure 4.2). The function for *Phragmites* live (R2 = 0.96, F = 123.90, $p < 0.0001$, n = 18) and dead (R2 = 0.63, F = 7.83, $p < 0.01$, n = 13) shoot density are shown in Table 4.1 (Eqn 3 & 4).

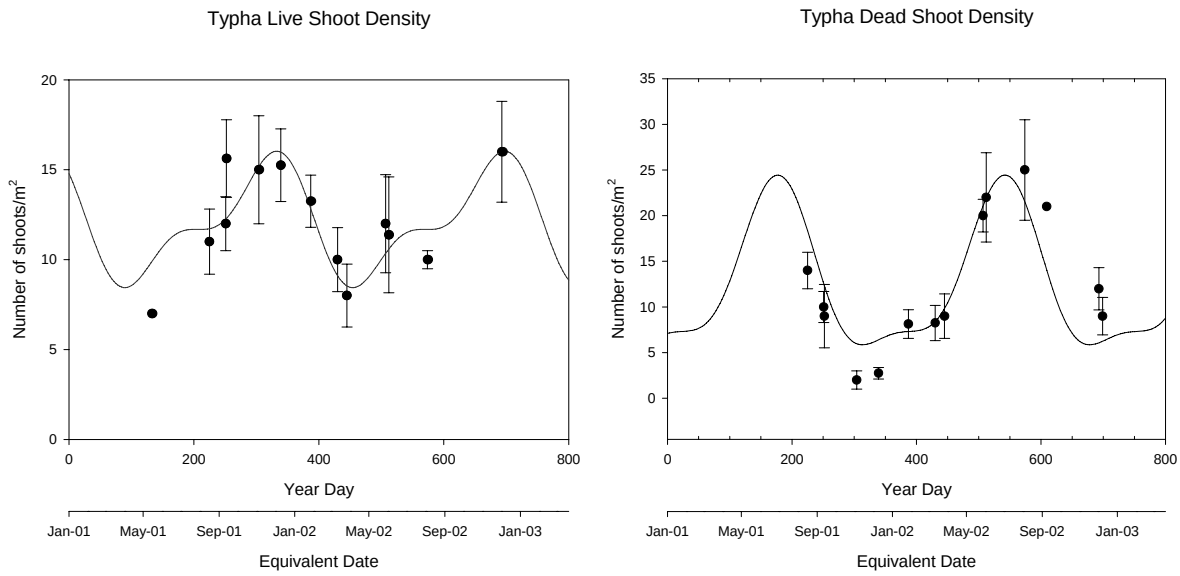

Figure 4.1. Changes to *Typha* shoot densities over time (means ± s.e.). Lines are the fitted functions.

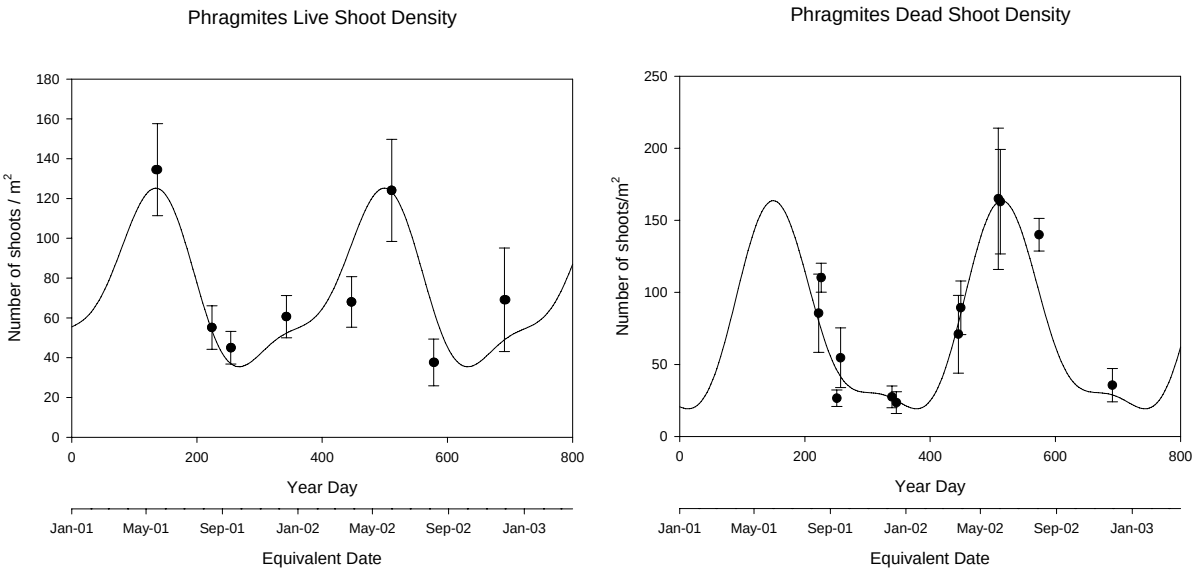

Figure 4.2. Changes to *Phragmites* shoot densities over time (means ± s.e.). Lines are the fitted functions.

As with *Typha*, the production of early-season shoots ahead of the main growth period resulted in secondary pulses in live and dead shoot densities. There was a slow increase in modelled live *Phragmites* shoot density from a minimum in late September of 35 shoots/m^2 up to 60 shoots/m^2 in January. January to May was the period of greatest increase in live shoot density; peaking at 125 shoots/m2 in mid-May. A fairly rapid loss of live shoots occurred from June to September. Dead shoot density increased rapidly from a minimum of 19 shoots/m^2 in January to 164 shoots/m^2 in June, then decreased to 38 shoots/m^2 in mid September before troughing again. Rates of increase and decrease in dead shoot density were about the same; whereas for live shoots the rate of increase was slower than the decrease. Rates of change to live shoot density were slower than for dead shoots.

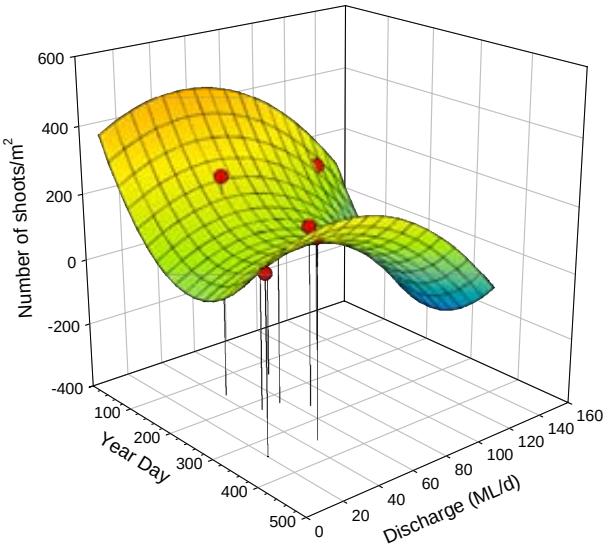

Figure 4.3. Changes to *Vallisneria* shoot density (points) with discharge and season; fitted function (mesh).

4.3.1.3 Persicaria

Mean shoot density for *Persicaria* at OVN was 462.85 shoots/m^2 (± 58.61); mean shoot biomass was = 297.3 g/m^2 (± 53.3) (Chapter 3).

4.3.1.4 Vallisneria

Although some seasonality was discernable in *Vallisneria* shoot density changes, the relationship appears to be complex, involving additional drivers such as discharge (Figure 4.3). The curve presented illustrates the pattern of changes to shoot density with discharge and season, rather than for use in mathematical modelling. The curve was three-dimensional with paraboloid curves for both the discharge-density relationship (with few shoots under very low or very high flows due to desiccation and light limitation, respectively) and the seasonal-density relationship (lowest number of shoots during periods of low temperature and short day length). While the trends described are theoretically sound, the limited range of discharges experienced during the study (e.g. only one sample point above 80 ML/d during the study period c.f. the annual average hydrograph for this site in Figure 2.10) has impaired development of a descriptive mathematical function for *Vallisneria* shoot density. Thus, modelling of *Vallisneria* organic matter will use a mean shoot density averaged over the entire data set (167.6 shoots/m^2 ± 10.8; n = 53).

Table 4.1. Summary of functions generated during overall model development.

Eqn	Function	Parameters					
	Shoot Density Equations	G_i = number of live shoots/m^2 on day *i* D_i = number of dead shoots/m^2 on day i					
1	*Typha* live shoot density $G_i = y_0+a*\sin(2\pi i/365+c)+a/2*\sin(4\pi i/365+d)$	y0 12.05	a 2.93	c 2.57	d 2.24		
2	*Typha* dead shoot density D_i = y0+a*sin(2πi/365+c) + a/3*sin(4πi/365+d)	y0 12.82	a 8.75	c -1.40	d -4.64		
3	*Phragmites* live shoot density G_i= y0+a*sin(2πi/365+c)+a/3*sin(4πi/365+d)	y0 73.12	a 40.13	c 5.74	d 2.92		
4	*Phragmites* dead shoot density D_i = y0+a*sin(2πi/365+c) + a/3*sin(4πi/365+d)	y0 73.30	a 68.04	c 5.21	d 2.82		
	Shoot component loss equations	BL_i = number of blades lost on day i SL_i = number of sheaths lost on day i PL_i = mass of stems lost on day i					
5	*Typha* blade loss rate BL_i = a/(1+e(-(i-x0)/b))	a 7.27	b 53.72	x0 340.52			
6	*Typha* sheath loss rate SL_i = a/(1+e(-(i-x0)/b))	a 5.54	b 71.02	x0 356.49			
7	*Typha* stem loss rate PL_i = a.e(-0.5(ln(i/x0)/b)^2)	a 0.08	b 0.35	x0 340.57			
8	*Phragmites* blade loss rate BL_i = a/(1+e(-(i-x0)/b))	a 14.12	b 18.67	x0 214.53			
9	*Phragmites* sheath loss rate SL_i = a/(1+e(-(i-x0)/b))	a 7.43	b 124.24	x0 416.73			
10	*Phragmites* stem loss rate PL_i = a*exp(-0.5*(ln(i/x0)/b)^2)	a 0.04	b 0.39	x0 319.08			
11	*Vallisneria* blade loss over time VB_i = y+a*sin(2*π*x/365+c)+a/2*sin(4*π*x/365+d)	a 2.078	c 1.207	d 2.171	y 9.483		
12	*Vallisneria* blade loss rate BL_i = a/(1+e(-(i-x0)/b))	a 5.11	b 10.79	x0 143.93			
	Litter production equations	BR_i = rate of blade loss on day i (# of blades lost/shoot/d) SR_i = rate of sheath loss on day i (# sheaths lost/shoot/d) PR_i = rate of stem loss on day i (g stem tissue lost/m^2/d) LR_i = total rate of litter production on day i (g DW/m^2/d) LP_i = total size of litter pool on day i (g DW/m^2)						
13	*Typha* blades BR_i = y0+a*sin(2πi/365+c) + a/5*sin(4πi/365+d)	y0 0.02	a 0.02	c 1.78	d 2.86		
14	*Typha* sheaths SR_i = y0+a*sin(2πi/365+c)	y0 0.01	a 0.01	c 6.97			
15	*Typha* stems PR_i = y0+a*sin(2πi/365+c)+a/3*sin(4πi/365+d)	y0 0.07	a 0.05	c 3.41	d 0.16		
16	*Typha* total litter production rate LR_i = y0 + a*sin(2πi/365 + c) + a/2*sin(4πi/365 + d) + a/2*sin(6πi/365 +e)	y0 1.07	a 0.16	c 0.65	d 2.72	e 1.19	

Table 4.1. cont.

Eqn	Function	Parameters					
	Litter production equations	BR_i = rate of blade loss on day i (# of blades lost/shoot/d) SR_i = rate of sheath loss on day i (# sheaths lost/shoot/d) PR_i = rate of stem loss on day i (g stem tissue lost/m^2/d) LR_i = total rate of litter production on day i (g DW/m^2/d) LP_i = total size of litter pool on day i (g DW/m^2)					
17	*Typha* total litter pool size $LP_i = y0 + a*i$	y0 0.57	a 1.10				
18	*Phragmites* blades $BR_i = y0+a*\sin(2\pi i/365+c) + a/3*\sin(4\pi i/365+d)$	y0 0.05	a 0.07	c 3.21	d -1.43		
19	*Phragmites* sheaths $SR_i = y0+a*\sin(2\pi i/365+c) + a/3*\sin(4\pi i/365+d)$	y0 0.02	a 0.02	c 2.10	d -1.20		
20	*Phragmites* stems $PR_i = y0+a*\sin(2\pi i /365+c) +a/2*\sin(4\pi i /365+d)$	y0 0.96	a 0.70	c 3.80	d 1.13		
21	*Phragmites* total litter production rate $LR_i = y0+a*\sin(2\pi i /365+c)+a/3*\sin(4\pi i /365+d)$ $+a/6*\sin(6\pi i /365+e)$	y0 2.24	a 1.99	c 3.75	d 0.26	e 3.20	
22	*Phragmites* total litter pool size $LP_i = -a*\sin(2\pi i/365-c)+d*I - y0$	y0 80.11	a 115.68	c 0.95	d 2.23		
23	*Vallisneria* blades $BR_i = y0+a*\sin(2\pi i/365+c) + a/5*\sin(4\pi i/365+d)$	y0 0.06	a 0.03	c 4.61	d 2.15		
24	*Vallisneria* total litter production rate $LR_i = y0+a*\sin(2\pi i/365+c) + a/5*\sin(4\pi i/365+d)$	y0 3.56	a 1.73	c 4.61	d 2.15		
25	*Vallisneria* total litter pool size $LP_i = a*\sin(2\pi i /365+c) + d*x - y0$	y0 14.49	a 100.29	c 3.04	d 3.56		

4.3.2 Shedding of Shoot Components

4.3.2.1 Typha

Shoot monitoring revealed similar patterns of senescence and loss of dead biomass components to those demonstrated by biomass partitioning (Chapter 3). The loss of blades and sheaths from *Typha* shoots followed a sigmoidal pattern. Curves were fitted to blade and sheath loss data, allowing the definition of functions to predict mean numbers of blades and sheaths lost per shoot for a given day of the year (Figure 4.4). The functions for blade ($R^2 = 0.98$, $F = 145.69$, $p < 0.0005$, $n = 7$) and sheath ($R^2 = 0.99$, $F = 231.96$, $p < 0.005$, $n = 5$) loss from shoots are shown in Table 4.1 (Eqns 5 and 6).

Both the rate of blade loss and total number of blades lost were greater than for sheaths, with blade loss commencing before sheath loss rather than structures being shed simultaneously. Sheath bases were retained to form a shoot “stump” which persists for several years (pers. obs.).

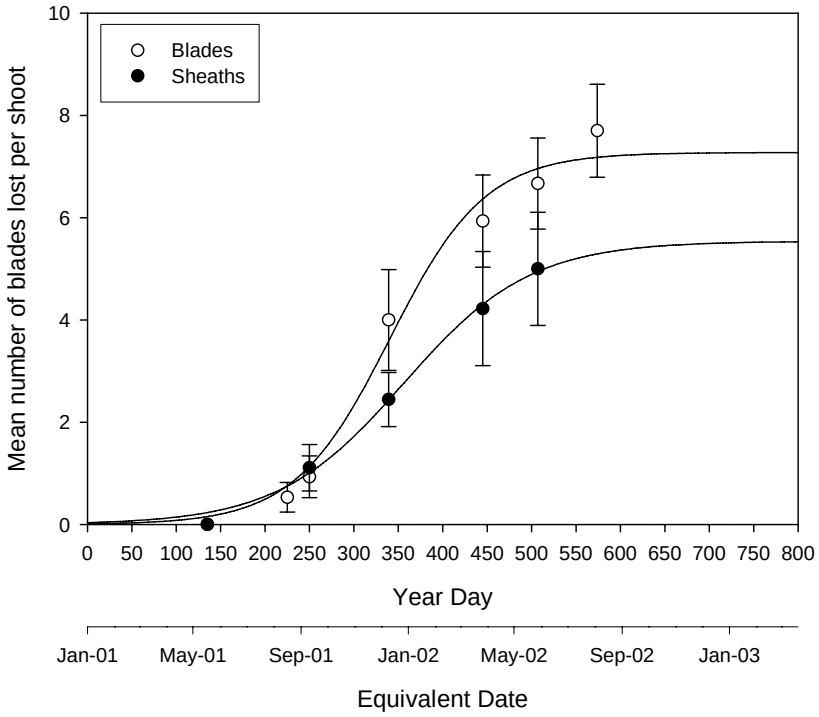

Figure 4.4. Loss of blades and sheaths from *Typha* shoots over time. Data points are mean numbers of blades and sheaths lost per shoot (± s.e.). Lines are the fitted functions.

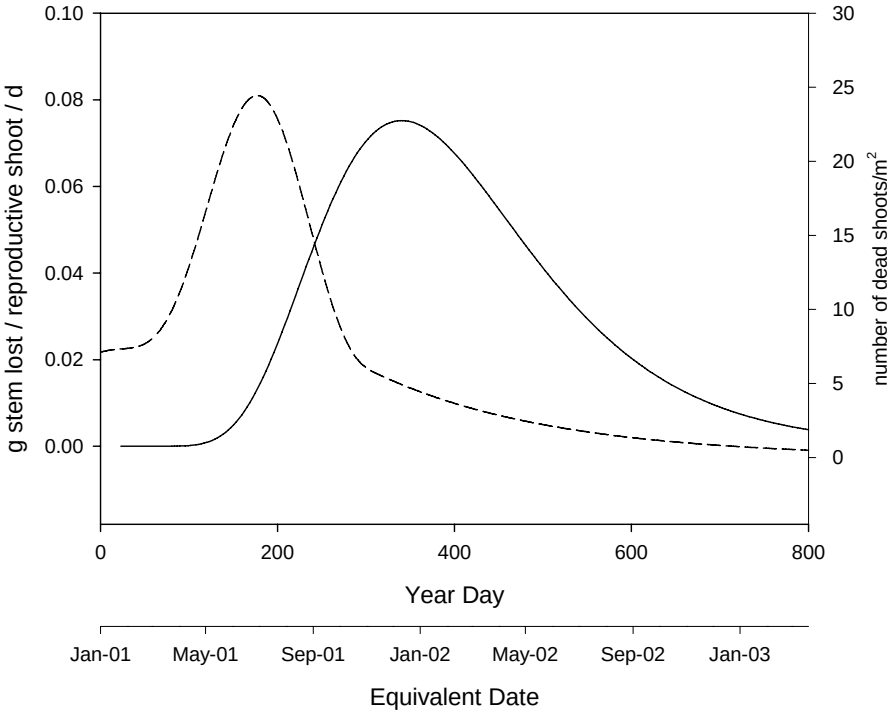

Figure 4.5. Changes to stem loss rate from a single cohort of *Typha* shoots over time estimated from mass loss data spread over a two year period commencing as dead shoot density starts to decrease (solid line). The curve shape was restricted so that the area under the curve equates to the mean mass of dead stem tissue per shoot at BAR. Dashed line is the *Typha* dead shoot density curve for a single cohort of shoots extrapolated to the same period.

Because the method of calculating fragmentation of stems was different from that for blades and sheaths, the initial curve produced was one describing changes to the rate of stem tissue loss over time (Figure 4.5) rather than the sigmoidal mass loss curves shown for blades and sheaths. The curve developed followed a log-normal function (Table 4.1 Eqn 7). Stem loss commenced in June and peaked in December (0.075 g/reproductive shoot/d) before tailing off to zero over the next 2½ years.

4.3.2.2 Phragmites

Patterns of senescence and tissue loss similar to those for *Typha* were apparent from shoot monitoring of *Phragmites* at both sites. Again, sigmoidal curves were appropriate for blade and sheath loss (Figure 4.6); the functions developed for *Phragmites* blade loss ($R^2 = 0.93$; $F = 54.03$; $p < 0.05$; $n = 9$) and sheath loss ($R^2 = 0.67$; $F = 16.00$; $p < 0.1$; $n = 16$) over time are shown in Table 4.1 (Eqns 8 and 9).

Pronounced differences were observed between modelled loss rates and maxima of blades and sheaths for *Phragmites* compared to *Typha*. Blade loss occurred nearly seven times faster than sheath loss. Sheaths were wrapped tightly around the stem and most remained attached to the stem for periods up to 2 years. After months to years of air-drying and aerial decomposition the stems became very brittle and broke off, with sheath material often still attached, to enter the litter pool (pers. obs.).

Similar to *Typha*, the development of a stem mass loss curve for *Phragmites* used a different approach from that used for blades and stems, and so a rate curve was again the starting point for later modelling of litter production in *Phragmites* (Figure 4.7). Utilising some biomass loss data plus literature values and observations of stem fragmentation in the field, the curve developed to describe *Phragmites* stem loss (Table 4.1 Eqn 10) demonstrated commencement of stem tissue loss concurrent with shoot collapse (decline in dead shoot density) in June (Figure 4.7). Stem loss rate peaked in November (0.036 g/shoot/d), followed by a period of gradual decline to zero over the next 3 years (Figure 4.7).

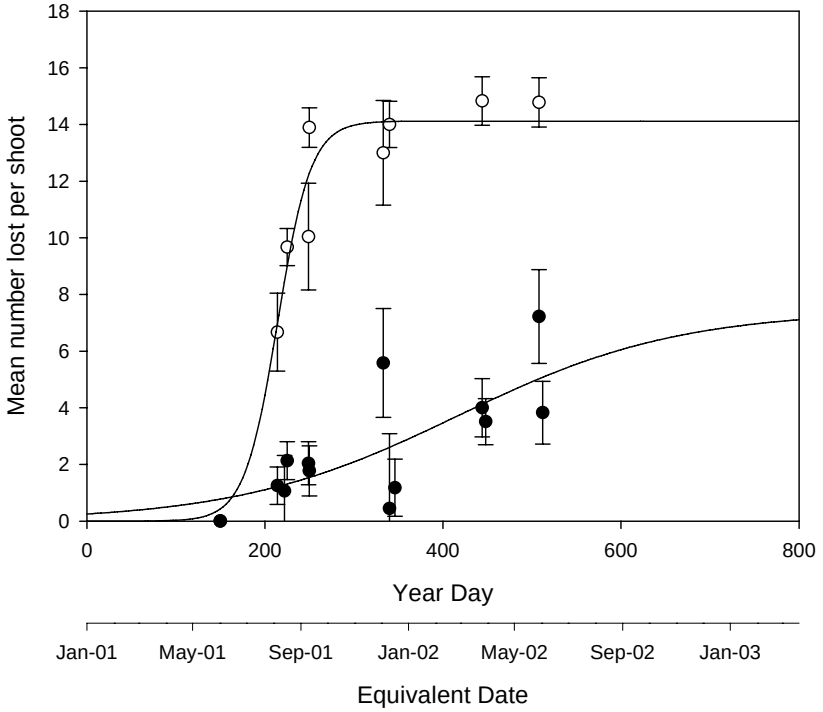

Figure 4.6. Loss of blades and sheaths from *Phragmites* shoots over time. Data points are mean numbers of blades and sheaths lost per shoot (± s.e.). Lines are the fitted functions.

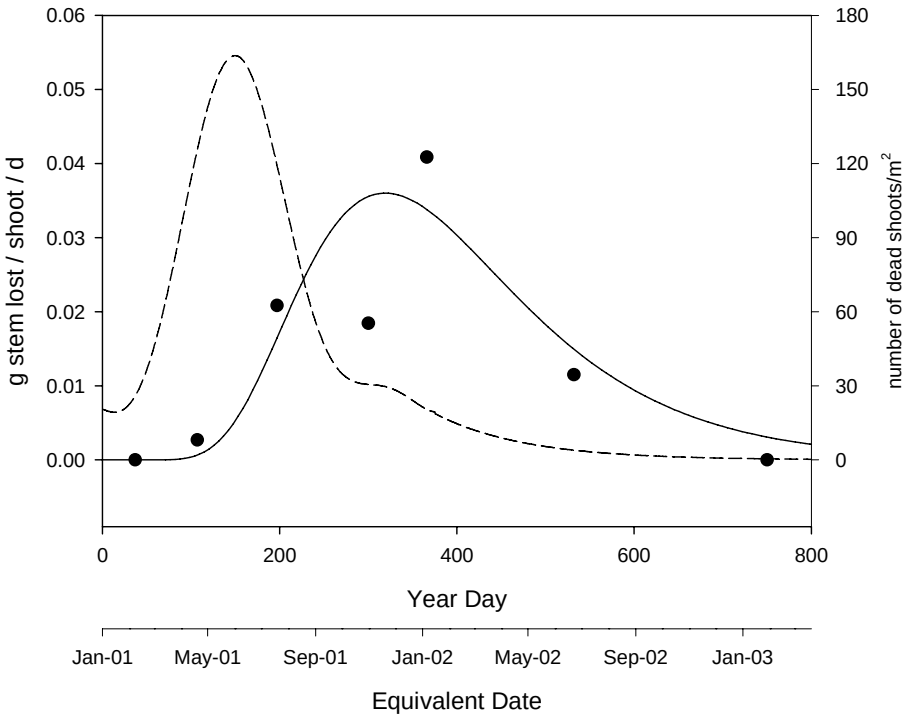

Figure 4.7. Changes to stem loss rate from a single cohort of *Phragmites* shoots over time (points) calculated from % loss of initial stem mass data and literature estimates (Asaeda et al., 2002). Solid line is the curve fitted to this data, with the stem loss period limited to two years (Asaeda et al., 2002 and pers. obs.) and the curve shape restricted so that the area under the curve equates to the mean mass of dead stem tissue per shoot at BAR. Dashed line is the *Phragmites* dead shoot density curve for a single cohort of shoots extrapolated to the same period (Asaeda et al., 2002).

4.3.2.3 Vallisneria

The growth form of *Vallisneria* is such that new blades are continually being produced as old leaves senesce and are shed (leaf turnover). Additional blade production and loss overlay baseline leaf turnover in this species, causing changes to shoot composition (total quantities and ratios of biomass components). It is this change in shoot composition, rather than leaf turnover, which is described in this section. Temporal changes in blade number per shoot were observed in harvested *Vallisneria* shoots (Figure 4.8) (Eqn 11 in Table 4.1; R2 = 0.84, F = 13.39, $p < 0.05$, n = 8). The pattern of blade loss in *Vallisneria* was again sigmoidal (Figure 4.8), producing the function shown in Table 4.1 (Eqn 12) ($R^2 = 0.97$; F = 77.81; $p < 0.1$; n = 6).

Based on the modelled data, *Vallisneria* above-ground shoot composition changed rapidly over 8 weeks in late autumn/ early winter, with an average loss of 5.1 blades per shoot. *Vallisneria* shoots never lost all of their leaves, retaining 5 – 9 blades until growth recommenced in spring. The rate of loss of *Vallisneria* blades was much greater than for biomass components of either *Phragmites* or *Typha*.

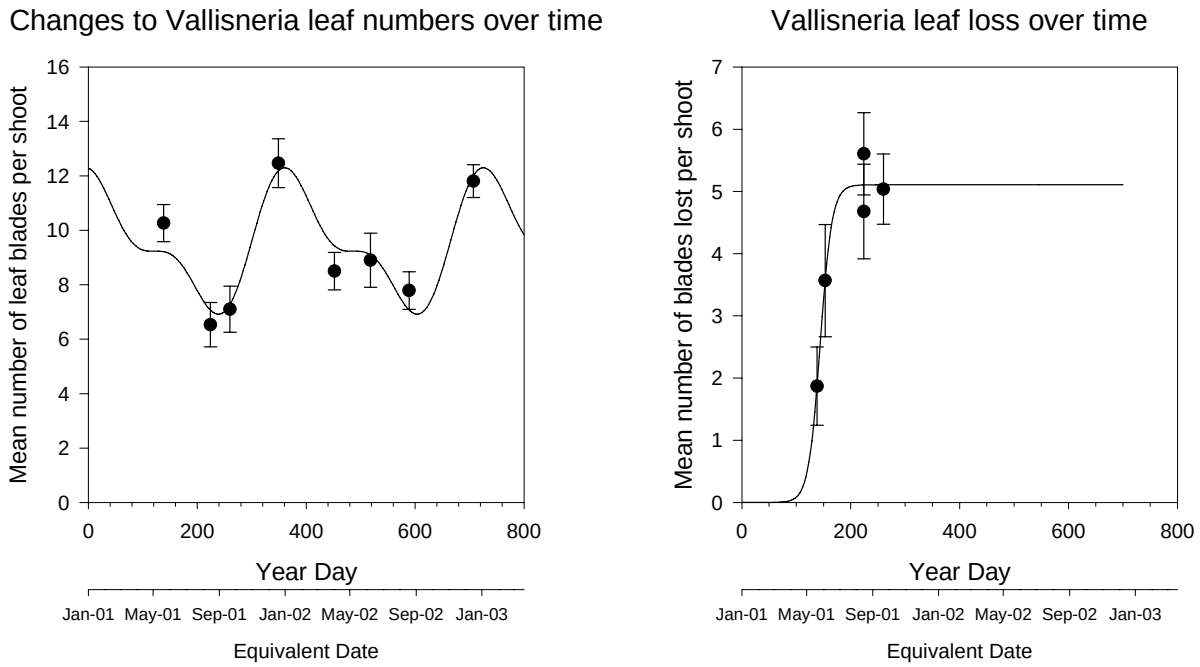

Figure 4.8.Changes to number of blades per *Vallisneria* shoot and loss of blades from *Vallisneria* shoots over time. Data points are mean numbers of blades (± s.e.). Line is the fitted function.

4.3.3 Litter Production

Blade and sheath loss rates were determined from the difference between dead blade and sheath counts on individual shoots from sequential field trips expressed as rates per day. Expression on a rate basis allowed the sigmoidal patterns of cumulative litter loss for *Typha*, *Phragmites* and *Vallisneria* shown in Figures 4.4, 4.6 and 4.8 to be converted to cyclical peaked curves (Figures 4.9, 4.12 and 4.15). While all blade and sheath material was shed in one season, negating the need to adjust calculations for overlapping cohorts, transfer of *Typha* and *Phragmites* stems to the litter pool was modelled over two years. To account for overlap between sequential cohorts, stem loss per shoot from one cohort was multiplied by the expected dead shoot density for that cohort during its second year (Figures 4.5 and 4.7) and added to stem litter production from the subsequent cohort during its first year. Thus, annual cycles of stem litter production were able to be produced (Figures 4.10 and 4.13). Fourier analysis was used to fit waveforms to blade, sheath and stem loss data for all species with an assumed periodicity of 365 days.

To calculate litter production in macrophyte beds between two time points, litter production rates per shoot were multiplied by the shoot density for the period of interest and mean mass per litter component. Where more than one biomass component contributed to litter, total litter production was determined by summing litter production from each component. Modelled litter production rates and cumulative totals (litter pool sizes) for *Typha*, *Phragmites* and *Vallisneria* are shown in Figures 4.11, 4.14 and 4.16, respectively. Functions were fitted to these data to enable direct prediction from year-day.

4.3.3.1 Typha

The functions describing changes in *Typha* blade, sheath and stem loss rates over time are shown in Table 4.1 (Eqns 13, 14 and 15) (BLADES: $R^2 = 0.65$, $F = 25.81$, $P < 0.0001$, $n = 22$; SHEATHS: $R^2 = 0.34$, $F = 6.81$, $P < 0.005$, $n = 14$; STEMS: $R^2 = 0.97$, $F = 9{,}465$, $p < 0.0001$, $n = 800$).

The maximum rate of modelled blade loss for *Typha* occurred in January at 0.044 blades per shoot per day, whereas modelled sheath loss rates peaked in February at 0.019 sheaths per shoot per day (Figure 4.9) and stem loss rate peaked in July at 0.135 g per m^2 per day (Figure 4.10). Rates of change of modelled sheath loss rate were less than those for blades and stems, with blade and stem loss rate increasing rapidly but decreasing more slowly. Some degree of blade, sheath and stem loss occurred throughout the entire year (no extended periods of zero litter production occurred during the 365 day period).

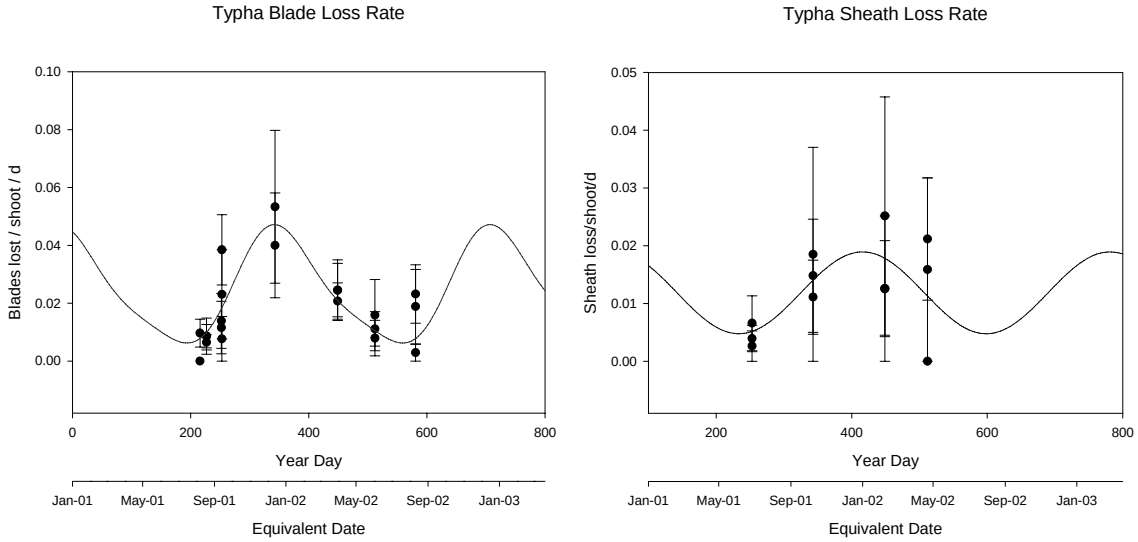

Figure 4.9. Changes to rates of blade and sheath loss from *Typha* shoots over time (means ± s.e). Lines are the fitted functions.

The function describing total *Typha* litter production rate is shown in Table 4.1 (Eqn 16) (R^2 = 0.95, F = 4,000, P < 0.0001, n = 800). Rates of litter production in *Typha* beds (Figure 4.11 a) followed a double-peaked waveform, producing a slightly "bumpy", but generally linear increase in litter pool size over time (Figure 4.11 b). A simple linear regression with slope of 1.10 and intercept of 0.57 was fitted to modelled *Typha* litter pool size changes (g DW/m^2) (Table 4.1 Eqn 17: R^2 = 0.99, F = 537,877, p < 0.0001, n = 800).

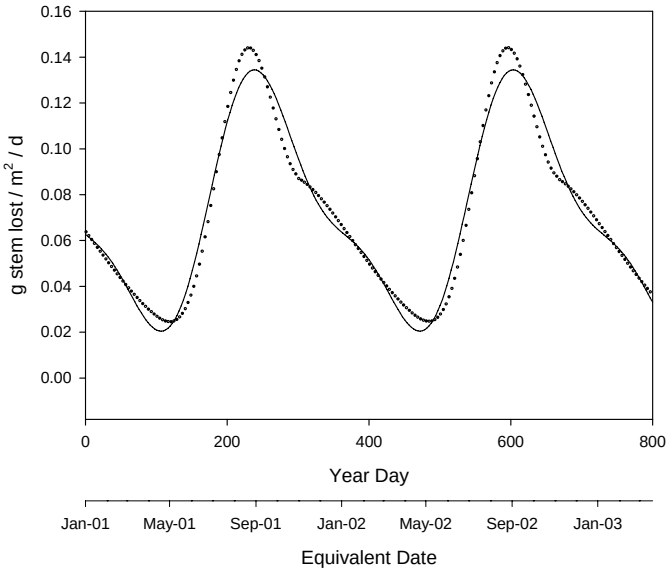

Figure 4.10. Annual stem loss from *Typha* shoots calculated for overlapping cohorts (points), assuming a frequency of reproductive shoots of 1 in 5. Line is the fitted function.

Litter production patterns in this species were mostly relatable to the interaction between changes in blade and sheath loss rates and dead shoot density. Maximum litter production occurred in January (1.28 g/m^2/d), with the second highest peak in May (1.26 g/m^2/d) (Figure 4.11). The minimum rate of litter production throughout the year was 0.84 g/m^2/d, occurring in late July. The first peak of the curve was due to the occurrence of peak blade loss rate despite dead shoot density at this time being minimal. The second peak and initial small hump were driven mainly by dead shoot density (peak and 50% of maximum, respectively); sheath loss rate also contributed to the second peak whereas stem loss made its major contribution to total litter production as the small initial hump. Annual litter production for *Typha* was 402 g/m^2 (c.f. peak standing biomass of 1,700 g/m^2).

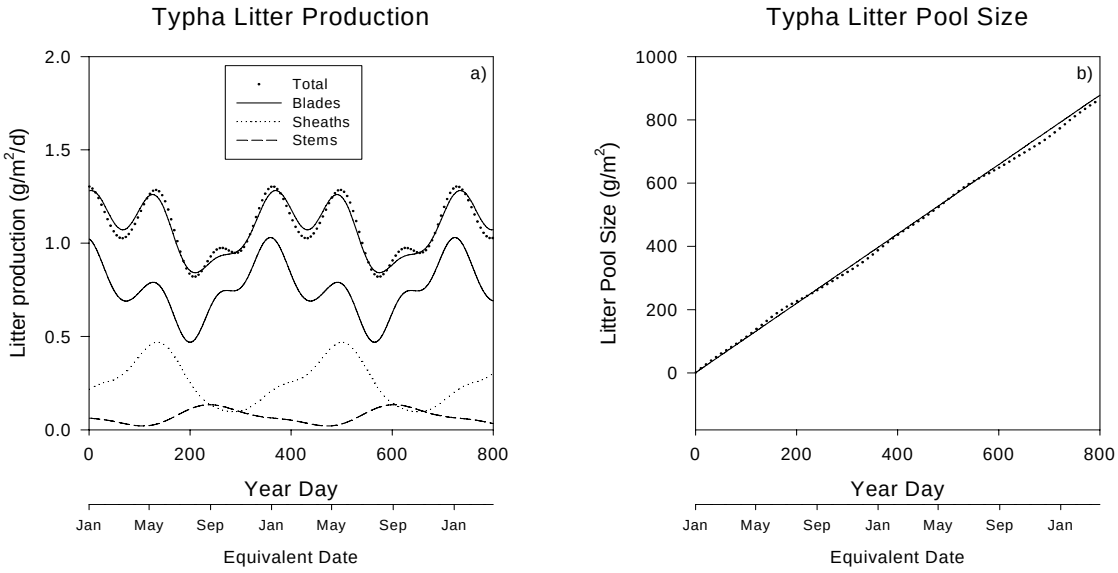

Figure 4.11. Changes to *Typha* litter production rate (a) and pool size (b) over time. The contributions of blades (solid line), sheaths (dotted line) and stems (dashed line) to litter production are shown in a). Data points are modelled values. Lines are the fitted functions.

4.3.3.2 Phragmites

Rates of abscision of *Phragmites* blades, sheaths and stems to the litter pool were also modelled (Figures 4.12 and 4.13). The equations for blade loss rate ($R^2 = 0.68$; $F = 22.23$; $p < 0.005$; $n = 13$), sheath loss rate ($R^2 = 0.86$; $F = 42.30$; $p < 0.005$; $n = 11$) and stem loss rate ($R^2 = 0.96$; $F = 11,434$; $p < 0.0001$; $n = 800$) are shown in Table 4.1 (Eqns 18, 19 & 20).

Large differences in the modelled peak rate of losses occurred for *Phragmites* blades and sheaths, with maxima of 0.14 and 0.039 units lost per shoot per day, respectively (Figure 4.12). Maximum blade loss occurred in late September, with the peak spanning 8 months and followed by a 4 month period of effectively zero blade loss. In contrast, the sheath loss cycle spanned most of the year, and there was a greater degree of variability in sheath loss rates than blade loss

rates. Rates of increase and decrease of blade loss were the same, and much higher than those for sheaths. The differences in sigmoidal loss curves for *Phragmites* blades and sheaths were reflected in the modelled litter production waveforms. Sheath loss rates increased relatively rapidly from June to October, associated with increasing blade loss rates – a proportion of sheaths were ripped off as blades were shed. Blade loss ceased in October, followed by the gradual loss of sheaths until March. The remainder of the sheath biomass was retained on standing stems. Modelled stem loss rate was lowest in late March (0.081 g/m^2/d), rising rapidly to its peak in late July (1.89 g/m^2/d) (Figure 4.13). The decline in stem loss rate involved two periods of similar rate change (July – November and January – March) separated by a period of stable stem losses (November – January).

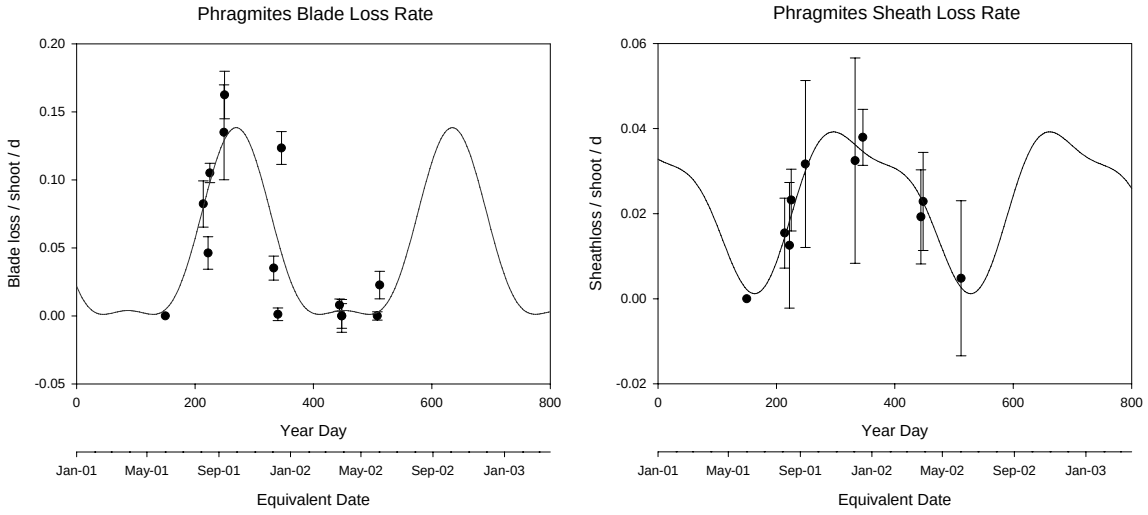

Figure 4.12. Changes to rates of blade and sheath loss from *Phragmites* shoots over time (means ± s.e). Lines are the fitted functions.

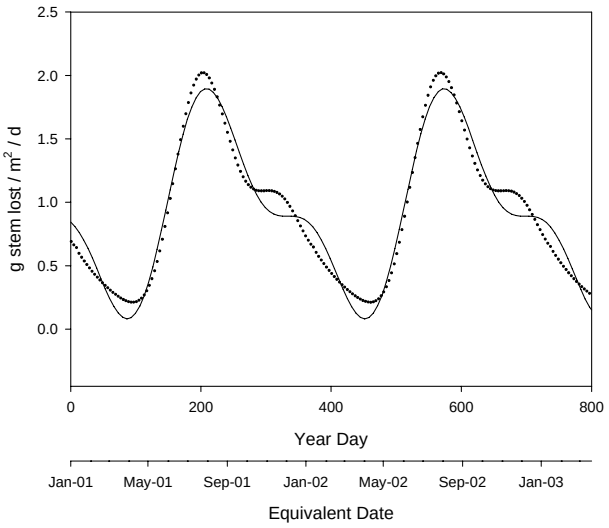

Figure 4.13. Annual stem loss from *Phragmites* shoots calculated for overlapping cohorts (points). Line is the fitted function.

The function describing changes to total litter production rate for *Phragmites* ($R^2 = 0.96$; $F = 4{,}529$; $p < 0.0001$; $n = 800$) is shown in Table 4.1 (Eqn 21). Seasonality in litter production (Figure 4.14 a) caused the litter pool size to increase in a step-wise fashion (Figure 4.14 b), with low rates of increase for the half-year when litter production rates are low and rapid increase when litter production is maximal. The equation developed to describe this pattern used a sine curve increasing linearly over time ($R^2 = 0.99$; $F = 418{,}754$; $p < 0.0001$; $n = 800$) (Table 4.1, Eqn 22).

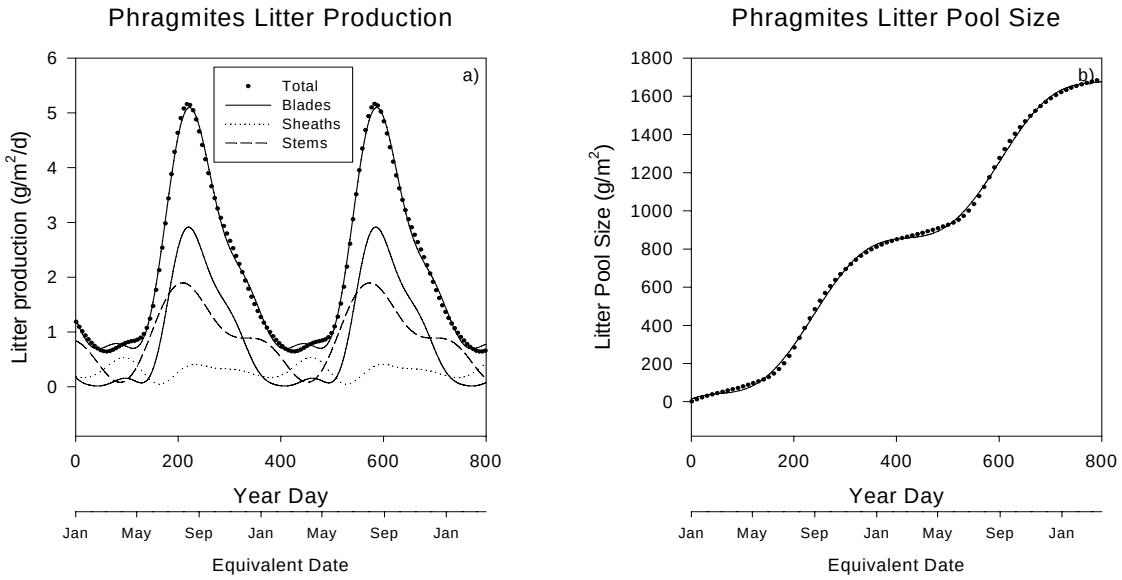

Figure 4.14. Changes to *Phragmites* litter production rate (a) and pool size (b) over time. The contributions of blades (solid line), sheaths (dotted line) and stems (dashed line) to litter production are shown in a). Data points are modelled values. Lines are the fitted functions.

Blade and stem loss rates were strong drivers of litter production in *Phragmites* compared to shoot density. The main peak of litter production in this species occurred during the peak blade loss period, despite dead shoot density of only 50% of maximum. Similarly, when dead shoot density approached its maximum (and sheath loss rate was about 50% of maximum), only a small peak occurred in total litter production because blade loss at this time was nearly zero. Despite stem loss from a single cohort peaking in December, stem litter production actually peaked at a similar time as blades (July – August), because of litter production by the previous year's cohort plus the interaction between dead shoot density and stem loss rate. The maximum modelled rate of litter production by *Phragmites* was 5.10 $g/m^2/d$ in August and the minimum was 0.69 $g/m^2/d$ in February. Total annual litter production by *Phragmites* (829 g/m^2 c.f. peak standing biomass of 3,760 g/m^2) was twice as large as for *Typha*.

4.3.3.3 Vallisneria

For this study, *Vallisneria* litter production was defined as the combination of leaf turnover plus blade losses associated with gross changes in shoot composition. Partial blade losses were not accounted for. Leaf turnover was not measured in this project, however data are available from other work on this and similar species. Blanch et al. (1998) estimated *Vallisneria* leaf turnover rates in a range of water depths and turbidities. The leaf turnover rate selected for use (0.037 blades/shoot/d) was intermediate between those of two depth treatments (39 and 49 cm) used by Blanch et al. (1998), due to differences in turbidity of their mesocosms and the river water at BRO.

The second litter component was assessed in this project (Section 4.3.2.3). Blade losses due to seasonal changes in shoot structure were added to the baseline turnover rate to determine total *Vallisneria* litter production throughout the year (Figure 4.15). The equation describing litter production changes over time for *Vallisneria* ($R^2 = 0.73$; $F = 19.30$; $p < 0.05$; $n = 21$) is shown in Table 4.1 (Eqn 23).

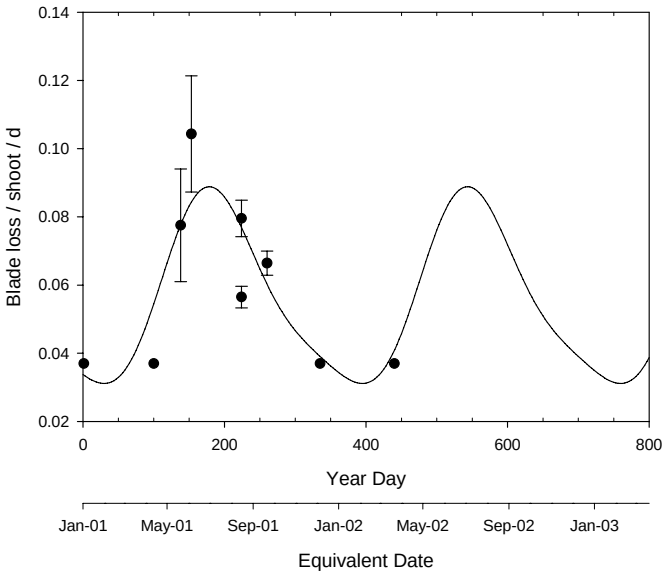

Figure 4.15. Changes to rates of blade loss from *Vallisneria* shoots over time. Data points are mean numbers lost/shoot/d (± s.e). Line is the fitted function.

Modelling of *Vallisneria* litter production assumed zero nett loss of shoot components during the peak growth period, commencing in December & continuing until commencement of major shoot compositional changes (and hence major blade loss) determined from the blade loss curve (early April). Thus, litter production over summer and early autumn was due almost entirely to blade losses from leaf turnover (Figure 4.15). The peak of modelled blade loss (0.089 blades/shoot/d) occurred in late June, decreasing over winter and spring.

The function developed to model total litter production in *Vallisneria* beds was basically the same as for blades, incorporating constants for shoot density and mean blade mass ($R^2 = 1$; $F = 3 \times 10^{13}$; $p < 0.0001$; $n = 800$) (Figure 4.16 a) (Table 4.1, Eqn 24). As with *Phragmites*, changes in *Vallisneria* litter pool size over time followed a sine wave increasing linearly with time (Figure 4.16 b) (Table 4.1 Eqn 25: $R^2 = 0.99$, $F = 3{,}692{,}671$; $p < 0.0001$; $n = 800$). Because constants were used for shoot density and mean blade dry weight for this species, litter production patterns were driven solely by changes in blade loss rates. The maximum rate of litter production for *Vallisneria* (5.58 g/m^2/d) was slightly higher than that for *Phragmites* and much higher than for *Typha*, resulting in an annual litter production total 1½ to 3 times larger (1,295 g/m^2 c.f. peak standing biomass of 620 g/m^2) than the emergent species.

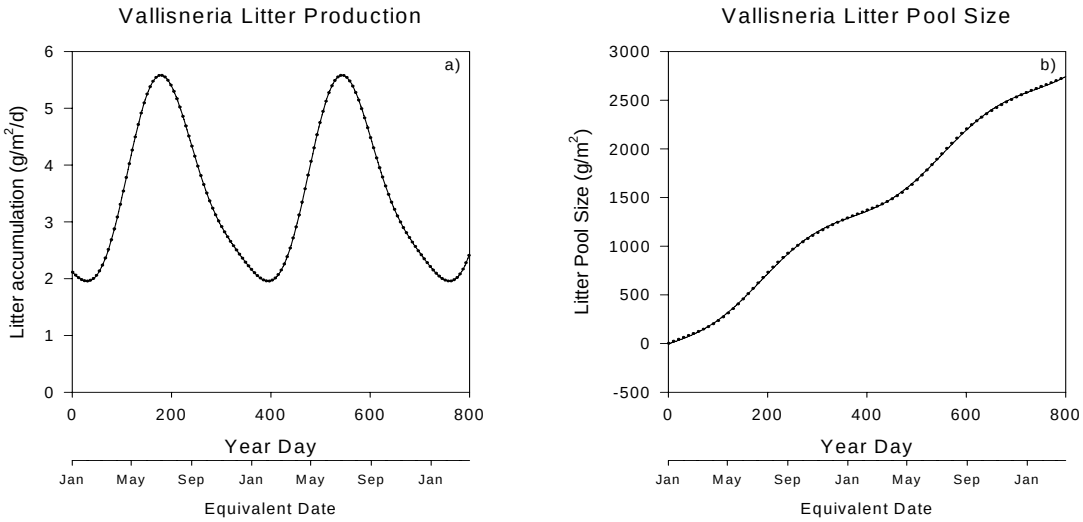

Figure 4.16. Changes to *Vallisneria* litter production rate (a) and pool size (b) over time. Data points are values modelled from blade loss data. Lines are the fitted functions.

4.3.4 Standing Litter

Only a relatively small amount of standing litter was present in exposed *Typha* beds at BAR on the collection date (41 g/m^2 – Table 4.2). Much more litter occurred in *Phragmites* beds at BAR (254 g/m^2) than BRO (44 g/m^2 – Table 4.2). The equivalent of standing litter in *Vallisneria* beds, POM trapped in the canopy, comprised 18 g/m^2 (Table 4.2).

Table 4.2. Standing litter collections from exposed and inundated bed areas for different species at BAR and BRO compared to predicted litter from modelling (g DW/m^2). Means ± s.e. (n).

Date	Site	Species	Measured Litter	Modelled Litter
5/08/2002	BAR	Typha	40.6 ± 6.5 (3)	52
6/08/2002	BAR	Phragmites	253.8 ± 145.0 (2)	310
12/08/2002	BRO	Phragmites	43.8 ± 33.2 (2)	1
19/5/2001	BRO	Vallisneria	17.8 ± 5.5 (6)	14

4.3.5 Modelling Macrophyte Organic Matter

In order to compile the observed changes in litter production and pools of live and dead standing material into a model of organic matter available for input under different flow scenarios, it was necessary to incorporate measures of mass, apply scaling factors and determine bed inundation under given flows (as per Chapter 2).

4.3.5.1 Standing OM

Standing OM available for input into the channel was calculated by multiplying shoot densities by the bed area in the reach for each species. Total numbers of shoots for each species in each reach are shown as the dotted curves in Figures 4.17 – 4.21. The maximum numbers of dead *Typha* and *Phragmites* shoots at BAR (331,700 and 2,230,300, respectively) were 1.5 times the maximum number of live shoots for the respective species at this site (217,500 and 1,705,500) (Figures 4.17 and 4.19). *Phragmites* shoots were far less abundant at BRO than at BAR – the maximum live number was 38,800 whereas dead shoot number peaked at 50,700 (Figure 4.21). Using constant values for *Vallisneria* and *Periscaria* shoot densities, the total numbers of shoots for these species were 80,400 at BRO and 2,999,300 at OVN, respectively (Figures 4.20 and 4.21).

4.3.5.2 Litter Accumulation and POM Inputs

Litter accumulation in emergent macrophyte beds was defined as litter produced within exposed bed areas which had not been previously inundated. To calculate litter accumulation, litter production in exposed beds on a given day was added to the litter pool size from the previous day and any POM inputs for that day were subtracted (with POM inputs calculated as the proportion of the litter pool (by area) inundated on that day). In order to compare litter production and accumulation dynamics within a single year under different flow regimes, litter accumulated in previous years was excluded from the scenarios run.

It should be noted that the use of terminology for modelling *Vallisneria* litter is slightly different to that for the emergent species. Whereas “accumulated litter” of emergent species refers to litter that is exposed in beds and not undergoing leaching, in *Vallisneria* the vast majority of litter is produced in inundated beds and hence enters the water immediately to commence leaching. While some of this litter is immediately washed away to contribute to transported riverine POM and hence acts as a non-point-source of DOM, other litter is retained in the canopy as a point-source or “hot spot” of DOM release to the rest of the system (“accumulated litter”). Modelling of *Vallisneria* litter accumulation assumed that all litter produced in inundated beds on a given day was retained in the canopy until discharge increased, flushing an estimated 50% of litter out of beds (“POM inputs”). Any litter produced in exposed

beds was assumed to remain in place until water levels rose to inundate exposed beds. The proportion of litter accumulated in exposed beds which then entered the transported POM pool was calculated as the proportion of exposed bed area inundated by increasing water levels multiplied by the pool size of litter accumulated in exposed beds.

In my modelling, POM inputs are disregarded in subsequent calculations of litter pool size, despite the fact that a proportion of the tissue would actually still remain in the reach (either within the macrophyte beds, deposited higher up on banks, swept away to form leaf packs elsewhere in the reach or incorporated into sediment). This is because the vast bulk of readily leachable organic matter is released from macrophyte tissues within the first 24 hours of inundation (see Chapter 5), and so subsequent immersions would probably not contribute substantially to nutrient releases and hence fuelling of secondary production in the river without the additional action by physical and biological forces to degrade the physical structure/ structural integrity of the tissues (although further work is required into patterns of OM release from macrophyte tissues which have been repeatedly wetted and dried). POM degradation rates from the literature (e.g. leaf pack studies) could be applied to modelled POM inputs predicted in this thesis to estimate persistence times of macrophyte POM, however this type of longer-term modelling is outside the scope of this project and will not be performed here.

4.3.6 Application of Models

Reach-scale standing organic matter pool sizes, litter production, litter accumulation and POM inputs were modelled using current macrophyte distributions and a range of flow management strategies. As shown in Chapter 2, the proportion of total macrophyte bed area inundated throughout the year varies depending on the hydrograph at each site (see Chapter 2). For emergent macrophyte species during periods of exposure, inputs of macrophyte organic matter to the river channel do not occur or are minor. Upon inundation, a pulse of macrophyte OM enters the river channel in the form of accumulated leaf litter (POM). The pool of standing OM (live and dead standing shoots) will also be wetted, potentially releasing DOM. For submerged species and inundated emergent macrophytes, on-going bed immersion results in a continual, low-level input of leachate from inundated standing shoots plus litter input directly into the water column.

Predictions of litter production and accumulation from my model were validated by comparison to standing litter data from collections made within *Typha* and *Phragmites* beds at BAR and *Phragmites* and *Vallisneria* beds at BRO during the study period and by comparison with alternative methods of calculation proposed in the literature. Estimates of annual litter production by *Typha* and *Phragmites* from my model were similar to values produced from mass-balance calculations using factors described by other workers. Approximately 18% of

peak live *Typha* biomass is translocated back to rhizomes upon senescence (Roberts and Ganf, 1986), and 25% of peak biomass has been reported to be lost due to aerial decomposition (Welsch and Yavitt, 2003). Some biomass might be expected to be respired off prior to senescence (1.2% - compiled from Asaeda et al., 2005, including the respiration figure for rhizomes (0.3%) applied to stems) and shedding of reproductive structures would account for an additional 200 g/m^2 at my study site. Seventy-two percent of remaining biomass has been suggested to contribute to litter production (Roberts and Ganf, 1986). At BAR, peak biomass for *Typha* during this study was 1,700 g/m^2 (mean shoot mass of 106 g multiplied by maximum shoot density of 16 shoots/m^2). Subtracting the factors outlined above and applying the 72% litter production coefficient produced an estimate of annual litter production of 540 g/m^2 using a mass-balance approach. The prediction from my model for annual litter production by *Typha* at BAR was 402 g/m^2. Similarly, annual litter production in *Phragmites* is approximately 40% (Soetaert et al., 2004) of annual nett photosynthetic production (peak biomass less production from rhizome resource remobilisation at the start of the growth season (18% – Soetaert et al., 2004), resorption of leaf production (3% – Soetaert et al., 2004), respiration (1.7% - Asaeda and Karunaratne, 2000) and the proportion translocated back to the rhizome upon senescence (26% – Asaeda and Karunaratne, 2000)). At BAR, *Phragmites* peak live biomass (mean live shoot mass of 30.1 g multiplied by maximum live shoot density of 125 shoots/m^2) was 3,760 g/m^2. Nett photosynthetic production was calculated as 1,930 g/m^2 after subtracting the factors described above. Annual litter production for *Phragmites* at this site estimated from these calculations was 770 g/m^2. The estimate produced by my model was 830 g/m^2.

Predictions of litter accumulation by my model were compared to standing litter collections made at the field sites during the study (Table 4.2). Predictions for *Typha* (52 g/m^2) and *Phragmites* (310 g/m^2) at BAR and *Vallisneria* (14 g/m^2) at BRO were quite close to litter accumulation observed in the field (41, 254 and 18 g/m^2, respectively). While litter accumulation predicted for *Phragmites* at BRO (1 g/m^2) was much lower than mean standing litter on the collection date (44 g/m^2), this mean was calculated from only two samples (due to some samples being lost) and variability was very high (range 11 – 77 g/m^2), making it difficult to determine if the model prediction was inaccurate or the standing litter collection sample size had not sufficiently encompassed the degree of variability at this site and the calculated mean is an overestimate.

In general, the model has performed well in predicting litter production and accumulation in macrophyte beds at the study sites and in comparison with calculation methods proposed by other workers, although litter accumulation in *Phragmites* beds at BRO needs further validation.

4.3.6.1 Typha

Applying the litter accumulation and standing OM models to the current annual average hydrograph at BAR (Figure 4.17 Current Hydrograph a), *Typha* beds were totally exposed between the 14th February and 15th March as well as between the 2nd April and the 23rd August, with varying degrees of inundation in the intervening periods. This flow regime caused inundation of *Typha* beds during spring and summer, when live shoot density was highest and dead shoot density lowest (Figure 4.17 Current Hydrograph b and c). Under more natural flow conditions (Figure 4.17 Historic Hydrograph a), *Typha* at BAR would be inundated over an extended period covering the peak and decline of dead shoot density as well as the rise to maximum of live shoot biomass (Figure 4.17 Historic Hydrograph b and c). During droughts, *Typha* beds at BAR would be exposed during summer and autumn, with minor bed inundation occurring throughout July – December, when live shoot density was high and dead shoot density low (Figure 4.17 Drought Hydrograph b and c). *Typha* beds were inundated all year round under the flood scenario, although maximum inundation depths and areas occurred from early June to late November, when live shoot densities were increasing to maximum and dead shoot densities decreasing (Figure 4.17 Flood Hydrograph).

Over an average year at BAR under current flows, 11% of total *Typha* litter production (5,310 kg) entered the water column by direct litter drop whereas 89% accumulated in beds and entered as pulses upon inundation (Figure 4.18 Current Hydrograph b). The maximum size of the litter pool was 2,210 kg, from which the largest single pulsed input of 560 kg occurred in late August (total litter pool was inundated fully over 11 days) and 52 kg of which remained in the beds after one year (Figure 4.18 Current Hydrograph c). Under pre-regulation flow conditions, twenty-four percent of annual *Typha* litter production was in the form of continuous litter drop directly into the water column throughout June – January (Figure 4.18 Historic Hydrograph b). The timing of litter accumulation and POM inputs was very different to current conditions – the maximum litter pool size of 2,080 kg all entered the channel in a single pulse over 5 days in late May (maximum single pulse of 940 kg) (Figure 4.18 Historic Hydrograph c). Litter remaining in beds at the end of the year totalled 91 kg. The drought scenario produced similar patterns of litter accumulation and POM inputs as under current conditions, although again the timing of inputs was earlier in the year. Ninety-three percent of litter accumulated in beds (maximum litter pool size of 2,780 kg, which entered as a single pulse over 19 days in early July) (Figure 4.18 Drought Hydrograph b and c). Large quantities of litter remained in beds to be carried over to subsequent years (392 kg). Because *Typha* beds were inundated to some degree all year round under the flood scenario, a larger proportion of annual litter production fell directly into the water column (44%) than under the other scenarios modelled (Figure 4.18 Flood Hydrograph b). The maximum quantity of litter accumulated and largest single POM input were 70 and 35 kg, respectively, occurring in December (Figure 4.18 Flood Hydrograph c). Only 50 kg of litter remained in the reach at the end of the flood scenario year.

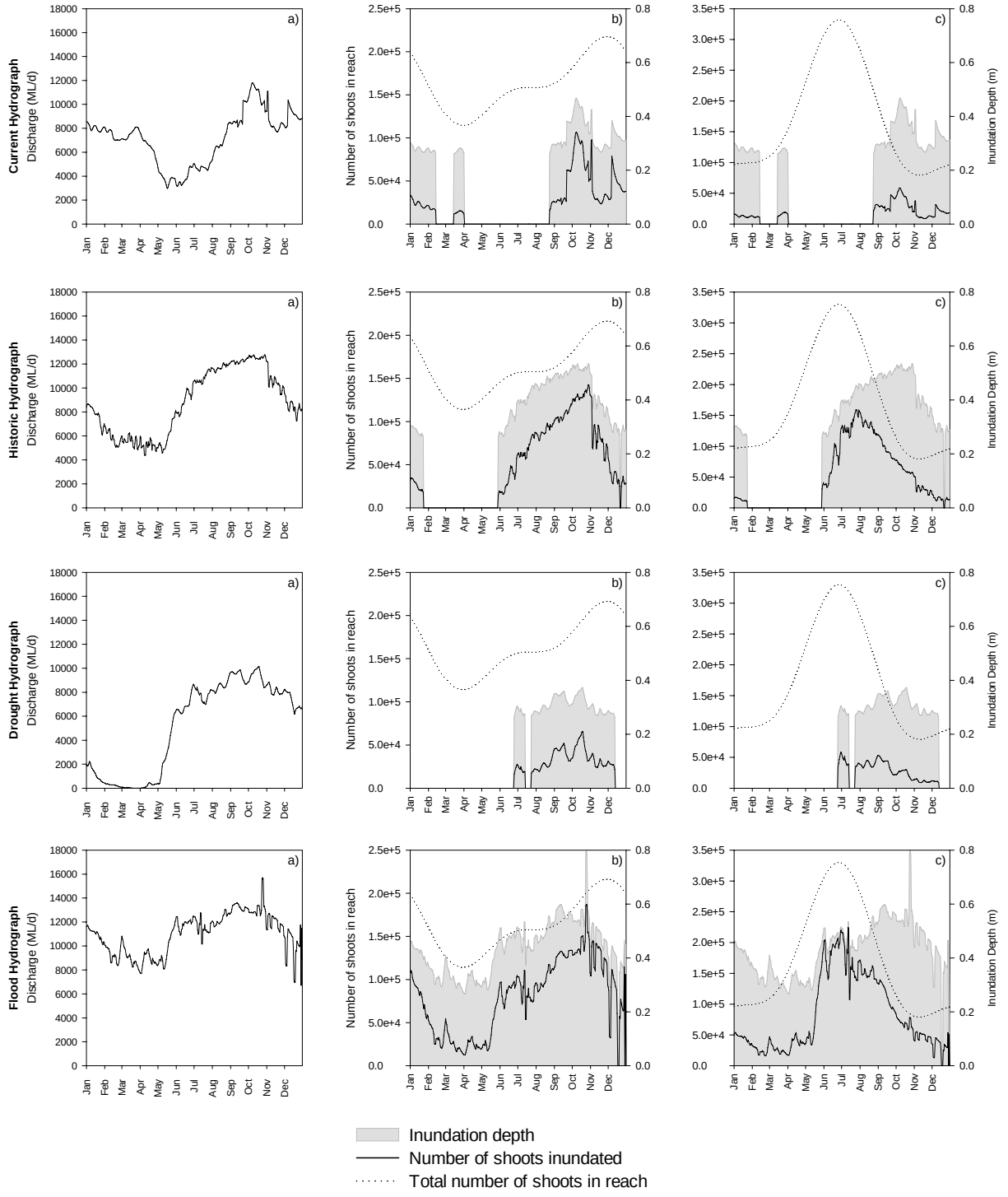

Figure 4.17. Changes to modelled *Typha* standing OM pools at BAR over time and inundation under different flow scenarios (grey filled areas show water depth inundating beds under different scenarios). The four flow scenarios modelled were (from top to bottom): current conditions, historical flows, drought conditions and flood. For each row, a) the hydrograph modelled, b) number of live shoots in reach inundated by specified flow conditions (solid line) compared to the total number of live shoots in the reach (broken line), c) number of dead shoots in reach inundated by specified flow conditions (solid line) compared to the total number of dead shoots in the reach (broken line).

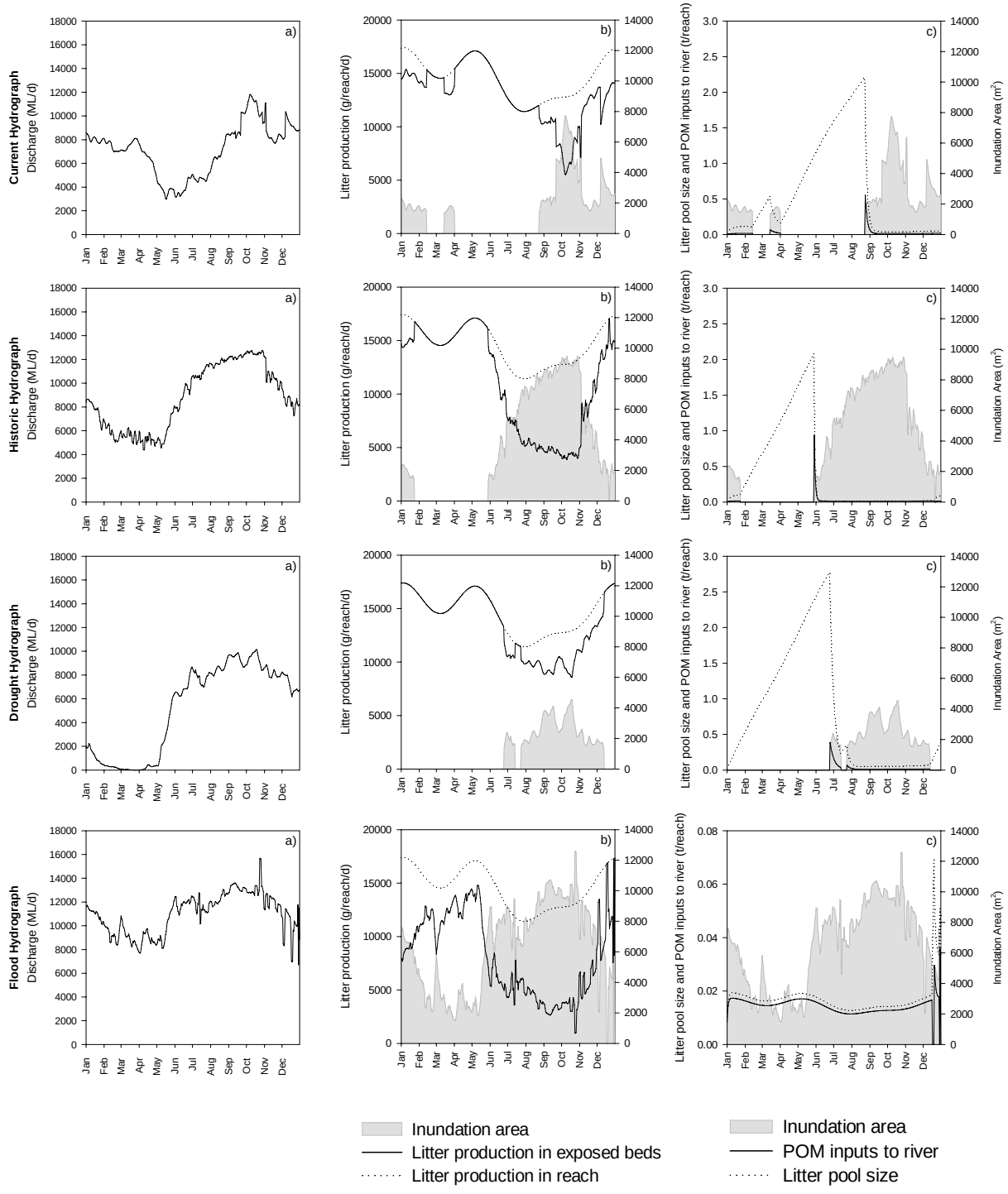

Figure 4.18. Changes to modelled *Typha* litter production, accumulation and inputs to the river at BAR over time for different flow scenarios (grey filled areas show bed area inundated under different scenarios). The four flow scenarios modelled were (from top to bottom): current conditions, historical flows, drought conditions and flood. For each row, a) the hydrograph modelled, b) litter production in exposed bed areas (solid line) compared to total reach production (broken line), c) litter accumulation in exposed bed areas (broken line) and POM inputs to the river (solid line). Note different y-axis for litter pool size in the flood scenario.

4.3.6.2 Phragmites

Under current flow conditions at BAR, *Phragmites* beds were inundated for a very short period from mid September to November, and again briefly in December. At these times both live and dead shoot densities were very low (Figure 4.19 Current Hydrograph b and c). Considerable quantities of litter accumulated during the extended period of exposure (96% of the total annual litter production of 11,120 kg) (Figure 4.20 Current Hydrograph b). Input of accumulated litter occurred as several pulses when beds were inundated (largest pulse of 1,870 kg in September). The exposed litter pool comprised 780 kg at the end of the year. Prior to regulation, *Phragmites* beds at BAR would have been inundated for extended periods, reducing litter accumulation in beds (25% of annual total) and promoting more continual low-level inputs of POM throughout the year (Figure 20 Historic Hydrograph b and c). The largest single pulse of litter input occurring under this scenario would have been 330 kg flushed out of beds during June. The maximum litter pool size attained under natural flows was 2,170 kg compared to 7,910 kg under current conditions, with 670 kg carried over to the following year. Bed inundation would span both peaks and troughs of live and dead shoot biomass (Figure 4.19 Historic Hydrograph b and c).

Both live and dead *Phragmites* shoot densities were at their minima when inundation occurred under the drought scenario at BAR (Figure 4.19 Drought Hydrograph b and c). Droughts caused even more extreme litter accumulation than current conditions, with bed exposure for most of the year leading to only 2% of litter entering the water column directly during bed inundation (Figure 2.20 Drought Hydrograph b). Of the 10,880 kg of litter which accumulated in exposed beds, 81% entered the water column as pulses during September and October, with 2,250 kg (or 165 g/m^2) remaining in beds at the end of the year (Figure 2.20 Drought Hydrograph c). In contrast, extensive inundation of *Phragmites* beds occurred at BAR under the flood scenario (Figure 4.19 Flood Hydrograph b and c). Beds were only exposed for brief periods during February, March and April, causing staggered litter accumulation and pulsed POM inputs during this period (maximum single input of 260 kg in May) (Figure 4.20 Flood Hydrograph c). During the main inundation period (June to December), litter accumulation and POM inputs were approximately equal, because around half of the total bed area was inundated. Overall, 39% of annual litter production entered the water column as continual litter drop, whereas 61% entered as pulsed inputs (Figure 4.20 Flood Hydrograph b). The maximum litter pool size was 580 kg, with 108 kg carried over into the following year.

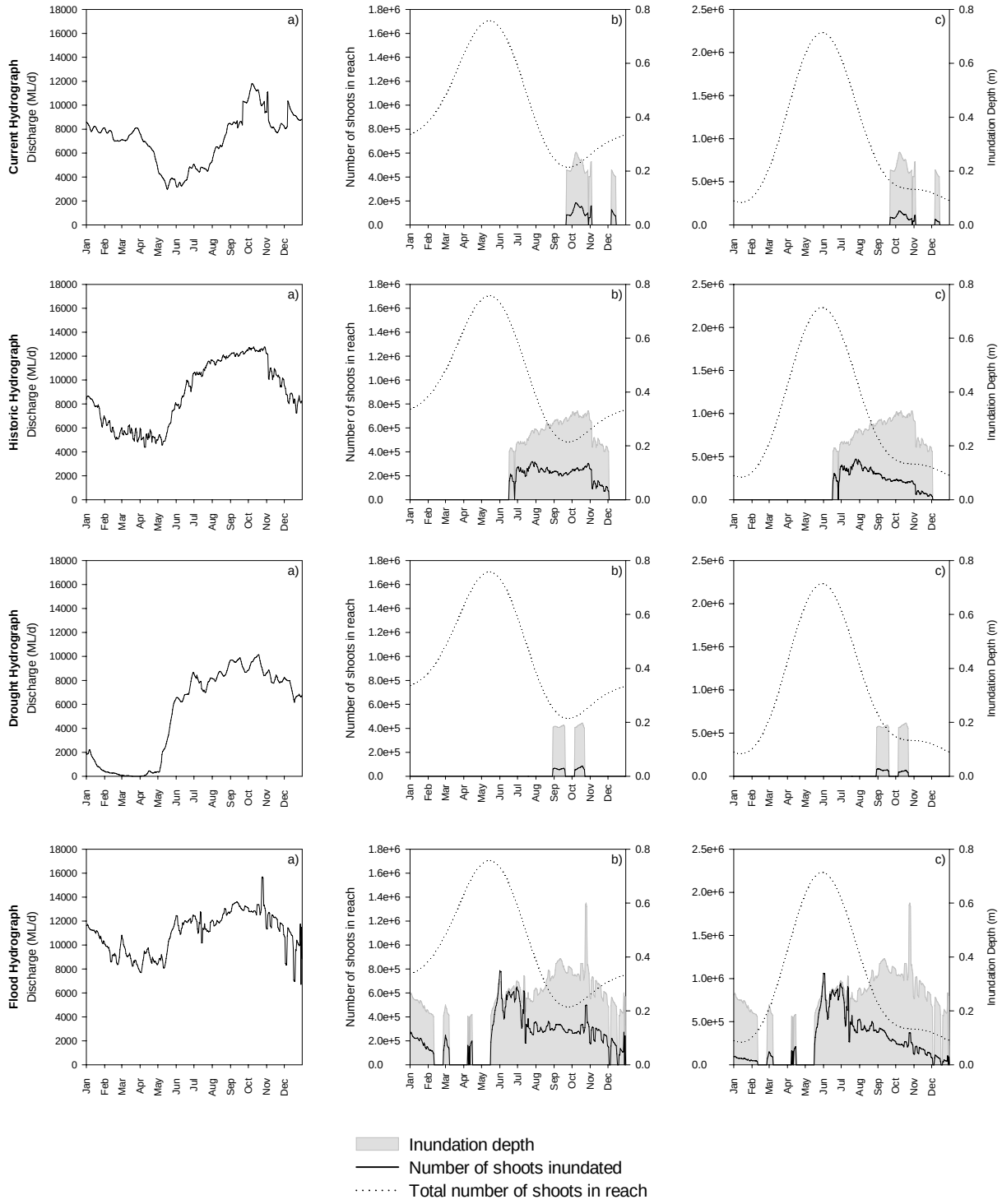

Figure 4.19. Changes to modelled *Phragmites* standing OM pools at BAR over time and inundation under different flow scenarios (grey filled areas show water depth inundating beds under different scenarios). The four flow scenarios modelled were (from top to bottom): current conditions, historical flows, drought conditions and flood. For each row, a) the hydrograph modelled, b) number of live shoots in reach inundated by specified flow conditions (solid line) compared to the total number of live shoots in the reach (broken line), c) number of dead shoots in reach inundated by specified flow conditions (solid line) compared to the total number of dead shoots in the reach (broken line).

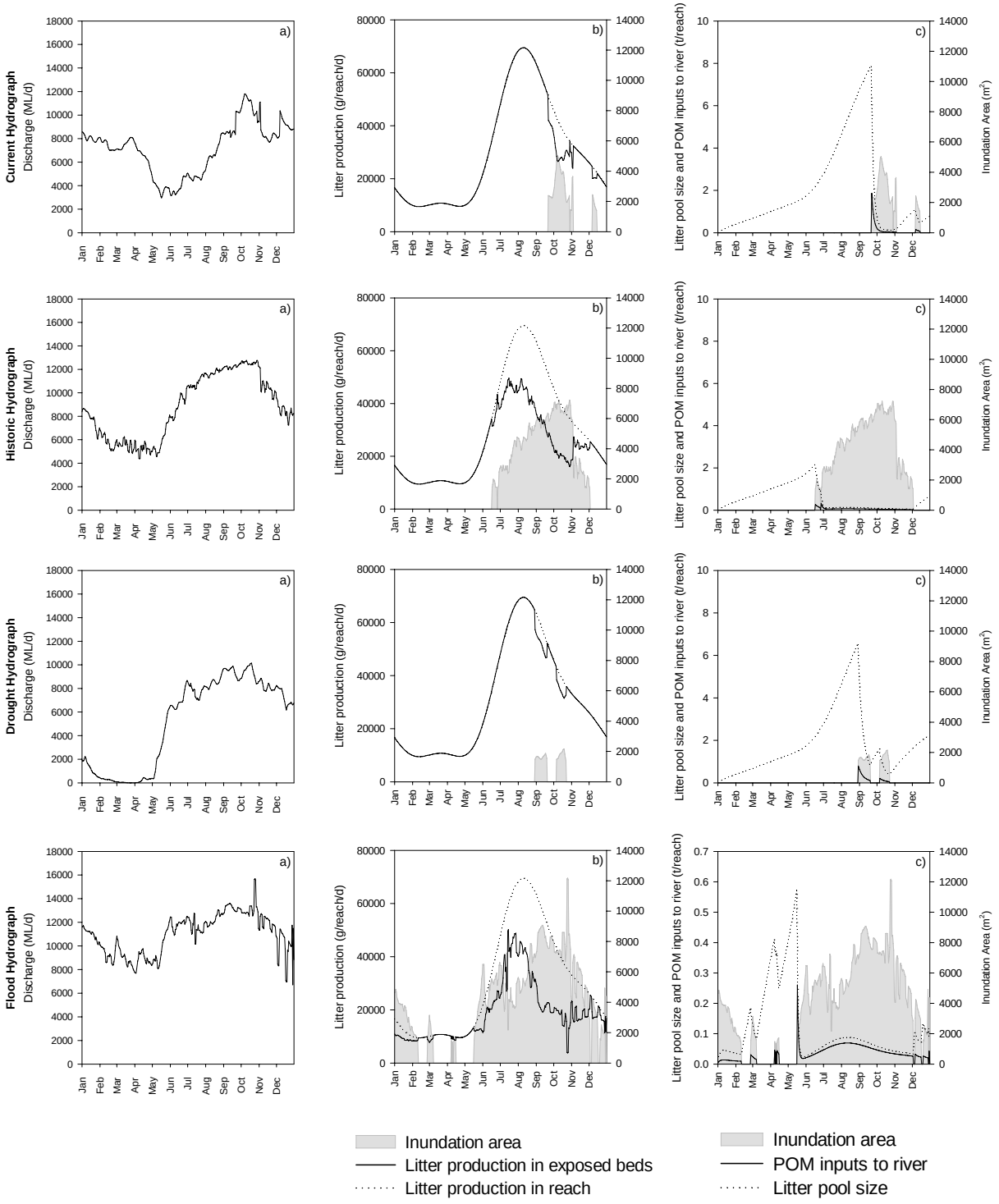

Figure 4.20. Changes to modelled *Phragmites* litter production, accumulation and inputs to the river at BAR over time for different flow scenarios (grey filled areas show bed area inundated under different scenarios). The four flow scenarios modelled were (from top to bottom): current conditions, historical flows, drought conditions and flood. For each row, a) the hydrograph modelled, b) litter production in exposed bed areas (solid line) compared to total reach production (broken line), c) litter accumulation in exposed bed areas (broken line) and POM inputs to the river (solid line). Note different y-axis for litter pool size in the flood scenario.

The majority of *Phragmites* bed area at the Broken River site was inundated continuously under current flow conditions. Both live and dead shoots were inundated, with peak inundation depths occurring when both live and dead shoot biomasses were minimal (Figure 4.21 Current Hydrograph b and c). Under current flow conditions at the Broken River site, the vast majority of the 253 kg of *Phragmites* litter produced in a year entered the reach directly, with only 1% accumulated in beds (Figure 4.22 Current Hydrograph b). The largest single pulsed input under this scenario was 2 kg in August and less than 1 kg of litter remained un-inundated at the end of the year. Similar results were produced under the historical flow scenario, with inundation of the majority of *Phragmites* bed area all year round, although the peak inundation period occurred slightly earlier in the year, immersing a greater biomass of both live and dead shoots (Figure 4.21 Historic Hydrograph b and c). As under current conditions, 99% of annual litter production entered the water column as direct litter drop, with the largest single input (2 kg) again occurring in August (Figure 4.22 Historic Hydrograph b and c). Less than 1 kg of litter was carried over into the following year.

During droughts at BRO, water levels were very variable and *Phragmites* beds were exposed for much of October – December, the period during which some of the greatest inundation depths usually occur (Figure 4.21 Drought Hydrograph b and c). Varying degrees of exposure and inundation continued up until May, when beds began to be fully inundated again, with total inundation from July onwards (Figure 4.21 Drought Hydrograph b and c). Thus, inundation of standing OM was quite flashy under this scenario, with peak inundation occurring during the peak and decline of both live and dead shoot density and periods of exposure occurring concurrently with periods of low shoot density. Drought conditions resulted in 72% of litter entering the channel directly (Figure 4.22 Drought Hydrograph b). The 70 kg of litter that accumulated in beds entered the water column in multiple small, rapid pulses (less than 2 kg at a time), with 10 kg of litter remaining in exposed beds at the end of the year (Figure 4.22 Drought Hydrograph c). Under the flood scenario, *Phragmites* beds at BRO were fully inundated from May to February, covering the peak and decline of both live and dead shoot biomass (Figure 4.21 Flood Hydrograph b and c). Flows were highly variable all year round, causing rapid changes in water level over the macrophyte beds and hence large fluctuations in bed areas inundated during the low flow period from February to May (Figure 4.21 Flood Hydrograph b and c). Five percent of annual litter production was accumulated in beds under this scenario, with three major pulsed inputs occurring in February (2.3 kg), March (2.7 kg) and May (3.5 kg) (Figure 4.22 Flood Hydrograph b and c). No standing litter remained un-inundated by the end of the year.

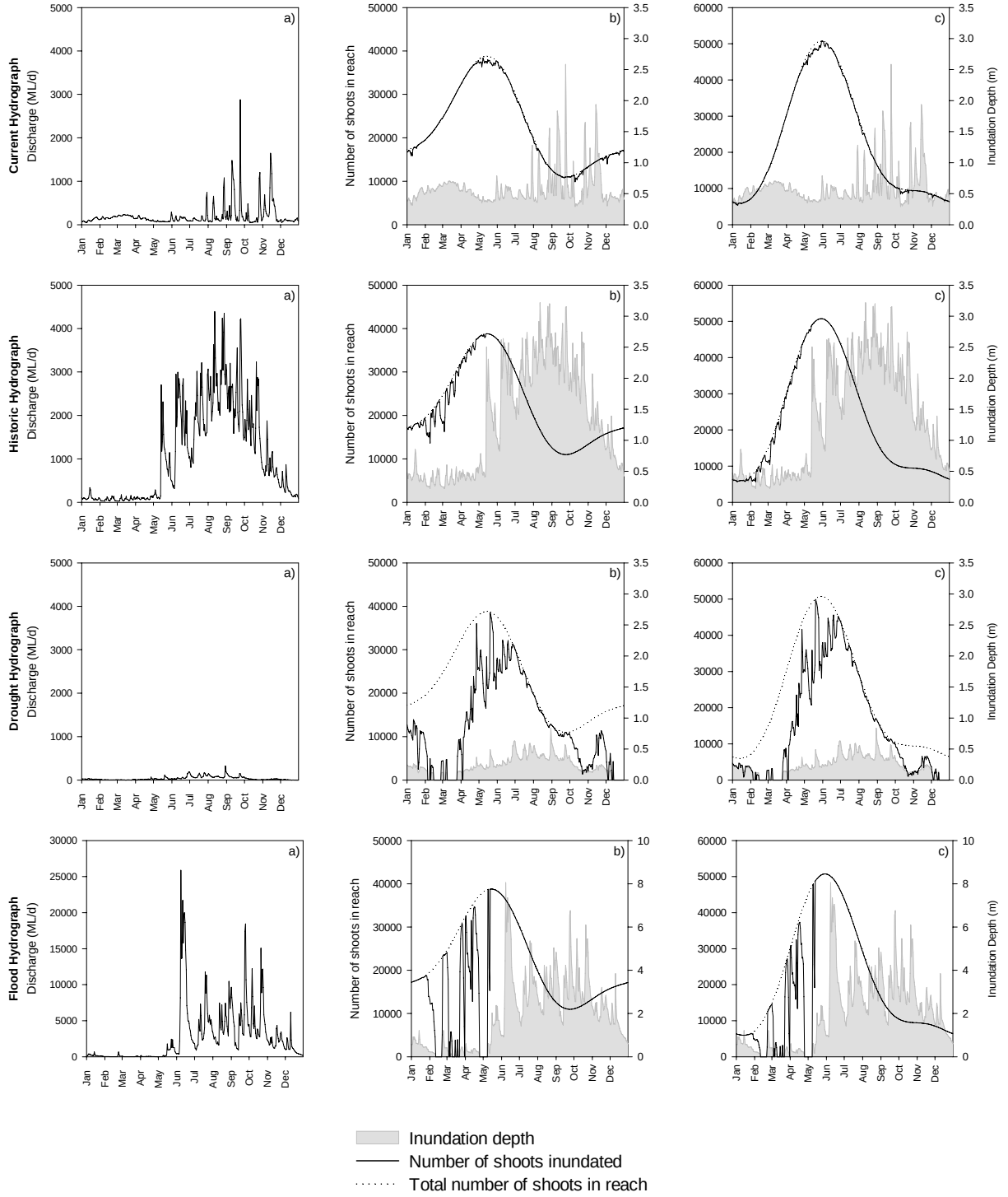

Figure 4.21. Changes to modelled *Phragmites* standing OM pools at BRO over time and inundation under different flow scenarios (grey filled areas show water depth inundating beds under different scenarios). The four flow scenarios modelled were (from top to bottom): current conditions, historical flows, drought conditions and flood. For each row, a) the hydrograph modelled, b) number of live shoots in reach inundated by specified flow conditions (solid line) compared to the total number of live shoots in the reach (broken line), c) number of dead shoots in reach inundated by specified flow conditions (solid line) compared to the total number of dead shoots in the reach (broken line). Note different scales on y-axes for discharge and inundation depth in the flood scenario.

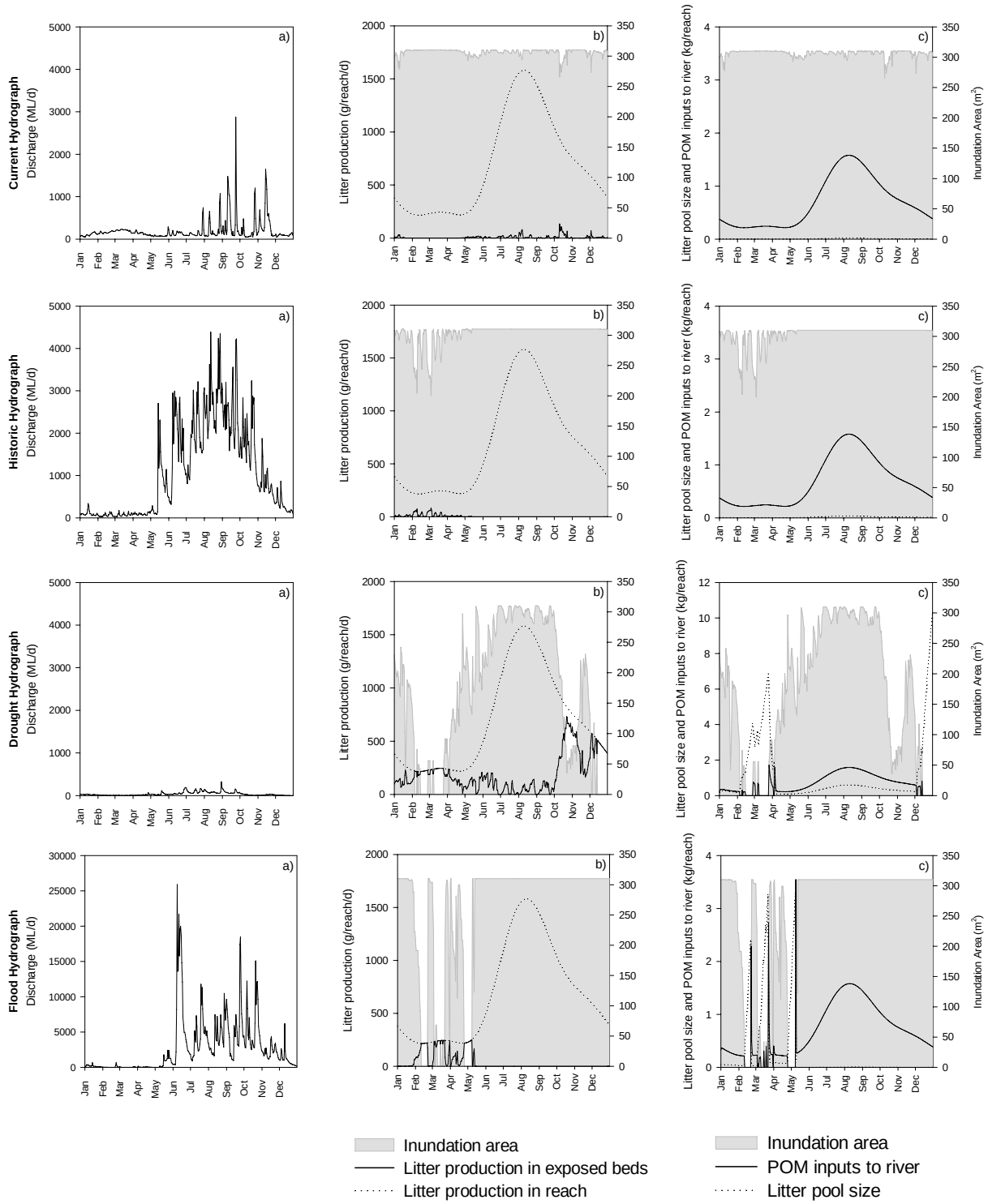

Figure 4.22. Changes to modelled *Phragmites* litter production, accumulation and inputs to the river at BRO over time for different flow scenarios (grey filled areas show bed area inundated under different scenarios). The four flow scenarios modelled were (from top to bottom): current conditions, historical flows, drought conditions and flood. For each row, a) the hydrograph modelled, b) litter production in exposed bed areas (solid line) compared to total reach production (broken line), c) litter accumulation in exposed bed areas (broken line) and POM inputs to the river (solid line). Note different y-axes for litter pool size in the drought scenario and discharge in the flood scenario.

4.3.6.3 Vallisneria

Under current average flow conditions a large proportion of the total number of *Vallisneria* shoots in the BRO reach were inundated for the majority of the year, with a mean water depth of 28 cm (Figure 4. 23 Current Hydrograph b). Historically, shoot inundation would have been much more seasonal, with many beds exposed over summer and autumn and total bed area inundation in winter and spring (mean water depth of 1 m) (Figure 4.23 Historic Hydrograph b). During droughts, however, large numbers of shoots would be totally exposed for much of the year, and those which were still submerged would be covered by shallower water (mean water depth over inundated beds of 15 cm) (Figure 4.23 Drought Hydrograph b). The flood scenario produced results similar to pre-regulation flows, with distinct seasonality of inundation, although inundation rates during low flow periods were greater and water overlying beds was deeper (mean of 1.8 m) (Figure 4.23 Flood Hydrograph b).

Under current flow conditions at BRO, the vast majority of *Vallisneria* litter was produced in inundated beds (Figure 4.24 Current Hydrograph b). Although discharges were quite low, rapid variation in flows caused frequent flushing of beds so that the litter pool was never very large (maximum of 19 kg) (Figure 4.24 Current Hydrograph c). The largest inputs (17 kg each) occurred in July and September.

Historically, patterns of litter production, accumulation and input were similar to current, although litter production in exposed beds was limited to spring and autumn, the maximum litter pool size and POM input were slightly larger (24 kg each) and the timing of peak POM input was earlier in the year (May), coinciding with the start of the high flow period (Figures 4.24 Historic Hydrograph b and c).

Very different results were produced under the drought scenario – most of the litter was produced in exposed beds and large quantities of litter accumulated in beds due to the lack of flushing by rising water levels (Figure 4.24 Drought Hydrograph b and c). While two large POM inputs occurred in April and May (80 and 91 kg, respectively), the peak input period actually occurred in winter. The maximum litter pool size was 139 kg and large quantities of litter remained in beds at the end of the year (112 kg) compared to current and historic conditions (3 and 5 kg, respectively). The extreme seasonality of flows under the flood scenario (Figure 4.24 Flood Hydrograph a) produced patterns of litter production, accumulation and litter input similar to droughts in the first half of the year and similar to historic conditions in the second half of the year (Figure 4.24 Flood Hydrograph b and c). The maximum litter pool size and POM input were both 56 kg, with peak litter input occurring in autumn – winter, and 24 kg of litter remained in the beds by the end of the year.

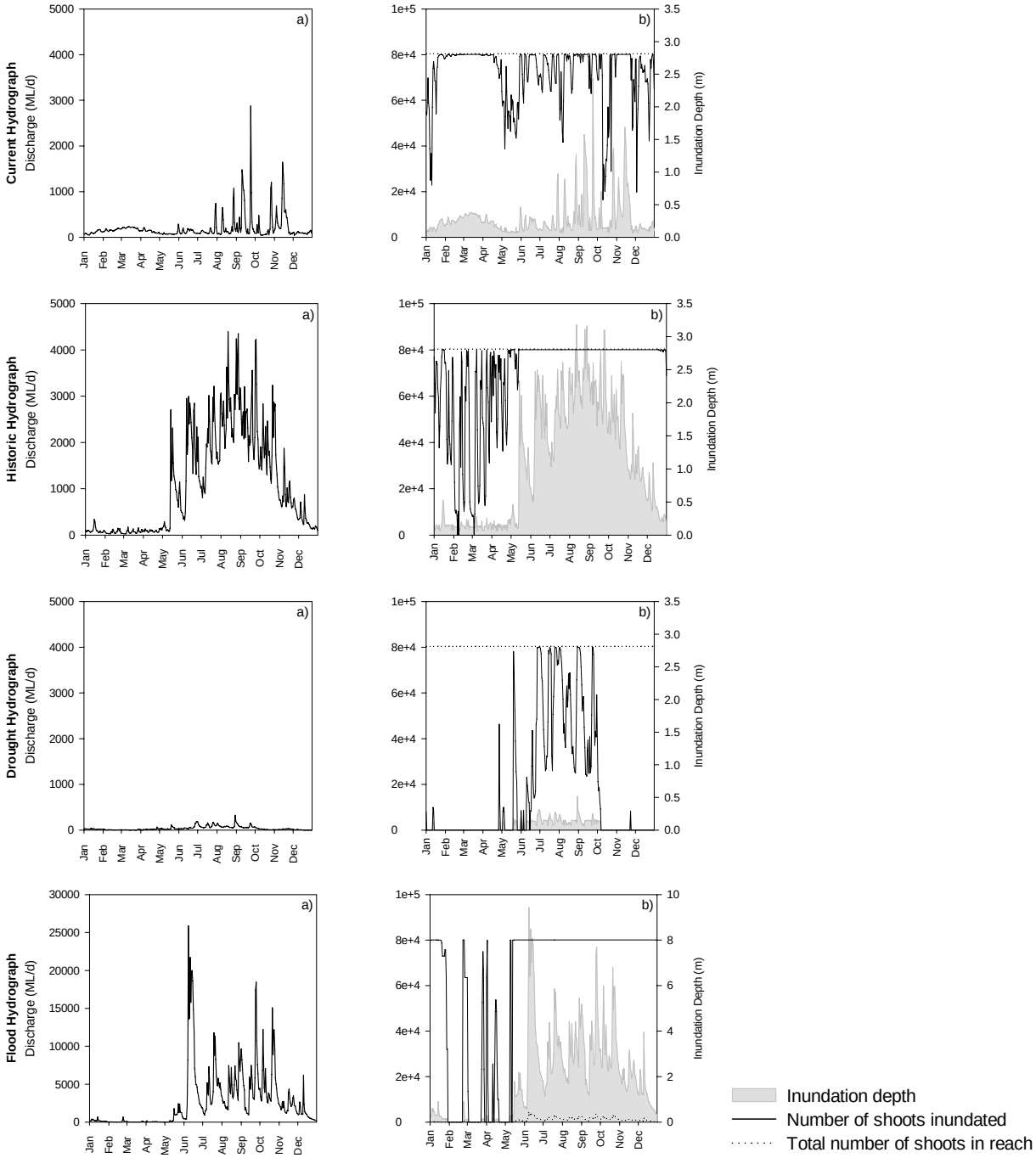

Figure 4.23. Changes to modelled *Vallisneria* standing OM pools at BRO over time and inundation under different flow scenarios (grey filled areas show water depth inundating beds under different scenarios). The four flow scenarios modelled were (from top to bottom): current conditions, historical flows, drought conditions and flood. For each row, a) the hydrograph modelled, b) number of shoots in reach inundated by specified flow conditions (solid line) compared to the total number of shoots in the reach (broken line). Note different scales on y-axes for discharge and inundation depth in the flood scenario.

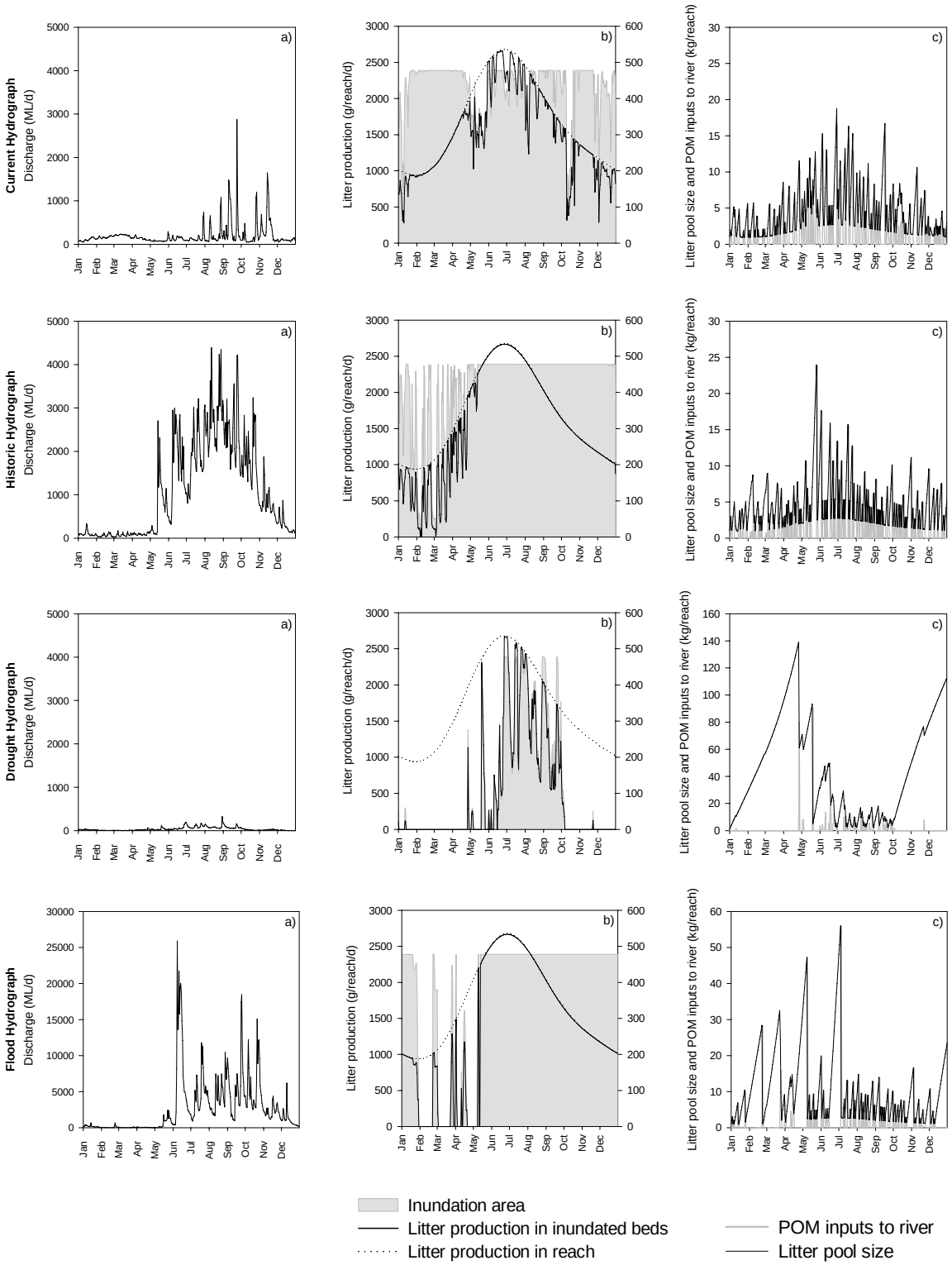

Figure 4.24. Changes to modelled *Vallisneria* litter production, accumulation and inputs to the river at BRO over time for different flow scenarios (grey filled areas show bed area inundated under different scenarios). The four flow scenarios modelled were (from top to bottom): current conditions, historical flows, drought conditions and flood. For each row, a) the hydrograph modelled, b) litter production in inundated bed areas (solid line) compared to total reach production (broken line), c) litter accumulation in *Vallisneria* canopy (both exposed and inundated bed areas) (black line) and POM inputs flushed from the beds into the river (grey line). Note different y-axes for litter pool size in the drought and flood scenarios and for discharge in the flood scenario.

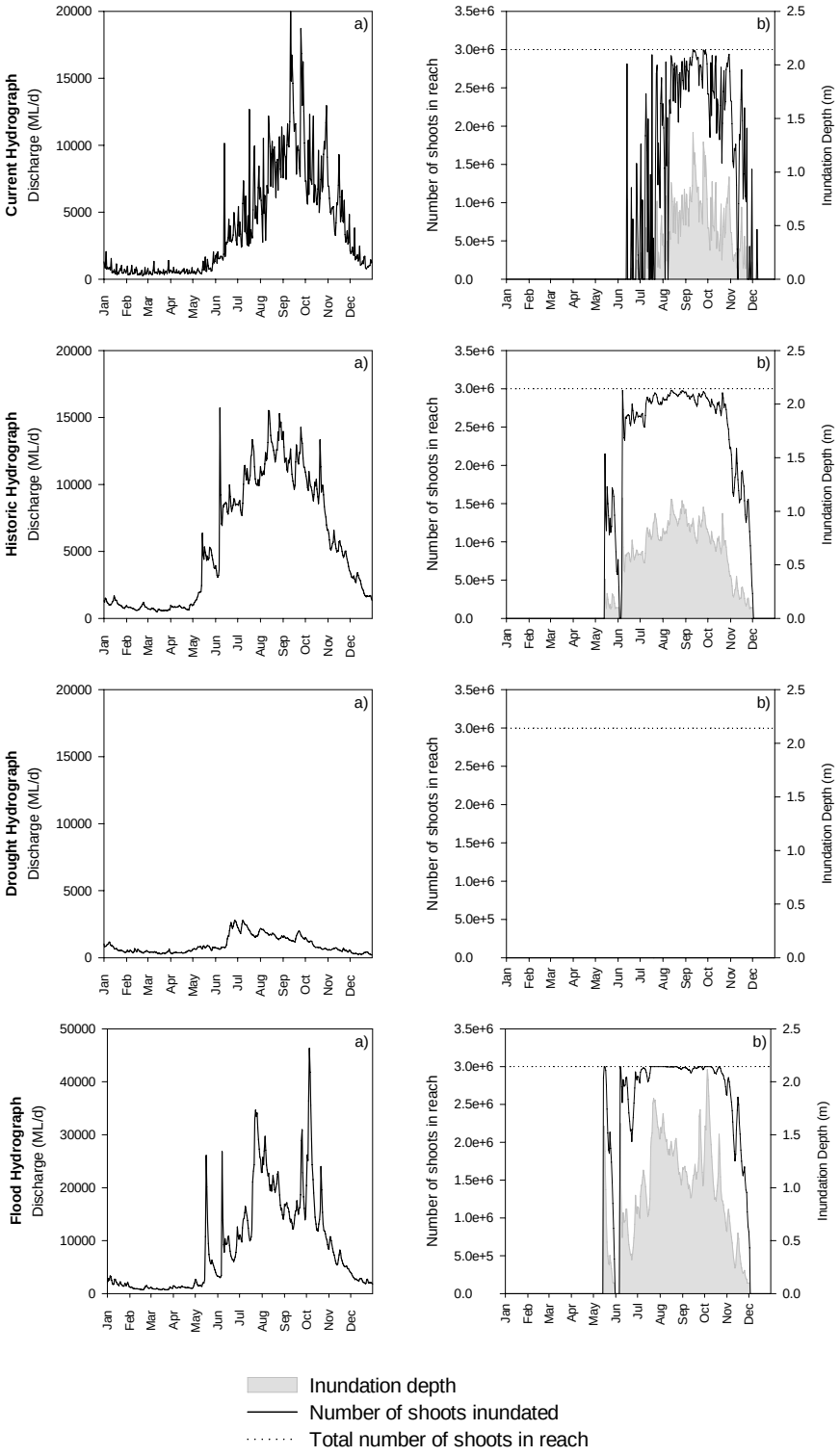

Figure 4.25. Changes to modelled *Persicaria* standing OM pools at OVN over time and inundation under different flow scenarios (grey filled areas show water depth inundating beds under different scenarios). The four flow scenarios modelled were (from top to bottom): current conditions, historical flows, drought conditions and flood. For each row, a) the hydrograph modelled, b) number of shoots in reach inundated by specified flow conditions (solid line) compared to the total number of shoots in the reach (broken line). Note different scale on y-axis for discharge in the flood scenario.

4.3.6.4 Persicaria

Persicaria shoot inundation patterns at OVN were similar under the current, historic and flood scenarios, with inundation of the majority of shoots in the reach from May to December (Figure 4.25). However, shoots were rapidly exposed and re-inundated during this period under current conditions, whereas historically and during floods they were constantly inundated. Water depths overlying inundated shoots averaged 50, 62 and 90 cm for the current, historic and flood scenario, respectively. During droughts, *Persicaria* beds at OVN would be exposed all year round (Figure 4.25 Drought Hydrograph b).

4.4 Discussion

The development of a quantitative method to estimate macrophyte organic matter available for input to lowland river channels required the formulation of functions to evaluate pools of, and rates of change to, standing live and dead organic matter and litter. The main functions developed describe changes to shoot density over time and rates of litter production from those biomass components making substantial contributions to litter. Incorporation of macrophyte distribution and inundation data from Chapter 2 and biomass component mean masses from Chapter 3 allowed scaling and modelling of different flow scenarios.

Variations in shoot densities over time were described for three of the four species under study, although no attempt was made to develop a mathematical equation for *Vallisneria* due to the limited scope of data. *Typha* shoot modelling revealed that although early season shoots were produced in autumn, the peak growth period for this species was in spring and peak biomass occurred in summer, a pattern often observed in this species (Mason and Bryant, 1975; Dickerman and Wetzel, 1985; Roberts and Ganf, 1986; Asaeda et al., 2005). The range of shoot densities observed for *Typha* in this study (live: 8 – 16 shoots/m^2; dead: 6 – 25 shoots/m^2; total: 19 – 32 shoots/m^2) were somewhat lower than those reported in most other studies (10 – 50 live shoots/m^2 (Dickerman and Wetzel, 1985; Asaeda et al., 2005); 20 – 60 dead shoots/m^2 (Asaeda et al., 2005); 30 – 100 shoots/m^2 total (Mason and Bryant, 1975; Froend and McComb, 1994)), although Miao and Sklar (1998) and Grace and Wetzel (1981) observed 25 or fewer shoots/m^2 in the Florida Everglades and a Michigan lake.

Patterns of modelled shoot density change over time were similar for *Phragmites* at both BAR and BRO, suggesting that observed trends are species-specific rather than being site-specific. Major increases in both live and dead *Phragmites* shoot densities occurred through autumn, with peak biomass occurring in summer. Other studies have reported peak *Phragmites* biomass in either summer (Kvet et al., 1969; Asaeda and Karunaratne, 2000; Soetaert et al., 2004) or autumn (Hocking, 1989; Rolletschek et al., 1999). Shoot densities observed for

Phragmites in the current study (live: 37 – 116 shoots/m^2; dead: 14 – 137 shoots/m^2; total: 64 – 252 shoots/m^2) were lower than in a eutrophic European estuary (126 – 587 shoots/m^2 – Soetaert et al., 2004), but higher than in two European lakes (39 – 62 shoots/m^2; Gessner, 2001; 0 – 170 shoot/m^2; Mason and Bryant, 1975).

Modelled shoot densities were 3 – 8 times higher for *Phragmites* than for *Typha*, which probably relates to differences in mean shoot biomass of these species (*Typha* shoots had four-fold greater mass) rather than large differences in productivity at these study sites (NAPP up to 3,500 g DW/m2 for *Typha* spp. (Mason and Bryant, 1975; Dickerman and Wetzel, 1985; Roberts and Ganf, 1986; Froend and McComb, 1994; Miao and Sklar, 1998; Asaeda et al., 2005) and up to 5,000 g DW/m2 for *Phragmites*, (Mason and Bryant, 1975; Allirand and Gosse, 1995; Gessner, 1996; Kohl et al., 1998; Rolletschek et al., 1999; Karunaratne et al., 2004; Soetaert et al., 2004), although some instances of much higher production (12,000 g/m^2) have been reported for *Phragmites* (Hocking, 1989; Asaeda and Karunaratne, 2000)). While *Vallisneria* shoot densities were high in comparison to the emergent species (2 – 3 times those of *Phragmites* and 14 – 17 times those of *Typha*), mean shoot mass was much lower ($1/12^{th}$ that of *Phragmites* and $1/47^{th}$ that of *Typha* (Chapter 3)). The differences in standing stocks of the emergent and submerged species may be driven by differential resource allocation, lower productivity in the submerged species, or shoot biomass turnover rather than accumulation in *Vallisneria* compared to the other two species. The preliminary model presented for *Vallisneria* shoot density changes driven by discharge and season presents an interesting opportunity for further study. One modification to the model which seems justified theoretically but which requires more data would be an alteration to the shoot density response at very low flows. Rather than replicating the temperature/discharge interaction predicted under medium and high flows, one might expect fewer shoots during periods of high temperature at low discharge (due to higher rates of desiccation), and conversely, greater shoot survival if exposure occurred during periods of low temperature. Future work to sample shoot density covering a range of discharge/time combinations is necessary to assess these predictions.

For both *Typha* and *Phragmites* shoot density modelling, losses from the live shoot pool did not always appear immediately in the dead shoot pool. For example, live *Phragmites* shoots lost from June to September do not cause an increase in the dead shoot pool at this time. Similarly, increases in dead shoot density can occur without apparent decreases in the live shoot pool (e.g. initial part of *Phragmites* dead shoot density peak). Rather than representing flaws in the observed or modelled data, these apparently unexplained appearances and disappearances are a consequence of measuring pools rather than rates. Principles of population ecology can be used to assist in interpretation of the processes underlying the observed changes in macrophyte

shoot densities (as per Dickerman and Wetzel, 1985; Carr et al., 1997), using shoot production, senescence, losses due to grazing, scouring, etc and recruitment of plantlets transported from upstream as equivalents of births (B), deaths (D), emigration (E) and immigration (I), respectively. Thus, shoot density observed at any given time is a function of B + I - D - E. For the species studied in this project, immigration rates are probably very low and not worth considering, however emigration (grazing by water rats, cattle, kangaroos; decomposition; litter drop; scouring; damage/ removal by wind action, water birds, falling tree limbs, burrowing animals; etc) is probably an important process affecting both live and dead shoot density. Thus, the following descriptive equations may be derived:

Live shoot density observed at a given time = $B - D - E_1$

Apparent dead shoot density at a given time = $D - E_2$

It should be noted that processes affecting emigration, and therefore emigration rates, will be different for live and dead tissues, hence the use of 'E_1' and 'E_2' notation above. At times when apparent rates of increase in dead shoot density are greater than losses from the live shoot pool, actual rates of live shoot production may be far higher than the changes in the pool size indicate. Similarly, when live shoots are lost without concurrent increases in the dead shoot pool, either some direct loss of live shoots is occurring which never enter the dead pool (E_1 – e.g. grazing) and/or live shoots are entering the dead shoot pool but that rapid removal (E_2 – e.g. litter loss) is masking the actual senescence rate.

The second major component of this work examined rates of loss of biomass components considered to be major contributors to litter over a 1 – 2 year period, in order to model litter production for the different species. Exclusion of some biomass components from this study, i.e. reproductive structures and below-ground biomass, was based on a combination of expert opinion (D. Williams, pers. comm.), the observed masses of particular components lost from shoots over time (Chapter 3) and evidence of standing litter composition in macrophyte beds (Chapter 3).

Of the biomass components assessed, patterns of loss are relatable to growth and senescence habits, i.e. phenology, of each species. Rather than being shed simultaneously, blade loss commenced before sheath loss in both *Typha* and *Phragmites* – fragile dead blades were shed readily and while some sheath tissue was concurrently torn from the shoot, most remained attached (more so for *Phragmites* than *Typha*). The submerged habit of *Vallisneria* resulted in continual colonisation by epiphytic growth, which increases with leaf blade age. The pattern of continuous production of new blades to replace old, epiphyte-covered blades (which are then discarded) in this species resulted in a continual low-level input of POM to the river. The leaf turnover rate used in modelling *Vallisneria* litter production in this study is comparable to rates

observed in seagrasses with similar growth forms as *Vallisneria* (West and Larkum, 1979; Wahbeh, 1984; Olesen and Sand-Jensen, 1994; Dennison and Alberte, 1986). Litter production due to leaf turnover is augmented by blade drop associated with gross changes in shoot composition in autumn. Reductions in above-ground biomass during autumn has been reported for *Vallisneria* elsewhere (Dawes and Lawrence, 1989; Kurtz et al., 2003), supporting the seasonal patterns observed in this study. Although *Vallisneria* has also been shown to decrease blade production with increasing turbidity (Blanch et al., 1998), there was no correlation between changes to turbidity and variations in leaf number per shoot in the present study (turbidity at BRO during this study was basically stable – data not presented here). Mean numbers of leaves per shoot observed in this study (7 – 12.5) were lower than values reported in the literature (16 – 71: Blanch et al., 1998; Kurtz et al., 2003).

Peak biomasses for *Typha*, *Phragmites* and *Vallisneria* observed in this study were 1,700 g/m^2, 3,760 g/m^2 and 620 g/m^2, respectively. Modelled litter production in *Vallisneria* in this study was much higher than for *Typha* or *Phragmites*, indicating that the smaller standing stock of *Vallisneria* is a result of rapid turnover of a small but productive biomass pool rather than slow biomass accumulation of standing stock due to low productivity. However, total annual production is not just the sum of standing stock and litter production – other sinks for production include respiration, translocation of resources to storage/over-wintering structures, reproductive losses and decomposition (Allirand and Gosse, 1995; Carr et al., 1997; Asaeda and Karunaratne, 2000; Asaeda et al., 2002; Soetaert et al., 2004; Asaeda et al., 2005). Of these, translocation to storage structures is probably a major sink for annual *Typha* and *Phragmites* production at the study sites, but probably not for *Vallisneria* in warm climates (Dawes and Lawrence, 1989) such as in south eastern Australian lowland rivers, where the lack of tuber production in this species has been noted previously (Blanch et al., 1998). If translocation to rhizomes is accounted for using estimates from the literature of 18% of NAPP for *Typha* (Roberts and Ganf, 1996) and 26% for *Phragmites* (Asaeda and Karunaratne, 2000), the biomass available to contribute to annual litter production for the emergent species becomes more similar to (*Typha*: 710 g/m^2) or surpasses (*Phragmites*: 1,810 g/m^2) annual estimates for *Vallisneria* (1,295 g/m^2). Shedding of reproductive structures in *Typha* would also be a substantial sink for production, given the biomass of flowers in this species (48 g, i.e. 25% of reproductive shoot mass or another 200 g/m^2 of NAPP). Clearly, alternative sinks for above-ground production are more important for the emergent species than the submerged species at the study sites.

Functions for shoot density changes and litter production were incorporated into a model of litter accumulation and shoot inundation for different flow scenarios using macrophyte distribution data and inundation curves from Chapter 2. Although limited data were available to

validate this final model, there was reasonable agreement between model predictions, field observations and estimates calculated using other techniques. Further validation would be beneficial before the final model is used for management interventions.

Modelled OM inputs under different flow scenarios showed that changes to management practices, such as flow regulation, can alter the timing, quantity and composition of OM inputs from macrophytes. Alterations to discharge quantity and timing affected the extent, duration and timing of exposure and inundation of macrophytes, which have implications depending on the species' tolerances for flooding and desiccation at different temperatures and periods in the growth cycle. In contrast to the limited degree of inundation experienced by *Typha* beds at BAR under current flow conditions, prior to regulation beds were inundated extensively during the peak period of shoot production. Differences in inundation patterns during shoot production periods could affect expansion of macrophyte bed areas and successful recruitment of new shoots to the population. *Phragmites* tends to occur at higher elevations than *Typha*, on banks and on the floodplain (Chapter 2), and so might be expected to be adapted to drier conditions (Blanch et al., 1999b). Prior to river regulation, ground-water conditions experienced by *Phragmites* growing on upper banks and the floodplain might have been similar to the drought scenario modelled, given that major rainfall events occur in autumn and winter in south eastern Australia (Bureau of Meteorology – data not shown). Natural flows result in the concurrence of 'wet' periods and the peak of live *Phragmites* biomass, with the greatest period of exposure occurring in late spring and summer, when live shoot density would be low. This indicates that the growth cycle of *Phragmites* may be adapted to have low live shoot biomass over late spring and summer, when ground-water availability under natural conditions would be limited.

Although not investigated in this study, changes to flow management would also impact on the distribution and abundance of macrophytes at each site as discussed in Chapter 2 (e.g. extended periods of exposure or flooding at BRO could wipe out *Vallisneria*, or conversely, further reductions in flow variability at BAR could encourage more widespread growth of *Typha*), which would in turn affect macrophyte OM inputs. Other water chemistry and physical parameters such as temperature, light attenuation, pH, etc. may also affect plant physiology and hence distribution, abundance and litter production of both emergent and submerged species. The higher temperatures associated with shallow water overlying *Vallisneria* beds during the drought (mean depth of 10 cm) may have resulted in increased litter production, higher shoot mortality and hence reduced bed area.

Partitioning of litter inputs into those which enter the river as direct drop versus in pulses may have flow-on effects for riverine functioning, providing either a diffuse, continual source of carbon or pulses of OM input. This carbon may be available immediately to higher trophic

levels, or require initial processing via the microbial loop (Findlay et al,. 1986; Moran et al., 1988; Meyer, 1994). Pulsed inputs of OM would provide a carbon resource for organisms with rapid response rates and short turnover times, such as microbes and zooplankton. In contrast, continual inputs are more likely to be utilised by larger, slower-growing fauna including caddis-flies, mayflies and other detritivorous or biofilm-grazing macro-invertebrates. Timing of inputs would be critical in supplying food during different life stages, such as the major growth period during the final instar stage of many macro-invertebrates (J. Hawking, pers. comm.). Comparisons of modelled litter inputs from emergent and submerged macrophytes suggest that differential supply types occur in different flow scenarios. Under natural conditions, emergent macrophytes provide a large, continual supply of OM during winter, probably benefiting larger, slow-growing predatory macro-invertebrates. Inputs from submerged species would be a mix of steady (autumn-winter) and pulsed (spring-summer) forms. River regulation causes greater exposure of emergent macrophyte beds during periods of litter accumulation, resulting in "hot spots" (both spatially and temporally) of macrophyte OM inputs upon inundation in spring/summer, which would cause rapid growth of biofilms and micro-crustacean grazers (D. Nielsen, pers. comm.), and fuel the emergence of macro-invertebrates with short life-cycles, such as caddis-flies and aquatic bugs. Although a regulated flow scenario was not modelled for *Vallisneria* at BRO, one would expect that the stable flows associated with regulation would result in greater accumulation of litter within beds, which would then act as a point-source of OM release. Thus, river regulation promotes pulsed inputs of macrophyte OM during spring/summer, potentially favouring riverine microbial and zooplankton production. However, as less of the annual litter production of emergent species actually entered the river in this scenario, secondary production based on macrophyte OM might be lower. These processes may be partly responsible for the paucity of macro-invertebrate fauna in regulated lowland rivers.

During droughts, emergent species would again provide pulsed OM inputs, however these would occur in autumn/winter. Inputs from submerged plants would depend on the nature of flows, with increasing flow variability (which was common in the hydrographs of the three study rivers during drought years – see Chapter 2) resulting in a diffuse supply of OM. The overall outcome would be a combination of pulsed and diffuse inputs during autumn/winter, with little OM release from macrophytes over summer. Lower water temperatures during autumn and winter would limit the response of microbial, zooplankton and macro-invertebrate communities to macrophyte inputs, however rates of release of DOM would probably also be slower than during warmer weather due to inhibition of both physico-chemical and biologically-mediated leaching processes (Bohman and Tranvik, 2001; Chapter 5).

The principles outlined above would suggest a similar combination of input types during a flood, with an initial pulse of OM input stimulating microbial and zooplankton production followed by a period of lower-level, continual inputs utilised by a range of organisms from higher trophic levels, depending on the timing of the flood. If flooding was in spring or autumn, enhanced biological activity would probably lead to rapid fragmentation and aerobic decomposition of macrophyte POM. In summer or winter, low oxygen levels and low temperatures, respectively, might inhibit activity levels of higher organisms, leading to the formation of leaf packs or incorporation of macrophyte POM into sediments and increased levels of anaerobic decomposition.

Generally, under natural conditions, input of litter from emergent species would be in the form of direct drop into the channel during May – December, with peak litter inputs for most species occurring in winter. The timing of these OM inputs is complementary to those of one of the other major contributors of carbon to lowland rivers, native riparian trees, which occur during summer (Bowen and Williams, in prep.; Gawne et al., submitted). During droughts, litter from emergent macrophytes would accumulate in exposed beds, but input would still most likely occur in late autumn/winter when the drought broke.

As temperature plays a role in microbial utilisation of OM, the timing of macrophyte inputs will be important to the in-stream microbial response generated. River regulation for irrigation purposes usually alters flows such that the highest discharges occur over summer. Current regulation at BAR has caused changes in the magnitude, composition and timing of macrophyte inputs compared to historical conditions. The interaction of these factors will affect the rates of leaching, bio-availability and microbial metabolism of DOM released from macrophyte tissues, as discussed in the following chapters.

4.5 Conclusion

Although management practices have substantially altered organic matter inputs to most south-eastern Australian lowland rivers, macrophytes still represent a major source of carbon to many of these systems. The introduction to this chapter revealed the gaps in our understanding of pools and fluxes of macrophyte POM in rivers, knowledge which is required to better understand the links between macrophyte production and the rest of the system. This study aimed to advance our understanding of litter production and variation in standing biomass over time in Australian lowland river macrophytes, and perform one of the first attempts at direct quantification of macrophyte POM inputs to rivers.

Quantitative models of sizes of, and rates of change to, standing live and dead biomass and litter pools were developed from assessments of litter production and shoot density changes over time in four common riverine macrophyte species. These models were incorporated with macrophyte distribution, inundation and biomass data to predict the effects of flow regime on the quantity, composition and timing of organic matter inputs from macrophyte beds to lowland river channels.

The different species showed different patterns of shoot density and litter production, composition and accumulation. Patterns of modelled shoot density change over time were similar across sites, and in comparison with the literature, suggesting that observed trends are species-specific rather than being site-specific. Alternative sinks for above-ground production (besides the litter pool) were more important for the emergent species than the submerged species at the study sites (e.g. translocation to rhizomes, reproductive losses).

Modelled OM inputs under different flow scenarios showed that changes to flow management can alter the timing, quantity and composition of OM inputs from macrophytes to rivers. Under natural flow conditions, emergent macrophytes provide a large, continual supply of OM during winter, probably benefiting larger, slow-growing macro-invertebrates. Pulsed inputs from submerged species in spring/summer would supply carbon to the system during the major growth period of many macro-invertebrate larvae. River regulation promotes pulsed inputs of macrophyte OM during spring/summer, potentially favouring riverine microbial and zooplankton production, although at lower levels due to the overall reduction in OM inputs. These processes may be partly responsible for the paucity of macro-invertebrate fauna in regulated lowland rivers.

This chapter provides fundamental information on pools and fluxes of macrophyte POM in Australian lowland rivers, linking macrophyte production with functioning in the rest of the system. Models developed represent the first attempt at quantifying inputs of macrophyte POM to rivers and enable prediction of inputs from macrophyte beds to lowland river channels under different flow conditions, allowing examination of some of the implications of altered OM inputs to the rest of the system.

Chapter 5. Leaching of dissolved fractions from macrophyte particulate organic matter.

5.1 Introduction

Inputs from macrophytes can represent a substantial and functionally important portion of the carbon budget of streams and rivers (Fisher and Carpenter, 1976; Findlay et al., 1986; Gawne et al., submitted). Dissolved carbon from aquatic plants can enter aquatic ecosystems as photosynthetic exudate or from leaching of particulate material once immersed (Wetzel, 1969; Wetzel and Manny, 1972a; Wetzel and Manny, 1972b; Findlay *et al*, 1986). While rates of photosynthate exudation from aquatic plants may be quite small in most river systems (approximately 4% of net shoot production – Wetzel and Manny, 1972b), other forms of dissolved organic matter from macrophytes may be important, given that particulate inputs can represent a major carbon source in lowland rivers (see Chapter 4).

Studies of macrophyte leaching (Lush and Hynes, 1973; Otsuki and Wetzel, 1974; Hough and Wetzel, 1975; Pakulski, 1986; Mann and Wetzel, 1996) reveal a range of DOM release rates and quantities similar to those for terrestrial vegetation (Webster and Benfield, 1986; Baldwin, 1999; Moore and Dalva, 2001). Rates of DOM release from plant tissues are usually fastest within the first 24 – 48 hours of immersion (Godshalk and Wetzel, 1978a; Otsuki and Wetzel, 1974; Harrison and Mann, 1975; Baldwin, 1999). Unfortunately, macrophyte leaching experiments have often involved extensive pre-treatment of samples (such as freezing, drying and grinding), resulting in data which may not be immediately applicable to the estimation of DOM release from POM in the field. Also, studies generally utilise one type of tissue (usually leaves) from a single species. The few studies which have examined leaching patterns of different macrophyte tissues demonstrated greater quantities of DOM release from leaves than from stems (Kominkova *et al.*, 2000) and from senescent tissues than green (Mann and Wetzel, 1996).

The major metabolic pathway for DOM leached from macrophytes is through the microbial loop (Findlay *et al.*, 1986; Moran et al., 1988; Meyer, 1994; Findlay *et al.*, 1998). DOM leached within the first 24 – 48 hours is comprised mainly of low molecular weight compounds (under 10 000 Da) (Amon and Benner, 1996; Mann and Wetzel, 1996), many of which can be rapidly utilised by bacteria (Kaplan *et al.*, 1980). Bacterial growth efficiencies on macrophyte OM range from 9 to greater than 90% (Linley and Newell, 1984; Findlay *et al.*, 1986; Meyer *et al.*, 1987; Mann and Wetzel, 1996; del Giorgio and Cole, 1998), and probably relate to varying proportions of rapidly-utilisable labile DOC and more recalcitrant compounds (Wetzel and Manny, 1972a; Findlay *et al.*, 1986).

As with terrestrial plant OM, rapid breakdown rates have been reported for macrophyte tissues and leachates with lower C:N and C:P ratios (Gessner, 2000a; Polisini and Boyd, 1972; Hodkinson, 1975; Godshalk and Wetzel, 1978b; Moran and Hodson, 1989; Polunin, 1982; Kominkova *et al.*, 2000; Sinsabaugh et al., 1993; Gessner and Chauvet, 1994; Godshalk and Wetzel, 1978a), or lower proportions of structural components such as fibre and lignin (Gessner, 2000a; Godshalk and Wetzel, 1978b; Godshalk and Wetzel, 1978a; Sinsabaugh et al., 1993; Kominkova *et al.*, 2000). Growth form has also been proposed to influence macrophyte decomposition (ie. to affect bio-availability) (Godshalk and Wetzel, 1978a), with the hierarchy of decomposition presented as floating plants > submerged plants > emergent plants (with interpretation based on the presence or absence of humic compounds).

The composition of a leachate will affect its bio-availability, due to nutrient ratios, the presence of inhibitory compounds or varying sizes and complexity of molecular compounds. Organic matter from aquatic plants has been characterised by analysis of nutrient content (mainly carbon, nitrogen and phosphorus – Polisini and Boyd, 1972; Hodkinson, 1975; Godshalk and Wetzel, 1978b; Moran and Hodson, 1989; Polunin, 1982; Gessner, 2000a; Kominkova *et al.*, 2000; Sinsabaugh et al., 1993; Gessner and Chauvet, 1994; Godshalk and Wetzel, 1978a). The carbon content of leachates has been quantified using UV absorbance (Findlay *et al.*, 1998; Godshalk and Wetzel, 1978a; Wheeler, 1976; Baldwin, 1999) although some authors found that relationships were not constant over all molecular weight fractions (Godshalk and Wetzel, 1978a; Wheeler, 1976). Fluorescence spectroscopy has been used to broadly characterise the chemical composition of dissolved organic compounds (Coble, 1996; Mobed et al., 1996; Baker and Genty, 1999; Mayer et al., 1999; Baker, 2001; McKnight et al., 2001; Westerhoff et al., 2001; Baker, 2002a; Baker, 2002b; Ohno, 2002; Alberts and Takacs, 2004; Yamashita and Tanoue, 2004), including plant leachates (Godshalk and Wetzel, 1978a; Senesi, 1990; McCarthy *et al.*, 1997; Findlay *et al.*, 1998; Howitt, 2003).

Comparisons of macrophyte DOM release between species, tissue types and tissue states are currently limited by a lack of research effort, the small number of species and tissue types assessed, and the use of a variety of different approaches in different studies. Interpretation of leaching data and prediction of leaching under field conditions is further limited by unnatural sample pre-treatments and the paucity of quantitative data over time scales less than 1-2 days. This study aimed to compare the rates of release and composition of DOM leached from a range of green and senescent tissues from four macrophyte species with different growth forms. It was hypothesised that:

- rates and total quantities of DOM release would be greater from tissues with lower proportions of structural tissues (e.g. leaf blades rather than stems);
- rates and total quantities of DOM release would be greater from senescent tissues than green;
- rates and total quantities of DOM release would be greater from emergent plant tissues than from submerged species;
- the composition of leachates derived from green tissues would indicate a higher degree of bio-availability than those from senescent tissues; and
- the composition of leachates derived from submerged plant species would indicate a higher degree of bio-availability than those from emergent and semi-terrestrial plants.

A range of biomass components collected from various macrophyte species in the field were used in time-course leaching experiments in the laboratory to determine rates and maxima of leaching of dissolved fractions from particulate organic matter. The composition of leachates derived from these experiments was assessed using nutrient analysis and three-dimensional fluorescence excitation-emission spectra.

5.2 Methods

5.2.1 Plant Material

Dead plant material from *Typha orientalis*, *Phragmites australis*, and *Persicaria prostrata* were collected from lowland reaches (BAR, BRO and OVN) of three rivers in south eastern Australia (Murray, Broken and Ovens Rivers) from May 01 – December 02 as described in Chapter 3 (Table 5.1). Material was dried to a constant weight at 60 ^{o}C in a Thermoline D120 dehydrating oven and stored until required for use in experiments. Live plant material from the above species, and live and dead *Vallisneria gigantea* tissues, were freshly collected just before each experiment from Woolshed Creek, the Murray River at Mungabareena Reserve or the Murray River near Hume Weir, all at Albury (Table 5.1). Tissues were wiped to remove any dirt or obvious epi -flora or -fauna. Tissue types assessed were a subset of the biomass components described in Chapter 3 (Table 5.2).

Table 5.1. Summary of collection locations for live and dead plant material of each species.

Species	Collection Sites for Different Tissues	
	Live Tissues	*Dead Tissues*
Phragmites australis	Murray River, Mungabareena	BAR, BRO
Typha domigensis	Woolshed Creek, Thurgoona	BAR
Persicaria prostrata	Murray River, Mungabareena	OVN
Vallisneria gigantea	Murray River, Hume Weir	Murray River, Hume Weir

Table 5.2. Summary of tissue types used in leaching experiments.

Species	Blades	Sheaths	Stems	Whole Shoot
Phragmites australis	L, D	L, D	L, D	-
Typha domigensis	L, D	L, D	L, D	-
Persicaria prostrata	-	-	-	L, D
Vallisneria gigantea	L, D	-	-	-

L = live tissue; D = dead tissue

5.2.2 Leaching Experiments

5.2.2.1 Experimental Setup

Leaching experiments were carried out with a range of OM loadings in order to avoid saturation effects of maximum leaching rate and total DOM release from each tissue type (Table 5.3). At high loadings, maximum DOM release would be expected, however the potential for inaccurate leaching rate measurement increases due to physico-chemical limitations (e.g. solution becoming saturated). Maximum leaching rates would be expected to occur at low OM loadings, however error may be introduced as the detection limit of equipment is approached. Thus, three OM loadings were utilised for each tissue type, covering 1.5 to 2 orders of magnitude. Masses of live tissue used were 5 – 10 times those for dead tissues to account for the differences between "wet" weights of fresh tissue and dry weights of dead tissue, and thus ensure that similar dry weights were added to each flask.

Leaching assessments were conducted over a series of six experiments (Table 5.3) due to logistical limitations. Weighed samples of each tissue type were cut into 0.5 – 5 cm^2 pieces and placed into conical flasks. Controls had no plant material added. RO water was added to the flasks, which were then covered with parafilm or cotton wool bungs. Plant tissues were leached with gentle agitation on an orbital shaker for 48 hours in the dark at 20 ^oC (Figure 5.1). Samples (5 ml) were removed at 8 – 10 time points throughout the incubation for assessments of dissolved organic matter, with the volume removed from each flask replaced with an equal volume of RO water. Volumes removed and replaced were not incorporated into final leaching calculations as they comprised less than 10% of the total flask volume.

Table 5.3. Summary of leaching experiments performed.

Experiment	Tissue Types	Loadings (g/L)	Replicates
A	Typha Sheath D	1, 10, 25	3, 3, 3
	Above + Azide	1, 10, 25	3, 3, 3
	Controls	0	3
	Controls + Azide	0	3
B	Typha Sheath L	1, 10, 50	3, 3, 3
	Above + Azide	1, 10, 50	3, 3, 3
	Controls	0	3
	Controls + Azide	0	3
C	Pers Shoot D	0.1, 1, 10	3, 3, 3
	Phrag Blade D	0.1, 1, 10	3, 3, 3
	Typha Blade D	0.1, 1, 10	3, 3, 3
	Vall Shoot D	0.1, 1, 10	3, 3, 3
	Control	0	9
D	Pers Shoot L	1, 10, 50	3, 3, 3
	Phrag Blade L	1, 10, 50	3, 3, 3
	Typha Blade L	1, 10, 50	3, 3, 3
	Vall Shoot L	1, 10, 50	3, 3, 3
	Controls	0	3
E	Phrag Sheath L	1, 10, 50	3, 3, 3
	Phrag Sheath D	0.1, 1, 10	3, 3, 3
	Phrag Stem L	1, 10, 50	3, 3, 3
	Controls	0	3
F	Phrag Stem D	0.1, 1, 10	3, 3, 3
	Typha Stem L	1, 10, 50	3, 3, 3
	Typha Stem D	0.1, 1, 10	3, 3, 3
	Controls	0	3

L = live tissue, D = dead tissue; Pers = *Persicaria*, Phrag = *Phragmites*, Vall = *Vallisneria*

Figure 5.1. Photograph showing experimental setup: flasks containing plant tissues and RO water rest on an orbital shaker table within a darkened enclosure in a constant temperature room set to 20^{o}C.

Because the plant tissue contained microbial communities which would utilise the DOM as it leached out, the extent of microbial uptake during incubation was assessed by performing a series of experiments where one of the treatments was sterilisation (achieved by adding sodium azide at a final concentration of 2.5 mM to flasks containing plant material and RO water) (Table 5.3).

5.2.2.2 DOM Assessments

The concentration of DOM in the flasks was monitored over time, using absorbance at 250 nm as a surrogate for dissolved organic carbon content (Godshalk and Wetzel, 1978a; Wheeler, 1976; Baldwin, 1999). Leachate samples were centrifuged at 3000 rpm for 10 minutes (Beckmann Allegra 6R centrifuge) to remove particulate material and absorbance measured at 250 nm against an RO-water blank. Leachates with $Abs_{(250)}$ greater than 1.5 were diluted prior to final measurement then corrected for the dilution factor. Coefficients for converting absorbance units to carbon content were generated by assessing the carbon content of a sub-set of absorbance samples (stored at -20 ^{o}C). Carbon content was measured using a Model 1010 Total Organic Carbon Analyser (O.I. Analytical, Texas) as per the APHA Total Organic Carbon Method 5310C (Eaton et al., 1995).

5.2.3 Leachate Composition

Leachates obtained after 48 hours of incubation (Figure 5.2) for each treatment were retained for compositional analysis and use in later microbial response experiments. Leachates were sterilized by passing sequentially through a coarse mesh net, GF/F and 0.2 µm pore size membrane filters, into autoclaved bottles.

Figure 5.2. Photograph showing examples of leachates obtained from different macrophyte tissues.

5.2.3.1 Nutrient Analysis

Total carbon, nitrogen and phosphorus content of leachates derived from each tissue type were determined. Carbon analysis followed the procedure outlined above, whereas simultaneous analysis of total nitrogen and phosphorus involved persulphate digestion on a Lachat Instruments QuickChem 8000 Flow Injection Analyser (Hosomi & Sudo, 1986) performed by J. Pengelly at the Analytical Chemistry Laboratory of the Murray-Darling Freshwater Research Centre. This lab operates under national standards of QA and QC.

5.2.3.2 Fluorescence Excitation-Emission Spectra

Three-dimensional excitation-emission matrix (3D-EEM) fluorescence spectroscopy of leachates obtained from leaching experiments was conducted within 3 hours of completion of each leaching experiment. Sample absorbance from 200 to 600 nm was determined prior to fluorometry using a Varian Cary 1E UV-VIS spectrophotometer. Samples were diluted until absorbance at all wavelengths was below 1.5 absorbance units, to minimise fluorescence quenching due to inner-filtering. 3D-EEM analysis was performed using a Hitachi F4500 fluorescence spectrophotometer and 1cm quartz cuvettes. Excitation wavelengths ranged from 200 to 400 nm and emissions were assessed from 200 to 600 nm over 5 nm increments. Fluorometry was performed twice on each diluted sample: once without pH amendment and once with pH adjusted to 2 with 1 M HCl. Raw data from the fluorometer was converted to a form suitable for plotting using a MS Excel macro created by Zygmunt Lorenz, Julia Howitt and Shane Perryman of the MDFRC. 3D-EEM contour plots were created using Sigmaplot 8.0 for Windows. Peak locations were determined using a MS Excel macro written by myself which excludes Rayleigh and Raman artefact lines from analysis and allows customisation of search area, window search size and minimum peak height. Peak heights were expressed as a percentage of maximal fluorescence for each sample after subtracting mean background fluorescence. Maximum intensities of sample replicates differed by less than 10%. Relative fluorescence data for each peak location were compiled for all samples and used as variables in non-parametric multi-variate analyses.

5.2.4 Water Column Nutrients

Water samples were collected from within inundated macrophyte beds at BAR, BRO and OVN on each field trip (see Chapters 2 and 3 for field sampling details and site descriptions). Samples for total nitrogen and phosphorus were collected directly into 70 mL plastic jars and frozen. Samples for dissolved organic carbon were collected with a 20 mL syringe and filtered through a 0.2 µm pore-size membrane syringe filter. Three drops of concentrated (80%) phosphoric acid was added to each sample to remove inorganic carbon and samples were stored at -20 ^{o}C. Samples were analysed using the methods outlined above for DOC, TN and TP.

5.2.5 Statistical Analyses

Analyses of variance (ANOVA) were used to determine if differences in leaching rates and maxima derived from different loading treatments, live and dead tissues, and different tissue types were significantly different, and to examine differences between tissue type and species combinations (Systat version 10). Sigmaplot version 8.0 for Windows was used for data plotting, curve-fitting and ANOVA of fitted functions. Primer version 5 for Windows was used for non-parametric multi-variate analyses of 3D-EEM data.

5.3 Results

5.3.1 Leaching Experiments

Leaching rates and maxima were obtained for all treatments by fitting the following exponential rise to maximum curve (95% of R^2 values > 0.7; all $p < 0.01$, min n of 7):

y = a*(1-exp(-b*x))

where

x = time in hours

a = leaching maximum

b = leaching rate

The reliability of parameter description was always very high for leaching maxima (all $p < 0.005$), but less certain for leaching rate, especially at the lowest OM loading levels (all $p < 0.05$ for medium and high loadings; all $p < 0.1$ for lowest loadings). Leaching rates and maxima were averaged across replicates within each treatment (Table 5.3) for comparisons between treatments.

Sodium azide was added as a sterilising agent to examine whether microbial communities attached to the plant tissues had any effect on leaching. Sterilisation with azide did not significantly alter leaching rates or maxima of dead plant material (Figure 5.3). In live tissues, however, the sterilisation treatment did have a significant effect on leaching rates (Figure 5.3; all $p < 0.005$, $F > 33.12$, $n = 6$ for all comparisons). Rather than acting to inhibit microbial uptake of released OM however, sterilisation suppressed the rates of release of OM from live tissues (average of 40% reduction in leaching rate). While sodium azide has been found to alter the transfer of compounds through cell membranes, this occurs due to inhibition of active, ATP-reliant transfer across the membrane rather than by affecting membrane permeability. In my study, decreased release of dissolved organic matter was observed from green plant tissues treated with azide. For azide to be affecting DOM release in this case, the live plant tissues would have to be actively transporting DOM out of their cells, which is highly unlikely.

A more likely explanation is that the azide inhibited the activity of microbes associated with the plant tissue which were facilitating release of DOM. Thus, leaching suppression observed in sterilised treatments indicates that release of DOM from live tissues involves biologically mediated processes. As microbial communities present on macrophyte tissue did not appear to remove DOM at a significant rate, and in fact may be enhancing DOM release, interference with these processes was considered undesirable and so azide treatments were discontinued.

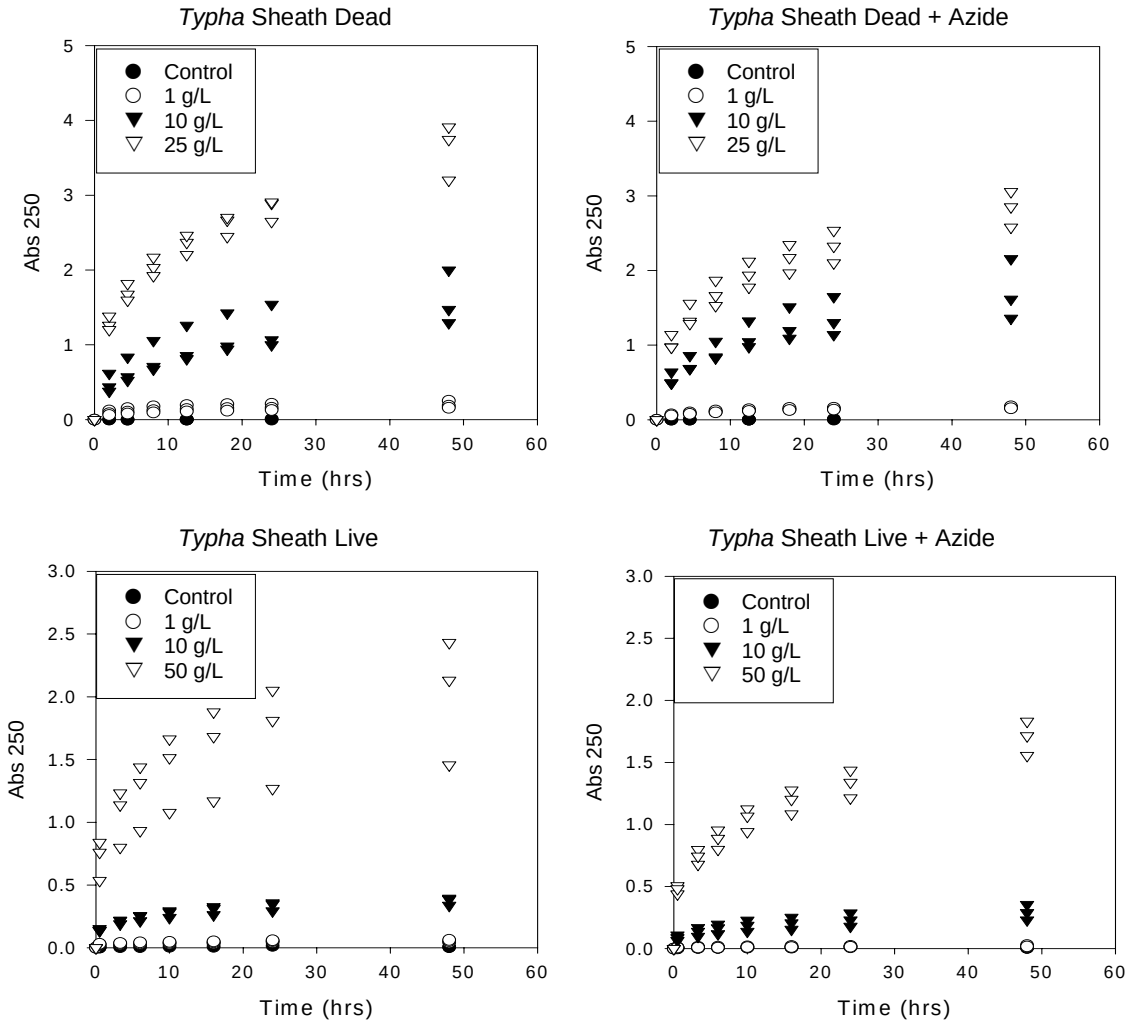

Figure 5.3. Leaching of DOM from live and dead *Typha* sheaths and the effects of sterilisation.

Patterns of release of DOM from different types and loadings of macrophyte tissues are shown in Figures 5.3 – 5.7 (note different y-axis scales on live and dead plots) and Tables 5.4 and 5.5. Within the one tissue type, leaching rates were generally higher for higher loading treatments, although some limitation was observed (presumably due to saturation effects) at the highest loadings (Table 5.4; all $p < 0.05$, $F > 4.9$, $n = 6 – 18$). *Typha* sheaths and stems (live and dead) showed the opposite pattern, with fastest DOM release from lower loadings (all $p < 0.005$, $F > 11.0$, $n = 6 – 18$). For leaching maxima, half of the tissue types assessed showed no significant differences among different loadings (Table 5.5). Where significant differences did occur, the greatest total DOM release was from lower loadings (all $p < 0.01$, $F > 5.2$, $n = 6 – 18$).

Table 5.4. Leaching rate coefficients determined from exponential curve fits to leaching data from different loadings of each tissue type/species combination.

Species	Tissue	Dead tissue loading levels			Live tissue loading levels		
		0.1 g/L	1.0 g/L	10 g/L	1.0 g/L	10 g/L	50 g/L
Persicaria	Shoot	0.101	**0.277** ^{A}	**0.266** ^{A}	**0.155** ^{C}	**0.353** ^{C}	**1.471** ^{C}
Phragmites	Blade	0.112	**0.240** ^{A}	**0.235** ^{A}	0.620	**1.124** ^{C}	**7.797** ^{C}
	Sheath	0.246	**0.370** ^{A}	**0.388** ^{A}	0.785	**2.179** ^{C}	**1.813** ^{C}
	Stem	**0.169** ^{A}	**0.095** ^{A}	**0.146** ^{A}	**0.554** ^{C,D}	0.423 ^{C}	**0.672** ^{D}
Typha	Blade	0.102	**0.164** ^{A}	**0.168** ^{A}	0.400 ^{C}	**2.407** ^{C,D}	**3.776** ^{D}
	Sheath	**0.211**	0.112	0.158	**0.248**	0.192 ^{C}	0.171 ^{C}
	Stem	**1.161** ^{A,B}	**0.528** ^{A}	0.156 ^{B}	1.804	**0.326** ^{C}	**0.314** ^{C}
Vallisneria	Shoot	bd	0.978	**1.916**	bd	bd	bd

Note: The same superscript letter indicates that leaching rates for different loading levels within a given tissue type were not significantly different at p = 0.05; bd = below detection limits; bold = rate value/s used for later cross-tissue and –species comparisons (where there is more than one value in bold text these were averaged).

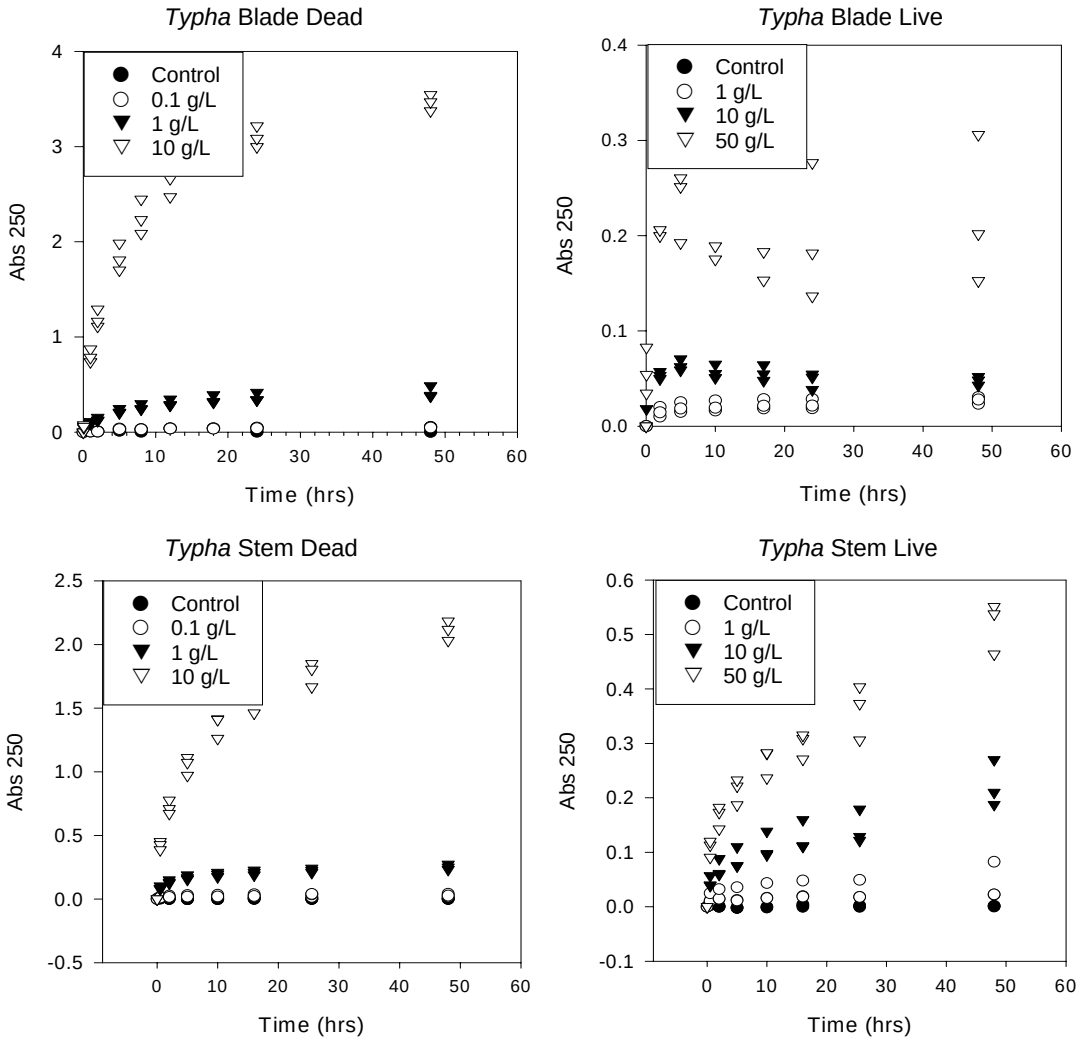

Figure 5.4. Leaching of DOM from live and dead *Typha* blades and stems.

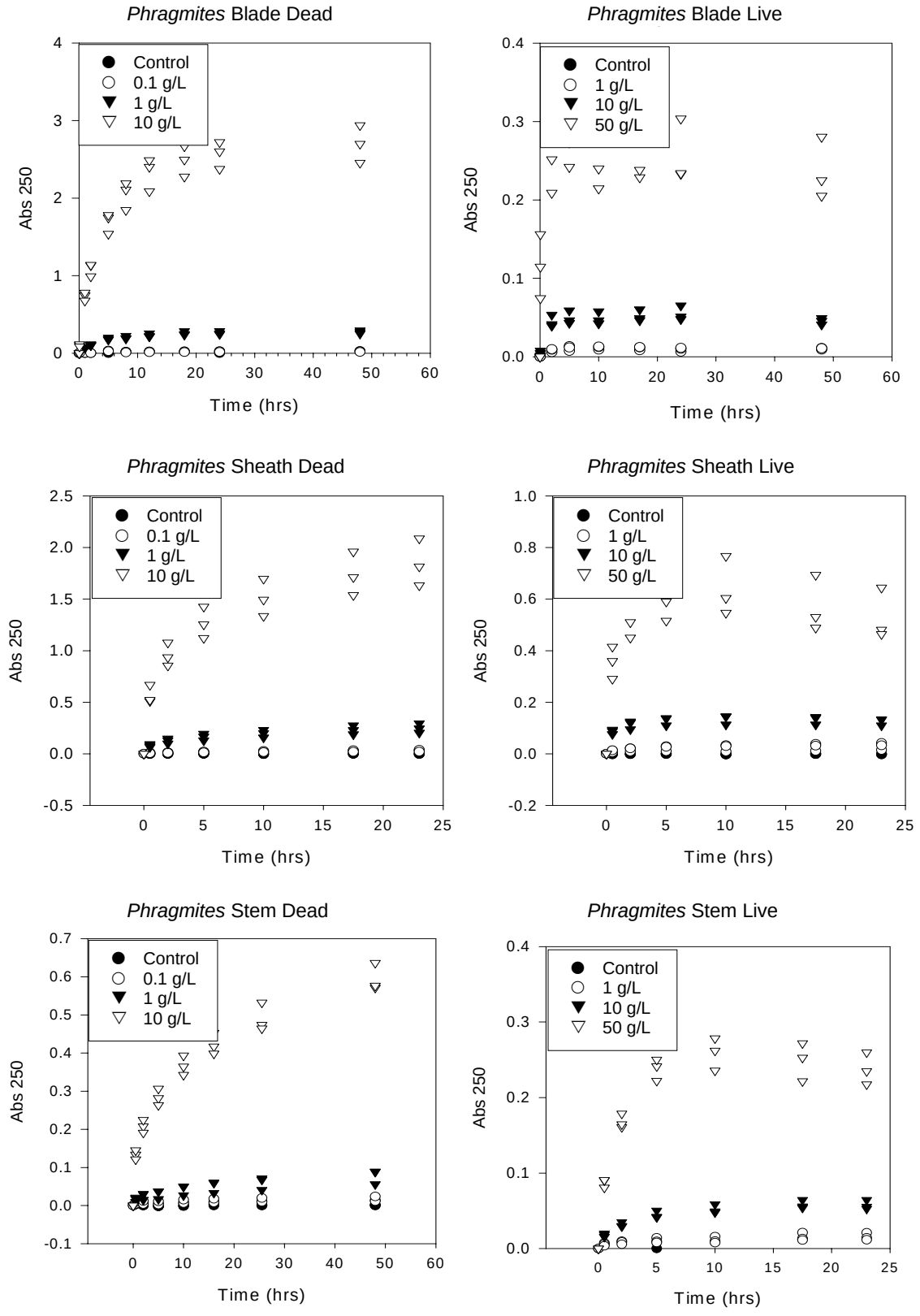

Figure 5.5. Leaching of DOM from live and dead *Phragmites* blades, sheaths and stems.

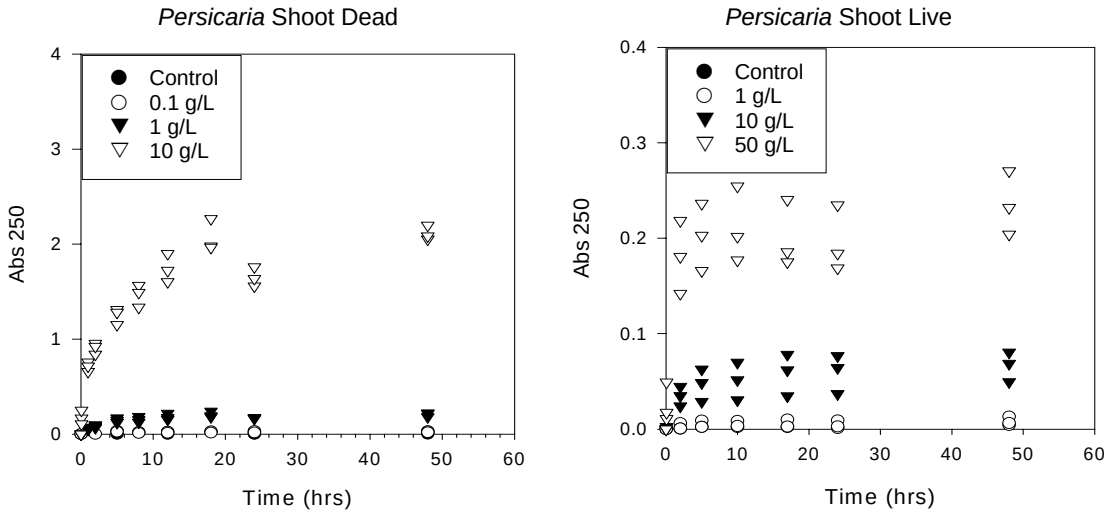

Figure 5.6. Leaching of DOM from live and dead *Persicaria* shoots.

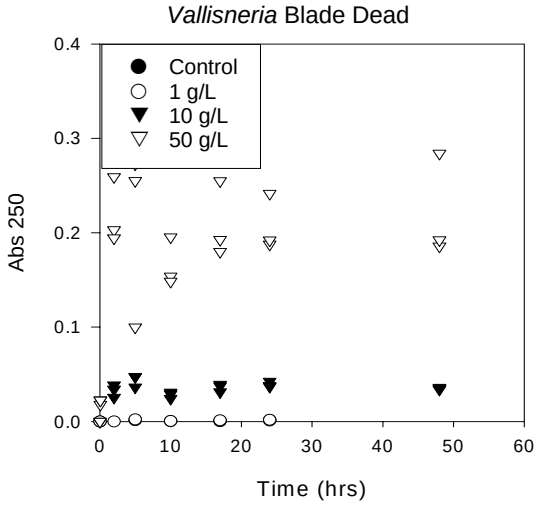

Figure 5.7. Leaching of DOM from dead *Vallisneria* blades (Abs $_{250}$ values for live *Vallisneria* blade leachates were never significantly different from controls (ie zero) for any loading).

Table 5.5. Comparison of leaching maxima (mg C/g DW tissue) determined from different loadings of each tissue type/species combination.

Species	Tissue	Dead tissue loading levels			Live tissue loading levels		
		0.1 g/L	1.0 g/L	10 g/L	1.0 g/L	10 g/L	50 g/L
Persicaria	Shoot	**24.32** ^{A}	**17.50** ^{A}	**17.05** ^{A}	**0.65**^{C}	**0.54**^{C}	**0.38** ^{C}
Phragmites	Blade	**13.90** ^{A}	**15.75** ^{A}	**15.62** ^{A}	**0.65**	0.31 ^{C}	0.32 ^{C}
	Sheath	**17.09** ^{A}	**13.70** ^{A}	**10.30** ^{A}	**1.61** ^{C}	**0.78** ^{C}	**0.71** ^{C}
	Stem	**8.85**	4.40 ^{A}	3.23 ^{A}	**0.84**	0.34 ^{C}	0.30 ^{C}
Typha	Blade	**30.78**	23.15 ^{A}	19.81 ^{A}	**1.44**	0.33 ^{C}	0.27 ^{C}
	Sheath	**10.30** ^{A}	**8.85** ^{A}	7.67	**2.84** ^{C}	**2.03** ^{C}	**2.17** ^{C}
	Stem	**16.21** ^{A}	**13.09** ^{A}	**11.51** ^{A}	**1.50**^{C,D}	**0.78** ^{C}	0.38 ^{D}
Vallisneria	Blade	bd	**0.20** ^{A}	**0.23** ^{A}	bd	bd	bd

Note: The same superscript letter indicates that leaching maxima for different loading levels within a given tissue type were not significantly different at p = 0.05; bd = below detection limits; bold = rate value/s used for later cross-tissue and – species comparisons (where there is more than one value in bold text these were averaged).

The assessment of DOC content of leachate sub-samples from the absorbance measurements allowed the development of standard curves for translating absorbance units into carbon content. Linear regressions fitted to pooled species data had a reasonable fit ($R^2 = 0.95$, $p < 0.0001$, $F = 1208$, $n = 58$), however it seemed more sensible to analyse species separately in case the relationship between absorbance and DOC concentration was species dependent. Linear regressions were fitted to data for each species studied (Figure 5.8), with the slope of the line providing the carbon conversion factor (all $R^2 > 0.96$, $p < 0.005$, $F > 45$, $n > 3$). Leaching maxima measured as absorbance units were then able to be converted to milligrams of carbon leached per gram of tissue (Figure 5.9 b).

Comparison of leaching rates and maxima across all tissue type/species combinations (Figure 5.9 and Tables 5.6 and 5.7) show marked differences between tissue type, species and tissue status (live versus dead). Significant differences were observed between live and dead leaching rates and maxima for pooled tissue types and species. The leaching rate of live tissues was 1 to 6 times greater than that of dead tissues ($p < 0.005$, $F = 10.6$, $n = 93$), but the leaching maxima were only 3 to 25% of dead ($p < 0.0001$, $F = 141.1$, $n = 104$). For those species for which equivalent tissue types were available (live and dead blades, sheaths and stems of *Phragmites* and *Typha*), leaching rate and maxima data were compared across species. Significant differences between species were observed for rates of DOM release from all tissues except live blades, with dead *Phragmites* blades leaching faster than dead *Typha* blades ($p < 0.0001$, $F = 76.5$, $n = 12$), *Phragmites* sheaths (live and dead) leaching faster than *Typha* sheaths (live and dead) (live: $p < 0.0001$, $F = 114.3$, $n = 9$; dead: $p < 0.005$, $F = 22.7$, $n = 9$), and the reverse pattern for stems (live: $p < 0.005$, $F = 23.5$, $n = 9$; dead: $p < 0.01$, $F = 9.7$, $n = 15$). Maximum OM released from different emergent plant tissues also showed significant species differences except for stems, with more OM leached from *Typha* tissues (all $p < 0.05$, $F > 4.8$, $n = 6 – 18$).

When comparing all tissue type and species combination (Figure 5.9 a), live blades from *Phragmites* and *Typha* had the fastest leaching rates (leaching coefficients of 4.5 and 3.1, respectively). Rates of DOM release from live *Phragmites* sheaths and *Typha* stems (2.0 and 1.8) were similar to that from dead *Vallisneria* blades (1.9). Live *Phragmites* stems were similar to live *Persicaria* shoots and dead *Typha* stems (0.6, 0.7 and 0.8, respectively). Leaching rate coefficients from all other tissues were below 0.4 (Figure 5.9 a).

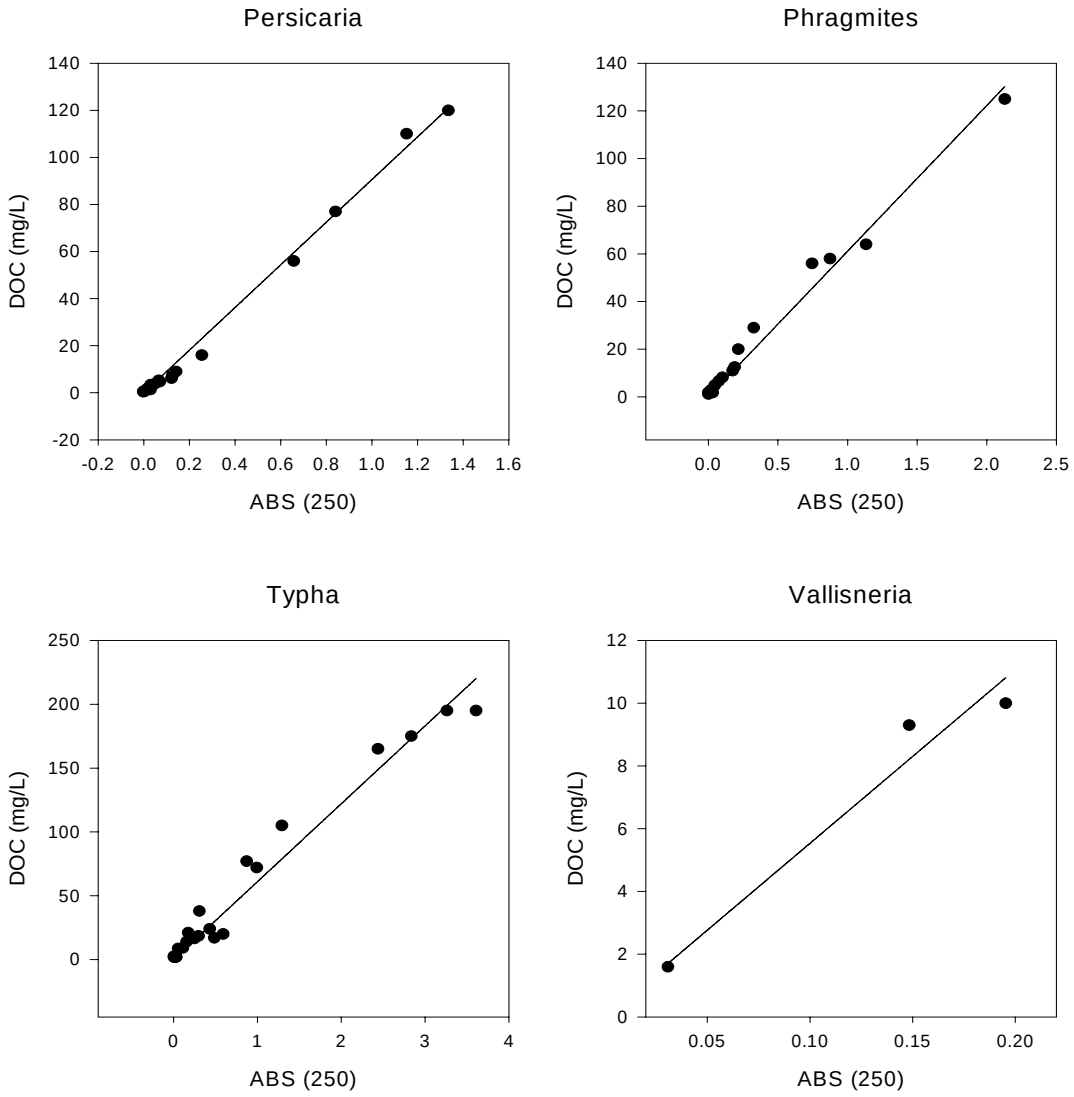

Figure 5.8. Relationship between carbon content and absorbance at 250 nm for leachates derived from different species (pooled tissue types). Linear regressions (lines) have been fitted to the data points.

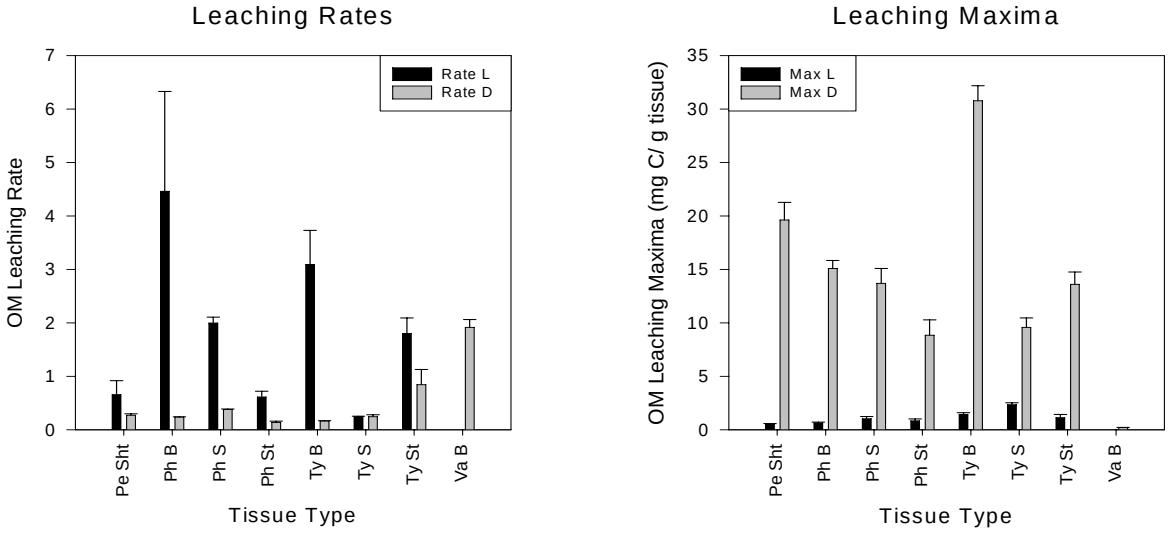

Figure 5.9. Leaching rate coefficients and leaching maxima for different macrophyte tissues (means ± s.e.). Species: Pe = *Persicaria*, Ph = *Phragmites*, Ty = *Typha*, Va = *Vallisneria*; Tissues: Sht = shoot, B = blade, S = sheath, St = stem

Table 5.6. Results of ANOVA comparisons of leaching rates across species and tissue types for live (top right of table) and dead (bottom left of table) tissues.

RATE	Pe Sht	Ph B	Ph S	Ph St	Ty B	Ty S	Ty St	Va Sht	
Pe Sht		*	*	ns	*	ns	*	*	
Ph B	ns		ns	ns	ns	ns	ns	*	
Ph S	*	*		*	ns	*	ns	*	
Ph St	*	*	*		*	ns	*	*	
Ty B	*	*	*	ns		*	ns	*	LIVE
Ty S	ns	ns	*	*	*		*	*	
Ty St	ns	ns	ns	*	*	ns		*	
Va Sht	*	*	*	*	*	*	*		
DEAD									

Note: * = significantly different at p = 0.05; ns = not significantly different.
Species codes: Pe = *Persicaria*; Ph = *Phragmites*; Ty = *Typha*; Va = *Vallisneria*
Tissue codes: Sht = shoot; B = blade; S = sheath; St = stem

Table 5.7. Results of ANOVA comparisons of leaching maxima across species and tissue types for live (top right of table) and dead (bottom left of table) tissues

MAX	Pe Sht	Ph B	Ph S	Ph St	Ty B	Ty S	Ty St	Va B	
Pe Sht		*	*	*	*	*	*	*	
Ph B	ns		ns	ns	*	*	ns	*	
Ph S	ns	ns		ns	ns	*	ns	*	
Ph St	ns	*	ns		ns	*	ns	*	
Ty B	*	*	*	*		*	*	*	LIVE
Ty S	*	*	*	ns	*		*	*	
Ty St	ns	ns	ns	ns	*	*		*	
Va B	*	*	*	*	*	*	*		
DEAD									

Note: * = significantly different at p = 0.05; ns = not significantly different.
Species codes: Pe = *Persicaria*; Ph = *Phragmites*; Ty = *Typha*; Va = *Vallisneria*
Tissue codes: Sht = shoot; B = blade; S = sheath; St = stem

Dead *Typha* blades released the greatest amount of DOM per gram of tissue (31 mg C/g tissue), followed by dead *Persicaria* shoots (20 mg/g) (Figure 5.9 b). Dead *Phragmites* blades and sheaths were similar to dead *Typha* stems (14 – 15 mg C/g tissue), whereas dead *Phragmites* stems were similar to dead *Typha* sheaths (9 and 10 mg C/g tissue, respectively). The total quantities of DOM released from all live tissues, and from dead *Vallisneria* blades, were very low (<0.02 – 3 mg C/g tissue). DOM leached from live and dead tissues represented, on average, 1% and 21% respectively, of the initial carbon content of the tissue (Figure 5.10). The exception was *Vallisneria* blades, where 0% of live and less than 1% of dead tissue carbon was leachable (Figure 5.10). Of the carbon which was able to be leached from each tissue type, at least 80% leached out within the first 24 hours following inundation (Figure 5.).

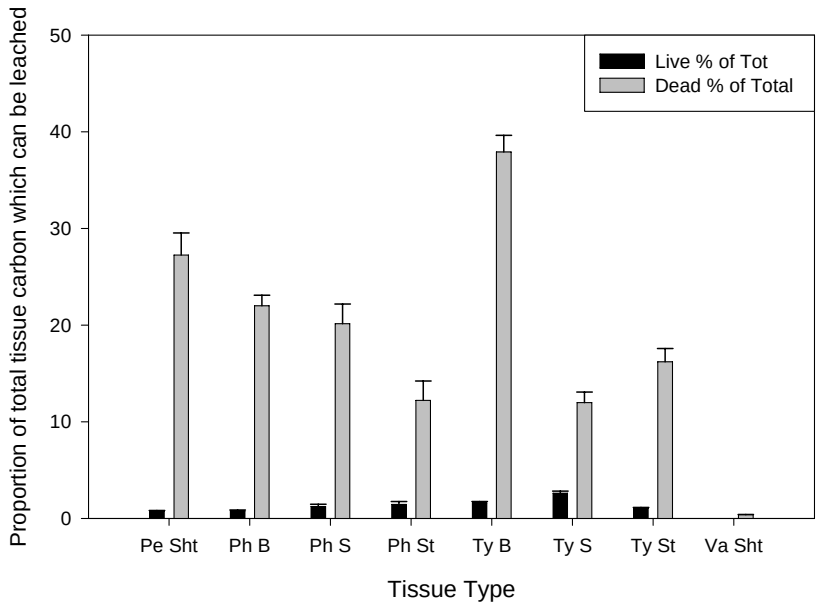

Figure 5.10. Proportion of initial tissue carbon leached from different macrophyte tissues (means ± s.e.).
Species: Pe = *Persicaria*; Ph = *Phragmites*; Ty = *Typha*; Va = *Vallisneria*
Tissues: Sht = shoot; B = blade; S = sheath; St = stem

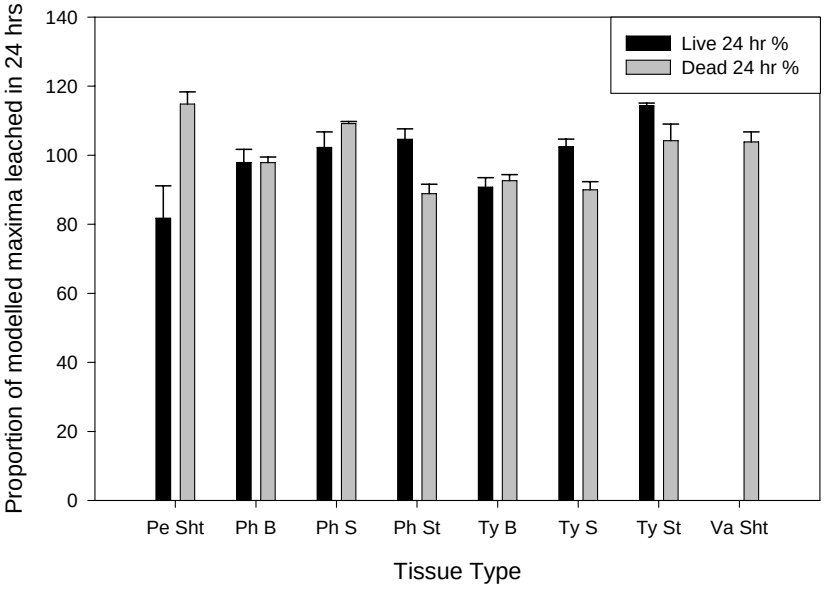

Figure 5.11. Proportion of modelled maxima leached in 24 hrs (means ± s.e.).
Species: Pe = *Persicaria*; Ph = *Phragmites*; Ty = *Typha*; Va = *Vallisneria*
Tissues: Sht = shoot; B = blade; S = sheath; St = stem

5.3.2 Nutrient Analysis

The carbon concentration of leachates derived from live macrophyte tissues was always lower than that derived from dead tissues (Table 5.8). While carbon content varied among tissue types, there seemed to be no repeated cross-species pattern of association of tissue type with carbon level. The highest carbon content of all the leachates was derived from dead *Persicaria* shoots (214 mg/L), followed by dead blades and sheaths from *Typha* (189 and 172 mg/L, respectively) and *Phragmites* (157 and 113 mg/L, respectively) (Table 5.8). Leachates derived from live and dead *Vallisneria* blades had the lowest carbon content (below detection levels and 12 mg/L, respectively), with low carbon concentrations also in live *Typha* blade (12 mg/L), live *Phragmites* stem (15 mg/L), live *Phragmites* blade (16 mg/L) and live *Persicaria* shoot (18 mg/L) leachates.

Live plant tissues produced leachates with lower nitrogen concentrations than equivalent dead tissues (Table 5.8), except for *Typha* sheaths, where leachate from green material had twice the nitrogen content (4.2 mg/L) as that from dead tissue (2.1 mg/L). Again, no trends were apparent in nitrogen content of different tissue types. Nitrogen content was high in leachates derived from dead *Vallisneria* blades (24.3 mg/L), dead *Phragmites* blades (8.5 mg/L), dead *Phragmites* stems (6.3 mg/L) and live *Typha* sheaths (4.2 mg/L). Low nitrogen concentrations occurred in live *Typha* blade (0.5 mg/L), live and dead *Persicaria* shoot (both 0.6 mg/L), live *Typha* stem (0.7 mg/L) and live *Phragmites* stem (0.8 mg/L) leachates.

As with nitrogen, phosphorus content was lower in live tissue leachates than dead for all tissue types except *Typha* sheaths, and no pattern was discernable in relation to tissue type (Table 5.8). Leachates derived from live and dead *Typha* sheaths (3.9 and 2.5 mg/L, respectively), dead *Vallisneria* blades (1.8 mg/L) and dead *Phragmites* stems (1.7) had the highest concentrations of phosphorus. Phosphorus content was low in leachates from live *Phragmites* blades (0.012 mg/L), live and dead *Persicaria* shoots (both 0.018 mg/L), live *Phragmites* sheaths (0.020 mg/L) and live *Typha* stems (0.020 mg/L).

As leachate bio-availability was not directly measured (as DOC removal or metabolism), surrogates of bio-availability have been used to infer leachate quality, hereafter referred to as "inferred" or "presumed" bio-availability. Leachate bio-availability was presumed to be high where C:N and C:P ratios were low, but N:P ratios were high. Substantial variation in inferred leachate bio-availability occurred across tissue type, tissue status and species. Leachates derived from live tissues of *Persicaria, Typha* and *Vallisneria* were generally inferred to be more bio-available than those derived from their equivalent dead tissues. *Typha* sheaths produced leachate with higher presumed bio-availability than blades, which were higher than stems. In contrast, leachates from dead *Phragmites* tissues generally had higher presumed bio-availability than those from live tissues, with the order of inferred bio-availability being stems > blades > sheaths.

Table 5.8. Nutrient composition of leachates derived from different macrophyte tissues

Tissue Type	C mg/L	N mg/L	P mg/L	C : N	C : P	N : P	C : N : P
Persicaria Shoot Live	17.7	0.63	0.018	28	1004	35	1004:35:1
Persicaria Shoot Dead	213.5	0.63	0.018	342	12084	35	12084:35:1
Phragmites Blade Live	15.7	0.88	0.012	18	1273	71	1273:71:1
Phragmites Blade Dead	156.8	8.53	0.433	18	362	20	362:20:1
Phragmites Sheath Live	32.4	1.24	0.020	26	1619	62	1619:62:1
Phragmites Sheath Dead	112.8	2.90	0.087	39	1301	33	1301:33:1
Phragmites Stem Live	14.5	0.78	0.037	19	392	21	392:21:1
Phragmites Stem Dead	30.0	6.27	1.700	5	18	4	18:4:1
Typha Blade Live	12.1	0.48	0.043	25	279	11	279:11:1
Typha Blade Dead	189.1	0.91	0.527	207	359	2	359:2:1
Typha Sheath Live	104.3	4.20	3.900	25	27	1	27:1:1
Typha Sheath Dead	171.8	2.06	2.520	84	68	1	68:1:1
Typha Stem Live	22.0	0.65	0.020	34	1120	33	1120:33:1
Typha Stem Dead	108.2	1.13	0.060	95	1803	19	1803:19:1
Vallisneria Blade Live	bd	0.76	0.033	<0.03*	<0.6*	23	0.6:23:1*
Vallisneria Blade Dead	11.5	24.33	1.767	0.5	6	14	6:14:1

bd = below detection levels (0.02 mg/L); * ratios calculated using C = 0.02 mg/L

Comparing across species and tissue types, dead *Persicaria* shoot leachate had the lowest inferred bio-availability of all tissues (C:N:P of 12,084:35:1); other leachates with low inferred bio-availability were those derived from live *Persicaria* shoots (1,004:35:1), dead *Phragmites* sheaths (1,301:33:1), and live and dead *Typha* stems (1,120:33:1 and 1,803:19:1, respectively). Ratios indicating the highest presumed bio-availability occurred in leachates derived from live and dead *Vallisneria* tissues (C:N:P of 0.6:23:1 and 6:14:1, respectively). However caution must be taken in interpreting live *Vallisneria* leachate nutrient ratios, which were calculated using a maximum carbon content (0.02 mg/L) because carbon levels were below detection limits (0.02 mg/L). Leachates from dead *Phragmites* stems (18:4:1), live *Typha* sheaths (27:1:1), live *Typha* blades (279:11:1), dead *Phragmites* blades (362:20:1) and live *Phragmites* stems (392:21:1) also had relatively high inferred bio-availability.

5.3.3 Fluorescence Excitation-Emission Spectra

Three-dimensional EEM fluorometry of macrophyte leachates demonstrated the presence of compounds similar to those reported elsewhere. A summary of known peak locations for specific compound types is shown in Figure 5.12 (Coble, 1996; Mobed et al., 1996; Baker and Genty, 1999; Mayer et al., 1999; Baker, 2001; McKnight et al., 2001; Westerhoff et al., 2001; Baker, 2002a; Baker, 2002b; Ohno, 2002; Alberts and Takacs, 2004; Yamashita and Tanoue, 2004).

Humic-acid like compounds occur between EX 215 to 280 nm and EM 405 to 475 (bottom right of contour plots). For similar excitation wavelengths, proteinaceous compounds fluoresce at shorter wavelengths (EM 285 – 365 nm; bottom and middle left of plots). Humic acid-like substances which tend to occur in marine systems and fulvic acid-like substances fluoresce at similar wavelengths as humic acid-like compounds, but require longer excitation wavelengths to do so (EX 390 – 330 nm and EX 305 – 355 nm, respectively; top right of plots). Generally there is a trend of increasing molecular weight of compounds moving towards the top right of the plot. Three-dimensional EEM data are usually presented as contour plots (Figures 5.13 – 5.18), with the main area of interest lying between the two artefactual Raleigh scatter bands. Peaks observed in contour plots for each tissue type and species (Figures 5.13 – 5.18) are summarised (Figure 5.19) in relation to the known peak locations shown in Figure 5.12.

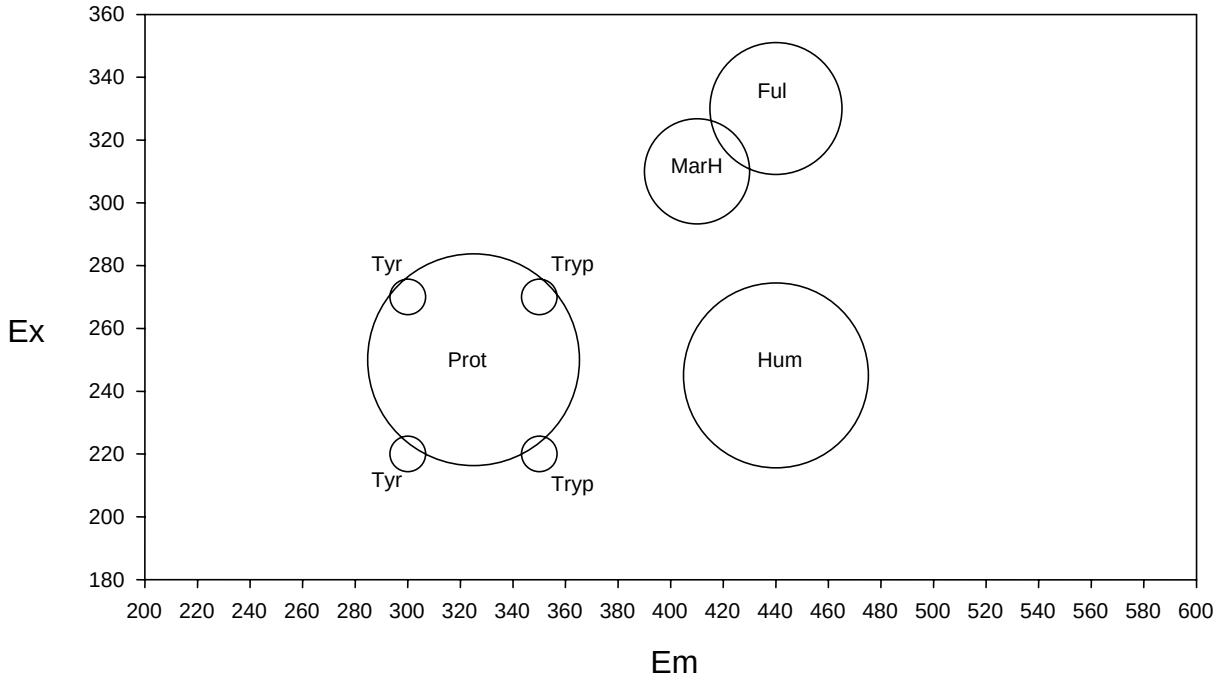

Figure 5.12. Plot showing known locations of 3D-EEM peaks for specific compound types. Hum = humic acid-like; Ful = fulvic acid-like; MarH = marine humic acid-like; Prot = proteinaceous (Tyr = tyrosine-like; Tryp = tryptophan-like).

The potential for pH, inner-filtering and metal complexation to affect the location and size of peaks measured with three-dimensional excitation-emission fluorometry was assessed by comparing results for unmodified sample replicates with pH-modified replicates and performing calculations with and without *a posteriori* absorbance correction. Lowering sample pH caused peaks to be smaller and more diffuse than unmodified samples (Figures 5.13 and 5.14 a and c). While sharpening of peaks was apparent after absorbance correction in some leachates (Figure

5.13 b c.f. a), in other samples peaks became almost undetectable, and substantial artefactual "noise" was introduced at low excitation wavelengths (Figure 5.14 b c.f. a). The combination of pH modification and absorbance correction on the dilute samples used in this study produced almost unusable spectra (Figures 5.13 d and 5.14 d). Thus, it was decided that data would not have the absorbance correction applied and only pH-unmodified results are presented.

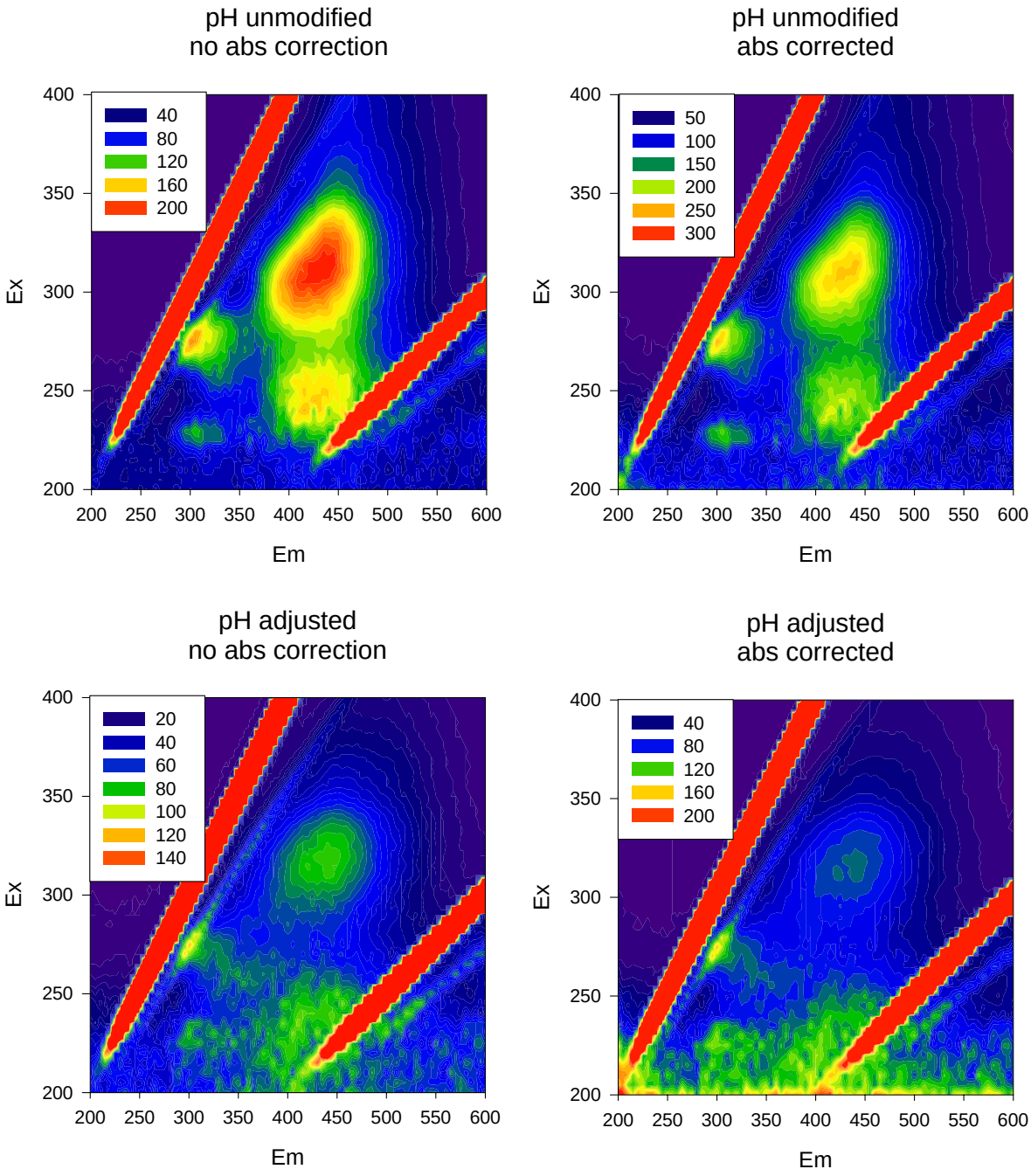

Figure 5.13. Contour plots of EEM data. Absorbance correction and pH adjustment trials on leachate from dead *Typha* sheaths.

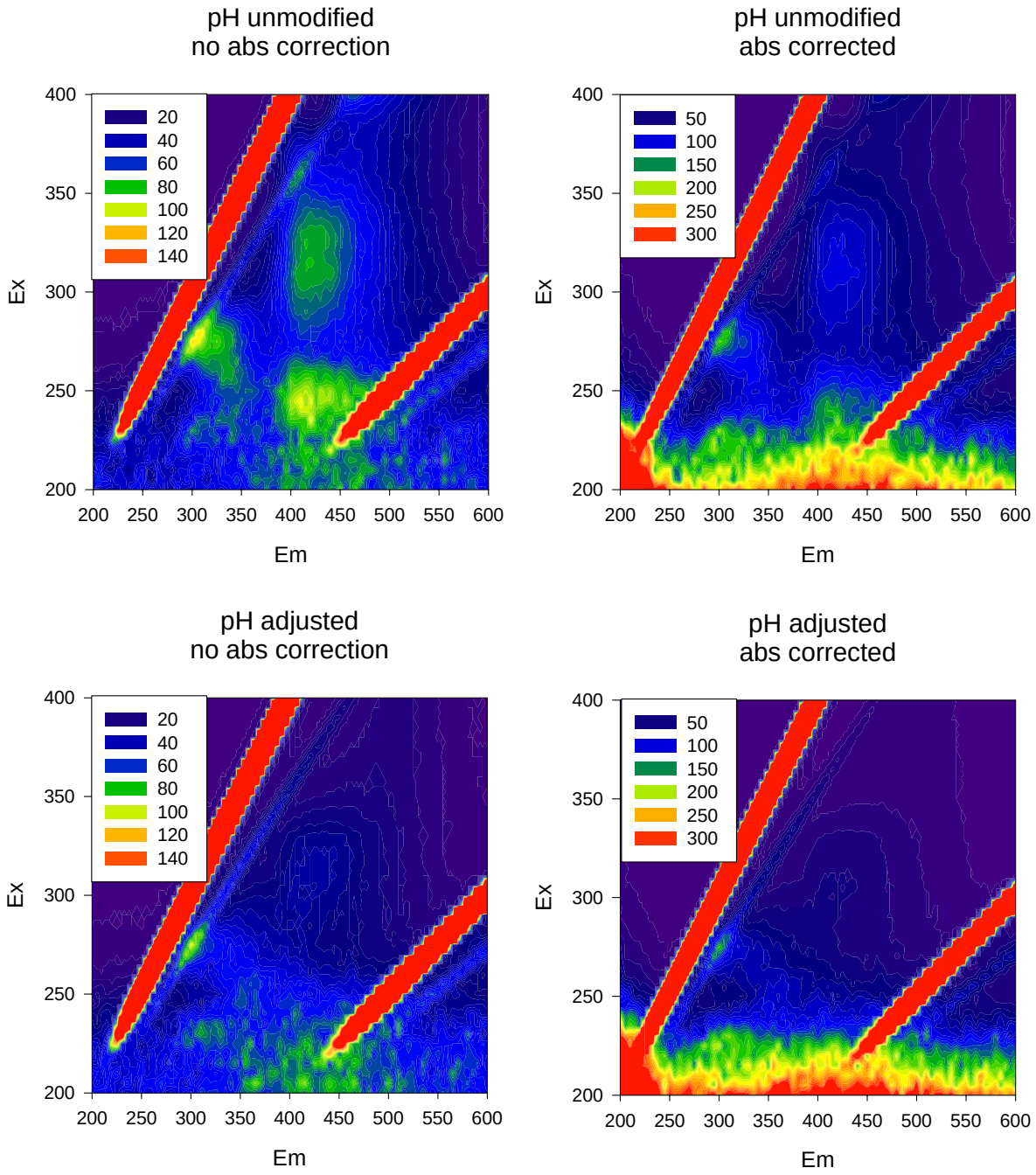

Figure 5.14. Contour plots of live *Typha* sheath leachate EEM data. Absorbance correction and pH adjustment trials.

Substantial differences were observed between 3D-EEM contour plots of leachates from different species, tissue types and live and dead tissues within the one tissue type (Figures 5.15 – 5.18). In general, leachates from live tissues showed peaks at low excitation wavelengths and the presence of proteinaceous compounds. In contrast, leachates from dead tissues had more humic material.

5.3.3.1 Typha

Leachates derived from different *Typha* tissues were comprised of quite different compounds (Figure 5.15, 5.19). Very few carbon compounds were present in stem leachates, with some proteinaceous substances in leachates from live stems and no defined peaks in leachates from dead stems (although some diffuse products appeared along the 200nm excitation band, which may represent chlorophyll or protein breakdown products). Four distinct peaks were detected in live sheath leachates (2 proteinaceous, a humic acid-like and a marine humic compound) and while peak location did not appear to change in senescent tissues, the proportions of these four compound types were markedly different. Five peaks representing proteinaceous and humic-like compounds occurred in leachates from live *Typha* blades, with loss of the proteins and the introduction of a marine humic substance upon senescence.

5.3.3.2 Phragmites

As well as displaying substantial differences in composition based on tissue type, leachates derived from *Phragmites* tissues also displayed the greatest differences between live and dead samples (Figure 5.16, 5.19). Carbon compounds observed in *Phragmites* live stem leachates were limited to two proteinaceous substances. As stems senesced, humic acid-like and marine humic compounds appeared in addition to the proteins. Live sheaths produced leachates similar to dead stems (which were also similar to leachates from *Persicaria* shoots and *Typha* sheaths), with a high proportion of marine humic compounds. In leachates derived from dead *Phragmites* sheaths, there was a shift away from the 4-peak pattern: marine humics were still present, with additional humic-like substance peaks occurring at different locations to live material, and the proteinaceous compounds were lost. Only two peaks were detected in leachates from *Phragmites* blades – in live samples these were proteinaceous (tryptophan-like) and in dead samples these were humic compounds (humic acid-like and fulvic acid-like).

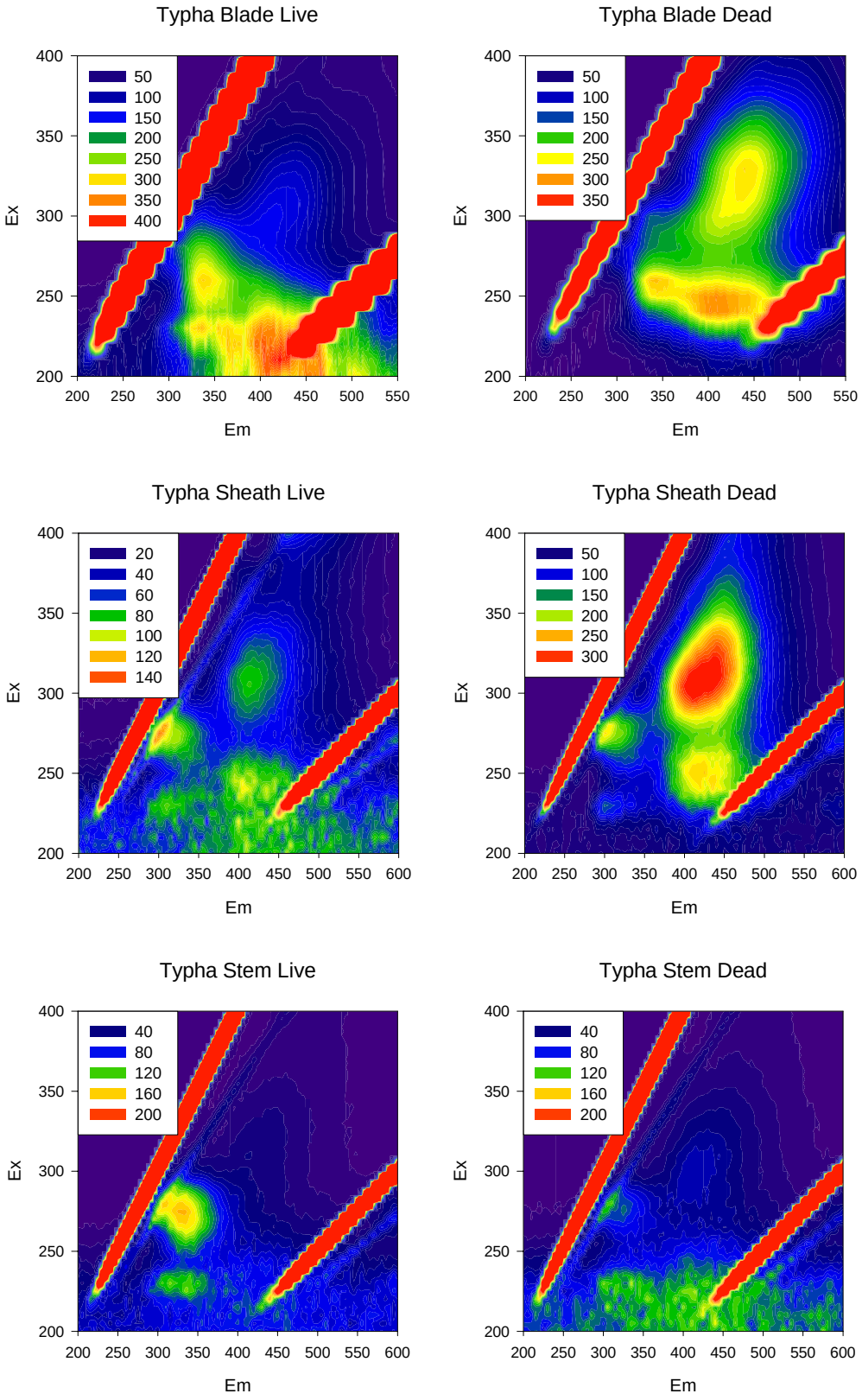

Figure 5.15. Contour plots from EEM analyses of leachates derived from *Typha* tissues.

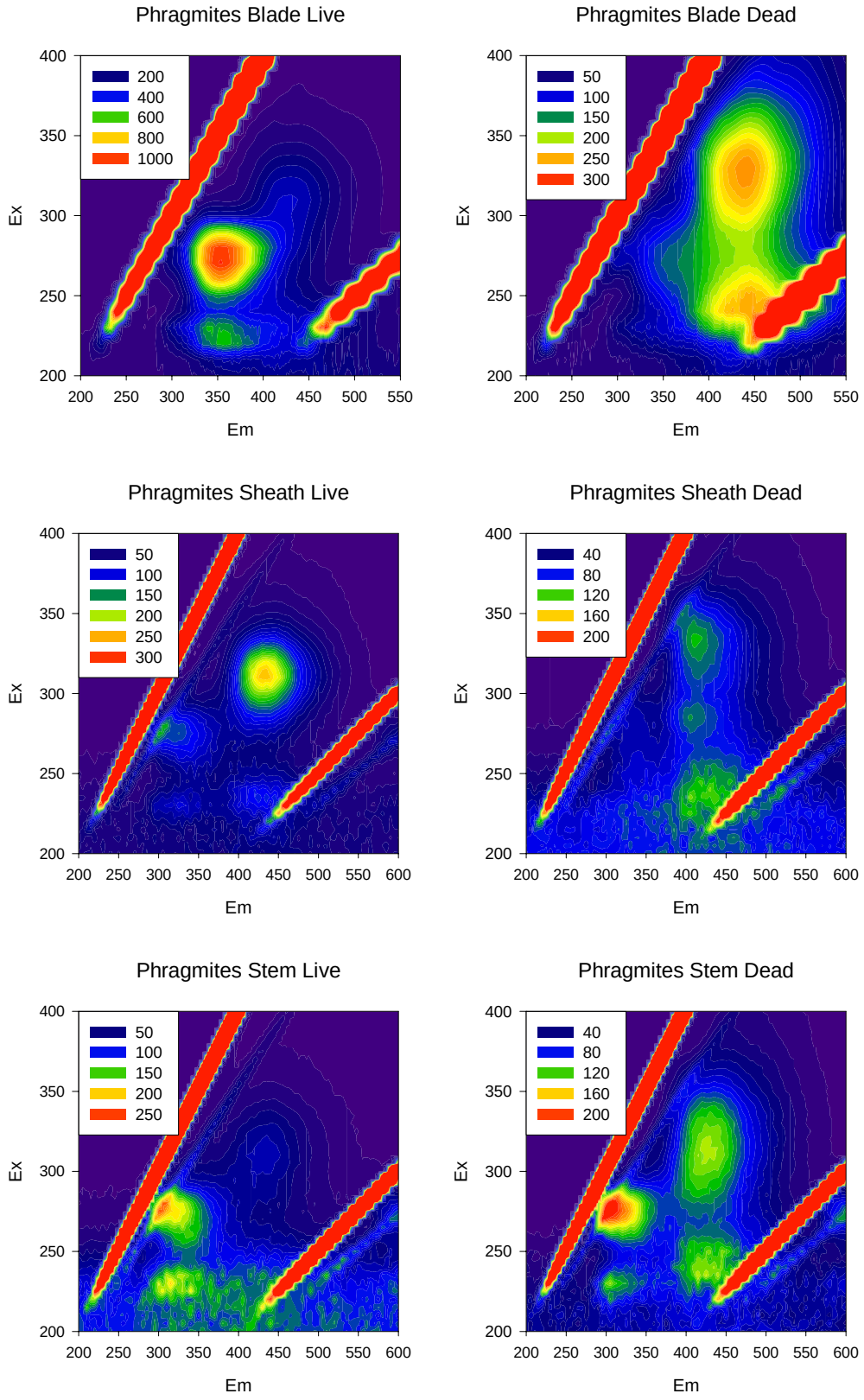

Figure 5.16. Contour plots from EEM analyses of leachates derived from *Phragmites* tissues.

5.3.3.3 Persicaria

Leachates derived from whole *Persicaria* shoots (Figure 5.17, 5.19) were similar to those from *Typha* sheaths, with two proteinaceous peaks, one humic acid-like peak and one marine humic peak detected in both live and dead samples. Leachates from senescent tissues had increased proportions of the protein-like substances.

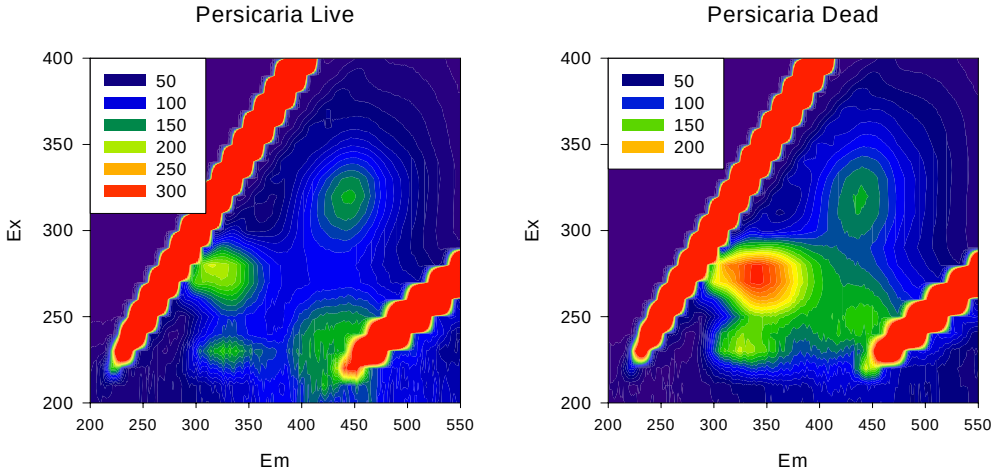

Figure 5.17. Contour plots from EEM analyses of leachates derived from *Persicaria* shoots.

5.3.3.4 Vallisneria

No peaks were detectable in leachates derived from live *Vallisneria* tissues. Dead *Vallisneria* leachates displayed two very faint proteinaceous peaks and a row of indistinct peaks at an excitation wavelength of 200 nm, which may represent chlorophyll and its breakdown products (Figure 5.18, 5.19).

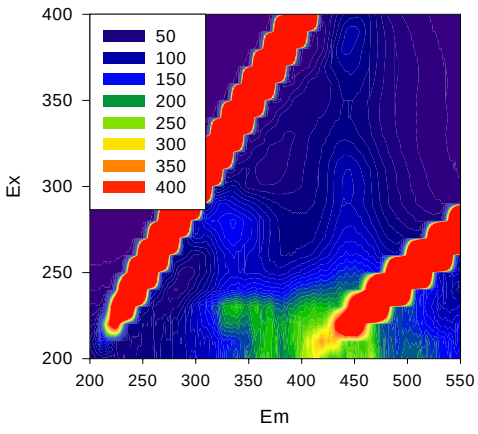

Figure 5.18. Contour plot from EEM analysis of leachate derived from dead *Vallisneria* shoots (no peaks were detected in leachates derived from live *Vallisneria* tissues).

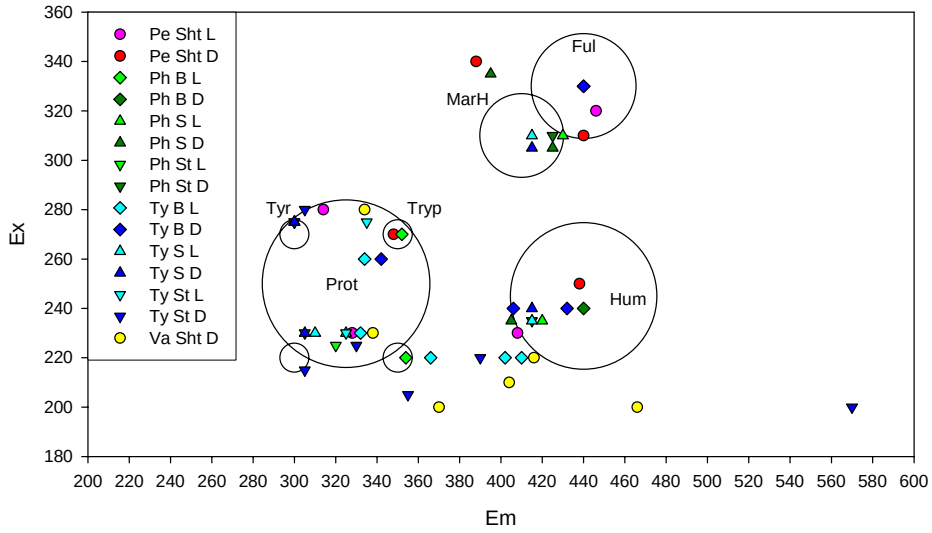

Figure 5.19. Plot showing locations of EEM peaks for different macrophyte tissue leachates in relation to the known locations of specific compound types. Species: Pe = *Persicaria*; Ph = *Phragmites*; Ty = *Typha*; Va = *Vallisneria*; Tissues: Sht = shoot; B = blade; S = sheath; St = stem; Status: L = live; D = dead

MDS ordination summarised the multi-variate analysis of peak locations and proportional peak height for each leachate (Figure 5.20). This plot demonstrates the high degree of similarity between replicates for each leachate type. Leachates derived from the following tissue pairs appear close together on the plot due to their similarity in carbon composition: live *Phragmites* blades and live *Typha* stems (bottom right of diagram, near 'A'); dead *Phragmites* stems and live *Typha* sheaths (near 'C' on the diagram); live *Typha* blades and dead *Vallisneria* shoots (bottom centre of diagram). The members of these leachate pairs also had similar levels of presumed bio-availability based on nutrient ratios.

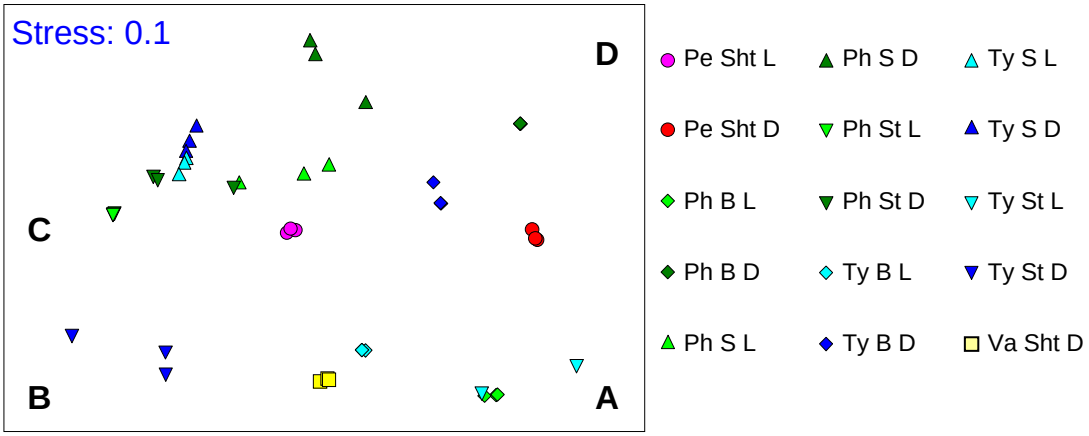

Figure 5.20. MDS plot of EEM data showing two-dimensional separation of leachates from different macrophyte tissues based on similarity of peak locations and proportional peak height. Species, tissue and status codes as per Figure 5.19

5.3.4 Water Column Nutrients

Nutrients in the main river channel and within macrophyte beds at each site were determined when beds were inundated. These data were obtained to determine if macrophyte bed inundation produced measurable changes in river nutrients and to validate predictions of nutrient additions to rivers from macrophyte inundation modelling (Chapter 7). While DOC levels in macrophyte beds at BAR were usually quite similar to those in the main river channel, levels of TN and TP were usually higher (Figure 5.21). The Broken River had much higher nitrogen and phosphorus concentrations than the Murray River at Barmah. Higher DOC levels were measured in macrophyte beds than in the river channel at this site only once, whereas at other times these values were similar (Figure 5.22). On occasions, TN and TP were higher in macrophyte beds than in the main river channel at BRO, but generally they were similar to river values. Nutrient levels at OVN were similar to BAR, and while TN and TP concentrations in *Persicaria* beds were higher than in the river channel on the date tested, DOC levels were lower (Figure 5.23).

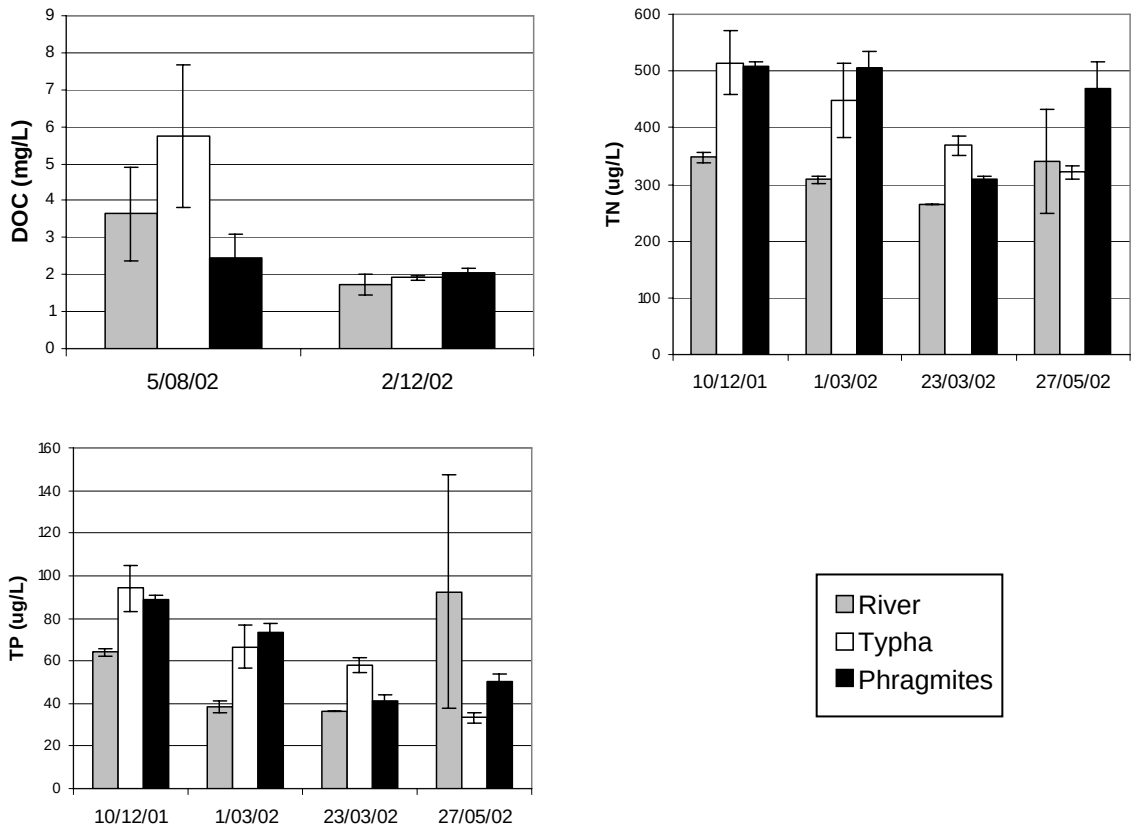

Figure 5.21. Comparison of water column nutrients within macrophyte beds and the main river channel at BAR (means ± s.e.).

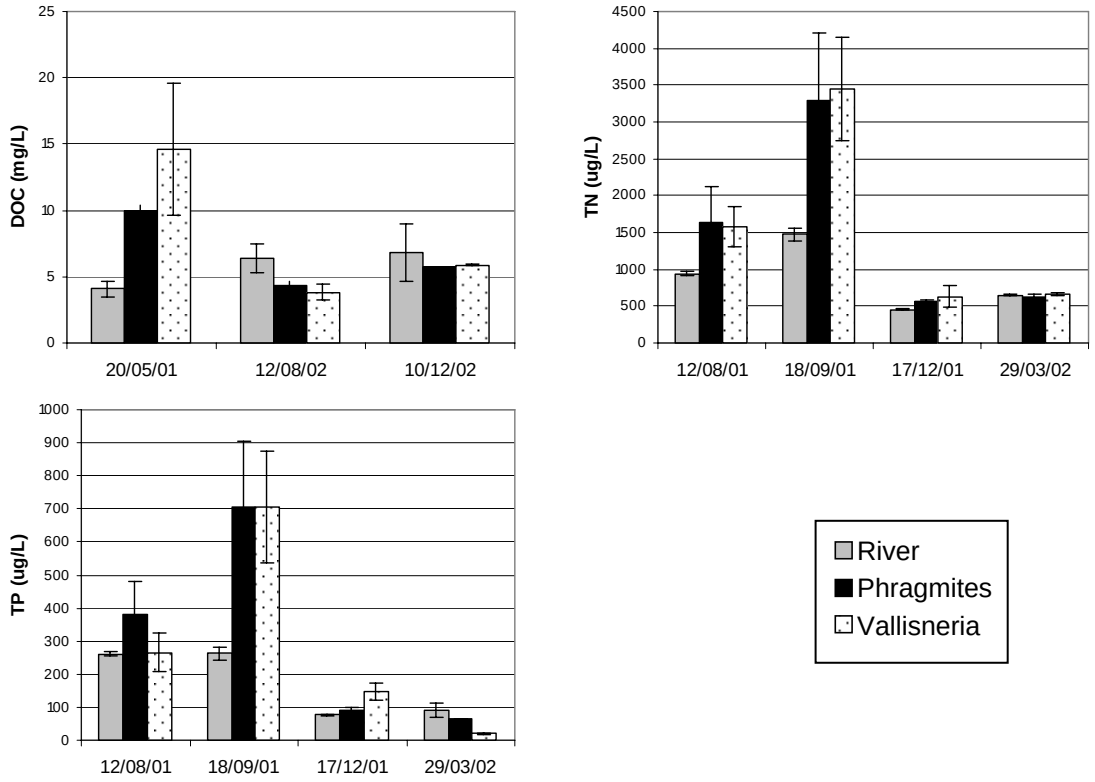

Figure 5.22. Comparison of water column nutrients within macrophyte beds and the main river channel at BRO (means ± s.e.).

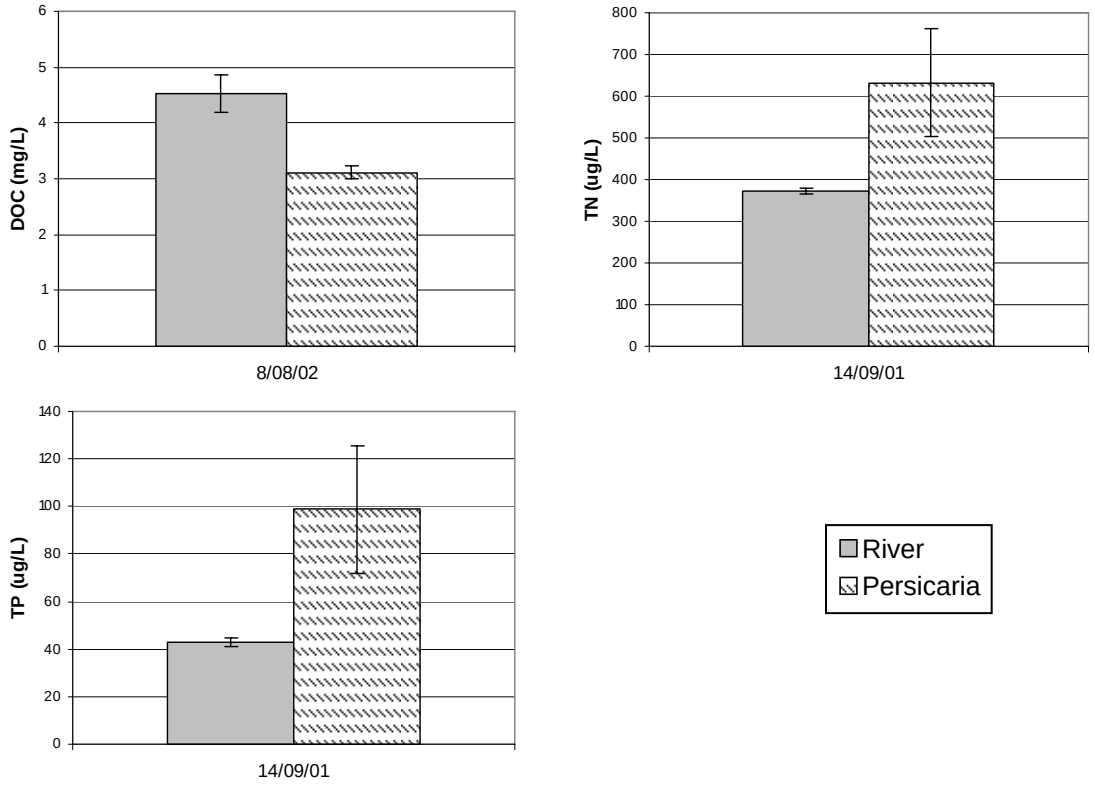

Figure 5.23. Comparison of water column nutrients within macrophyte beds and the main river channel at OVN (means ± s.e.).

5.4 Discussion

This study determined rates of release, quantities and composition of DOM leached from a range of green and senescent tissues from four macrophyte species. Patterns of DOM release from macrophyte tissues fit exponential rise to maximum curves, with the greatest leaching occurring in the first 24 hours of immersion, as has been reported in other studies (Godshalk and Wetzel, 1978a; Otsuki and Wetzel, 1974; Harrison and Mann, 1975; Baldwin, 1999). In the laboratory, slow release of DOM from tissues might be expected to continue over longer time periods, with concurrent uptake and utilisation by microbes leading to slow growth of microbial populations. Under field conditions, colonisation by complex biofilms and the action of shredding invertebrates would alter patterns of DOM release (Webster and Benfield, 1986; Bohman and Tranvik, 2001). Comparisons of leaching from different macrophyte tissues revealed that tissue status (live or dead) had the greatest effect on rates and quantities of DOM release. As initially hypothesised, dead tissues leached greater quantities of DOM than live (4 – 30 times more). Similar results have been observed for other emergent macrophyte species, with DOC release from senescent tissues 5 to 25 times higher than from green when samples were not pre-treated (Mann and Wetzel, 1996). Microbially-mediated release of DOM may be responsible for the faster rates of leaching from live tissues than dead observed in the present study. This phenomenon has been implicated previously in River Red Gum leaching experiments (Baldwin**,** 1999). Either the live tissues themselves or an exudate may be supporting active colonies of microbes, whereas the microbial community on standing dead tissues may be mostly dormant. When live tissues are immersed, there is an immediate release of DOM, either from the tissues due to the action of the microbes or as an exudate from the functioning microbes. In contrast, immersion of dead tissues results in slower leaching rates, perhaps because there are fewer active microbial cells present to assist in DOM release and so only physico-chemical processes occur initially.

Although leaching from live tissues was faster than from dead tissues, much smaller quantities of DOM were released. This may reflect adaptations by aquatic and semi-aquatic plants to tolerate intermittent inundation of live shoots (Blanch et al., 1999; Li et al., 2004). Inundation for longer than species-specific tolerance limits would reduce a shoot's ability to limit loss of soluble components as it became more stressed, structurally compromised and finally started senescing.

The data provide some evidence for an inverse relationship between the proportion of structural compounds in plant tissue and its capacity for leaching, with greater and faster leaching from leaf blades generally than from sheaths or stems, as reported by Kominkova *et al.* (2000). However, this trend was confounded by *Vallisneria* blades (few structural compounds

but very low leaching rates and maxima), and dead *Persicaria* shoots (large structural component but high leaching maxima). Growth form may need to be considered in comparisons of macrophyte leaching and decomposition (Godshalk and Wetzel, 1978a). Whereas *Vallisneria* might be expected to have pronounced leaching based on its paucity of structural components, its submerged habit has probably resulted in extensive adaptations to resist leaching from live tissues. Conversely, the semi-terrestrial nature of *Persicaria* may have resulted in a reduced resistance to leaching, aligning this species' leaching patterns closer to those of terrestrial plants (e.g. River Red Gum can leach ~14% of initial tissue mass in 24 hrs (Baldwin, 1999), whereas the average for macrophytes from this study was ~7% and for *Persicaria* was ~10%). Within a single growth form (emergent plants), tissue type was more important than species in determining differences in leaching maxima.

Across the species and tissue types assessed in this study, the quantity of DOM released from dead tissues represented an average of 20% of tissue carbon. While these data are similar to values reported for *Typha latifolia* (Lush and Hynes, 1973), Kominkova *et al.* (2000) showed DOM release from dead *Phragmites australis* blades and stems was less than 1%. However, material used by Komincova *et al*. (2000) was either over one year old (stems) or from the current season's growth, but collected at the end of autumn in an area of high rainfall (922 mm annual rainfall at nearby Bern, Switzerland – data from the Euro Weather website (http://www.eurometeo.com/english)), and so might be expected to have already undergone substantial leaching by rainfall. The effects of multiple wetting and drying cycles on DOM releases and leachate composition from macrophyte tissues are unknown, however it would be expected that leaching rates and maxima would be reduced with sequential wetting cycles, with leachates increasingly comprised of higher molecular weight, recalcitrant compounds.

On average, only 1% of tissue carbon leached out of live macrophyte tissues, a value even lower than the 4% of biomass expected to be lost due to excretion of photosynthate (Wetzel and Manny, 1972b). As reported in other leaching studies (Godshalk and Wetzel, 1978a; Otsuki and Wetzel, 1974; Harrison and Mann, 1975; Baldwin, 1999), the vast majority of leachable carbon (greater than 80% for all tissue types) was released from macrophyte tissues within the first 24 hours of immersion.

While the carbon contents of leachates from live macrophyte tissues were always lower than leachates from equivalent dead tissues, the opposite was true for nitrogen and phosphorus content (except for leachates derived from live and dead *Typha* sheaths). Some evidence was provided by the data for a link between growth form and leachate nutrient status, with both carbon and phosphorus content showing trends from the semi-terrestrial mudflat hydrophyte (*Persicaria*), through the emergent macrophytes (*Phragmites* and *Typha*) to the submerged

species (*Vallisneria*) (with carbon decreasing and phosphorus increasing through this progression). No trend was apparent in leachate nutrient contentvariation with tissue type (i.e. blades, sheaths, stems).

Interesting patterns of nutrient composition were observed in leachates derived from live and dead *Typha* sheaths and live *Vallisneria* blades. *Typha* sheath leachates had very high nitrogen and phosphorus content which is not explained by the presence of unusual tissue structure or its tissue nutrient content (mid-range N and P compared to the other species and tissue types assessed – see Chapter 3). One explanation for the high nutrients is the presence of thick mucilage between each sheath, which was not removed during leaching experiments and which may contain high proportions of soluble N and P. Similarly, relatively large quantities of N and P were present in live *Vallisneria* leachates despite carbon levels being below detection limits. Although all leaves were wiped to remove epiphytic growth, these nutrients may have been released from remnants of biofilm attached to the leaf which may have been damaged, but not fully removed, by leaf pre-treatment.

The bio-availability of leachates in this study was inferred from C:P, C:N and N:P ratios. Use of nutrient ratios is a very broad approach to estimating bio-availability which generalises across a range of organic matter types (Godshalk and Wetzel, 1978; Valiela et al., 1984; Webster and Benfield, 1986; Moran and Hodson, 1989; Atkinson and Cairns, 2001; Lee and Bukaveckas, 2002). It is not a definitive technique, and other factors must be taken into account, such as the types of compounds comprising each of the nutrients (e.g. high versus low molecular weight carbon compounds) and the presence of inhibitory compounds. While dead *Vallisneria* blades did not conform to the standard model of C:N:P (ie. Redfield Ratio of 106:16:1), having high N and P but very low C, it was considered highly bio-available in this study because the small quantity of carbon present comprised low molecular weight compounds, and hence would be more easily metabolised by microbes than some of the more abundant, but larger molecules comprising the carbon content of other leachates (e.g. humic and fulvic acid-like substances) (Amon and Benner, 1996).

As initially hypothesised, leachates derived from live macrophyte tissues generally had nutrient ratios indicative of higher bio-availability than leachates from dead tissues, although *Phragmites* blades and stems produced leachates with the opposite trend. The other hypothesis proposing a trend of increasing inferred bio-availability from semi-terrestrial through emergent to submerged macrophyte leachates was also generally supported by the data. *Vallisneria* tissues produced highly labile leachates, *Persicaria* leachates were among the most refractive and leachates derived from the various types of emergent plant tissue were spread throughout the range of inferred bio-availability.

Several studies that have used fluorescence techniques to examine carbon compounds have noted changes to peak location and size due to pH differences between samples, "inner filtering" caused by solution absorption of excitation or emission wavelengths, or the influence of metal complexation on organic molecules (Mobed et al., 1996; Westerhoff et al., 2001; Ohno, 2002; Tucher et al., 1992; McKnight et al., 2001). The effects of inner-filtering and metal complexation on leachate fluorescence were assessed in this study by comparisons of spectra produced by raw data and that which had been pH-adjusted and corrected for sample absorbance. While inner-filtering may be important in undiluted leachate samples (Howitt, 2003), absorbance correction (McKnight et al., 2001) applied to diluted samples in this study decreased the resolution of fluorescence peaks and introduced substantial artefactual "noise" at low excitation wavelengths (i.e. where sample absorption was greatest). Other studies have found it unnecessary to correct for absorbance where samples were dilute (Westerhoff et al., 2001; Baker, 2001; 2002a; 2002b). Fluorescence peaks were again more diffuse in spectra produced after pH modification – peak heights were reduced and background fluorescence levels were higher than in unmodified samples. Similar effects were observed by Westerhoff et al. (2001), with a reduction in pH from 7 to 3 causing minor differences in peak locations but substantial decreases in maximal fluorescence (average of 30 – 40% reduction in peak height with some peaks more severely affected, becoming almost undetectable). The combination of pH modification and absorbance correction on the dilute samples used in this study produced almost unusable spectra, and therefore these practices were discontinued.

The locations of peaks observed from 3D-EEM analyses of macrophyte leachates were comparable to those of known compound types from the literature, such as humic and fulvic acid-like substances and proteinaceous compounds (Coble, 1996; Mobed et al., 1996; Baker and Genty, 1999; Mayer et al., 1999; Baker, 2001; McKnight et al., 2001; Westerhoff et al., 2001; Baker, 2002a; Baker, 2002b; Ohno, 2002; Alberts and Takacs, 2004; Yamashita and Tanoue, 2004). The occurrence of low molecular weight nitrogenous substances, such as the proteinaceous compounds observed in leachates from live tissues in this study, has been used as an indicator of high bio-availability, whereas higher molecular weight humic compounds (which occurred more often in leachates derived from dead macrophyte tissues in this study) are often considered to be more recalcitrant (Godshalk and Wetzel, 1978; Amon and Benner, 1996). The distribution of leachates in two-dimensional MDS space based on 3D-EEM data was related to the proportions of different compounds present. In the bottom right corner (labelled 'A'), leachates are dominated by tryptophan-like substances, with chlorophyll and its degradation products being introduced towards 'B'. In the area around 'C' are leachates which contain tyrosine-like compounds. As humic compounds appear in leachates, their position moves

towards ‘D’. For nearly all leachates, there was movement toward ‘D’ with senescence, indicating that, while greater quantities of DOM are released from dead macrophyte tissues, these leachates tend to contain higher molecular weight humic compounds and so are not as labile as leachates derived from live tissues (with the exception of *Phragmites*).

5.5 Conclusion

Macrophytes in rivers and wetlands are regularly inundated by changing water levels. Leaching of inundated macrophyte tissues contributes dissolved organic matter (DOM) to the water column, fuelling secondary production by aquatic microbes. This study determined rates of release, quantities and composition of DOM leached from a range of green and senescent tissues from four macrophyte species with different growth forms. The majority of DOM release occurred within 24 hours of inundation. While live tissues leached DOM more quickly than dead tissues, only small quantities of DOM were released (1% of tissue carbon), and this process appeared to be microbially mediated. Much larger quantities of DOM were released from dead macrophyte tissues (20% of tissue carbon), however these leachates generally had lower presumed bio-availability than DOM released from live tissues (inferred from nutrient composition and fluorescence excitation-emission spectra). The data provide some evidence for an inverse relationship between the proportion of structural compounds in plant tissue and its capacity for leaching, with greater and faster leaching from leaf blades than from sheaths or stems within a single growth form. Growth form appeared to affect leachate nutrient composition, with carbon decreasing and phosphorus increasing from the semi-terrestrial mudflat hydrophyte, through the emergent macrophytes to the submerged species. Inferred leachate bio-availability also followed this trend.

Given the paucity of comparative, quantitative studies of leaching from untreated macrophyte tissues, this work represents a major advance in our understanding of DOM release from aquatic plants. Information on leachate bio-availability provides a potential link to microbial utilisation, and hence to the rest of the system. Data are immediately applicable to the estimation of DOM release from POM in the field, allowing extrapolation of DOM release processes and potential microbial utilisation to the reach scale.

Chapter 6. Responses of riverine microbial communities to flow-induced changes in carbon inputs.

6.1 Introduction

Carbon entering lowland rivers can originate from a range of autochthonous and allochthonous sources including organic matter (OM) transported from upstream, algal production (both attached and planktonic), macrophytes, riparian vegetation, interaction with the floodplain and in-stream and terrestrial fauna (Robertson et al, 1999). Heterotrophic microbes play a critical role in aquatic ecosystems in the breakdown and assimilation of carbon compounds, leading to the production of inorganic carbon and incorporation into microbial biomass, continuing carbon transfer back through the food-web (Meyer, 1994).

Microbial communities in temperate Australian lowland rivers are often carbon limited and show rapid responses to inputs of organic matter (Rees, unpub.; also see Benner et al., 1995). It is possible that river and catchment management practices have altered the timing and composition of organic matter inputs, thus changing in-stream carbon dynamics.

Riverine microbial responses to carbon inputs can be assessed using bacterial production rates, respiration rates and bacterial ectoenzyme analysis, among other things (Cole et al., 1988). Respiration assessment provides a relatively easy and inexpensive method of determining microbial activity and responses to nutrients, environmental variables, etc., and can be performed under laboratory conditions or in the field (Jahnke and Craven, 1995). Ectoenzyme analysis offers a different approach, allowing more detailed insight into microbial responses to particular substrates. Ectoenzymes are enzymes that are secreted across the cell membrane and react on polymeric substrates outside the cell. Ectoenzymes for degrading particular organic compounds are produced in response to the presence of those compounds; patterns and rates of enzyme activity can be used to infer sources and quantity of organic matter present (Chrost, 1992; Hoppe, 1993; Sinsabaugh and Findlay, 1995).

Alterations to the proportions of organic matter supplied from different sources will affect microbial functioning due to differences in the composition of the material. While not often explicitly defined, bio-availability has been described in terms of bacterial growth efficiency (BGE), biomass production, growth rates and respiration rates. Bio-availability is affected by source species (Mann and Wetzel, 1996), growth form (Godshalk and Wetzel, 1978a) and prior desiccation (Harrison and Mann, 1975; Godshalk and Wetzel, 1978a). Bacterial growth efficiencies on emergent macrophyte DOM (Findlay et al., 1986; Findlay et al., 1992; Mann and Wetzel, 1996) are substantially lower than those reported for algal and submersed macrophyte leachates (Linley and Newell, 1984; Findlay et al., 1992), but higher than those reported for terrestrial inputs (Meyer et al., 1987). Higher bacterial growth efficiencies have been observed on leachates derived from green tissues compared with senescent tissues (Mann and Wetzel, 1996).

Major causes of variation in supply of carbon to lowland rivers include autotrophic species composition, abundance and distribution, temporally variable plant production and senescence cycles, and the accumulation, input, photochemical processing and transformation (by microbial utilisation, adsorption or complexation) of organic matter. River hydrology is an over-arching driver of many of these factors, affecting community structure, productivity, and OM inputs from phytoplankton, macrophyte and biofilm communities, OM accumulation within channels and adsorption by particles. Of these, flow-induced changes to OM inputs are likely to have the most immediate and substantial effects on riverine microbial functioning (Leff and Meyer, 1991; Benner et al., 1995). It is hypothesised that flow changes alter relative proportions of OM inputs from different sources, which in turn affect microbial functioning due to differences in bio-availability.

The aim of this chapter was to assess responses of in-stream microbial communities to flow-induced changes in carbon source by addressing the following questions:

1. Do rates and patterns of microbial carbon use vary under different flows?
2. Do riverine carbon inputs vary under different flow conditions?
3. Is riverine microbial functioning affected by altered carbon inputs and can patterns of microbial carbon metabolism be related to specific carbon sources?

A combination of field and laboratory techniques were used to address each of the above questions:

1. Rates of community respiration and bacterial ectoenzyme activities were measured under different flow conditions at three lowland river field sites.
2. Changes to entrained carbon (DOM and POM) were determined and changes to important potential carbon sources were modelled for different discharges at the three field sites.
3. Microbial responses to different OM types were determined from *in situ* measurements of substrate-induced respiration, ectoenzyme patterns at field sites during inundation of macrophyte beds and ectoenzyme patterns induced by laboratory manipulations of OM.

6.2 Methods

6.2.1 Study Sites

Field study sites were located along lowland reaches (BAR, BRO and OVN) of three rivers in south-eastern Australia (Murray, Broken and Ovens Rivers) (fully described in Chapter 2). *In-situ* measurements of community respiration were conducted on eight occasions between May 2001 and December 2002, with the sampling schedule designed to target a range of flow events (base flow, rising and falling limbs, flood, etc.). On each field trip, samples were also collected to assess water column dissolved organic carbon (DOC) and nutrient concentrations (total nitrogen and total phosphorus – TN and TP), particulate organic matter (POM) content, and bacterial ecto-enzyme activities. River flow data for each site covering the study period were obtained from DIPNR/DSE.

6.2.2 Effects of Flow on Microbial Functioning

6.2.2.1 Water Column Community Respiration

In-situ respiration chambers were used to assess water column community respiration under different flow conditions. The six chambers (3.5 L) were constructed from PVC pipe fittings with integrated pumps for recirculating water within each chamber (Figure 6.1). Water temperature and dissolved oxygen (DO) concentration were logged every four minutes. Chambers were filled with river water on-site, DO probes calibrated and allowed to stabilise, and then chambers were sealed under water. Changes in dissolved oxygen were monitored over short incubation periods (4 – 6 hours), to ensure that the initial response of the microbes was being assessed rather than any subsequent changes to the population within the chamber.

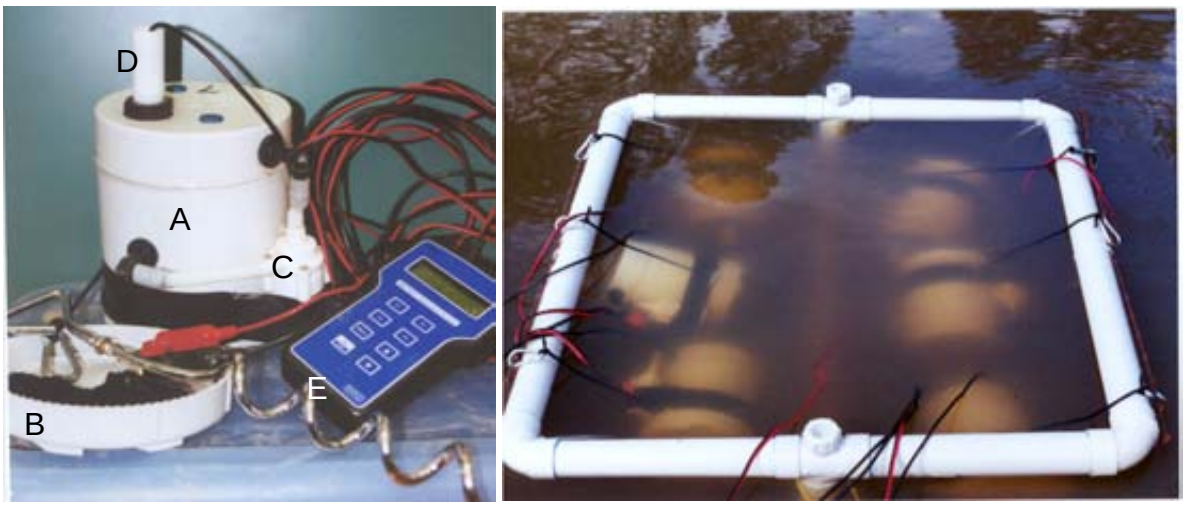

Figure 6.1. Apparatus used to assess community respiration rates in the field. Left: Chambers were constructed of a PVC pipe segment sealed on one end (A) with a screw on lid (B). Submersible pumps (C) circulated water within the chambers to maintain flow past the membrane of the dissolved oxygen probe (D). Data were logged every 4 minutes (E). Right: Method of deployment of chambers in the field. Cables running to the DO loggers and pump batteries can be seen.

6.2.2.2 Bacterial Ecto-Enzyme Activities

Enzyme analyses on river water samples were used to assess the forms of carbon being utilised by microbial communities at each site on each field trip (i.e. under different flow conditions). Water samples were collected from the main river channel on each trip and frozen for later analysis. Fluorogenically labelled (Methylumbelliferyl (MUB) linked) substrates were selected to cover a range of carbon sources in lowland rivers (Table 6.1).

Stock solutions of 100 mM bicarbonate (pH 8.2) or phosphate (pH 7.0) buffers were prepared, autoclaved and stored at 4 ^{o}C for use in the preparation of standards and substrate solutions. Substrate solutions (1 mM) were prepared in 5 mM bicarbonate or phosphate buffers (Table 6.2) with aggressive stirring at 4 ^{o}C. MUB-butyrate was prepared fresh before each assay; the other enzyme substrates were stable stored at 4 ^{o}C for up to one week. Equal volumes of enzyme substrate were added to thawed, unfiltered water samples (x 4); final substrate concentrations were 500 µM. Samples were incubated at 20 ^{o}C in the dark and fluorescence was monitored over time (365 nm excitation and 450 nm emission with 5nm EM and EX slit widths). Two fluorometers were used during the study – a Hitachi F4500 (reading single 2 ml cuvettes) and a Labsystems Fluoroskan II 96-well plate reader (300 µl well volume), the latter allowing much greater through-put of samples. Comparisons of results produced by the different fluorometers were performed before switching between them, with good agreement between results and an improvement in precision obtained with the plate reader.

Table 6.1. Enzymes selected for assessment in this study and the substrates used to assay them.

Enzyme	Abbrev	Substrate	Solvent*		
			Bicarb	*Phos*	*Milli-Q*
fatty acid esterase	EST	MUB-butyrate		**X**	
α-1,4-glucosidase	α-GLU	MUB-α-D-glucoside	**X**		
β-1,4-glucosidase	β-GLU	MUB-β-D-glucoside	**X**		
β-D-xylosidase	XYL	MUB-β-D-xyloside	**X**		
β-N-acetylglucosaminidase	NAG	MUB-β-N-acetylglucosamine	**X**		
endo-peptidase	PEP	MUB-guanidine			**X**

* Bicarb = 5 mM sodium bicarbonate buffer, pH 8.0; Phos = 5 mM phosphate buffer, pH 7.0; MilliQ = 0.2 µm pore size membrane filtered distilled water

Short incubation periods (max. of 8 hours, but generally 4 – 6 hours) were critical for ensuring that results represented activity occurring in the river at the time of sampling rather than being an artefact of incubating the microbes with a bio-available substrate (increases in activity were observed over long incubation periods in larger volume samples presumably because the bacterial population increased or switched on production of enzymes to match the added substrate; plateauing was observed in some occasions with the plate reader as the small quantities of substrates were used up). Background substrate degradation occurring during each analysis was quantified using boiled sample blanks. A 10 ml sub-sample of each sample was boiled for 1 min and allowed to cool. Any volume lost by evaporation was replaced with Milli-Q water. Blanks were then processed as for water samples. Initial rates of enzyme activity (which were linear) were calculated, with correction for abiotic substrate degradation by subtracting rates of fluorescence increase in boiled blanks. Fluorescence units were converted to nmol substrate hydrolysed/ml/min using the slopes of standard curves adjusted for fluorescence quenching. Standards (0.05 to 5.00 µM MUB) were prepared by serially diluting a 50 µM stock solution of MUB in 5 mM bicarbonate or phosphate buffer. Quenching of fluorescence can occur in samples due to absorption or scattering by particles/DOM or sample pH effects on fluorescence. Thus, standard curves were determined for each sample by adding equal volumes of sample to aliquots of the standard series and determining the slope of MUB concentration regressed with sample fluorescence. After each run, plates/cuvettes were rinsed in tap water, soaked in 5% HCl acid overnight and rinsed well with RO water.

6.2.3 Effects of Flow on Carbon Inputs

Changes to riverine carbon inputs in response to flow were estimated by measuring changes in DOM and POM in the water column under different flow conditions (entrained carbon) and modelling changes to important potential carbon sources under different discharges (channel inundation modelling).

6.2.3.1 Entrained Carbon

On each sampling trip, water samples for DOC, TN and TP concentration assessment were collected from the main river channel (group data from CRCFE project A200) and from within macrophyte beds where inundation had occurred. Nutrient samples (150 ml x 4) were collected into new or acid-washed PET jars (after initial rinsing in sample water) and frozen for later analysis. Simultaneous analysis of total nitrogen and phosphorus involved persulphate digestion on a Lachat Instruments QuickChem 8000 Flow Injection Analyser (Hosomi & Sudo, 1986) performed by J. Pengelly at the Analytical Chemistry Laboratory of the Murray-Darling Freshwater Research Centre (under national standards for QA and QC). Water (30 ml x 4) filtered through 0.2 um syringe filters was collected into sterile PP jars, preserved with 80% phosphoric acid and stored at -20 ^{o}C for DOC analysis. Blanks were obtained by filtering RO water into jars and processing in the same manner. Carbon samples were processed using an adaptation of APHA Total Organic Carbon Method 5310C (Eaton et al., 1995) using a Model 1010 Total Organic Carbon Analyser (O.I. Analytical, Texas) by John Pengelly at the MDFRC Analytical Lab. The concentration of particulate organic matter within the water column was assessed on each sampling occasion by filtering known volumes of river water (50 – 200 L) through drift nets (50 and 250 µm mesh size) into 150 ml PET collecting jars. Samples were frozen for later processing, involving concentration onto pre-ashed and weighed GF/C filters for dry weight and loss-on-ignition analyses.

6.2.3.2 Channel Inundation Modelling

Three-dimensional mapping of each reach, including distributions of macrophyte beds, was performed and incorporated into a GIS for each site. In combination with rating curves for each site, this allowed the prediction of macrophyte bed areas inundated, wetted sediment area, wetted perimeter and reach volume for different discharges (see Chapter 2 for details).

6.2.4 Effects of Carbon on Microbial Functioning

6.2.4.1 Enzyme Responses to Macrophyte Bed Inundation

On each field trip, if macrophyte beds were inundated then water samples were collected from within inundated beds, frozen and ectoenzyme activity rates measured as described above, to determine how *in situ* patterns of microbial activity varied in response to inputs of OM from known sources (inundated macrophytes).

6.2.4.2 Respiration Responses to OM Additions

Responses of riverine microbial communities to inputs of particulate organic matter from a range of sources were assessed. On each field trip, substrate-induced respiration rates were determined *in-situ* using macrophyte OM (which had not been previously inundated) added to the respiration chambers described above. Plant material was collected from macrophyte species studied at each site on the day of assessment, with material selected to be representative of that occurring in macrophyte beds at the time. Plant tissues were trimmed to the length of the respiration chambers and replicate batches were enclosed in pantyhose (to stop the POM from being sucked through the pump) and placed in the chambers. Chambers were then sealed under water and DO logged every four minutes for 4 – 6 hours. Control chambers had empty pantyhose added. Substrate-induced respiration rates were determined by subtracting control rates from treatments. It should be noted that respiration changes observed were in response to POM additions and whatever quantity of DOM was leached out of added POM during the experimental incubation period (4 – 6 hours).

6.2.4.3 Enzyme Responses to OM Additions

DOM leached from different types of particulate organic matter is comprised of different compounds with varying ratios of nutrients and potentially inhibitory compounds (Chapter 5). Given that bacteria produce enzymes in response to specific compounds, it might be expected that characteristic enzyme profiles would be associated with OM from different sources. An experiment was conducted to assess how patterns of riverine bacterial ecto-enzymes changed in response to inputs of carbon from different sources, and whether enzyme profiles could be used to determine primary carbon sources being utilised by riverine microbes at a given time. Leachates (50 ml) obtained from different carbon sources (Table 6.2) or Milli-Q water (controls) were added to 200 ml of freshly collected river water in 500 ml conical flasks (x 4 replicates) and incubated at 20^{o}C in the dark with gentle agitation for 2 weeks (Figure 6.2). Samples (5 ml) were removed from each flask after 1, 3, 6, 10 and 14 days and frozen for later enzyme analysis (method described above). Due to project time constraints, only the data for Day 1 samples were analysed and are presented here.

Table 6.2. Leachates used in the enzyme experiment.

Code	Material	Species	Source
Alg	Green algae whole cells	Scenedesmus sp.	R. Oliver culture
Gum	River Red Gum leaves, stems	Eucalyptus camaldulensis	Murray R. near Albury
Pers	Knotweed whole shoots	Persicaria prostrata	Murray R. near Albury
Phrag	Common Reed blades, sheaths, stems	Phragmites australis	Murray R. near Albury
Typha	Cumbungi blades, sheaths, stems	Typha domigensis	Woolshed Ck near Albury
Vall	Ribbonweed blades	Vallisneria gigantea	Murray R. near Albury

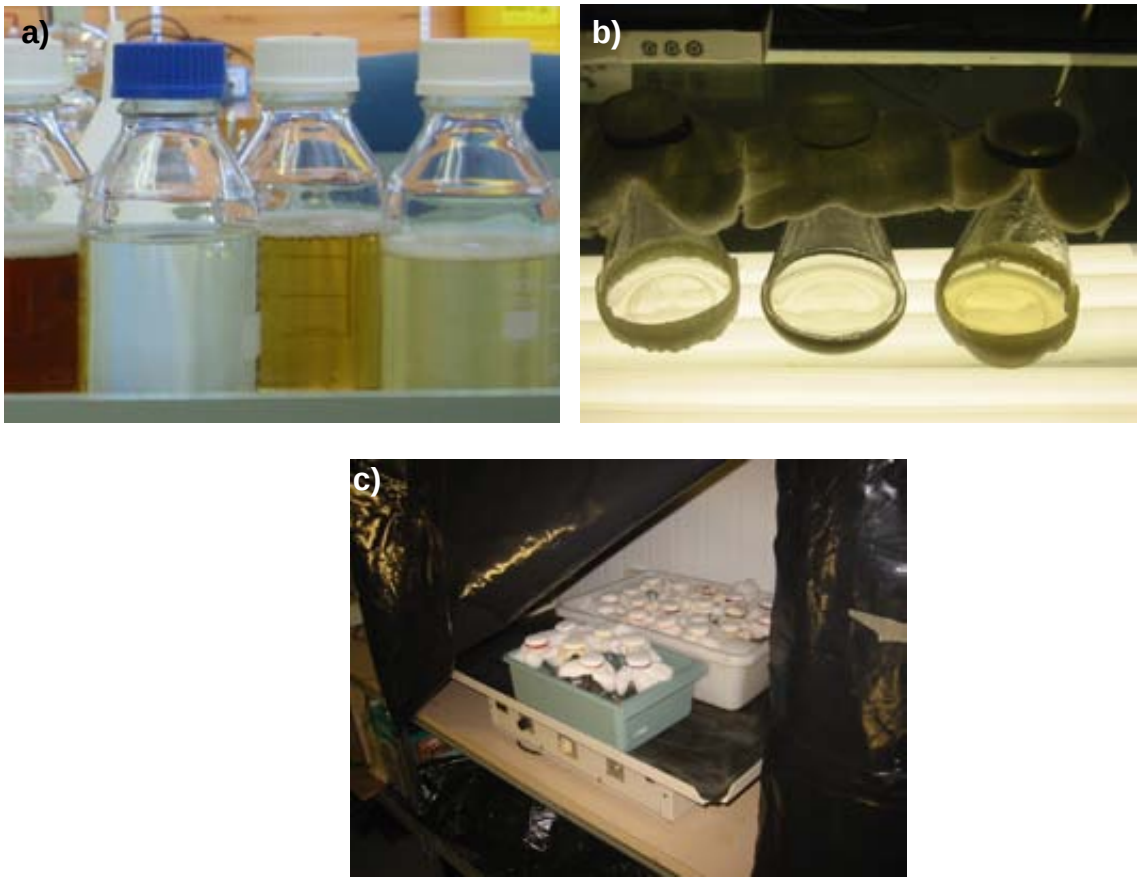

Figure 6.2. Enzyme experiment setup: a) leachates obtained from algae and higher plants; b) filter-sterilised leachate added to river water in flasks; c) flasks incubated in the dark with agitation. Samples were removed for enzyme analyses after 1, 3, 6, 10 & 14 days.

6.2.5 Statistical Analyses

In order to include flow as a categorical variable in analyses, flow data for each field trip at each site was classified by two parameters – stage (water level, gauge height) and action (stability, movement). The categories for stage were low, medium, high or flood, comparing the mean discharge over the week of the field trip to mean daily discharge calculated over several years. For BRO and OVN, low flows were those at 30% of the mean daily flow or lower, while medium flows were between 30% and 120% and flows were classified as high when they were over 120% of the mean. Because the Murray River is so highly regulated at the study site, with flows generally maintained at levels much higher than natural, low flows at BAR were defined as those below 70% of the mean, whereas flows between 70% and 130% of average were considered medium and above 130% were classified as high. Flow stability was determined from regressions over the 7 days preceding field trips compared to mean annual discharge, with changes in discharge of more than 5% at BAR and OVN and 10% at BRO classified as rising or falling limbs and less than this considered to be stable (steady).

Graphs were plotted and regressions fitted in Sigmaplot 8.0 for Windows. ANOVA was used to assess differences in mean respiration rates observed for POM treatments and controls, between flow categories for in-situ community respiration assessments, and between enzyme ratios for different flow categories and macrophyte species. Non-parametric multi-variate methods were used to analyse enzyme data (ANOSIM, BIOENV and MDS plots based on similarity matrices calculated for non-transformed data using standardised Euclidean distances).

6.3 Results

6.3.1 Site Characteristics

The characteristics of each site are summarised in Table 6.3. The Murray River was obviously the largest of the three rivers under study, with at least double the mean annual discharge and channel width of the Ovens and Broken Rivers. Much higher nutrient levels were observed at the Broken River site, possibly related to the occurrence of a town upstream (Benalla) or surrounding land-use, which was cleared cropping and grazing land. In contrast, OVN and BAR sites were surrounded by state forest and national park, with fairly dense native vegetation. Concentrations of particulate organic matter (POM) were similar across all sites, and showed a high degree of variability. Although large differences occurred in absolute values of macrophyte bed areas between the three sites (27,100, 794 and 6,200 m^2 at BAR, BRO and OVN), when standardised by reach area (determined from mean channel width multiplied by reach length – 199,880, 14,400 and 35,805 m^2, respectively) or mean annual discharge (2,544, 71 and 1,335 GL, respectively) the values were quite similar (AREA: 0.14, 0.06 and 0.17 and discharge: 10.65, 11.18, 4.64 for the three sites, respectively).

Table 6.3. Summary of site characteristics.

Characteristic	BAR	BRO	OVN
Degree of regulation	High	Moderate	Low
Mean Annual Discharge ± sd (GL)	2544 ± 281	71 ± 44	1335 ± 809
Reach Length (m)	2630	800	1085
Mean channel width ± sd (m) [++]	76 ± 5.71	18 ± 2.68	33 ± 6.44
Mean water depth ± sd (m) [++]	2.38 ± 0.49	0.39 ± 0.08	2.27 ± 0.90
Max water depth (m) [++]	4.69	0.96	5.85
Mean DOC ± sd (mg/L) [++]	3.36 ± 1.46	9.47 ± 7.88	3.04 ± 1.15
Mean TN ± sd (µg/L) [++]	331.6 ± 61.21	938.3 ± 487.3	381.1 ± 121.3
Mean TP ± sd (µg/L) [++]	41.69 ± 11.66	206.5 ± 145.5	49.08 ± 13.60
Mean POM > 50 µm ± sd (mg/L) [++]	0.32 ± 0.30	0.34 ± 0.31	0.28 ± 0.22
Mean POM > 250 µm ± sd (mg/L) [++]	0.10 ± 0.11	0.08 ± 0.08	0.38 ± 0.86
Area of macrophyte beds (m^2)	27100	794	6200
Riparian vegetation type	Dense younger River Red Gum (RRG)	Cleared pasture, some RRG, Acacia, poplars, willows	Dense, mixed age RRG, Callistemon, Acacia

[++] Group data from the CRCFE A200 project "Lowland Rivers Project Mark II", supplied by B. Gawne, I. Ellis, H. Gigney, Z. Lorenz

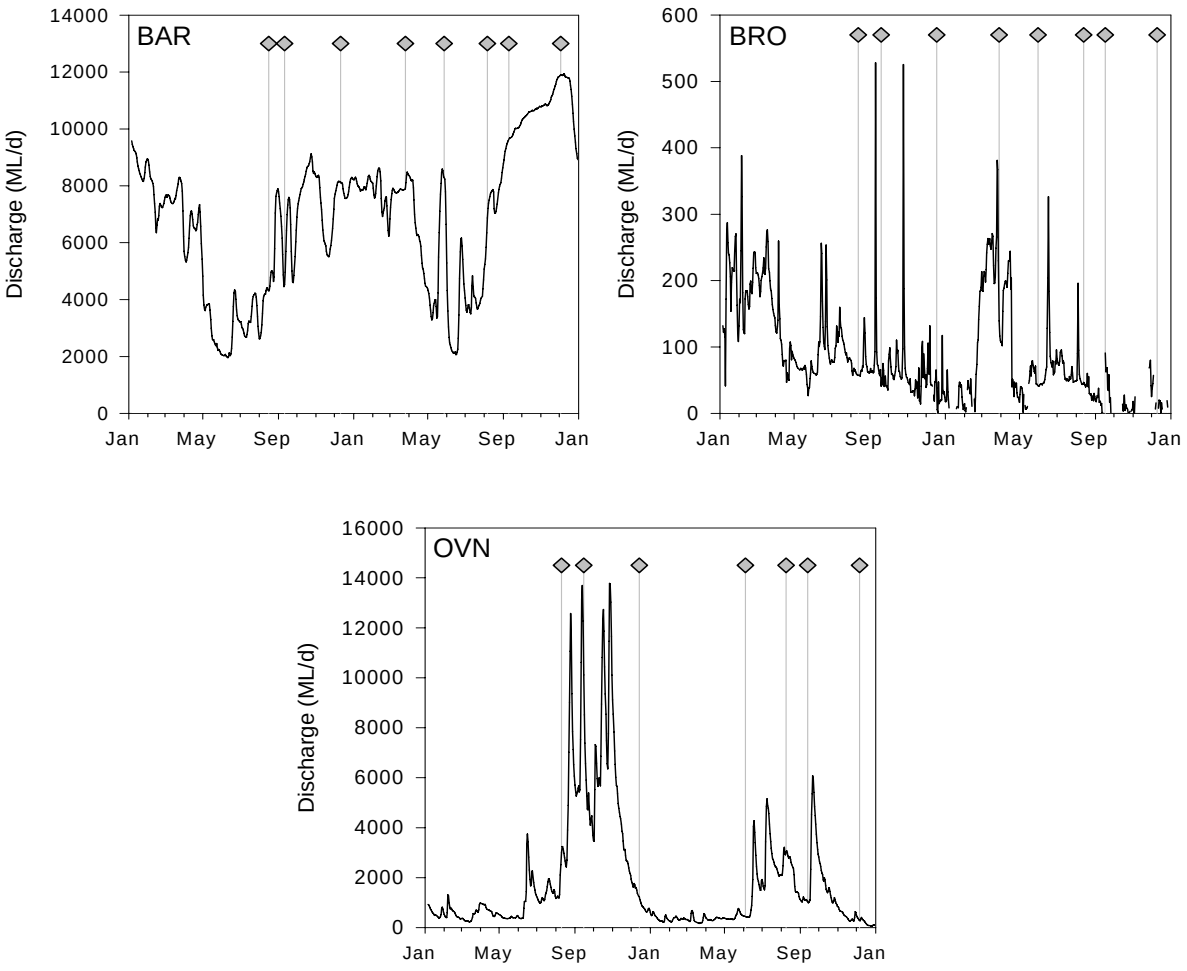

Figure 6.3. Hydrographs of the three study sites over the study period showing sampling occasions. Note different y-axis scales.

Hydrographs for each site over the study period are presented in Figure 6.3, with sampling occasions indicated. The summary and classification of flows during sampling occasions (Table 6.4) shows the effects of the drought on-going throughout this study, with generally low, stable flows occurring at the two least regulated sites (BRO and OVN). Mean and maximum water depths calculated over the study period for BRO were very low compared to the other sites. The flood in 2001 at OVN increased the mean and max water depths for this site despite the drought.

Table 6.4. Summary of flow classification characteristics for the different sites and sampling occasions.

Site	Date	Mean discharge during field trip		Stage	Change in discharge over previous week **			Action
		(ML/d)	*% ++*		*(ML/d)*	*% ^^*	*R^2*	
BAR	Oct-00			flood				rise
BAR	Dec-00			flood				fall
BAR	Aug-01	4323	62	low	26.2	0.6	0.41	std
BAR	Sep-01	4648	67	low	-455.0	-9.8	0.96	fall
BAR	Dec-01	8123	117	med	33.8	0.4	0.68	std
BAR	Mar-02	7969	114	med	-0.8	0.0	0.04	std
BAR	Jun-02	8277	119	med	80.0	1.0	0.32	std
BAR	Aug-02	6807	98	med	345.6	5.1	0.96	rise
BAR	Sep-02	9633	138	high	69.3	0.7	0.98	std
BAR	Dec-02	11891	171	high	26.2	0.2	0.94	std
BRO	Aug-01	57	30	low	-1.3	-2.3	0.83	std
BRO	Sep-01	54	28	low	-4.3	-7.9	0.69	std
BRO	Dec-01	36	19	low	16.6	45.5	0.26	rise
BRO	Mar-02	162	83	med	19.8	12.2	0.33	rise
BRO	Jun-02	41	21	low	-4.5	-11.0	0.65	fall
BRO	Aug-02	45	23	low	-1.1	-2.4	0.52	std
BRO	Sep-02	41	21	low	5.4	13.3	0.09	rise
BRO	Dec-02	0	0	low	-2.6	na	0.03	std
OVN	Aug-01	2920	80	med	311.5	10.7	0.83	rise
OVN	Sep-01	10302	282	flood	-942.0	-9.1	0.46	fall
OVN	Dec-01	1207	33	med	-69.3	-5.7	0.93	fall
OVN	Jun-02	439	12	low	-11.3	-2.6	0.97	std
OVN	Aug-02	3007	82	med	119.8	4.0	0.48	std
OVN	Sep-02	1030	28	low	-16.0	-1.6	0.70	std
OVN	Dec-02	288	8	low	-51.5	-17.9	0.94	fall

++ % of mean daily discharge
** calculated by linear regression of flow with date
^^ % of mean discharge during field trip

6.3.2 Effects of Flow on Microbial Functioning

Both rates of microbial activity (assessed from community respiration data) and patterns of microbial carbon use (as indicated by bacterial ecto-enzyme analyses) varied under different flows.

6.3.2.1 Community Respiration Responses

Respiration rates at each site varied on the different sampling trips. This variation was not related to DOC, TN, TP, POM, area of inundated macrophytes, the ratio of wetted sediment area to reach volume or phytoplankton GPP for either pooled samples or the separate sites (Figure 6.4; Table 6.5). There was a slight correlation with water temperature for pooled site data ($p < 0.05$, $F = 6.24$, $n = 23$), however the relationship only explained 19% of the variation. In contrast, respiration was strongly correlated with flow. When plotted by site, respiration at the different sites responded differently to changes in discharge (Figure 6.5). However, when the site data was pooled an interesting relationship with discharge emerged ($R^2 = 0.69$, $p < 0.0001$, $F = 17.07$, $n = 23$). Higher respiration rates occurred when discharge was very low (e.g. in the almost still pools at BRO) or very high (flood at OVN, high and rising water at BAR.

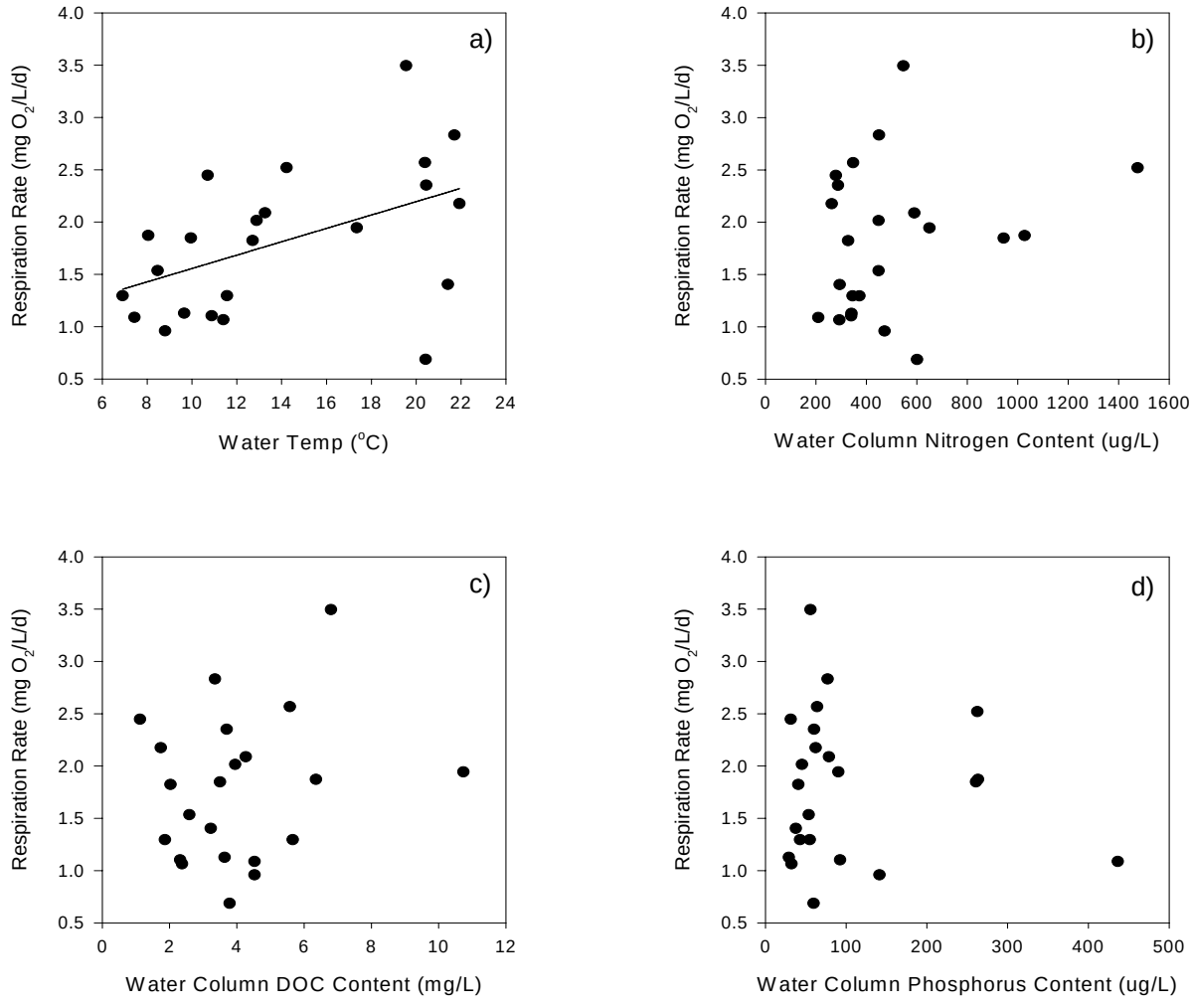

Figure 6.4. Comparison of community respiration rates to a range of potential drivers: a) water temperature, b) TN, c) DOC, d) TP.

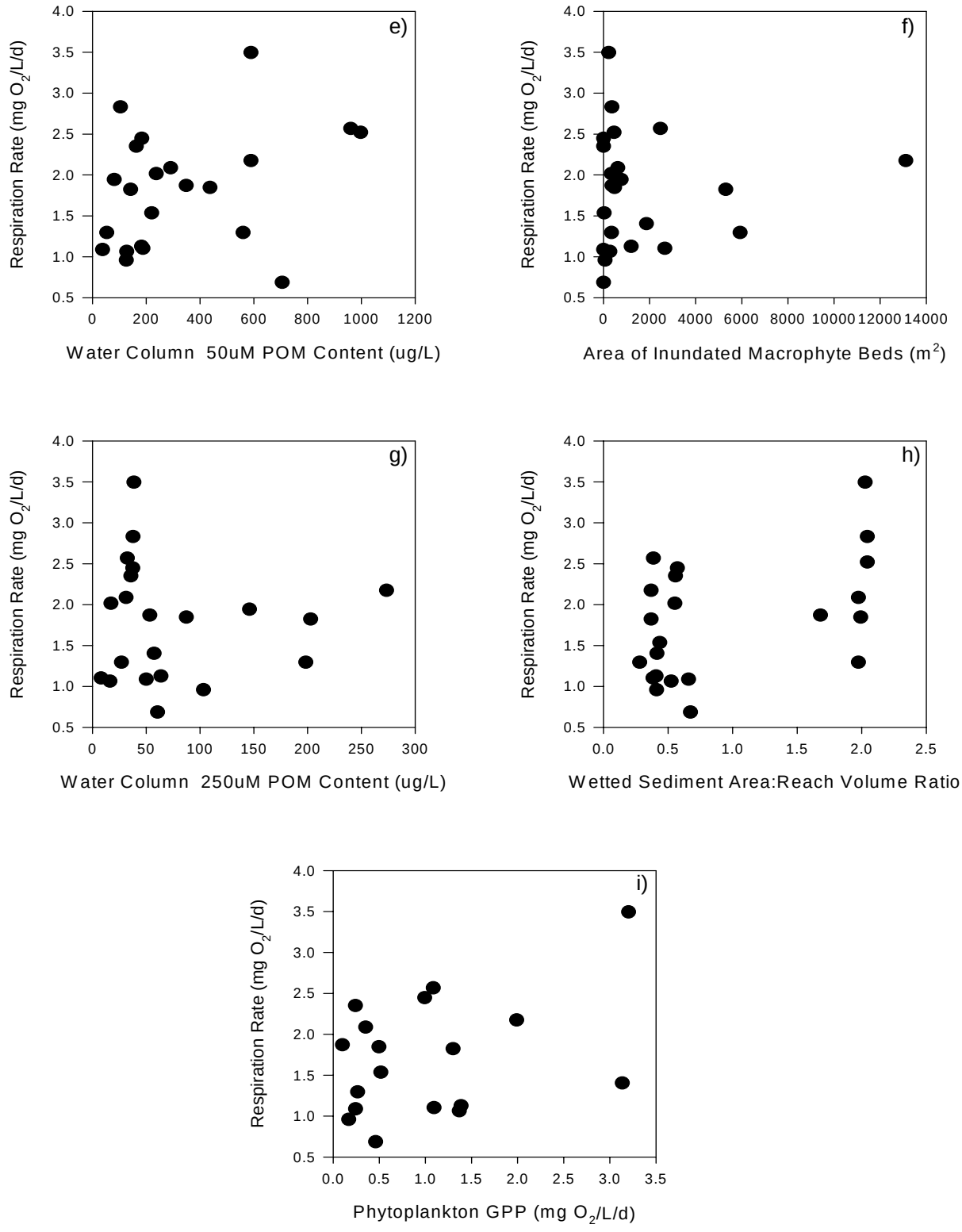

Figure 6.4 cont. Comparison of community respiration rates to a range of potential drivers: e) POM > 50 µm, f) macrophyte bed inundation, g) POM > 250 µm, h) wetted sediment to reach volume ratio, i) phytoplankton GPP.

Table 6.5. Summary statistics from analyses of linear regressions of community respiration versus a range of environmental parameters. Bold text has been used to highlight those parameters where the regressions were statistically significant at $p < 0.05$ or better.

Parameter	All Sites	BAR	BRO	OVN
Water Temp	**$R^2 = 0.19$**	$R^2 = 0.30$	$R^2 = 0.61$	$R^2 = 0.00$
	$p < 0.05$	$p < 0.5$	$p < 0.5$	$p < 1.0$
	$F = 6.24$	$F = 4.01$	$F = 12.04$	$F = 0.08$
	$n = 23$	$n = 8$	$n = 8$	$n = 7$
DOC	$R^2 = 0.00$	$R^2 = 0.06$	$R^2 = 0.00$	$R^2 = 0.18$
	$p < 0.5$	$p < 0.5$	$p < 1.0$	$p < 0.5$
	$F = 0.90$	$F = 1.44$	$F = 0.01$	$F = 2.28$
	$n = 22$	$n = 8$	$n = 7$	$n = 7$
TN	$R^2 = 0.01$	$R^2 = 0.00$	$R^2 = 0.00$	$R^2 = 0.22$
	$p < 0.5$	$p < 1.0$	$p < 1.0$	$p < 0.5$
	$F = 1.25$	$F = 0.23$	$F = 0.00$	$F = 2.74$
	$n = 23$	$n = 8$	$n = 8$	$n = 7$
TP	$R^2 = 0.00$	$R^2 = 0.00$	$R^2 = 0.00$	$R^2 = 0.00$
	$p < 1.0$	$p < 1.0$	$p < 1.0$	$p < 0.5$
	$F = 0.14$	$F = 0.26$	$F = 0.26$	$F = 0.75$
	$n = 23$	$n = 8$	$n = 8$	$n = 7$
POM 50	$R^2 = 0.06$	$R^2 = 0.58$	$R^2 = 0.06$	$R^2 = 0.00$
	$p < 1.0$	$p < 0.5$	$p < 1.0$	$p < 0.5$
	$F = 2.38$	$F = 9.41$	$F = 1.44$	$F = 0.99$
	$n = 22$	$n = 7$	$n = 8$	$n = 7$
POM 250	$R^2 = 0.00$	$R^2 = 0.00$	$R^2 = 0.00$	$R^2 = 0.00$
	$p < 1.0$	$p < 1.0$	$p < 1.0$	$p < 0.5$
	$F = 0.12$	$F = 0.97$	$F = 0.02$	$F = 0.63$
	$n = 22$	$n = 8$	$n = 8$	$n = 6$
Inundated macrophyte area	$R^2 = 0.00$	$R^2 = 0.05$	$R^2 = 0.02$	$R^2 = 0.00$
	$p < 1.0$	$p < 1.0$	$p < 0.5$	$p < 1.0$
	$F = 0.02$	$F = 1.35$	$F = 1.16$	$F = 0.08$
	$n = 23$	$n = 8$	$n = 8$	$n = 7$
Wet sediment: volume ratio	$R^2 = 0.19$	0.00	0.00	0.00
	$p < 1.0$	$p < 1.0$	$p < 0.5$	$p < 1.0$
	$F = 5.79$	$F = 0.20$	$F = 1.02$	$F = 0.00$
	$n = 22$	$n = 8$	$n = 7$	$n = 7$
Total enzyme activity	**$R^2 = 0.47$**	$R^2 = 0.15$	**$R^2 = 0.67$**	$R^2 = 0.00$
	$p < 0.0005$	$p < 0.5$	**$p < 0.05$**	$p < 1.0$
	$F = 17.88$	$F = 2.20$	**$F = 13.10$**	$F = 0.03$
	$n = 20$	$n = 8$	**$n = 7$**	$n = 5$

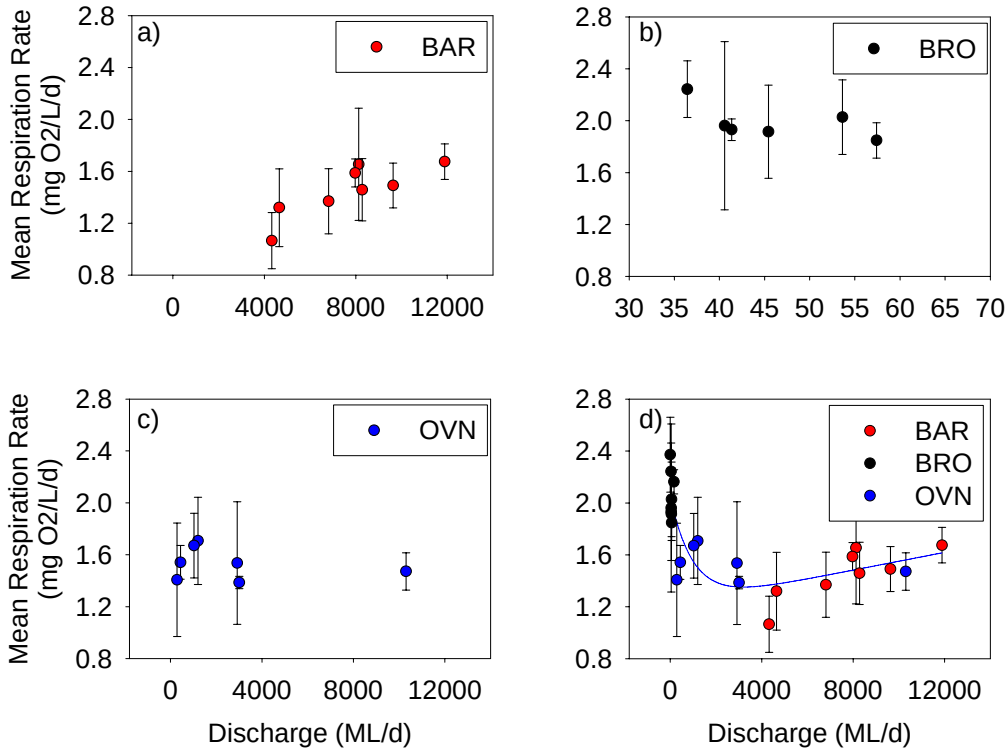

Figure 6.5. Relationship between discharge and community respiration at the three sites plotted separately (a, b, c), and together (d).

6.3.2.2 Bacterial Enzymatic Responses

As well as providing information about patterns of microbial carbon use at a given time, bacterial ecto-enzymes can indicate relative rates of metabolism, as demonstrated by their correlation with community respiration (Figure 6.6; $R^2 = 0.47$, $p < 0.0005$, $F = 17.88$, $n = 20$).

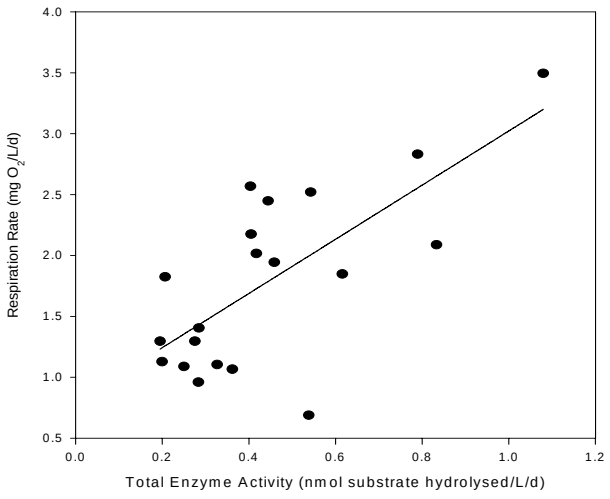

Figure 6.6. Correlation between total enzyme activity and water column community respiration in river water samples from all sites and sampling occasions.

No significant differences at $p < 0.05$ (ANOSIM) were observed in river enzyme patterns based on site, year or month (Figure 6.7 a, b, c; Table 6.6). Therefore, samples were pooled to analyse variation in response to flow. Patterns of microbial activity were affected more by water level variability than stage height (Figure 6.7 d, e). Pooled river samples from all three sites fall out into those taken during periods of steady flow, regardless of water level, and those taken on a rising or falling limb or during a flood (ANOSIM: Global $R = 0.49$, $p < 0.0001$; Table 6.6).

Table 6.6. ANOSIM output showing significance of groupings presented in Figure 6.7. Bold text highlights groups which are significantly different at $p < 0.05$.

Groups	R Stat	Sig Level %
Site – global stats	0.093	5.5
BAR, BRO	0.194	3.0
BAR, OVN	0.110	9.3
BRO, OVN	-0.014	48.4
Year – global stats	0.122	10.9
00, 01	0.291	9.1
00, 02	0.512	4.1
01, 02	0.004	41.5
Month – global stats	0.085	14.1
Sep, Aug	0.157	10.0
Sep, Dec	0.187	6.6
Sep, Mar	0.017	37.5
Sep, Jun	-0.013	50.5
Aug, Dec	0.416	1.6
Aug, Mar	0.038	36.5
Aug, Jun	0.012	40.5
Dec, Mar	0.088	23.0
Dec, Jun	0.072	18.3
Mar, Jun	-0.194	96.8
Stage – global stats	**0.279**	**0.1**
high, med	0.016	36.3
high, fld	**0.690**	**0.8**
high, low	0.063	22.1
med, fld	0.298	7.5
med, low	**0.203**	**3.6**
fld, low	**0.871**	**0.3**
Action – global stats	**0.487**	**0.1**
fld, rise	**0.403**	**2.4**
fld, fall	0.200	12.5
fld, std	**0.992**	**0.2**
rise, fall	-0.125	84.2
rise, std	**0.376**	**0.1**
fall, std	**0.675**	**0.2**

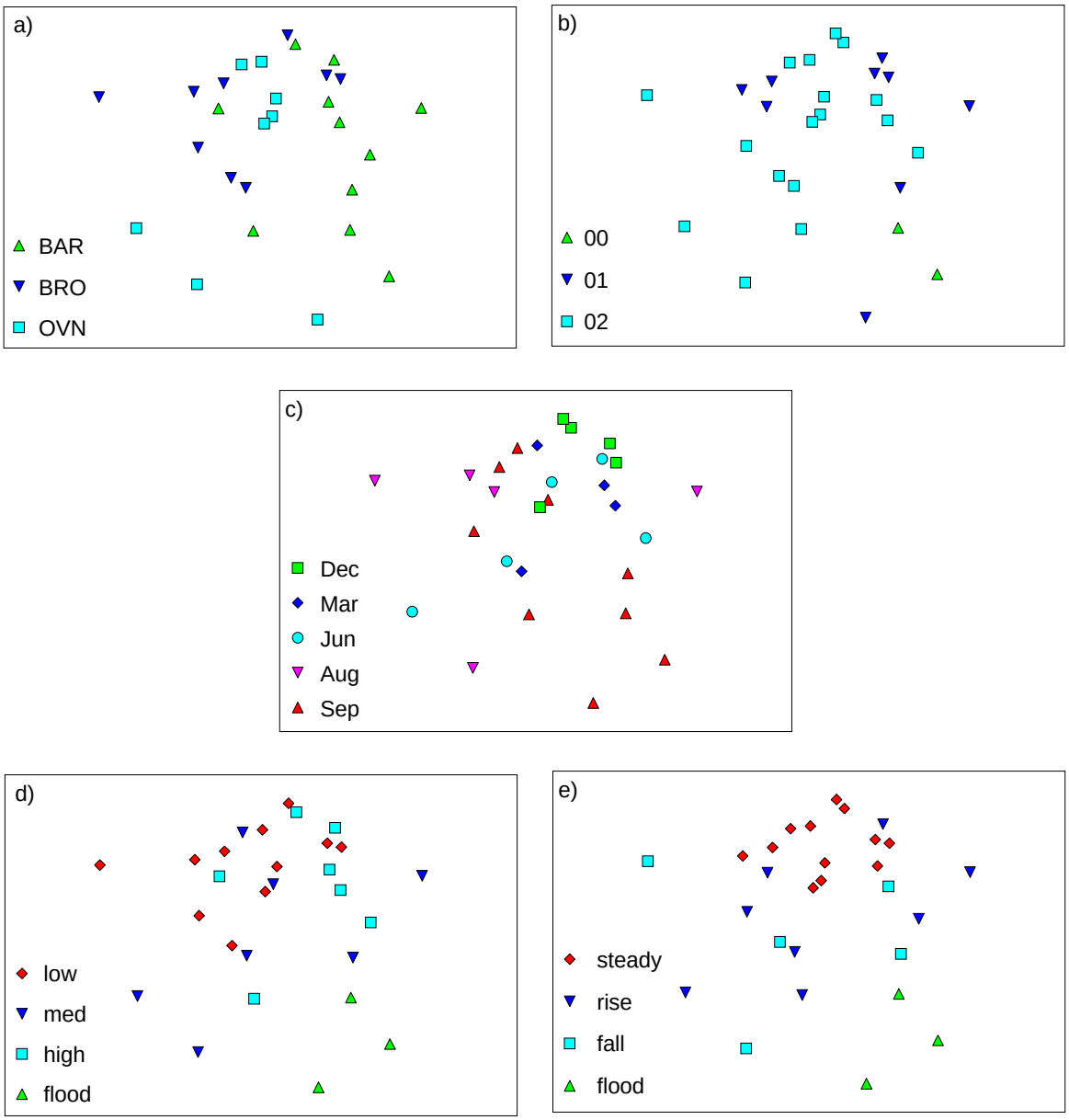

Figure 6.7. MDS ordinations of enzyme activities from river water samples at all sites and sampling dates grouped by a) site, b) year, c) month, d) water level and-e) water stability. Stress = 0.11.

BIOENV analysis indicated that these differences were driven mostly by PEP, NAG and α-GLU activities (R = 0.883; rising to 0.933 when XYL is also included). Activities of these enzymes are presented as overlays of the preceding MDS ordination in Figure 6.8, with bubble location following the sample distribution shown in the MDS and bubble size directly proportional to activity for each enzyme presented. During steady flows, microbial functioning appeared to be based on proteinaceous compounds (Figure 6.8 a), with a switch to carbohydrates, cellulose and chitin during a flood or when the water level changes (Figure 6.8 b, c, d). Xylosidase activity was highest toward the bottom left of the plot (Figure 6.8 d), corresponding to periods of water level change or flood at OVN. In contrast, the highest α-Glucosidase activity was induced by flow variability at BAR (Figure 6.8 c).

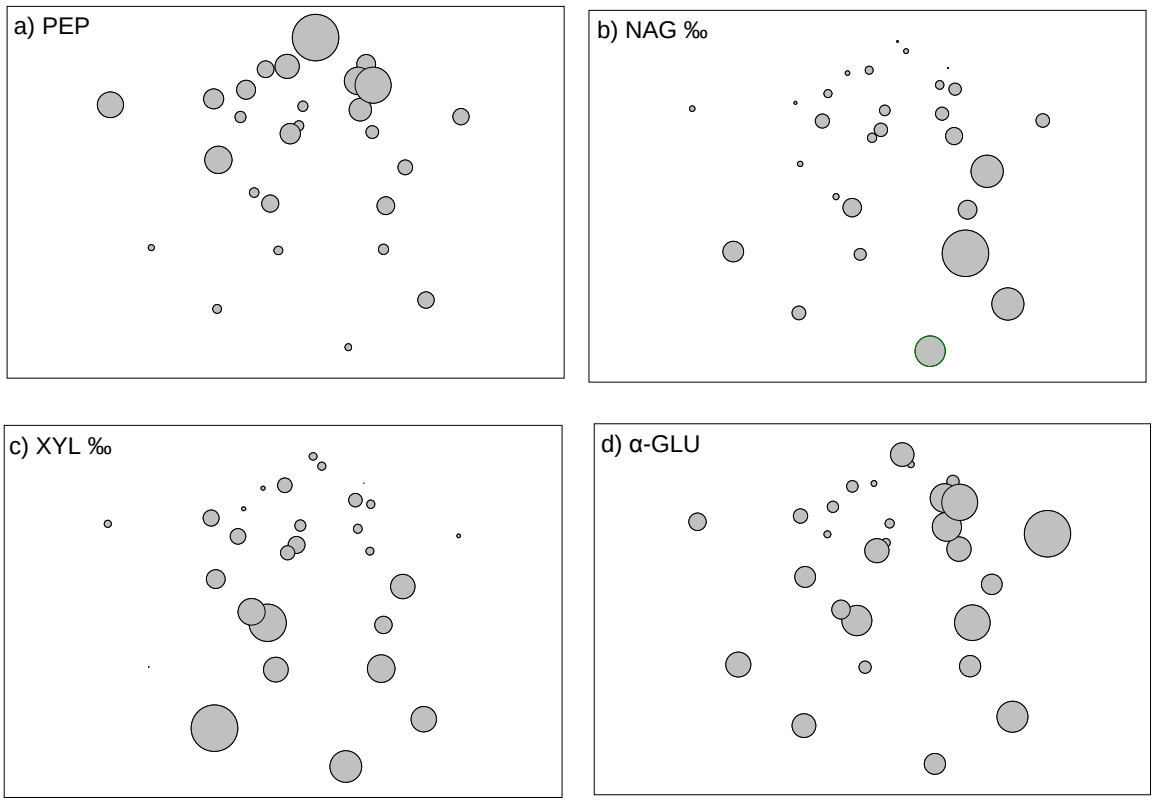

Figure 6.8. Activities of specific enzymes overlaid on the MDS presented in Figure 6.7 showing trends in a) peptidase (PEP), b) chitobiose (NAG), c) xylosidase (XYL) and d) alpha-glucosidase (α-GLU) driving separation of data points.

Under stable flows the PEP:CARB ratio of pooled river water samples was quite high (Figure 6.9 a). When water levels rose or fell, or floodplain inundation occurred, this ratio dropped markedly. The activity of chitobiose, represented as a proportion of total enzyme activity (NAG ‰) increased from steady flows through variable flows to flood conditions (Figure 6.9 b). XYL ‰ was similar under steady flows and falling limbs, increasing slightly as water levels rise to maximum levels during floods (Figure 6.9 c).

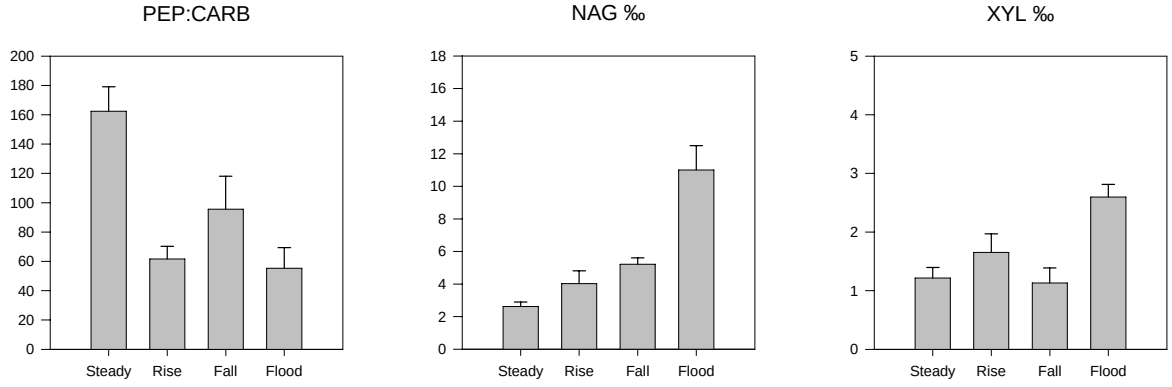

Figure 6.9. Changes to important enzyme parameters of pooled river samples with flow.

6.3.3 Effects of Flow on Carbon Inputs

Changes to riverine carbon inputs in response to flow were estimated by measuring changes in DOM and POM in the water column under different flow conditions (entrained carbon) and modelling changes to important potential carbon sources under different discharges (channel inundation modelling).

6.3.3.1 Entrained Carbon Assessments

No correlations were apparent between dissolved organic carbon concentration and discharge, current speed, stage or water level stability. Similarly, POM greater than 50 µm in size showed no relationship with flow variables. In contrast, POM greater than 250 µm was related to discharge (Figure 6.10; BAR: $R^2 = 0.60$, $p < 0.05$, $F = 11.68$, $n = 8$; BRO: $R^2 = 0.78$, $p < 0.005$, $F = 22.63$, $n = 7$; OVN: $R^2 = 0.91$, $p < 0.005$, $F = 52.01$, $n = 6$).

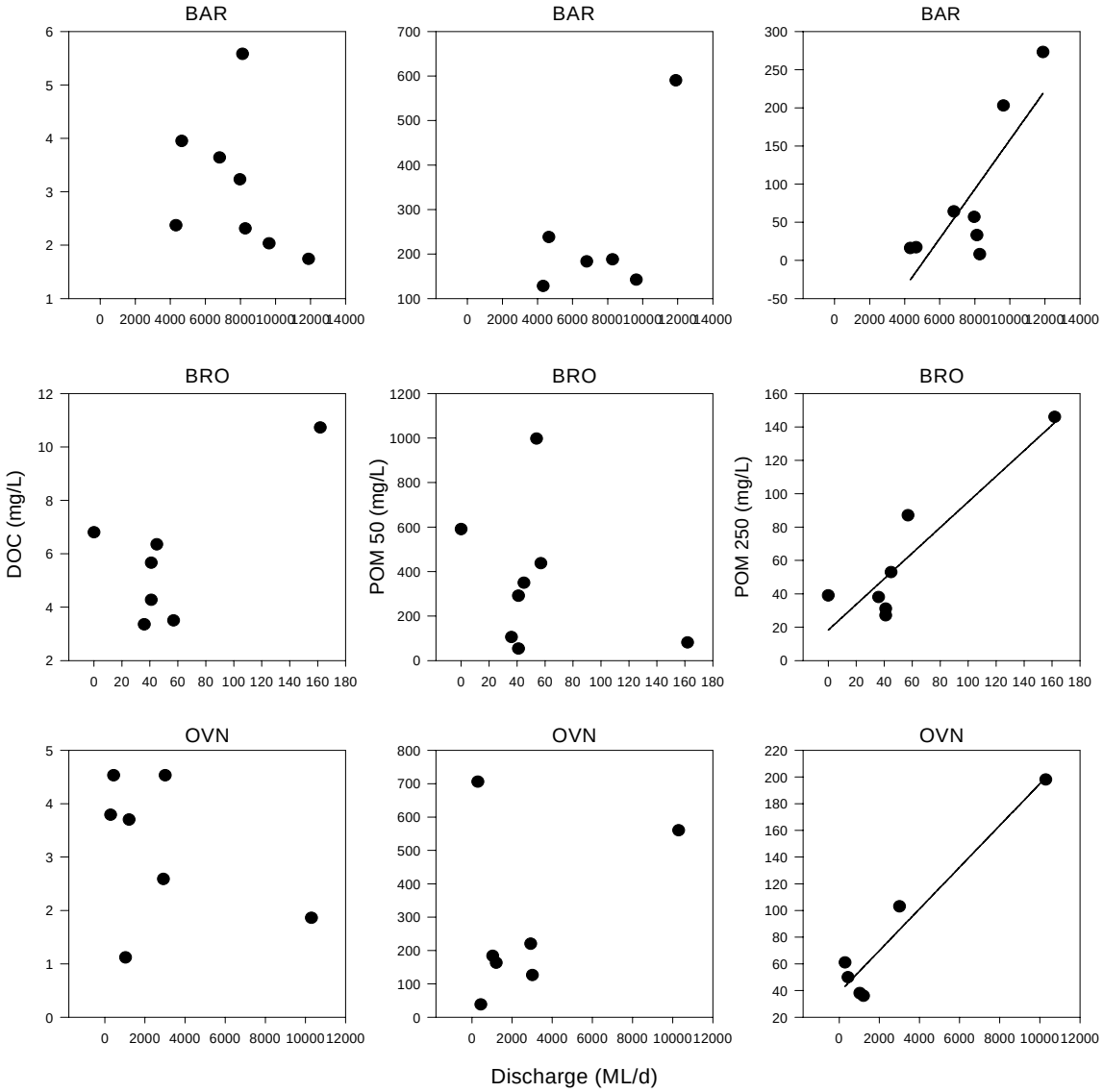

Figure 6.10. Plots of discharge versus three measures of entrained carbon for the three study sites. Left = DOC; Centre = POM > 50 µm; Right = POM > 250 µm.

6.3.3.2 Channel Inundation Modelling

Different discharges will inundate the channel, banks and any macrophyte beds within a given river to different degrees (although this is generally not a linear relationship) and cause changes in the proportions of wetted sediment to water volume. Patterns of change to total macrophyte bed areas inundated with discharges observed during field trips were quite similar at BAR and OVN (Figure 6.11 a), with relatively large discharges required to commence macrophyte inundation (see Chapter 2 for full details of macrophyte inundation modelling). In contrast, substantial areas of macrophytes are inundated even at low flows at BRO, due to the occurrence of submerged species at this site.

Similar patterns of change occurred in relation to wetted sediment area across the sites, with small reductions in flow at BRO causing far greater increases in the wetted sediment to reach volume ratio than at OVN or BAR (Figure 6.11 b). Comparisons of channel inundation characteristics with measures of entrained carbon generally revealed relationships with POM > 250 µm, with higher POM occurring when greater areas of macrophyte bed were inundated, and an inverse relationship for wetted sediment to reach volume ratio (Figures 6.12 and 6.13; BAR MACROPHYTES: $R^2 = 0.80$, $p < 0.005$, $F = 28.69$, $n = 8$; BRO MACROPHYTES: $R^2 = 0.40$, $p < 0.1$, $F = 5.06$, $n = 7$; BAR SEDIMENT: $R^2 = 0.61$, $p < 0.05$, $F = 12.11$, $n = 8$; OVN SEDIMENT: $R^2 = 0.90$, $p < 0.005$, $F = 44.75$, $n = 6$).

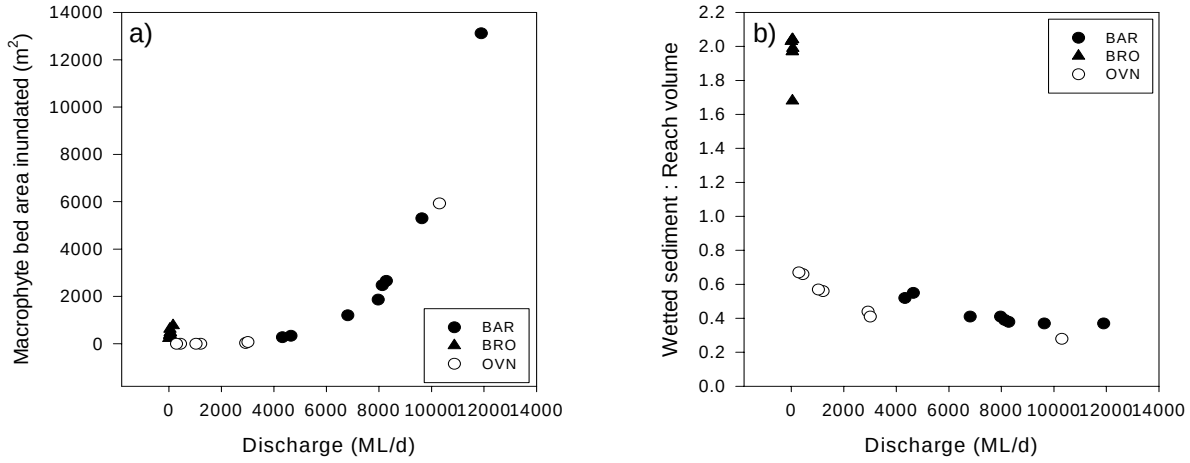

Figure 6.11. Relationship between discharge and channel inundation characteristics at each site: a) macrophyte bed area inundated (m^2), b) wetted sediment to reach volume ratio.

6.3.4 Effects of Carbon on Microbial Functioning

Riverine microbial functioning changed in response to carbon sources commonly found in lowland rivers, as evidenced by altered respiration rates and enzymatic patterns observed under field conditions and during experimental manipulations of carbon inputs.

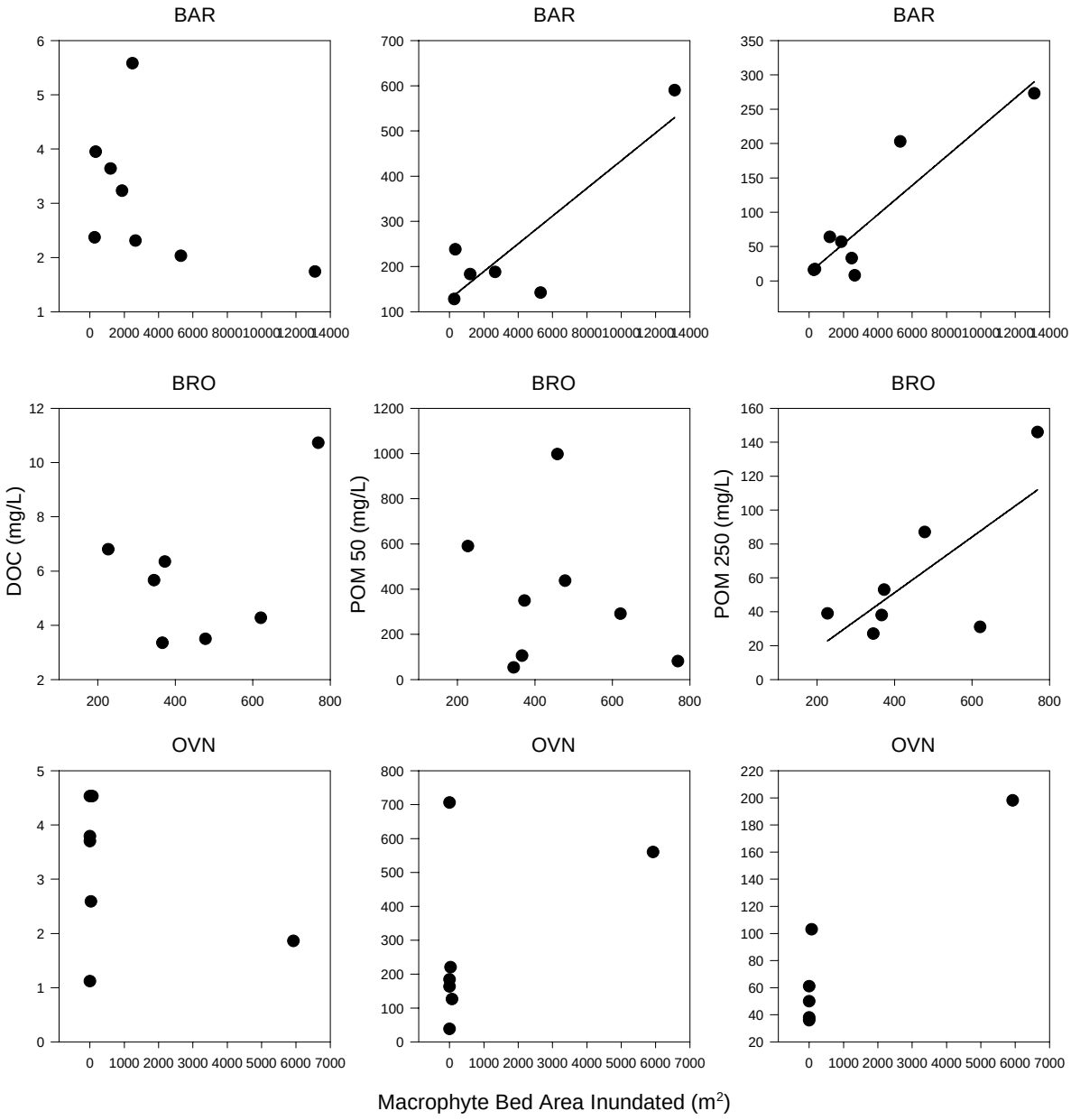

Figure 6.12. Plots of macrophyte inundation (m^2) versus three measures of entrained carbon for the three study sites. Left = DOC; Centre = POM > 50 µm; Right = POM > 250 µm.

6.3.4.1 Enzyme Responses to Macrophyte Bed Inundation

Enzyme data from macrophyte bed samples for all years were pooled because of the lack of significant differences between these groups (Figure 6.14 a; Table 6.7). While some differences between sites were detected based on enzyme data from macrophyte beds (Figure 6.14 b; ANOSIM: OVN different to other sites at $p < 0.05$, Global $R = 0.22$), these were probably driven by differences in the species assessed at each site. Enzyme patterns within macrophyte beds varied depending on species and month (Table 6.7). *Persicaria* samples separated from those taken from *Phragmites*, *Typha* or *Vallisneria* beds ($p < 0.05$), however no significant differences were found between the latter three species (Figure 6.14 c; Table 6.7).

Significant seasonal variation occurred in microbial carbon utilisation within macrophyte beds, with samples collected in August and September different from other months sampled, although not different to each other ($p < 0.01$; Figure 6.14 d, Table 6.7). Interactions between month and species were expected, however the lack of data within each pair-wise comparison (because macrophyte beds were not inundated in every month at every site) prohibited statistical analysis of this interaction.

Seasonal differences in microbial carbon utilisation in macrophyte beds were driven by variation in activities of PEP, NAG and XYL (BIOENV: R = 0.974), with inclusion of α-GLU improving the fit slightly (R = 0.980). Overlays of these enzymes on the MDS in Figure 6.14 demonstrate their influence on separation of data points (Figure 6.15). Peptidase activity was high in most species from December through March, decreasing through winter and spring to return to high levels in summer again (Figure 6.15 a). Peptidase activity in inundated *Persicaria* beds was always low. Xylosidase activity showed the opposite pattern to peptidase (Figure 6.15 c) while NAG and a-GLU provided separation along an axis perpendicular to the PEP-XYL separation (Figure 6.15 b, d).

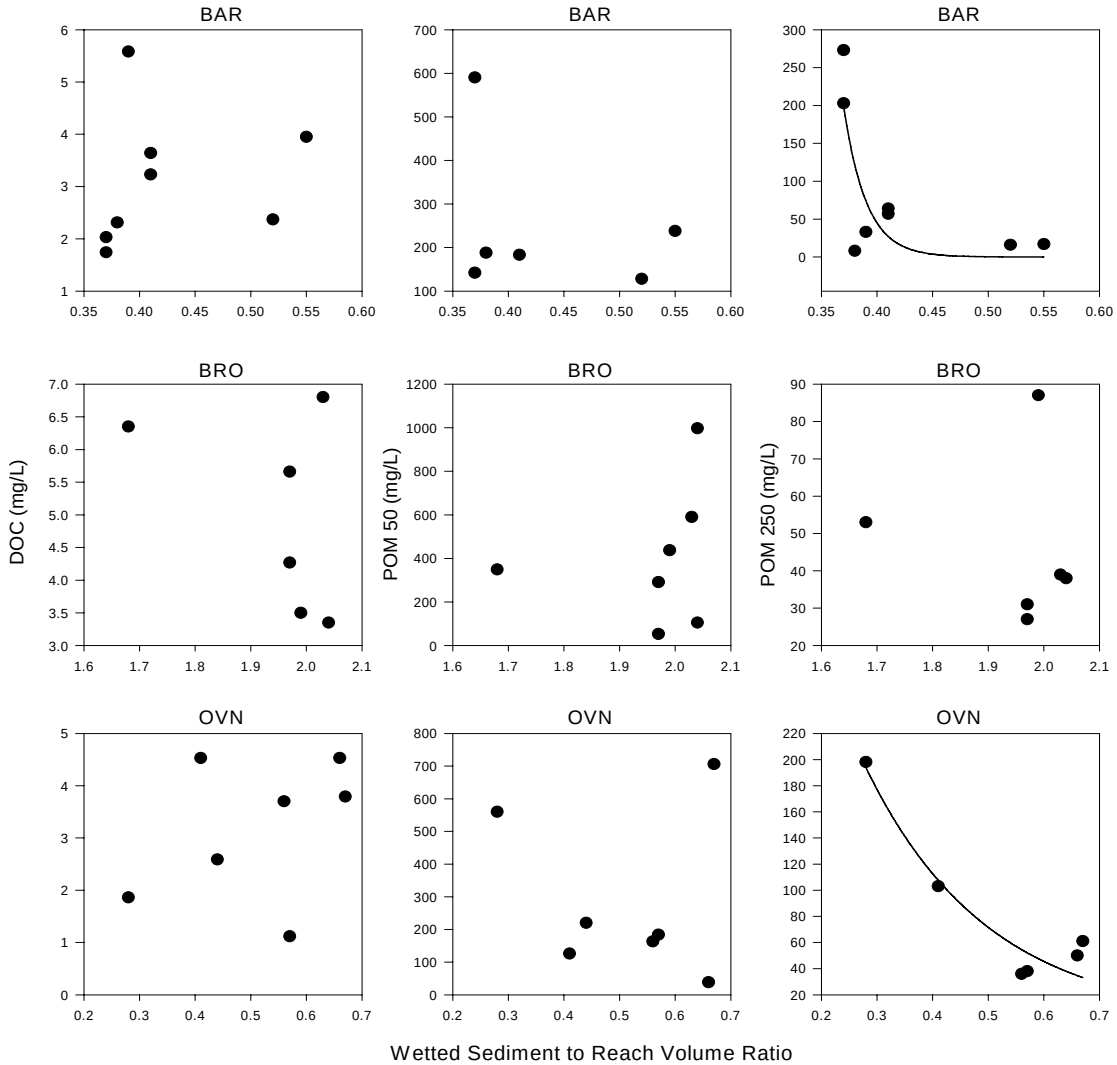

Figure 6.13. Plots of wetted sediment to reach volume ratio verses three measures of entrained carbon at the three study sites. Left = DOC; Centre = POM > 50 µm; Right = POM > 250 µm.

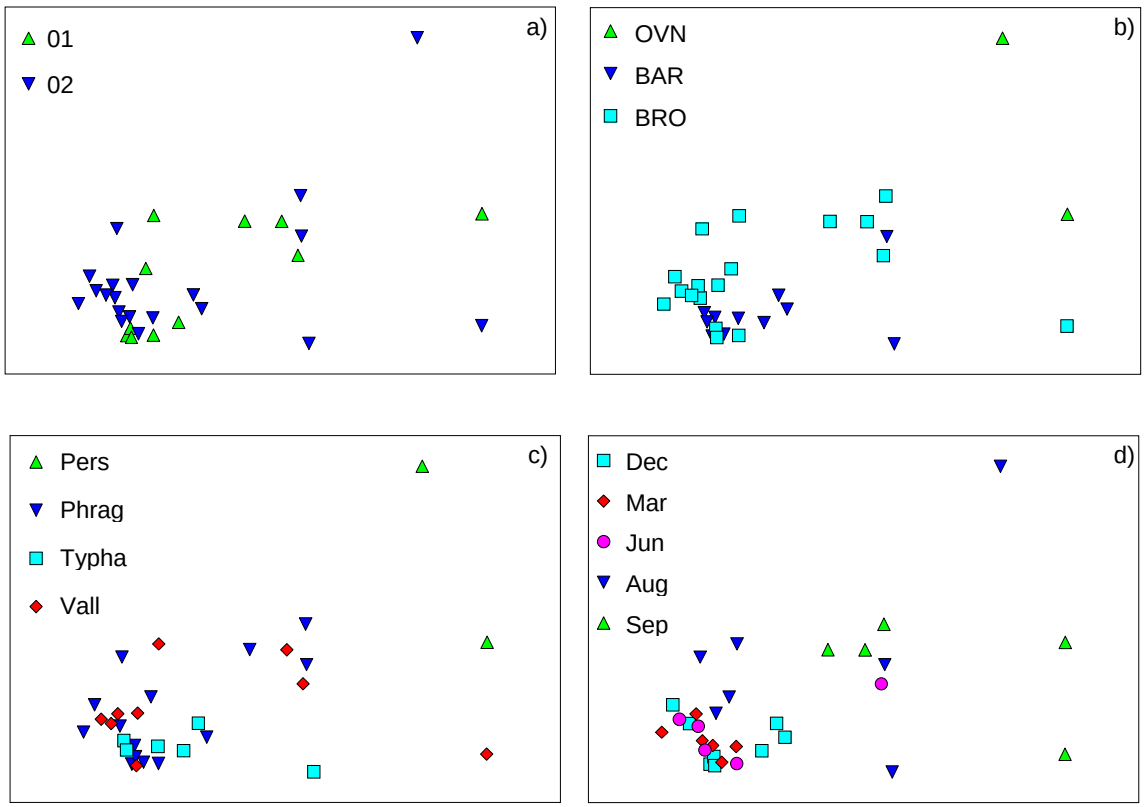

Figure 6.14. MDS ordinations of enzyme activities from macrophyte beds for all sites and sampling dates grouped by a) year, b) site, c) species and d) month. Stress = 0.06.

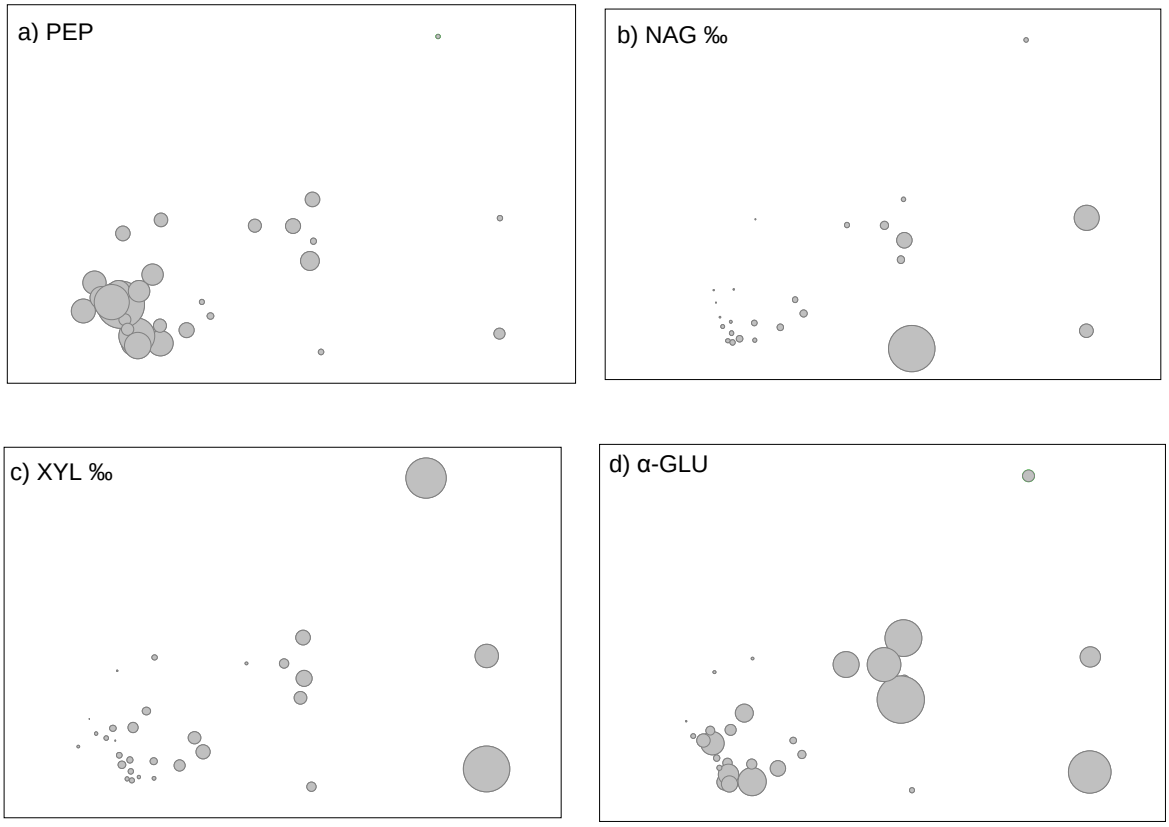

Figure 6.15. Activities of specific enzymes overlaid on the MDS presented in Figure 6.14 showing trends in a) PEP, b) NAG, c) XYL & d) α -GLU driving separation of data points.

Table 6.7. ANOSIM output showing significance of groupings presented in Figure 6.14. Bold text highlights groups which are significantly different at p < 0.05.

Groups	R Stat	Sig Level %
Site – Global Stats	**0.217**	**2.1**
OVN, BAR	**0.961**	**1.3**
OVN, BRO	**0.864**	**0.5**
BAR, BRO	0.025	28.5
Year – Global Stats	0.026	31.0
01, 02	0.026	31.0
Species – Global Stats	**0.137**	**4.9**
Pers, Phrag	**0.953**	**0.8**
Pers, Typha	**0.969**	**3.6**
Pers, Vall	**0.736**	**1.8**
Phrag, Typha	-0.075	65.1
Phrag, Vall	-0.011	48.3
Typha, Vall	-0.033	57.0
Month – Global Stats	**0.394**	**0.1**
Jun, Sep	**0.847**	**0.1**
Jun, Aug	**0.404**	**1.0**
Jun, Dec	-0.012	48.3
Jun, Mar	-0.074	81.8
Sep, Aug	0.110	17.6
Sep, Dec	**0.999**	**0.2**
Sep, Mar	**1.000**	**0.2**
Aug, Dec	**0.517**	**0.4**
Aug, Mar	**0.620**	**0.1**
Dec, Mar	-0.011	41.6

The ratio of peptidase to carbohydrases varied between macrophyte beds of different species, with very low values in *Persicaria* beds, increasing in *Vallisneria* and peaking in the emergent macrophyte species (Figure 6.16). Chitobiose activity (presented as parts-per-thousand of the total of all the enzyme activities assessed) was lowest in *Typha* beds and slightly higher in *Vallisneria* and *Phragmites* beds. However, peak chitobiose activity occurred when *Persicaria* became inundated (Figure 6.16). XYL ‰ activities in inundated macrophyte beds increased from the emergent species, to *Vallisneria*, with maximum values again in *Persicaria* beds (Figure 6.16).

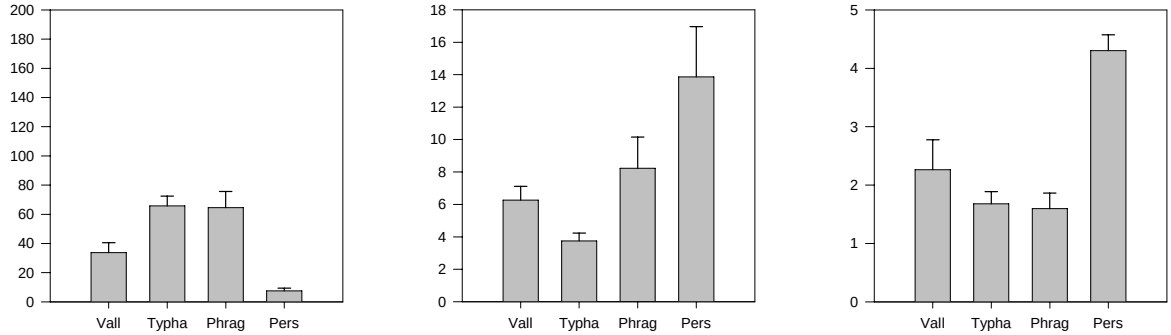

Figure 6.16. Enzyme parameters in different macrophyte beds.

6.3.4.2 Respiration Responses to OM Additions

For all incubations, rates of respiration with additions of OM were 2-10 times background levels (Figure 6.17), indicating that the macrophyte tissues represented highly bio-available carbon sources to the riverine microbial communities. Microbial responses to the macrophyte POM additions were apparent immediately after chambers were sealed and logging commenced (raw data traces not presented). Generally, additions of *Phragmites* tissue produced similar responses at BAR and BRO (2.4 – 6.2 mg O_2/g tissue/d; Figure 6.17). Additions of OM from the other emergent macrophyte under study (*Typha*) induced similar respiration rates as *Phragmites* (2.7 – 7.1 mg O_2/g tissue/d; Figure 6.17). In comparison to the other macrophytes, adding POM from emergent species caused moderate increases in microbial respiration that were independent of time of year. POM from *Vallisneria* generally induced much higher respiration rates than other macrophyte tissues (7.5 – 19.7 mg O_2/g tissue/d), with some variability through the year (Figure 6.17). Large temporal variation occurred in microbial responses to additions of *Persicaria* POM, which ranged from a minimum of 1.4 mg O_2/g tissue/d in August 2001 to 25.1 mg O_2/g tissue/d in December 2001 (Figure 6.17).

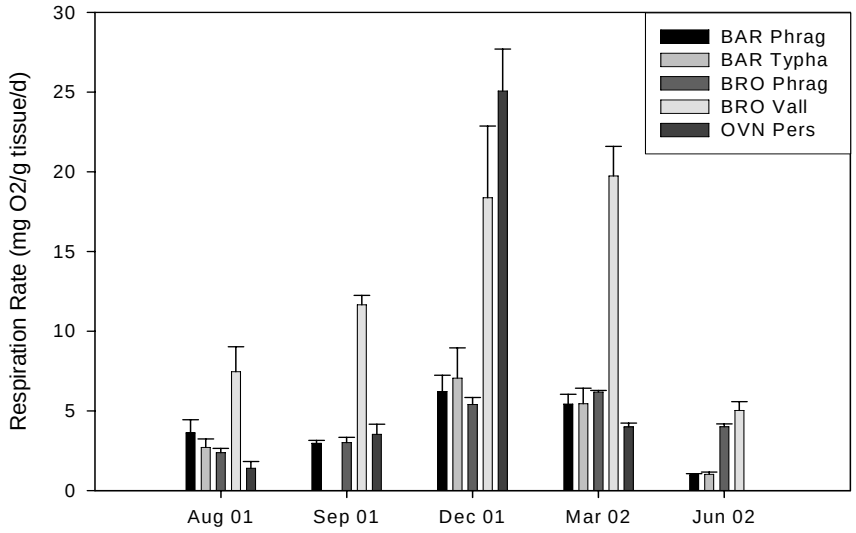

Figure 6.17. Changes to bio-availability of macrophyte POM throughout the growth season (based on microbial respiration responses to additions of POM in *in situ* experiments).

6.3.4.3 Enzyme Responses to OM Additions

Patterns of microbial activity changed in response to experimental manipulation of carbon availability (Figure 6.18; Table 6.8). After 24 hours, enzyme patterns in most treatments had changed significantly from controls, and were also significantly different from each other (ANOSIM: Global R = 0.859, p = 0.001); that is, unique enzyme profiles were produced in response to specific carbon sources. The algal treatment was the most different to the others whereas the two emergent macrophyte treatments (*Phragmites* and *Typha*) were quite similar to each other. When compared to the enzyme profiles generated by OM additions, the initial river water most closely resembled the profile for *Vallisneria*, a submerged macrophyte growing extensively at the collection site (Figure 6.18).

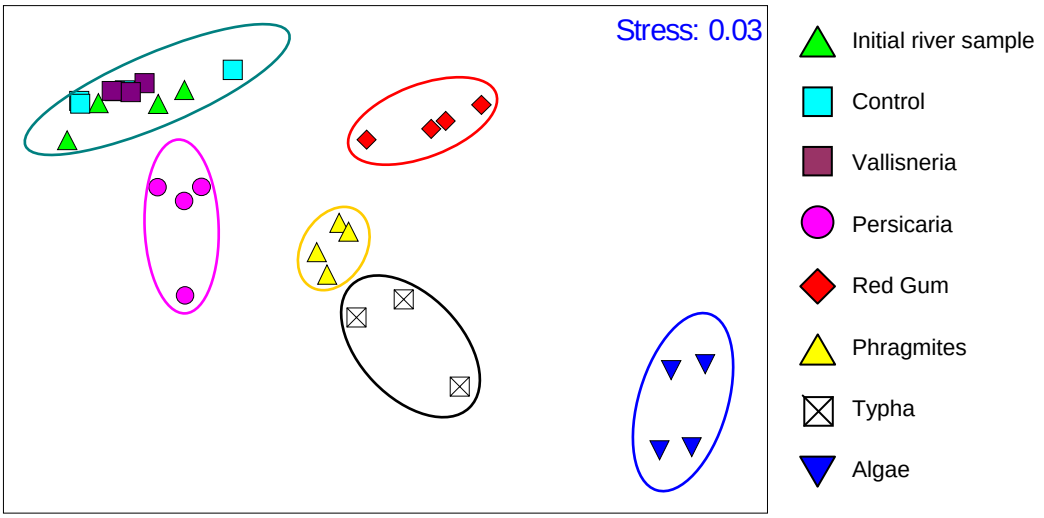

Figure 6.18. MDS ordination of enzyme data from the enzyme experiment. Data points within ellipses represent significant groupings at $p < 0.05$.

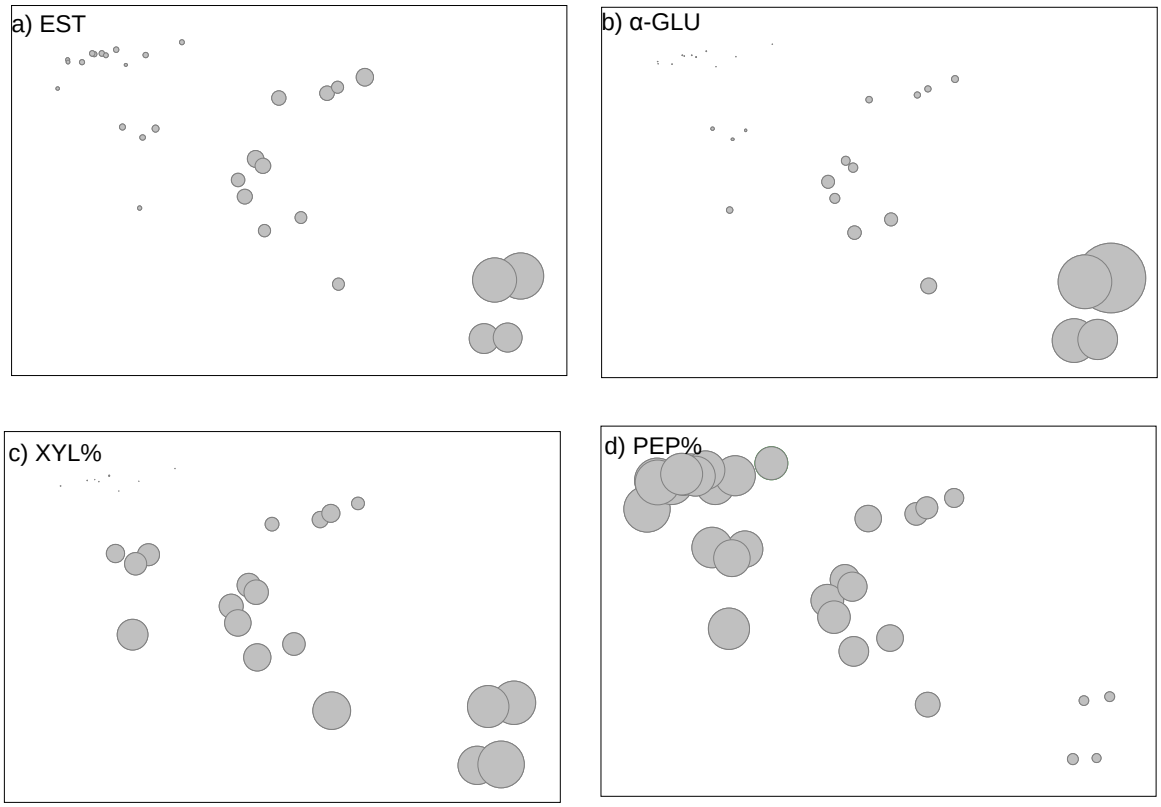

Figure 6.19. Activities of specific enzymes overlaid on the MDS presented in Figure 6.18 showing trends in a) EST, b) α-GLU, c) XYL and d) PEP driving separation of data points.

Drivers of enzyme profile variability induced by the different carbon sources were difficult to determine (BIOENV (PEP, NAG, α-GLU): R = 0.969; BIOENV (EST, β-GLU, XYL) R = 0.970). All enzyme activities were highest in the algae treatment and decreased towards the top left of the MDS, except for peptidase, which showed the opposite trend (Figure 6.19).

Table 6.8. ANOSIM output showing significance of groupings presented in Figure 6.18. Bold text highlights groups which are NOT significantly different at p < 0.05.

Groups	R Stat	Sig Level %
River Init, Alg	1.000	2.9
River Init, Cont	**0.031**	**37.1**
River Init, Gum	1.000	2.9
River Init, Pers	0.896	2.9
River Init, Phrag	1.000	2.9
River Init, Typha	1.000	2.9
River Init, Vall	0.417	2.9
Alg, Cont	1.000	2.9
Alg, Gum	1.000	2.9
Alg, Pers	1.000	2.9
Alg, Phrag	1.000	2.9
Alg, Typha	1.000	2.9
Alg, Vall	1.000	2.9
Cont, Gum	0.979	2.9
Cont, Pers	0.667	2.9
Cont, Phrag	1.000	2.9
Cont, Typha	1.000	2.9
Cont, Vall	**0.156**	**17.1**
Gum, Pers	1.000	2.9
Gum, Phrag	0.979	2.9
Gum, Typha	1.000	2.9
Gum, Vall	1.000	2.9
Pers, Phrag	0.99	2.9
Pers, Typha	1.000	2.9
Pers, Vall	0.854	2.9
Phrag, Typha	0.722	2.9
Phrag, Vall	1.000	2.9
Typha, Vall	1.000	2.9

6.4 Discussion

Flow manipulation is a major river management tool. In order to use this tool effectively, a better understanding is needed of flow-related ecological processes, including microbial community responses to flow. This study aimed to assess riverine microbial responses to different flow conditions, using a combination of field observations and experimental manipulations. It was hypothesised that changes in flow cause changes in organic matter inputs to rivers and that in-stream microbial communities respond to these altered carbon inputs, resulting in an indirect relationship between flow and in-stream microbial activity.

Water column community respiration rate varied with discharge, supporting the proposition of an indirect link between flow and microbial activity. Variation in this relationship in different rivers may represent site-specific responses or a single relationship with highest activity rates at the extremes of discharge (still pools and floods). During very low flows, warm waters with low current speeds and high nutrient levels would provide optimal conditions for heterotrophic microbial activity (Peters et al., 1987; White et al., 1991; Shiah and Ducklow, 1994). As water levels increase these conditions are diluted, so microbial respiration decreases (Leff and Meyer, 1991). Large inputs of carbon and nutrients as dry banks are inundated and during floods again push the system towards heterotrophy (Benner et al., 1995). Caution should be exercised in applying this interpretation to other systems, however, as data from three different rivers were used in the curve's development. Further investigation is required to determine if the relationship holds true within one river, although this may be difficult given that most Australian lowland rivers never experience their full range of natural flow conditions any more due to river regulation.

If the changes in respiration rate associated with flow were due to microbial metabolism of altered OM inputs, one would also expect different patterns of bacterial ecto-enzymes under different flow conditions. This study showed that patterns of microbial carbon use changed under different flow conditions (Figures 6.7 and 6.8), lending support to the hypothesis that flow-induced changes in carbon delivery affect microbial activity. Carbon sources used under steady conditions clearly changed as water levels rose, with similar types of carbon used during floods as on a rising limb. This supports the conjecture that rising water levels inundate previously dry channel areas, providing fresh pulses of highly bio-available (or at least different composition) OM.

Some enzyme parameters can be used as indicators of riverine microbial communities switching between primary OM sources. Under stable flows the PEP:CARB ratio in the main channel was quite high, becoming more similar to values observed in inundated macrophyte beds as water levels rose or fell, or floodplain inundation occurred (compare Figures 6.9 and 6.16).

During rising and falling limbs, NAG values were similar to those in submerged (*Vallisneria*) and inundated emergent macrophyte beds (*Phragmites* and *Typha*), while floods induced similar values as inundated *Persicaria*. Xylosidase activity in all rivers increased as water levels rose and peaked during floods, attaining values similar to those in inundated *Persicaria* beds.

Given that large quantities of DOM are rapidly leached from both live and dead macrophyte tissues (Chapter 5; Mann and Wetzel, 1996), flow variation, which alters the degree of macrophyte bed inundation, will affect carbon inputs. Wetting of soils and sediment is also known to lead to carbon release (Findlay et al., 1998), with bio-availability of sediment-derived compounds dependent upon the composition of soil humus and prior inundation patterns. In addition to altering carbon inputs, the ratio of wetted sediment to reach volume is important because of the effects of sediment microbial processing on whole stream metabolism – when the wetted sediment to reach volume ratio is high, these processes will represent a greater proportion of whole stream metabolism.

Rapid removal of low molecular weight, highly bio-available compounds from DOM (by bacterial degradation, complexing or adsorption) (Godshalk and Wetzel, 1978a) reduces the likelihood of their detection in water column DOC assessments. This may explain the lack of correlation between flow or channel inundation characteristics and DOC content in the present study, and between bacterial production and river DOC in other studies (Findlay et al., 1991; Rees et al., 2005). While high variability precluded the determination of relationships between flow or channel inundation and POM > 50 µm in the present study, changes in flow were found to influence the concentration of POM > 250 µm. No *in situ* measurements have been published of dissolved or particulate organic matter inputs from macrophyte beds under different flows, however Meyer et al. (1998) observed higher DOC (generated from in-channel leaf litter) during increasing discharges than during steady base flows. Modelling described in other chapters of this thesis attempts to estimate these fluxes, however it may be summarised that higher inputs of both POM and DOM would be expected with increasing macrophyte bed inundation, and in particular as water levels rise to inundate previously dry bed areas.

As recognised in a number of aquatic microbial studies (e.g. Godshalk and Wetzel, 1978a; Webster and Benfield, 1986; Sinsabaugh and Findlay, 1995; Wehr et al., 1999; Qiu et al., 2003), the current study demonstrated that riverine microbial functioning was closely linked to carbon dynamics. Different rates and patterns of microbial functioning were observed in response to inputs of different riverine carbon sources, indicating varying degrees of bio-availability between OM types (del Giorgio and Cole, 1998). Organic matter from algae and submerged macrophytes have been shown previously to be more bio-available than emergent macrophytes (Godshalk and Wetzel, 1978a; Linley and Newell, 1984; Findlay et al., 1986;

Findlay et al., 1992; Mann and Wetzel, 1996; Moran and Hodson, 1989). Emergent macrophyte OM is generally more labile than carbon from terrestrial vegetation (Meyer et al., 1987), which can at times even inhibit microbial production (Serrano and Boon, 1991; Wehr et al., 1999). Results from the present study followed this trend – generally *Vallisneria* OM bio-availability was greater than the emergent *Phragmites* and *Typha*, which were more bio-available than the semi-terrestrial low-growing hydrophyte *Persicaria*.

Temporal variability was observed in microbial respiration responses to additions of macrophyte POM. Rather than relating to temperature variation throughout the year (which would presumably not alter the relative bio-availability between species), this may reflect compositional changes of tissue throughout plant growth cycles. Temporal variability in macrophyte detrital decomposition processes may be linked to variable nitrogen and lignin content of plant tissues throughout the growth season (Moran and Hodson, 1989). Absolute rates of macrophyte POM induced microbial respiration were generally higher in summer, when peak live plant biomass occurs, and lowest in winter, particularly for *Persicaria*. Other workers have found differences in plant OM bio-availability based on tissue status (live or dead – Mann and Wetzel, 1996) or timing with respect to plant growth cycles (Findlay et al., 1998).

Analysis of microbial carbon use patterns (enzyme activities) from inundated macrophyte beds supported the POM respiration findings, with major differences between enzyme patterns driven by plant species inundated and month. Attempts have been made previously to link enzyme patterns observed in the field to specific carbon sources. Links between protease activity and algal production (Scholz and Boon, 1993; Talbot and Bianchi, 1997), possibly related to mucilaginous algal secretions (Smith et al., 1995), have resulted in some workers suggesting that high protease activity is an indicator of microbial processing of algal-generated carbon (Boschker and Cappenberg, 1998). α-glucosidase and β-glucosidase are associated with the breakdown of starch and cellulose, respectively, and are generally associated with decomposition of higher plant OM (Sinsabaugh and Findlay, 1995). In field studies, the activity of β-glucosidase was not affected by the presence (Scholz and Boon, 1993) or productivity (Chrost, 1992) of algae, although high rates were observed during breakdown of an algal bloom (Chrost, 1992). OM from plants with secondary thickening might be expected to induce xylosidase activity, which acts in the breakdown of xylan. High xylosidase activities have been reported in mesocosms amended with terrestrial vegetation detritus (Wehr et al., 1999). Patterns of enzyme activity observed in inundated macrophyte beds in the current study were similar to those described above. Higher xylosidase activity occurred in inundated beds of *Persicaria*, which is more similar to terrestrial vegetation than the other species. Peptidase and glucosidase activities were lower in *Persicaria* compared to the other macrophytes and EST was highest in *Vallisneria*.

Laboratory experiments were carried out to determine if specific OM sources induced characteristic enzyme activity profiles, which might be used to determine OM sources in use by riverine microbes in the field at a given time. Experimental carbon manipulations induced rapid changes to enzyme patterns (< 24 hrs), linked to compositional differences between the OM treatments (Findlay et al., 1998). Unique enzyme profiles were produced by the riverine microbes in response to additions of POM from specific sources, however these enzyme patterns differed from those observed under field conditions or described by other workers. All enzyme activities except PEP were highest in algal OM treatments. The highly bio-available nature of algal exudates (Bell et al., 1983) explains the high EST activity induced by algal leachates. Given the pre-treatment required to disrupt algal cells enough to obtain leachate for the experiment, it is not unreasonable that α -GLU and β -GLU activities were also high in algal treatments. While XYL activity was also high in algal treatments, its activity as a proportion of total enzyme activity was similar in nearly all treatments. This may be interpreted as xylan being present in all samples, but its low bio-availability inducing microbes to preferentially use other, more readily-degradable compounds first. In algal treatments, the compounds preferentially degraded (of those assayed) were carbohydrates – over 20% of total enzyme activity assessed was α - and β -GLU in algal treatments whereas in other treatments, activity rates of these enzymes were all below 6%. In most of the higher plant treatments, proteins represented the bio-available alternative to xylan, with PEP activity representing 45-80% of total enzyme activity after 24 hours of incubation. Given that all of the plant leachates contained proteins (see Chapter 5), the enzyme profiles after 24 hours may simply reflect a rapid pulse of highly labile proteinaceous DOM being used by microbes. Thereafter, the enzyme signature for these samples could be expected to switch to that reported in the literature and apparent in the field, of higher XYL and carbohydrase activities. High initial activities (12 hr) of protease in macrophyte OM treatments and carbohydrases in algal treatments have been observed in other carbon addition experiments (Wehr et al., 1999).

The lack of well replicated and controlled experiments on microbial respiration responses to additions of dissolved organic matter from riverine carbon sources presents a major gap in this work. While the POM addition experiments were reasonably comprehensive, direct comparison of the bio-availability of different macrophyte tissues obtained from these experiments is difficult because of differences in incubation temperatures and initial microbial community compositions. Also, the POM experiments were not able to isolate microbial carbon uptake and utilisation functions from processes relating to leaching of DOM from POM which might confound results (e.g. if DOM uptake by microbes was limited by leaching rate).

Understanding the detailed processes involved in microbial utilisation of compounds leached from macrophyte tissues thus remains a topic requiring further study, with possible questions regarding:

- the role of microbes already on plant tissues vs. in the water column;
- the effects of temporal variation in the release of compounds from plant tissues on leachate bio-availability after different periods/cycles of inundation;
- microbial feedback – microbes act on tissues to release different compounds.

Despite these limitations, flow-induced carbon variation effects on riverine microbes appears to be a real phenomenon, with the following summary of effects observed in the rivers under study. During steady flows, riverine microbes appeared to be utilising mainly carbon from planktonic sources, with a switch to higher plant carbon during a flood or when the water level changes. At this time the enzyme signal was very similar to that observed within macrophyte beds, where a considerable dependency on higher plant carbon would be expected. Changes in xylosidase activity indicated that flooding, in particular, appeared to cause inputs of OM from more woody terrestrial species which are more similar to *Persicaria* than other macrophytes assessed. Chitobioase activity during floods was also more similar to activities observed in inundated *Persicaria* beds than the other species, possibly due to inundation of terrestrial insects which may be more prevalent in the less frequently inundated mudflat hydrophyte or the triggering of macro-invertebrate emergence.

6.5 Conclusion

This chapter described the response of in-stream microbial communities at three sites in the Murray Darling Basin to different flow conditions (steady, falling, rising and flood). Both general activity (determined by dark respiration rates) and patterns of carbon utilisation (inferred from enzyme analysis) changed in response to different flow conditions, coincident with altered OM inputs. Patterns of microbial carbon use were shown to be specific to the carbon source which induced them. While further work is required to tease out temporal variation in enzyme profiles, they represent a potentially useful bio-assay for assessing *in-situ* utilisation of specific carbon sources by riverine microbes. This study shows that flow manipulation could be used by managers to affect inputs of OM from different sources and thus achieve goals with respect to microbial functioning. In particular, if vegetation is present within the channel, similar responses to those observed during floods may be obtained by relatively small-scale within-channel water level manipulations.

Chapter 7. Modelling microbial utilisation of macrophyte OM inputs under different flow conditions.

7.1 Introduction

The timing and composition of inputs of organic matter to lowland rivers are important as allochthonous organic matter can play a major role in lowland river function (Robertson et al., 1999). In Australia, factors affecting OM inputs have been immensely altered by river regulation and landscape management practices since European settlement.

The majority of Australian lowland rivers are highly regulated to supply water for irrigation, achieved through the storage and release of water from reservoirs. In many instances, flow release patterns are very different from those expected under natural conditions (e.g. under regulation, high flows occur in summer when rivers would have traditionally been at base flow or dried to a series of pools, and low flows occur in winter/spring when high flows would have been expected due to rainfall and snow-melt inputs). Other management practices have reduced riparian vegetation and macrophytes, removed large woody debris and reduced interactions between rivers and floodplains, altering the composition and timing of inputs of organic matter to our river systems.

Numerous studies of large lowland rivers overseas have found heterotrophic conditions, with associated high production levels by riverine bacteria (e.g. Findlay et al., 1998). In contrast, in-stream microbial production appears to be carbon-limited in many Australian rivers, resulting in conditions of P>R in many instances. This carbon limitation may be linked to the changes in reduced carbon loading described above.

Macrophytes represent potentially important sources of carbon for in-stream microbial production. Dissolved organic matter leached from macrophytes is thought to be highly bio-available and can be a major component of overall carbon loading to the system, even in rivers where the ratio of plant biomass to discharge is small (Findlay and Sinsabaugh, 1999;Gawne et al., 2002). OM inputs would occur through leaching of standing material or inputs of litter

during bed inundation, with some direct drop of litter into the water column also possible. Little work has been done to assess these or microbial processing of them. Species/growth form and seasonality will affect the type and status (degree of senescence) of tissue present and available for input at any time. Input will be affected by wind, distance to water and flow.

Microbial responses to variations in OM supply of importance to ecosystem functioning include oxygen consumption (potential for "black-water" events), competition with algae for inorganic nutrients (possible attenuation of algal blooms), food supply to higher trophic levels and the provision of inorganic carbon to the water column for autotroph production. As well as being important for improving our understanding of these interactions, knowledge about microbial functioning is critical for predicting system responses to management interventions.

This chapter brings together data from all preceding chapters into a single model of microbial responses to inputs of macrophyte organic matter under different flows, and ultimately highlights the importance of macrophyte-microbial interactions to ecosystem level functioning.

7.2 Methods

The modelling approach used in this chapter was based on the conceptual models of macrophyte OM inputs to rivers developed in Chapter 3 (Figures 3.22 – 3.24). These conceptual models propose that the majority of OM inputs occur due to macrophyte bed inundation, with only small quantities of OM entering the water column as direct litter drop when beds are exposed. Inundation of macrophyte beds causes entrainment of litter (POM) and leaching of both standing shoots and litter (DOM). In order to develop a predictive, quantitative model of these inputs, the following input parameters were required:

- macrophyte bed areas in a particular river reach (mapping)
- live and dead shoot densities throughout the year
- litter drop and accumulation rates (and mean dry masses of different litter components)
- bed area inundated for a given discharge
- depth of bed inundation for a given discharge (and hence lengths and dry weights of shoots inundated using shoot length to dry weight conversion factors)
- tissue carbon and nutrient contents
- rates of leaching of DOM from different plant tissue types (and C, N and P content of leachates)
- riverine microbial responses to various carbon inputs and water temperature

Model development in this chapter brings together the data presented in earlier chapters of this thesis. Data collection for each of the parameters listed above has been described in detail throughout this thesis, however each will be outlined briefly below.

7.2.1 Input Parameters

7.2.1.1 Mapping

As part of a larger project, three-dimensional mapping of the river channel and part of the floodplain was performed at each study site (Chapter 2). Locations of macrophyte beds and their vertical distribution within the channel were described and total bed areas for each species were determined at each site (m^2).

7.2.1.2 Shoot densities

Changes to the relative proportions of live and dead shoot densities throughout the year were determined from shoot counts in permanent field plots at each site (Chapter 4). Equations were developed to describe changes to shoot density (number of shoots/m^2) over time (Chapter 4). Data on the composition and biomass of live and dead shoots (Chapter 3) enabled conversion of density data to standing biomass (g/m^2).

7.2.1.3 Litter production

Changes to shoot composition over time were used to determine litter production by each species (Chapter 4). Again, curve-fitting produced equations describing the litter-fall patterns observed. Data on mean masses of individual biomass units (Chapter 3) allowed conversion of litter estimates (e.g. number of dead leaves/m^2) to mass per unit area (g/m^2).

7.2.1.4 Inundation modelling

Three-dimensional channel models from the river mapping were incorporated into a GIS for each site and a range of flow scenarios were simulated to determine water depths overlying macrophyte beds for a range of discharges (Chapter 2). Using shoot length to dry weight conversions obtained from biomass partitioning (Chapter 3), water depths were converted to a length, and hence mass (g), of macrophyte tissue inundated.

7.2.1.5 Tissue nutrient content

Data used for the OM input model were percent carbon, nitrogen and phosphorus content of those shoot components contributing to POM inputs (litter) for each species (Chapter 3).

7.2.1.6 Leaching

Rates and composition of DOM leached from each biomass component of each species were determined from laboratory experiments (Chapter 5). Curves were fitted to leaching rate data to predict DOM release due to macrophyte inundation. Leachate composition was described using nutrient content data and a broad assessment of the carbon compound types present.

7.2.1.7 Microbial responses

Substrate-induced respiration responses of riverine microbes were assessed in the field (Chapter 6) (mg O_2/g POM/d). Respiration rates were plotted against water temperature for each species and exponential curves were fitted (all $R^2 > 0.44$, $p < 0.2$) (Figure 7.1). Respiration coefficients were applied to modelled POM inputs (Chapter 4) to estimate initial microbial respiration induced by additions of fresh macrophyte OM under a range of flow scenarios ("rapid" rate). The slower microbial metabolism of litter which had been previously inundated was estimated by applying literature measurements of macrophyte POM half-life periods to accumulated litter which had been previously inundated ("slow" rate) (as per Pereira et al., 1994; Asaeda et al., 2000). Generally, exponential decay curves have been reported for macrophyte litter mass loss over time (e.g. Parnas, 1975; Webster and Benfield, 1986; Boulton and Boon, 1991), however these were simplified in the current modelling to a constant rate which would explain 100% of litter mass loss over the time periods specified in the literature for different species (typically 3 – 6 months) (e.g. Madsen and Adams, 1988). Oxygen consumption data were converted to carbon units using a respiration quotient of one. Bacterial production was estimated from respiration data using bacterial growth efficiencies (BGE) determined from the C:N ratio of the POM inputs (Figure 7.2 – logarithmic relationship between substrate bioavailability (C:N ratio) and BGE ($R^2 = 0.95$, $p < 0.0001$, $F = 118.54$, $n = 7$)) (Goldman et al., 1987; Blum and Mills, 1991; del Giorgio and Cole, 1998; Lennon and Pfaff, 2005; Buesing and Gessner, 2006).

Table 7.1 Temperature-response curves: y=a*exp(b*x)

Site	Species	a	b	R2	p	F	n
BAR	*Typha*	0.5882	0.1122	0.73	<0.1	9.04	4
BAR	*Phragmites*	0.9126	0.0883	0.68	<0.1	9.47	5
BRO	*Phragmites*	1.4609	0.0653	0.44	<0.2	3.36	4
BAR & BRO	*Phragmites*	1.1346	0.0777	0.65	<0.01	16.16	9
BRO	*Vallisneria*	4.9424	0.0651	0.58	<0.2	5.09	4
OVN	*Persicaria*	0.4250	0.1994	0.98	<0.01	124.54	4

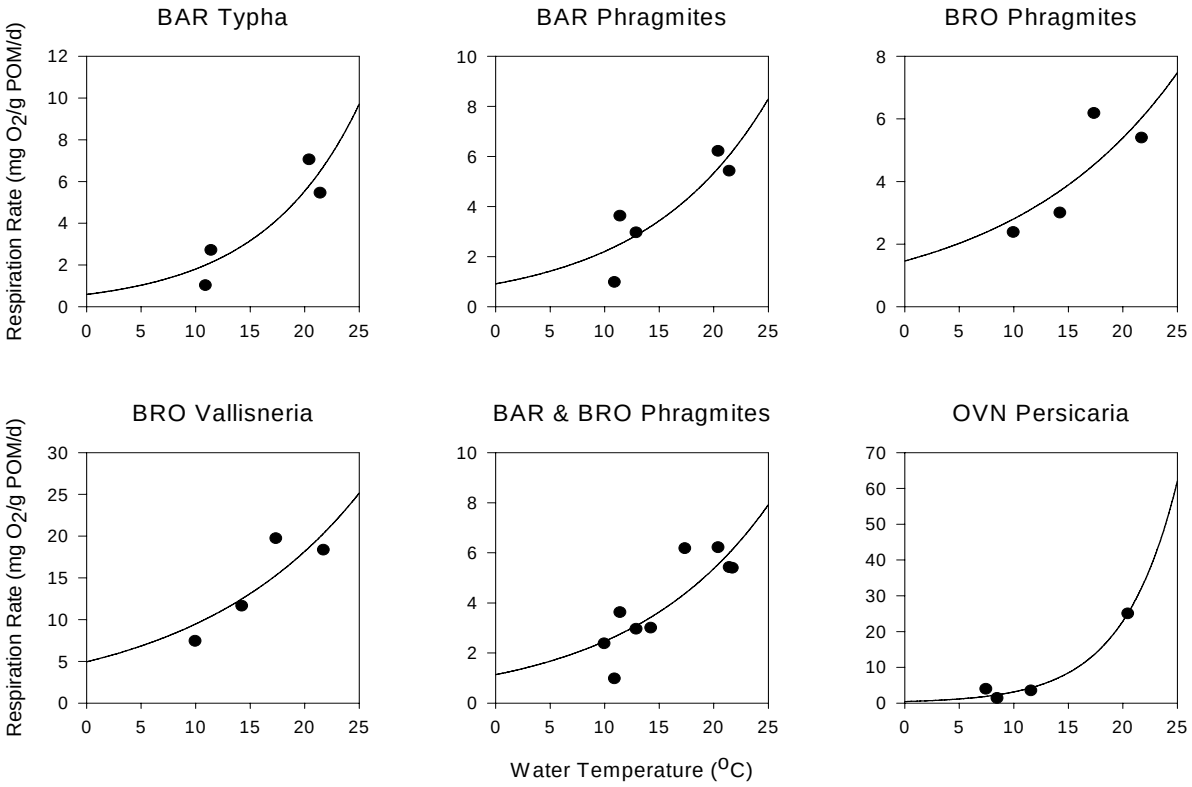

Figure 7.1. Changes to substrate-induced respiration rate with temperature (temperature response curves). Points are means of three replicates, lines are the fitted functions.

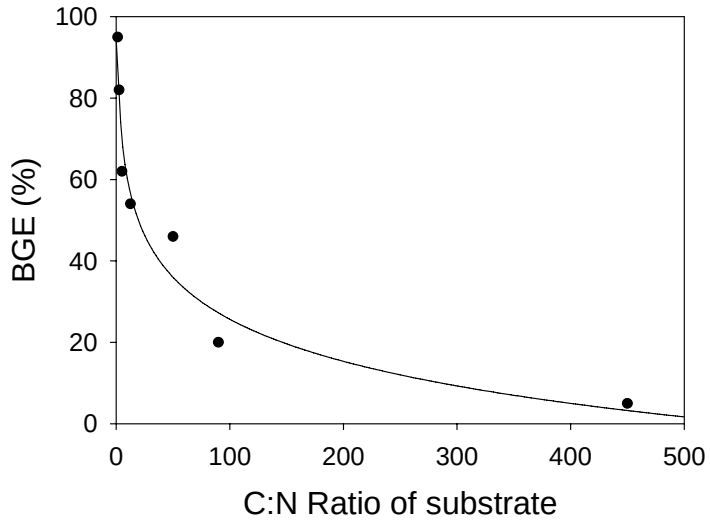

Figure 7.2. Changes to bacterial growth efficiency with C:N ratio of macrophyte POM. Data points extracted from literature (see text). Line is the fitted function.

7.2.2 Model Construction

As outlined in previous chapters, Sigmaplot 8.0 for Windows was used for curve-fitting to generate equations describing several of the parameters above. The final model of macrophyte OM inputs was constructed in MS Excel using VisualBasic.

7.3 Results

7.3.1 Macrophyte OM Input Modelling

Three equations were developed to describe POM inputs (litter) from inundated macrophyte beds, DOM inputs from inundated litter and DOM inputs from inundated standing shoots:

mg POC from litter = $\sum_{e}^{i=s}(L_i \cdot A \cdot K_p \cdot C_p)$ **[Eqn 1]**

mg DOC from litter = $\sum_{e}^{i=s}(L_i \cdot A \cdot K_p \cdot R_p)$ **[Eqn 2]**

mg DOC from shoots = $\sum_{e}^{i=s}[(G_i \cdot A \cdot W_i \cdot N_g \cdot R_g) + (D_i \cdot A \cdot W_i \cdot N_d \cdot R_d)]$ **[Eqn 3]**

Where;

i = Year Day; s = Start day of period of interest; e = End day of period of interest

L_i = rate of litter accumulation on day *i* (quantity of *p* / m^2 bed / d) (Chapter 4)

A = area of macrophyte beds (m^2 / km) (Chatper 2)

K_p = average dry weight of tissue type *p* (g DW / unit *p*) (Chapter 3)

C_p = carbon content of tissue type *p* (mg/g) (Chapter 3)

R_p = leaching rate of tissue type *p* (mg DOC / g DW plant tissue / d) (Chapter 5)

p = tissue type (e.g. dead *Typha* blades) (Chapter 3)

G_i = live shoot density on day *i* (# shoots / m^2 bed) (Chapter 4)

D_i = dead shoot density on day *i* (# shoots / m^2 bed) (Chapter 4)

W_i = water depth on day *i* (m) (Chapter 2)

N_p = shoot length to DW conversion for tissue type *p* (g DW / lineal m of shoot) (Chapter 3)

Inputs were expressed in nitrogen and phosphorus units using conversion factors generated from tissue and leachate nutrient ratios (Chapters 3 and 5).

7.3.2 Microbial Response Modelling

Riverine microbial respiration induced by additions of macrophyte organic matter was estimated using the following equation:

O_i = $(a_p \cdot e^{(b_p T_i)} \cdot P_i)/(v_i \cdot z)$ **[Eqn 4]**

Where;

i = Year Day

O_i = rate of oxygen consumption on day *i* (mg O_2/L/d)

a_p = temperature-response curve maximum coefficient for tissue type *p*

b_p = temperature-response curve rate coefficient for tissue type *p*

T_i = water temperature on day *i* (^{o} C)

P_i = POM inputs on day *i* (g)

v_i = reach volume on day *i* (ML)

z = volume conversion factor of 1,000,000

Current daily water temperature data were obtained for the three sites from the Department of Natural Resources and Environment (NSW) and the Department of Sustainability and Environment (VIC) and used for all scenarios due to a lack of historic monitoring. Water temperature data used for each of the sites is shown in Figure 7.3.

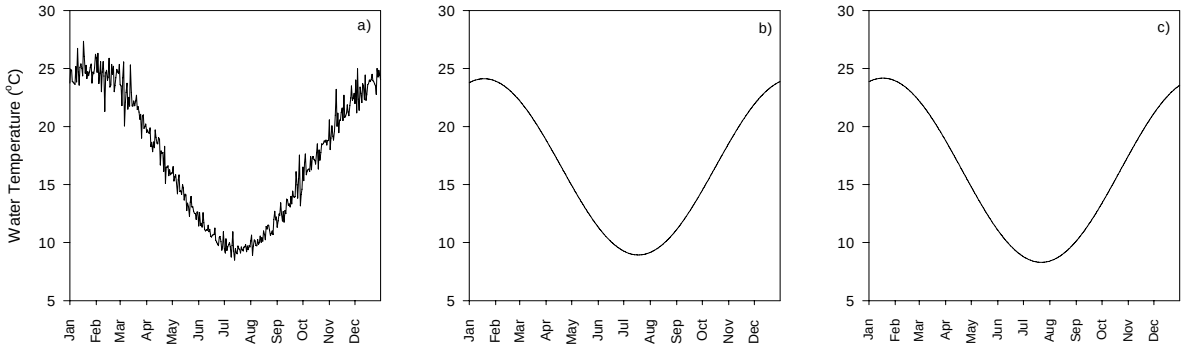

Figure 7.3. Water temperature data used in modelling microbial metabolism of macrophyte OM inputs – a) BAR, b) BRO, c) OVN

Respiration rates were converted to carbon units using a respiration quotient of one:

$$\mathbf{BR}_i = O_i / 32 \times 12 \qquad \textbf{[Eqn 5]}$$

Where;

i = Year Day

BR_i = rate of bacterial respiration on day *i* (mg C/L/d)

Bacterial production (BP) was calculated from respiration rates, with partitioning of carbon metabolism into respiration and biomass incorporation using bacterial growth efficiencies (BGE) based on the C:N ratio of the substrate (Figure 7.2).

$$\mathbf{BP_i} = BR_i / (1 - BGE_i) \cdot BGE_i \qquad \textbf{[Eqn 6]}$$

$$\mathbf{BGE_i} = c \cdot \ln^{(M_i)} + d \qquad \textbf{[Eqn 7]}$$

Where;

i = Year Day

BP_i = bacterial biomass production on day *i* (mg C/L/d)

BGE_i = bacterial growth efficiency for day *i* (%)

c = substrate-bioavailability-adjusted BGE rate coefficient = -14.908

M_i = C:N ratio of POM inundated on day *i* (litter and standing shoots)

d = substrate-bioavailability-adjusted BGE maximum = 94.34

Bacterial production was converted to nitrogen and phosphorus units using C:N:P mass ratio of bacterial cells of 9:2:1 (calculated from Goldman et al., 1987).

7.3.3 Model Compilation

These equations were compiled into Visual Basic code in Excel. A graphical user interface was developed for manipulating initial parameter values (Figure 7.4).

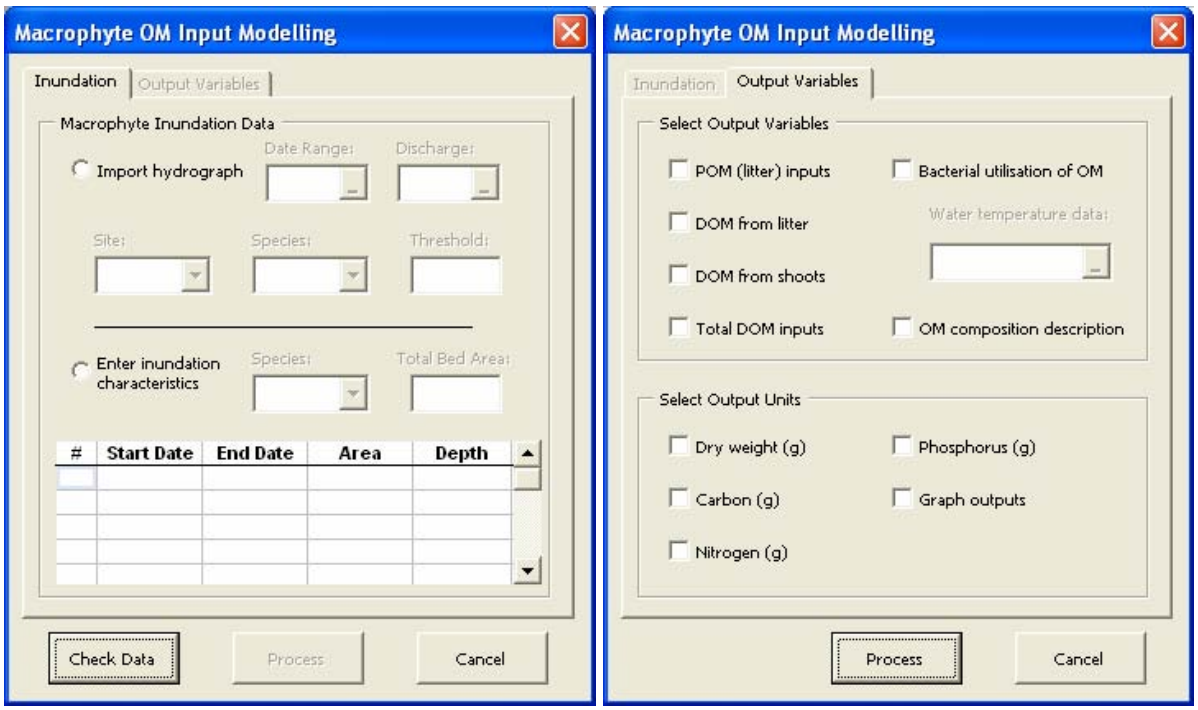

Figure 7.4. Screen shots of the graphical user interface developed for the macrophyte OM model.

7.3.4 Model Outputs – Microbial Metabolism

All scenario modelling in this chapter involved the application of hypothetical flow regimes (Chapter 2) to current channel morphologies and macrophyte distributions. Under sustained flows of one type, these parameters could be expected to change (e.g. recurring flashy floods could scour out the channel or extended droughts could restrict macrophyte bed areas). Also, modelling did not incorporate alterations to annual water temperature patterns under different flows, due to the unavailability of this data for the scenarios being modelled. It might be expected that warmer water temperatures would occur during droughts and possibly lower temperatures during flood years with increased snow melt inputs and larger reach volumes. Variation from the annual water temperature patterns used for modelling would have a major effect on the microbial metabolism predictions made in this chapter, especially for those plant tissues which had low bio-availability, where the effect of temperature on microbial metabolism became relatively more important (similar phenomenon reported by Felip et al., 1996).

7.3.4.1 Typha

Under current flow conditions, inputs of DOM from *Typha* at BAR (annual input of 8.0 kg C) were much lower than under pre-regulation flows (annual input of 30 kg C) and peaked in summer rather than winter/spring (Figure 7.5 b, d; Table 7.2). Similar levels of bacterial metabolism occurred during summer under these two scenarios (means of 18.5 and 11.2 µg C respired/L/d for current and historic scenarios, respectively), however bacterial production and respiration were much higher during winter historically (mean of 7.4 µg C respired/L/d compared to 0.7 under current flows) (Figure 7.5 b, d).

Under the drought and flood scenarios, peak DOM inputs occurred in winter/spring, although these were small during droughts (maximum of 117 g/L/d) compared to floods (406 g/L/d) (Figure 7.5 f, h; Table 7.2). Overall, bacterial metabolism based on macrophyte carbon was very low under the drought scenario (annual biomass production of 0.4 mg C/L). Although DOM inputs during summer under the flood scenario were only 2 – 3 times those under the current and historical flow scenarios, high water temperatures at this time of year resulted in very high bacterial metabolism, the vast bulk of which was respired (4.7 mg/L annually). Respiration rates during summer in flood years were 1.5 to 9 times higher than the other scenarios. Bacterial respiration and production levels during winter in flood years (6.4 and 1.6 µg C/L/d, respectively) were more similar to those under pre-regulation flows and droughts (4.7 – 7.4 and 1.1 – 1.8 µg C/L/d); than under current flows (0.7 and 0.2 µg C/L/d). Some macrophyte-OM driven microbial metabolism also occurred through autumn during flood years (10.5 µg C respired/L/d compared to 0 – 3.0 µg C/L/d under other scenarios) (Figure 7.5 h).

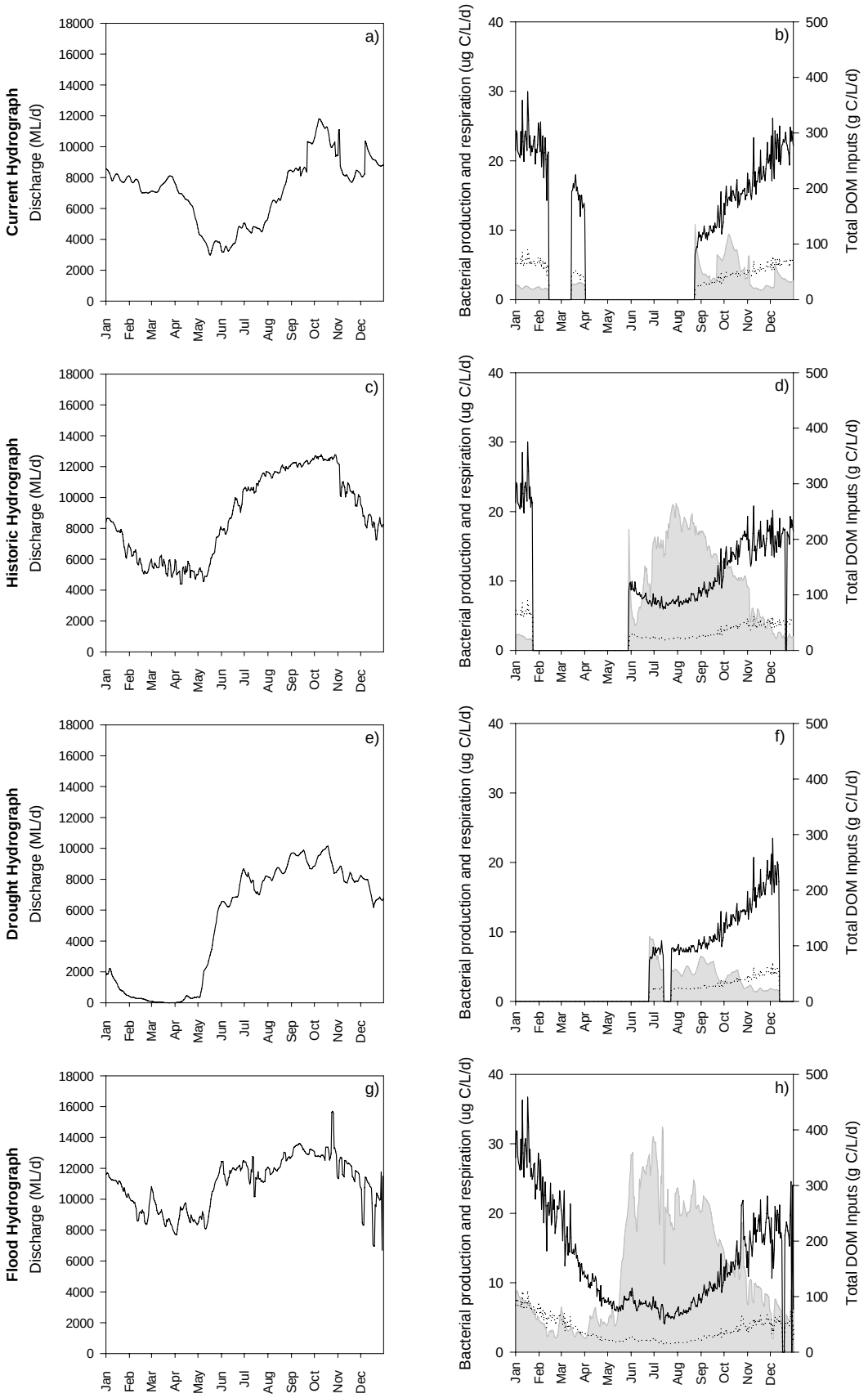

Figure 7.5. Modelling of microbial responses to inputs of *Typha* OM at BAR under different flow scenarios. In microbial response plots, dashed line indicates bacterial production, solid line indicates bacterial respiration and grey shading indicates DOM loading.

Table 7.2 Modelled DOM inputs and microbial response parameters under different flow scenarios for *Typha* at BAR

	Scenario			
Parameter	**Current**	**Historic**	**Drought**	**Flood**
DOM Inputs				
Mean*	22	82	21	148
Max*	135	264	117	406
Annual**	8.0	30	7.8	54
Respiration				
Mean#	9.1	8.0	4.9	13
Max#	30	30	23	37
Annual##	3.3	2.9	1.8	4.7
Production				
Mean#	2.2	1.9	1.2	3.1
Max#	7.2	7.2	5.6	8.9
Annual##	0.8	0.7	0.4	1.1

* g C/L/d ** kg C/L
# µg C/L/d ## mg C/L

Table 7.3 Modelled DOM inputs and microbial response parameters under different flow scenarios for *Phragmites* at BAR

	Scenario			
Parameter	**Current**	**Historic**	**Drought**	**Flood**
DOM Inputs				
Mean*	3.7	16	2.7	35
Max*	163	59	76	142
Annual**	1.4	5.9	1.0	13
Respiration				
Mean#	4.3	6.9	2.3	11
Max#	51	26	32	28
Annual##	1.6	2.5	0.9	4.0
Production				
Mean#	2.2	3.3	1.3	5.2
Max#	27	13	16	14
Annual##	0.8	1.2	0.5	1.9

* g C/L/d ** kg C/L
# µg C/L/d ## mg C/L

7.3.4.2 Phragmites

For all sites and scenarios, a higher proportion of the *Phragmites* organic matter metabolised by bacteria was incorporated into biomass than for *Typha* (mean BGE of 33% and 20%, respectively). While DOM loadings from *Typha* at BAR (7.8 – 54 kg C/L/yr) were greater than those from *Phragmites* at BAR (1.0 – 13 kg C/L/yr), the opposite was true for *Phragmites* at BRO (116 – 227 kg C/L/yr) (Tables 7.2, 7.3, 7.4). Patterns of microbial metabolism based on macrophyte OM followed this trend across species and sites.

Patterns of DOM input and microbial metabolism were quite similar for *Phragmites* at BAR under current flows to those during droughts, although peaks currently are larger and occur later in the year (maximum DOM inputs of 163 and 76 g/L and annual respiration rates of 1.6 and 0.9 mg C/L for current and drought scenarios, respectively) (Figure 7.6 b, f; Table 7.3). A more sustained, but still quite low level of DOM input occurred under historic flow conditions, spanning mid-June to December (annual input of 5.9 kg C/L) and resulting in the second highest level of microbial activity (2.5 mg C/L respired annually) (Figure 7.6 d, Table 7.3). The flood scenario produced substantially larger DOM inputs over much of the year (13 kg C/L annually). Correspondingly, high levels of bacterial metabolism occurred throughout the year during floods, with major peaks in June and October (4.0 mg C/L respired annually) (Figure 7.6 h; Table 7.3).

For all scenarios, DOM inputs from *Phragmites* at BRO were much higher than at BAR on a river volume basis (e.g. annual inputs for BRO and BAR under current flows were 227 and 1.4 kg C/L, respectively). Similarly, bacterial metabolism was higher at BRO, with particularly high levels of biomass production (e.g. 9.6 mg C/L annual production currently at BRO versus 0.8 mg C/L at BAR) (Tables 7.3 and 7.4).

While the maximum daily DOM inputs from *Phragmites* at BRO were similar under all scenarios (1263 – 1460 g C/L/d), total inputs over a year varied substantially due to the effects of mean reach volume (Current = 10; Historical = 32; Drought = 3; Flood = 57 GL) on the different annual loadings (Current = 1,902; Historical = 4,724; Drought = 750; Flood = 4,664 kg C), producing patterns of DOM input concentrations across the scenarios which contrasted with those at BAR (Figure 7.7).

Annual DOM input concentrations were highest in the current and drought scenarios (227 and 182 kg C/L, respectively), followed by the historic (177 kg C/L) and flood (116 kg C/L) scenarios (Table 7.4). Microbial production and respiration rates followed the trend of DOM inputs across scenarios, with 20 – 30 mg C/L respired annually under the current and drought scenarios compared to 14 – 18 mg C/L historically and during floods (Table 7.4). Under all flow scenarios at BRO, major DOM inputs from *Phragmites* occurred in autumn/winter, peaking in May-June (Figure 7.7). For all scenarios, peak periods of microbial activity were in summer (lower inputs but high water temperatures) and autumn (lower water temperatures but peak OM inputs), although late spring activity also occurred under the drought scenario (Figure 7.7 f).

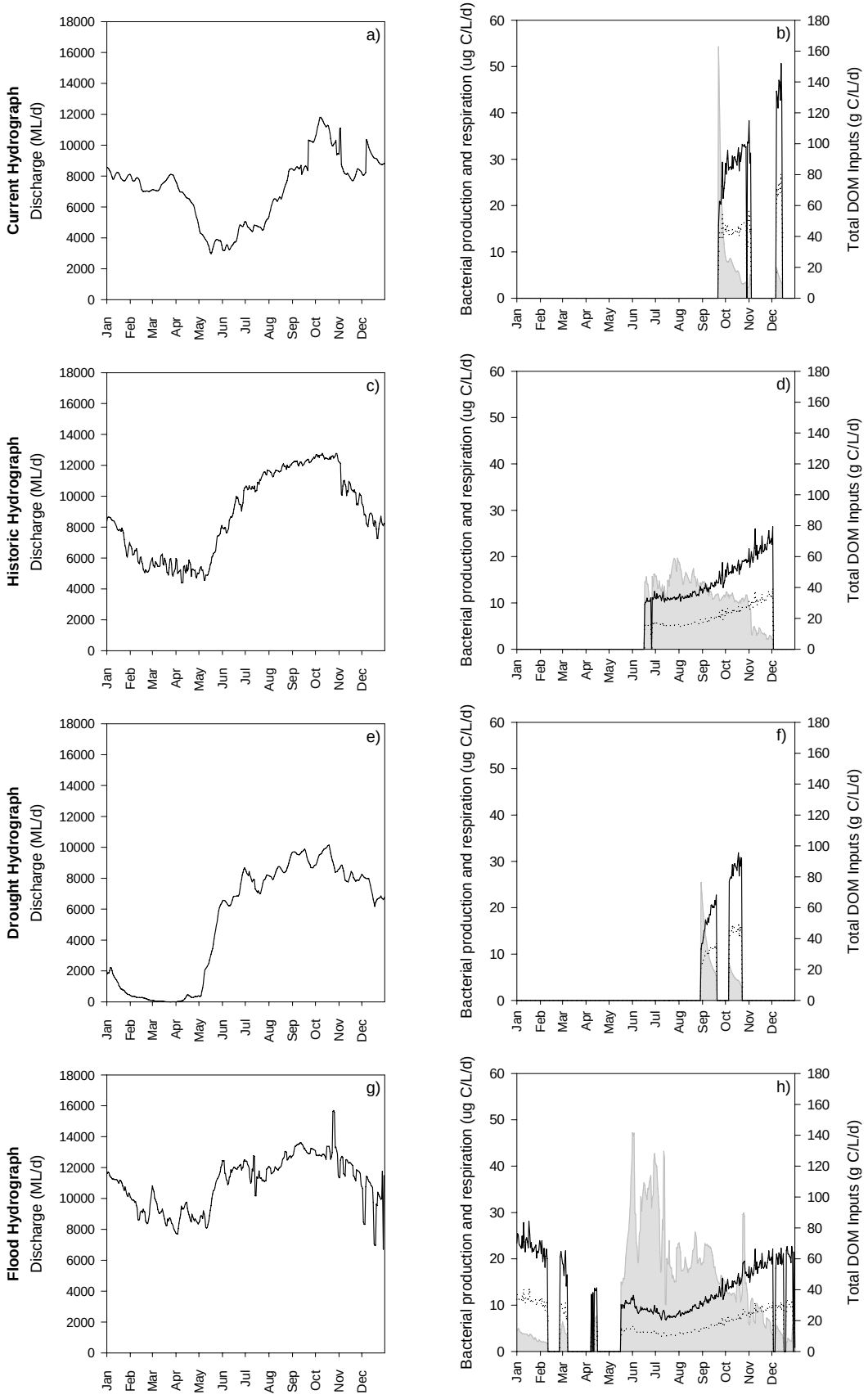

Figure 7.6. Modelling of microbial responses to inputs of *Phragmites* OM at BAR under different flow scenarios. In microbial response plots, dashed line indicates bacterial production, solid line indicates bacterial respiration and grey shading indicates DOM loading.

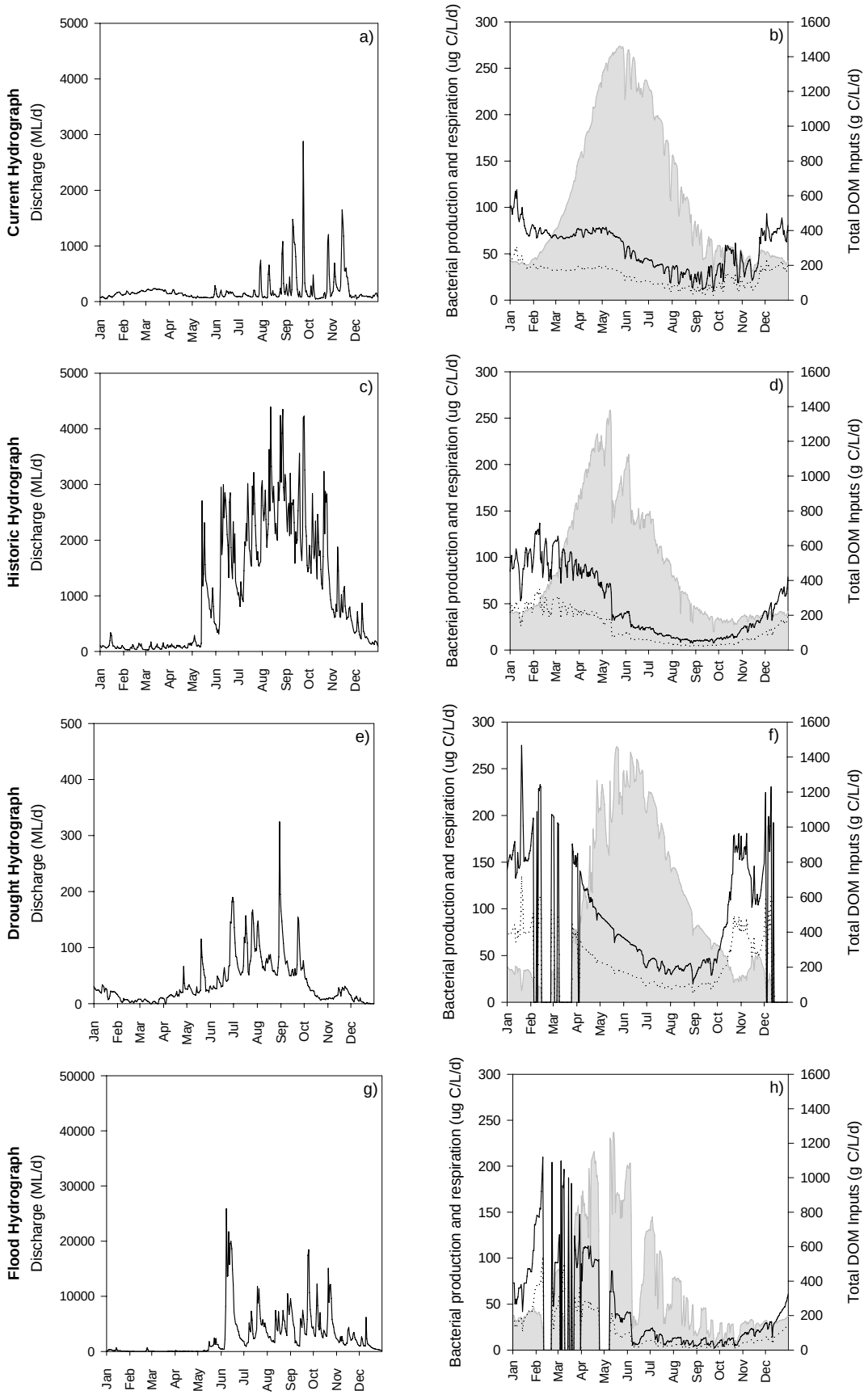

Figure 7.7. Modelling of microbial responses to inputs of *Phragmites* OM at BRO under different flow scenarios. In microbial response plots, dashed line indicates bacterial production, solid line indicates bacterial respiration and grey shading indicates DOM loading.

Table 7.4 Modelled DOM inputs and microbial response parameters under different flow scenarios for *Phragmites* at BRO

	Scenario			
Parameter	**Current**	**Historic**	**Drought**	**Flood**
DOM Inputs				
Mean*	621	485	497	318
Max*	1460	1379	1459	1263
Annual**	227	177	182	116
Respiration				
Mean#	56	49	79	39
Max#	119	137	275	210
Annual##	20	18	29	14
Production				
Mean#	26	23	38	18
Max#	57	66	135	104
Annual##	9.6	8.4	14	6.7

* g C/L/d ** kg C/L
\# µg C/L/d ## mg C/L

7.3.4.3 Vallisneria

Vallisneria DOM inputs at BRO were the lowest of all the species/site combinations assessed (mean of 0.2 – 0.3 g C/L/d; less than 130 g C/L/yr) (Table 7.5). Despite DOM inputs 1 – 3 orders of magnitude lower than the other species, bacterial respiration and biomass production on *Vallisneria* OM was comparable to, or less than an order of magnitude lower than, the other species (Table 7.5). While drought conditions produced the highest *Vallisneria* DOM inputs (124 g C/L annually), microbial metabolism was the second lowest under this scenario (11 mg C respired/L and 6.7 mg biomass C produced/L annually) (Table 7.5). The highest microbial respiration and production occurred under the current flows scenario (17 and 9.3 mg C/L/yr, respectively), which had slightly lower annual DOM inputs than during droughts (117 g C/L) (Table 7.5). Macrophyte-OM-driven microbial metabolism during floods was half that under historical flows on a volumetric basis (6.5 c.f. 14 mg C respired/L/yr), despite DOM inputs being only 20% lower (Table 7.5).

Under current flows, there was relatively little variation in DOM inputs from *Vallisneria* over the year, whereas microbial metabolism driven by these inputs varied considerably, with a major peak in January and numerous minor peaks throughout winter and spring (Figure 7.8 b). Historically, each year was divided into two distinct phases – higher DOM loading and high microbial metabolism during summer/autumn when flows were low, and low DOM loading and low microbial activity during winter/spring when flooding occurred (Figure 7.8 c, d).

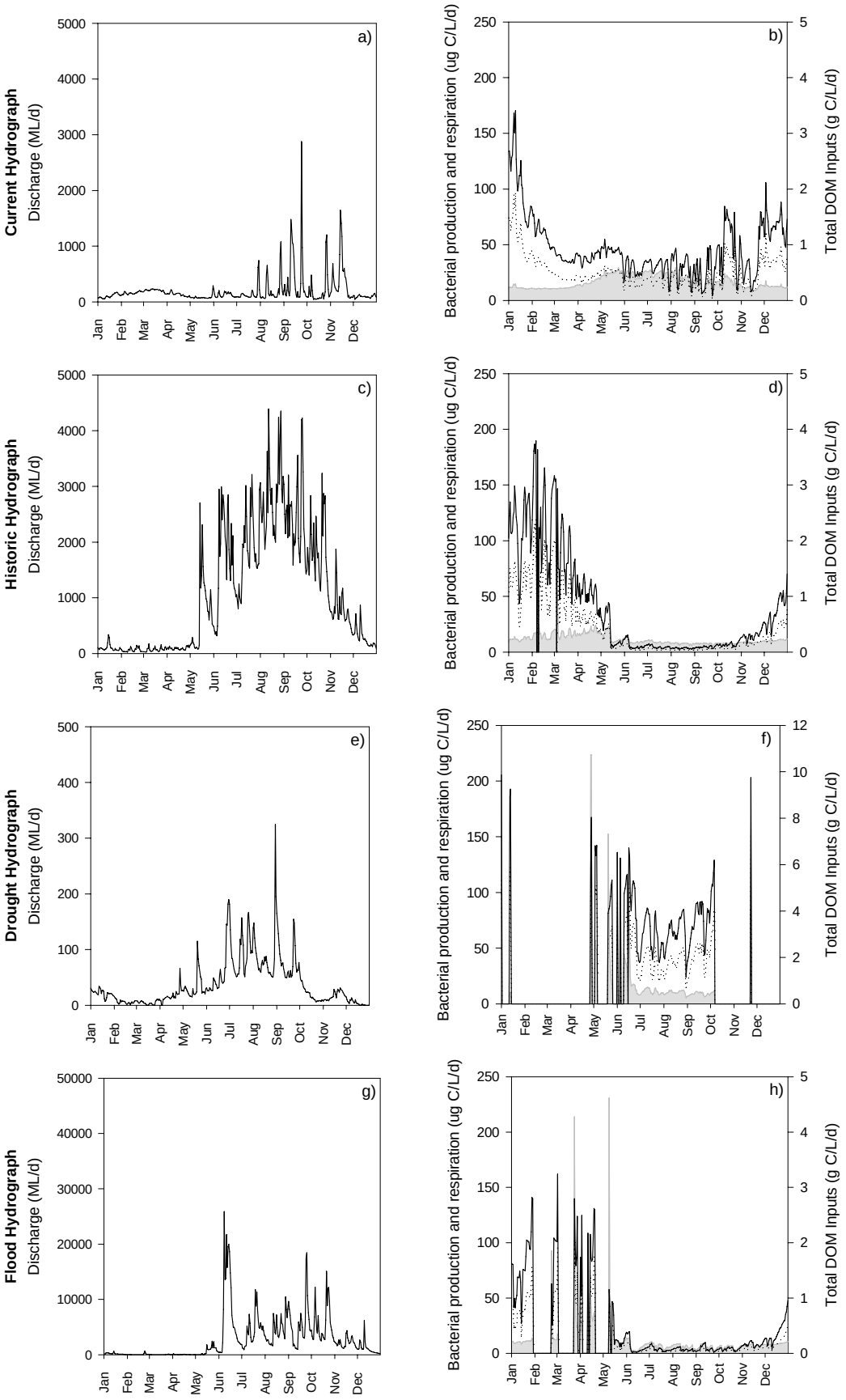

Figure 7.8. Modelling of microbial responses to inputs of *Vallisneria* OM at BRO under different flow scenarios. In microbial response plots, dashed line indicates bacterial production, solid line indicates bacterial respiration and grey shading indicates DOM loading.

Droughts produced very flashy DOM inputs and microbial metabolism because of highly variable flows – the major activity period was in winter/spring under this scenario (Figure 7.8 f). As with the drought scenario, floods caused long periods of minor DOM inputs and little microbial activity (although these occurred in winter/spring) interspersed with flashy peaks (mainly during autumn, as with the historic flow scenario) (Figure 7.8 h).

Table 7.5 Modelled DOM inputs and microbial response parameters under different flow scenarios for *Vallisneria* at BRO

	Scenario			
Parameter	**Current**	**Historic**	**Drought**	**Flood**
DOM Inputs				
Mean*	0.3	0.2	0.3	0.2
Max*	0.6	1.1	11	4.6
Annual*	117	82	124	64
Respiration				
Mean#	46	38	30	18
Max#	170	190	206	162
Annual##	17	14	11	6.5
Production				
Mean#	25	21	18	10
Max#	97	119	152	102
Annual##	9.3	7.8	6.7	3.6

* g C/L/d
\# µg C/L/d ## mg C/L

7.3.4.4 Persicaria

DOM inputs from *Persicaria* at OVN (0 – 2.4 kg C/L/yr) were of a similar magnitude to those for *Phragmites* at BAR (1.0 – 13 kg C/L/yr), however microbial metabolism was somewhat higher (0 – 21 mg C respired/L/yr c.f. 0.9 – 4.0 for *Phragmites* at BAR) (Tables 7.3 and 7.6). Indeed, macrophyte OM induced microbial metabolism at OVN was of a similar magnitude to others driven by inputs of great quantity (*Phragmites* at BRO: 14 – 29 mg C respired/L/yr) or quality (*Vallisneria* at BRO: 6.5 – 17 mg C respired/L/yr) (Tables 7.4 – 7.6).

The annual DOM loading from *Persicaria* at OVN was similar across most scenarios (1.6 – 2.4 kg C/L – Figure 7.9 b, d, h) except for droughts, where no inputs occurred due to complete exposure of macrophyte beds all year round (Figure 7.9 f). Similarly, minor differences occurred between annual respiration and production rates under current, historical or flood conditions (16 – 21 mg C respired/L/yr and 8.5 – 11 mg biomass C produced/L/yr) (Table 7.6). Under current flows, peak DOM loading from *Persicaria* at OVN occurred during winter/spring (Figure 7.9 b). There was a steady increase in microbial activity from the commencement of the wet season as

temperatures increased, with peak microbial activity occurring in late spring (maximum daily microbial respiration of 393 µg C/L) (Table 7.6). Historically, similar patterns of DOM loading and microbial metabolism occurred as under current conditions, although rate increases commenced earlier in the year (annual DOM loading and bacterial respiration of 2.4 kg C/L and 21 mg C/L compared to 1.6 kg C/L and 16 mg C/L under current flows) (Figure 7.9 d). During droughts, macrophytes at OVN were not inundated at all, and hence all riverine microbial metabolism would be based on algal production, riparian inputs (which may be quite high during droughts) or other carbon. DOM inputs from *Persicaria* during floods were dominated by several large peaks (in July, September and November) compared to the fairly stable inputs once inundation commenced in June under historic flows (Figures 7.9 d, h). The maximum daily microbial respiration rate was higher during flood years than historically (384 c.f. 332 µg C /L/d) (Table 7.6).

Table 7.6 Modelled DOM inputs and microbial response parameters under different flow scenarios for *Persicaria* at OVN

	Scenario			
Parameter	**Current**	**Historic**	**Drought**	**Flood**
DOM Inputs				
Mean*	4.4	6.5	0	6.2
Max*	14	14	0	14
Annual**	1.6	2.4	0	2.3
Respiration				
Mean#	43	56	0	58
Max#	393	332	0	384
Annual##	16	21	0	21
Production				
Mean#	23	30	0	31
Max#	212	180	0	208
Annual##	8.5	11	0	11

* g C/L/d ** kg C/L # µg C/L/d ## mg C/L

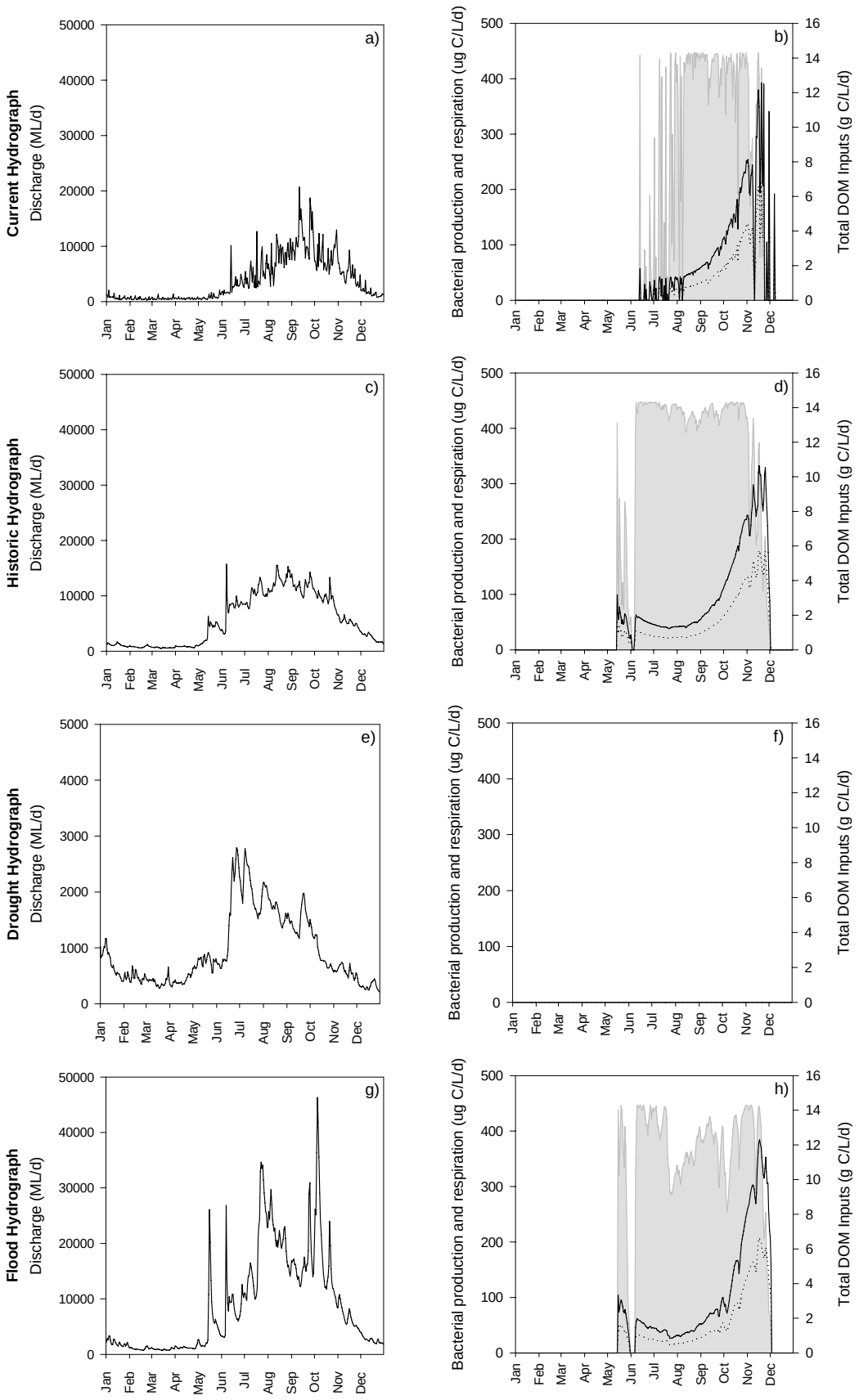

Figure 7.9. Modelling of microbial responses to inputs of *Persicaria* OM at OVN under different flow scenarios. Note different scales on y-axes of hydrographs for different scenarios. In microbial response plots, dashed line indicates bacterial production, solid line indicates bacterial respiration and grey shading indicates DOM loading.

7.3.5 Model Outputs – Bacterial Growth Efficiency

For the modelling in this chapter, BGE was determined from the nutrient composition of OM inputs on a given day. As nutrient status changed with plant phenology, so too did the proportion of metabolised carbon which was channelled into microbial biomass, with varying degrees of change in BGE over time for each species. Annual variation in BGE on OM from emergent macrophyte species was very small across the scenarios assessed; less than 3% for *Typha* and 6% for *Phragmites*. BGE on *Typha* OM peaked in winter at around 19.7% (only slight variations occurred between scenarios modelled so only one scenario per species is shown in Figure 7.10 as an example of the seasonal patterns observed), whereas maximal BGE on *Phragmites* OM occurred in summer (up to 40.7%) (Figure 7.10 a, b). *Vallisneria* OM induced more variable growth efficiency coefficients (generally around 10% variation), with no apparent seasonal pattern (max. of 43.8%) (Figure 7.10 c). Because the modelling of *Persicaria* OM inputs did not incorporate variability in shoot composition over the year, BGE was (probably artificially) stable at 35.1%.

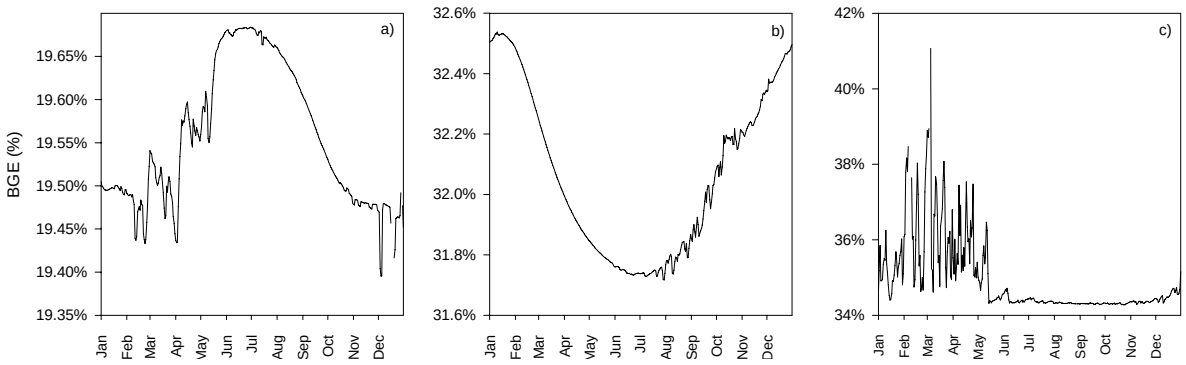

Figure 7.10. Examples of changes to modelled BGE on inundated macrophyte OM over a year (plots show only one of the four scenarios run for each species at each site)
a) *Typha*, b) *Phragmites* and c) *Vallisneria*.

7.3.6 Model Outputs – Ecosystem Level Effects

Microbial respiration rates based on macrophyte OM inputs from my modelling were compared to water column bacterial respiration rates obtained from in-situ oxygen consumption in chambers (Chapter 6), with the fraction due to phytoplankton respiration subtracted (data provided by R. Oliver) to estimate water column heterotroph respiration, the majority of which would be due to aquatic microbes.

In all cases, total microbial respiration from macrophyte OM inputs at a site (all species) was less than the total water column bacterial respiration, but of the same order of magnitude, indicating that the values produced from my modelling represent acceptable estimates of macrophyte-OM-induced microbial metabolism (Table 7.7).

Table 7.7 Contributions of different riverine carbon sources to annual microbial respiration under current flow conditions (µg C/L/yr).

	Bacterial Respiration on Different Riverine Carbon Sources			Total Bacterial Respiration	
	Macrophyte Inputs	*Phytoplankton NPP*	*Riparian Litter Inputs*	*Modelled*	*Measured*
BAR					
Typha	3315				
Phragmites	1573				
Total	4888	34542	26026	65456	72735
% measured bacterial respiration explained	**7%**	**47%**	**36%**	90%	
BRO					
Phragmites	20359				
Vallisneria	16878				
Total	37237	8616	26309	72162	67359
% measured bacterial respiration explained	**55%**	**13%**	**39%**	107%	
OVN					
Persicaria	15731				
Total	15731	-8250	52053	79949	121648
% measured bacterial respiration explained	**13%**	**10%***	**43%**	66%	

* assigned an arbitrary contribution of phytoplankton carbon to riverine microbial metabolism of 10% because net phytoplankton production at this site appeared to be negative

Incorporating estimates of nett OM inputs from phytoplankton (R. Oliver) and riparian leaf litter (my own calculations, based on Gawne et al. submitted) at the three sites allowed a comparison of the major carbon sources utilised by riverine bacteria under current flow conditions. The assumptions underlying these comparisons were that no grazing of any of the autotroph carbon was occurring (ie. all macrophyte and riparian POM inputs and phytoplankton biomass pass through the microbial loop); that BGE on algal carbon was 50% (del Giorgio and Cole, 1998); that the riparian tree density and productivity at BAR, BRO and OVN were similar to those at field sites with similar adjacent land use for which riparian litter input data were available; that BGE on River Red Gum litter was 20% (terrestrial litter value from Meyer et al., 1987) and that inundated Red Gum litter degraded over two years (Glazebrook and Robertson, 1999).

At BAR, respiration on macrophyte OM accounted for only 7% of riverine microbial metabolism, with phytoplankton and riparian vegetation providing the bulk of carbon used by microbes at this site (47% and 36%, respectively) (Table 7.7). In contrast, macrophytes represented the major driver of microbial metabolism in the Broken River, comprising 55% of annual riverine bacterial respiration. Riparian litter was the second highest contributor to

microbial metabolism at this site (39%), with phytoplankton carbon responsible for only 13% of riverine bacterial respiration (Table 7.7). At OVN, only 66% of total annual bacterial respiration could be explained by metabolism of macrophyte, algal and riparian carbon, indicating that alternative carbon sources are contributing to microbial respiration at this site (e.g. ground-water inputs). Of the carbon sources for which estimates were available, riparian vegetation represented the major driver of microbial metabolism (43%) with macrophyte inputs responsible for 13% of bacterial respiration (Table 7.7).

7.4 Thesis Overview and Synthesis

The vertical distributions of different macrophyte species presented in Chapter 2 is summarised in Figure 7.11, with elevations adjusted around the bank full water level for each site. Vertical distributions varied from 2.5 – 4.5 m below bank full level for the fully aquatic *Vallisneria*, through ranges centred on the bank full level for the emergent *Typha* and *Phragmites* to the semi-terrestrial *Persicaria*, which occurred up to 2.5 m above the high water mark.

For different flows, each of these species would be inundated to different degrees. This thesis has focused on two aspects of flow – water level (e.g. gauge height or discharge) and flow variability. Four categories of flow were described in Chapter 2 (Table 7.8), components of which have been related to macrophyte inundation, OM inputs and microbial functioning used throughout this thesis.

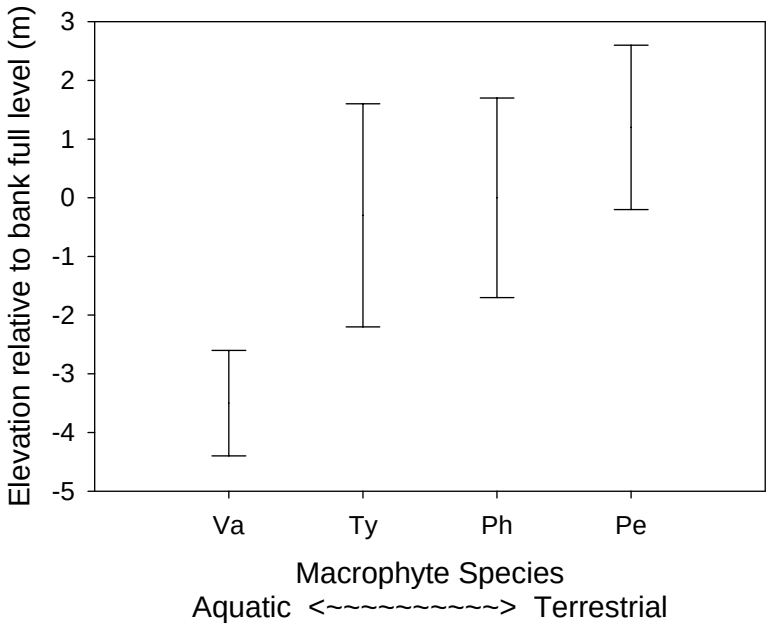

Figure 7.11. Relative macrophyte vertical distributions.
Species codes: Va = *Vallisneria*, Ty = *Typha*, Ph = *Phragmites*, Pe = *Persicaria*

These four flow types were used in scenarios to model inundation of standing shoots and leaf litter (Chapter 4), with tissue mass, nutrient content and leaching data (Chapters 3 and 5) used to estimate DOM inputs to the water column from inundated POM (this chapter). When reported as a direct loading per m^2 of macrophyte bed rather than as concentrations (Tables 7.2 – 7.6), a trend of increasing inputs from the terrestrial to aquatic species is apparent (Figure 7.12 – note log scale on z-axis). This is due to a combination of time spent inundated, magnitude of litter production and levels of DOM release.

Table 7.8 Flow categorisation with respect to water level and variability.

Flow Code	Water Level	Variability	Flow Type	Study reach with similar flow
A	Low	Low	Drought	-
B	Low	High	Historic	BRO
C	High	High	Flood	OVN
D	High	Low	Regulated	BAR

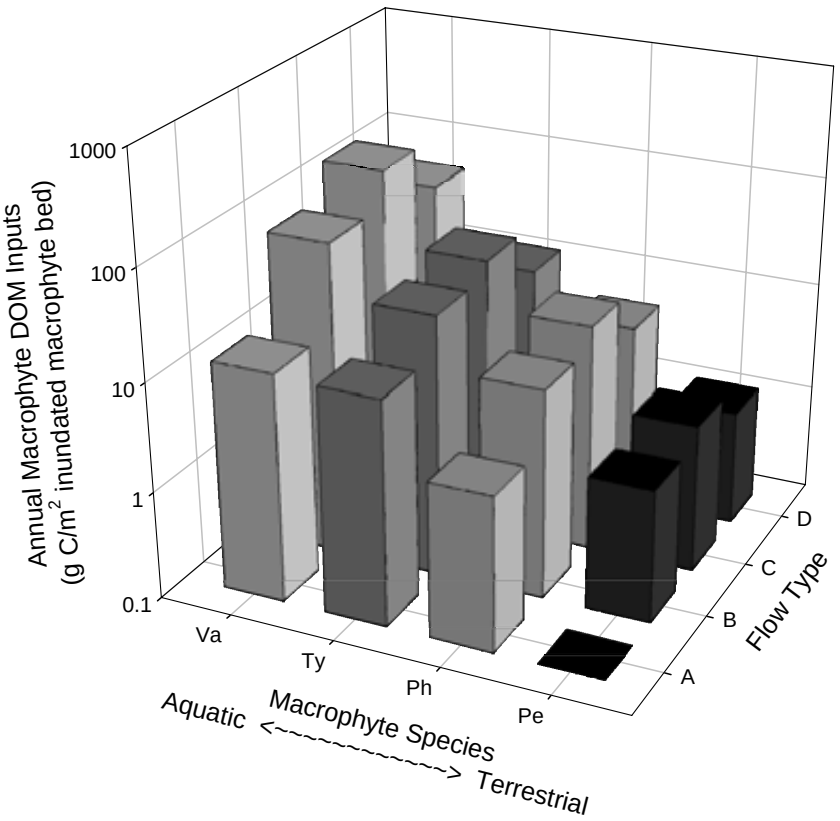

Figure 7.12. Summary of DOM inputs from different macrophytes under different flows. Species codes: Va = *Vallisneria*, Ty = *Typha*, Ph = *Phragmites*, Pe = *Persicaria*

Due to its low vertical distribution, *Vallisneria* experiences the greatest degree of inundation of all species under any flow type. Lacking any storage structures in the climate of the study region, this species focuses more energy on leaf, and hence litter production than the emergent species, which produce extensive spreading rhizomes. So despite having lower quantities of DOM leaching from intact tissues, *Vallisneria* has the greatest DOM inputs on an areal basis of all species studied. In contrast, the very high levels of DOM release from *Persicaria* shoots do not make as great an impact on stream DOM inputs because of their infrequent inundation. The emergent species experience intermediate levels of inundation and also have intermediate levels of litter production and DOM release.

It is also important to note from this figure that flow variability has a greater effect on macrophyte OM inputs than water level. The flow types with high flow variability (B & C) always have higher OM inputs for a given species than those with low variability (A & D), regardless of water level.

It was hypothesised in Chapter 6 that flow-induced inputs of OM from different riverine sources, including macrophytes, would affect riverine microbial functioning. A relationship between discharge and microbial community respiration was observed (Figure 7.13), however as demonstrated in section 7.3.6 of this chapter, this metabolism is based on several riverine carbon sources whose importance varies under different flows.

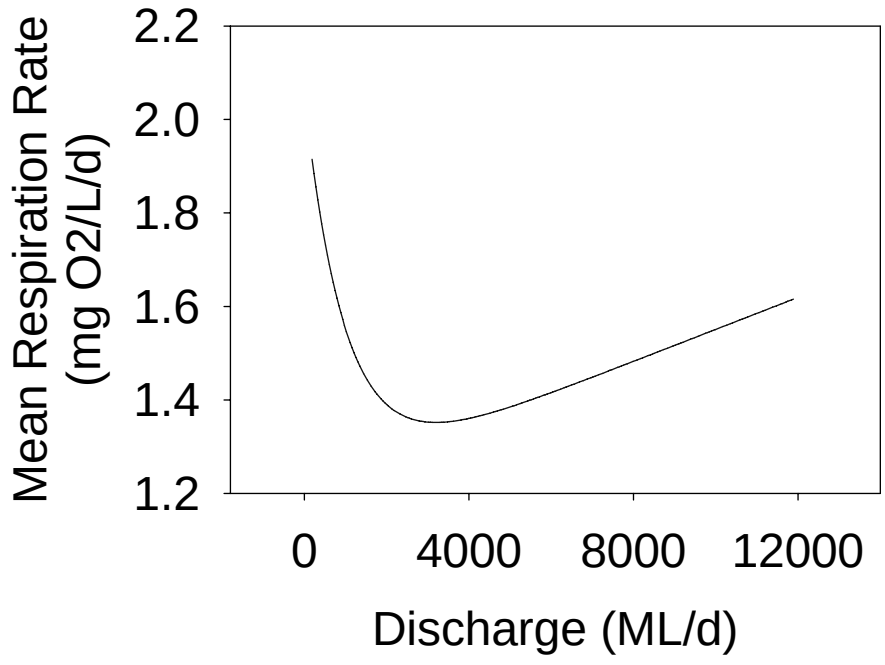

Figure 7.13. Relationship between discharge and community respiration.

The importance of flow variability to changing microbial carbon use was emphasised in Chapter 6, where riverine bacterial carbon utilisation patterns were driven more by flow variability than water level. During steady flows, microbial metabolism was based on proteinaceous compounds (probably from phytoplankton), with a switch to carbohydrates and cellulose from higher plants as water levels changed, and chitinous compounds (e.g. insect exoskeletons) and cellulose (probably from semi-terrestrial macrophytes and riparian vegetation) most important during floods. This interpretation of qualitative changes to microbial carbon use patterns was supported by observed changes in contributions of different riverine OM sources to microbial community respiration presented earlier in this chapter (Table 7.9).

Table 7.9 Contributions of different riverine OM sources to microbial community respiration (%).

Site	Phytoplankton NPP	Macrophyte OM	Riparian OM	Other	Most Similar Flow Type
BAR	**47**	7	36	10	D
BRO	13	**55**	39	0	B
OVN	10	13	**43**	33	C

By combining the contribution of different carbon sources at the three study sites under current flows with macrophyte DOM inputs modelled for different flows and microbial responses to known carbon sources, a conceptual model of the relative importance of different riverine carbon sources to microbial community metabolism under different flows was developed (Figure 7.14).

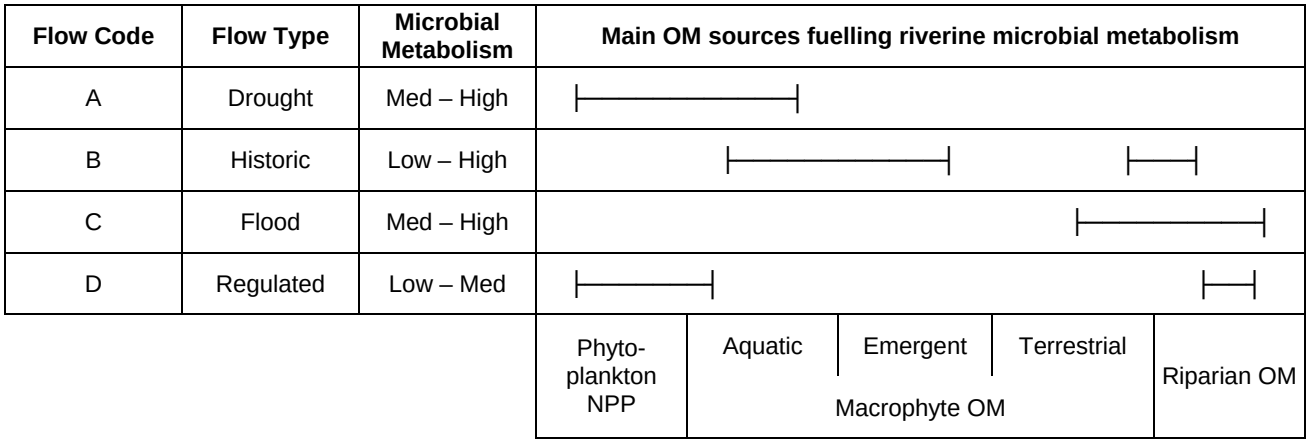

Figure 7.14. Conceptual model of relative importance of riverine carbon sources to microbial community metabolism under different flows.

Historically, microbial metabolism in rivers in the south-eastern region of the Murray-Darling basin was probably quite variable and driven by different OM sources during different parts of the hydrograph. Both fully aquatic and emergent macrophytes would have been important for much of the year, with the more terrestrial macrophytes and riparian OM inputs important during high flows. Under regulated flows, phytoplankton inputs dominate the low to medium levels of microbial metabolism in most lowland rivers, although riparian inputs can be important in reaches with intact riparian vegetation. During droughts, microbial metabolism will be high (as per Figure 7.13) and driven primarily by the few macrophytes remaining inundated (fully aquatic, or submerged, species) plus high levels of phytoplankton productivity. During flood years, the high microbial metabolism is driven mainly by OM inputs from semi-terrestrial macrophytes and riparian vegetation. From this conceptual model it becomes apparent that macrophyte OM inputs are a significant but temporally variable component of lowland river organic matter dynamics and that flow variability is a critical driver of OM inputs and riverine microbial metabolism in temperate Australian lowland rivers.

7.5 Discussion

The over-arching aim of this thesis was to develop a predictive model of inputs of macrophyte organic matter to rivers under different flows and estimate microbial responses to these inputs. This has been achieved by the integration of data and functions, presented in earlier chapters, into a series of equations describing particulate and dissolved organic matter inputs from standing live and dead shoots and the litter pool, and microbial respiration and biomass production induced by these OM inputs. The final equations were compiled into computer code and a graphical user interface developed to simplify usage, providing the capacity to rapidly simulate OM inputs and microbial responses induced by a range of hypothetical flow scenarios.

Modelling macrophyte OM inputs and microbial responses under different flows showed that degree of regulation had a major impact on OM inputs and microbial metabolism. As the water level at the highly-regulated BAR is maintained at a relatively high level all year round, macrophytes grow quite high up on the banks (Chapter 2). A small change in discharge (as a proportion of mean discharge) at this site caused large changes in bed areas inundated and hence OM inputs (Chapter 4), while the dilution effect was minimal. So, using current macrophyte distributions, there was generally a positive relationship between discharge and DOM inputs and microbial metabolism at this site (drought < current < historical < flood). Microbial metabolism and DOM inputs were restricted to summer/autumn under current flows compared to the greater emphasis on winter/spring inputs and microbial activity evident under unregulated flows.

At the less-regulated Broken River site, much of the flow variability has been retained since regulation. Macrophytes grow low down in the channel and are inundated even at very low discharges (Chapter 2). High flows don't substantially alter the bed areas inundated, but cause major changes in discharge relative to the mean at this site, so the dilution effect is strong, producing a negative relationship between discharge and DOM inputs/microbial activity (generally flood < historical < current < drought). Because the Ovens River is essentially unregulated and floods frequently as part of its natural flow cycle, the flood, historical and current flow scenarios all produced very similar results with respect to macrophyte OM inputs and microbial metabolism. Under these flows, macrophyte beds were generally either fully exposed or fully inundated, with little partial inundation occurring. The drought scenario followed this pattern for summer, but low inflows during winter/spring caused total bed exposure at this time of year as well. Other flow scenarios with varying discharges and degrees of variability (e.g. regulation for irrigation) could inundate only portions of the total macrophyte bed area and would be expected to produce quite different results for OM inputs and microbial metabolism for this site. However, any hydrographs generated to run these scenarios would be entirely fabricated and so it was not considered appropriate to attempt this.

For *Typha* and *Phragmites* at BAR and *Persicaria* at OVN, DOM inputs were lower under current flows than historically. At BRO, while total loadings followed this pattern, dilution during high flows historically caused a reversal of this trend when DOM concentrations were considered. Despite maximum DOM inputs occurring in winter/spring for nearly all scenarios (across all plant species), the highest microbial activities were generally in summer/autumn, due to temperature effects. This may be partly explained by the use of a constant rate of microbial metabolism for the "slow" decomposition of previously inundated litter throughout the year, when in reality the breakdown rate would be higher during the initial litter inundation period (winter/spring) and taper off the longer the litter was wetted. If low temperatures do limit microbial utilisation of macrophyte-derived OM in winter/spring then the excess might appear as DOM in the water column which would be transported downstream.

Microbial metabolism levels predicted from my modelling (biomass production range of 0 – 290 µg C/L/d) were of a similar magnitude to those reported for the Murray River from direct measurements of bacterial production (20 – 560 µg C/L/d) (Rees et al., 2005). In comparison to other riverine autotrophs, macrophyte OM at times represented a major carbon source for microbial metabolism at the study sites, supporting 7 – 55% of water column bacterial respiration under current flow conditions. It might be expected that under flow conditions where macrophytes provide greater OM inputs to the system, (e.g. during floods at BAR), that water column bacterial metabolism would be even more strongly linked to aquatic plant carbon.

For all species and sites, bacterial respiration was always greater than biomass production. Modelled bacterial growth efficiency (BGE) in this study ranged from 17% (on *Typha* OM) to 44% (on *Vallisneria* OM), with intermediate levels of carbon incorporation into bacterial biomass from *Phragmites* and *Persicaria* OM (31 – 40% BGE). Growth efficiencies on vascular plant carbon ranging from 9 – 90% have been reported (reviewed in del Giorgio and Cole, 1998). Workers assessing production and respiration of riverine microbes without specific carbon additions commonly report growth efficiencies around 30% for freshwater systems worldwide (del Giorgio and Cole, 1988), with 35 – 38% reported for the Murray River (Rees et al., 2005). At different times of the year, proportionally more of the macrophyte carbon metabolised by bacteria was incorporated into biomass than respired. Timing of peaks in BGE was related to nutrient composition of inundated macrophyte OM and hence was species-specific. Further increases in BGE might be expected during extended periods of daylight (ie. summer) when photolysis of large, recalcitrant organic compounds (such as humic and fulvic acids) would produce smaller, more bio-available molecules (Anesio et al., 2000; Howitt, 2003).

BGE values of less than 50% in this study indicate that less than half of the carbon inputs from macrophytes would enter the food chain directly following microbial metabolism, with the majority catabolised to CO_2. However, this doesn't necessarily mean that the carbon is not used by the rest of the system. Depending on weather conditions, flow and channel morphology, gas exchange between the atmosphere and water column in lotic systems can be quite limited. The degree of mixing within the water column (both laterally and at depth) also affects how evenly the gas transferred from the atmosphere is distributed throughout a river for use by autotrophs. Thus, macrophytes (and sometimes algae) are often limited by supply of inorganic carbon (CO_2) in lotic systems (Lehman, 1978; Weber et al., 1981; Stevenson, 1988; Madsen and Sand-Jensen, 1991; Invers et al., 2001) and so microbes can form an important link between the large pools of organic carbon often present in rivers and carbon-limited autotrophs, supplying respired inorganic carbon to autotrophs to be fixed in photosynthesis (Chrost, 1992; evidence in Hietz, 1992). Of the carbon which is incorporated into microbial biomass, traditional models of aquatic food webs suggest transmission of energy to higher trophic levels via flagellates and protozoan grazers through zooplankton, macro-invertebrates and thence to high-order predators such as fish, birds, amphibians, etc. Recent stable isotope studies have suggested that the contribution of microbial biomass to higher trophic levels is minimal (Delong and Thorp, 2006). However, the effect of passage through the microbial loop on isotope signatures is unknown, thus making it difficult to tease out the role of microbes in aquatic food-webs. Empirical work on grazing of microbial biomass by protozoans (e.g Wright & Coffin, 1984; Riemann, 1985; Servais et al., 1985; Findlay et al., 1986; Hulot et al., 2001), and clearance rates of these by zooplankton (Fenchel, 1982; Sherr et al., 1983; Andersen and Fenchel, 1985), indicate that this certainly is a viable pathway for transmission of microbial carbon to higher trophic levels.

Microbial metabolism values generated in this work have been scaled to the water column volume of the whole river reach. Depending on the exchange of water between macrophyte beds and the rest of river, however, there may be more of a situation of "hot-spots", where microbial metabolism within the beds is much higher than the rest of the water column and based almost entirely on macrophyte carbon. This in turn would lead to hot-spots of protozoan, macro-invertebrate and higher-order production, so sampling of fauna or detritus within the main river channel may not reveal the linkages occurring within macrophyte beds.

Flow management is a powerful tool for altering aquatic ecosystems, known to affect channel morphology, bird and fish breeding and concentrations of particles and dissolved compounds in the water column. This work has shown that it can also be used to influence macrophyte organic matter inputs to rivers and microbial responses, affecting whole stream metabolism and food web interactions.

While scenario modelling in this chapter used current macrophyte distributions, these would be expected to change if particular flow regimes were maintained. For example, continuing drought at BRO would probably cause large reductions in bed areas of *Vallisneria*, which has limited tolerance to exposure and desiccation (Blanch et al., 1999b) and a shift in the vertical distribution of *Phragmites* (Walker et al., 1994) such that shoots would be totally submerged when moderate flow levels returned. Flow regimes (such as extended droughts or increased regulation) which caused a reduction in *Vallisneria* bed area would also probably result in domination by *Phragmites*, which has greater tolerances to a wide range of water levels (Blanch et al., 1999b). This would result in the reduction of inputs of highly-bio-available OM from *Vallisneria* (which currently support around 25% of the microbial metabolism in the river), producing lower microbial activity and a greater proportion of carbon respired than incorporated into biomass.

A return to more natural flow conditions at BAR would most likely result in a reduction of the *Typha* population, which has limited tolerance for variation in water level (Walker et al., 1994). Conversely, *Phragmites*, which can withstand extreme changes in water level, could well expand to cover far greater areas of this site. While, in general, *Phragmites* OM induced higher BGEs than *Typha* OM, highly-bio-available DOM could be leached from different *Typha* tissues at different times throughout the year. For example, very high nitrogen and phosphorus concentrations were detected in leachates derived from *Typha* sheaths (particularly those from live tissues), which contained high proportions of proteinaceous compounds (Chapter 5). Thus, a reduction in the diversity of carbon compounds entering the water column might be induced by restoring the natural flow regime, although other species of macrophyte might recolonise the river channel and floodplain carbon would also play a greater role.

The major effect of temperature on microbial metabolism has important implications for managing flows which inundate carbon sources such as macrophyte beds (Howitt et al., 2005). Where inundation occurs in summer, rates of microbial metabolism are 2 – 7 times higher than a similar flow event occurring in winter, possibly leading to a low oxygen event. This effect is compounded if beds have not been flushed the previous winter/spring to wet the large standing stock of litter and initialise the leaching and microbial colonisation stages.

The predictive model of macrophyte OM inputs and microbial responses developed throughout this thesis represents a major step forward in our understanding of macrophyte-microbe interactions and our ability to manage our river systems. As well as making predictions about the dominant species at the study sites, the integration of data and functions developed throughout this thesis into a computer model means that the code can easily be modified to address other management issues of current interest, such as:

- the effect of different species compositions, population sizes and distributions of macrophytes to OM inputs and stream functioning (e.g. effects of revegetation)
- how alterations to channel morphology could modify macrophyte distributions and affect OM inputs through the influence of bank slope on degree of inundation under different flows (e.g. channelisation, repairing erosion and reinforcing with rip-rap)
- additional flow scenarios – regulation of currently unregulated systems, increasing flow variability, introducing low-flow periods, etc.

7.6 Conclusion

This chapter integrated data presented in earlier chapters into a model of microbial utilisation of macrophyte OM inputs to rivers under different flow conditions. Application of this model was demonstrated by predicting OM inputs and microbial responses induced by a range of hypothetical flow scenarios. Degree of regulation had a major impact on OM inputs and microbial metabolism, through the effects of flow variability on macrophyte vertical distributions, relative proportions of macrophyte bed inundation and dilution effects. Positive relationships between discharge, DOM inputs and microbial metabolism (drought < current < historical < flood) were observed at the most highly regulated site. While a similar pattern occurred at the less regulated site in terms of total loading to the reach, dilution effects resulted in a reversal of this trend on a reach volume basis. Microbial metabolism and DOM inputs were restricted to summer/autumn under regulated flows compared to the greater emphasis on winter/spring inputs and microbial activity evident under unregulated flows.

Comparison to bacterial production measurements in lowland rivers by other workers validated the levels of microbial metabolism predicted by my model. Comparison to other riverine carbon sources demonstrated the importance of macrophyte OM to riverine microbial metabolism (supports 7 – 55% of water column bacterial respiration under current flow conditions). Modelled bacterial growth efficiency in this study ranged from 17 to 44%, with variation both among species and throughout plant growth cycles. As the majority of macrophyte carbon metabolised by microbes was catabolised to CO_2, microbes may potentially provide an important link between the large, but generally unavailable organic carbon pool and carbon-limited autotrophs.

The predictive model of macrophyte OM inputs and microbial responses developed throughout this thesis represents a major step forward in our understanding of macrophyte-microbe interactions and our ability to manage our river systems. This work has shown that flow manipulation can be used to influence macrophyte organic matter inputs to rivers and microbial responses, affecting whole stream metabolism and food web interactions.

Literature Cited

Abal, EG; Loneragan, N; Bowen, P; Perry, CJ; Udy, JW; Dennison, WC (1994) Physiological and morphological responses of the seagrass *Zostera capricorni* Aschers. to light intensity. *Journal of Experimental Marine Biology and Ecology* **178:** 113-129

Alberts, J. J. and Takacs, M. (2004) Total luminescence spectra of IHSS standard and reference fulvic acids, humic acids and natural organic matter: comparison of aquatic and terrestrial source terms. *Organic Geochemistry* **35:** 243 – 256

Allen, H.L. (1976) Dissolved organic matter in lakewater: characteristics of molecular weight size-fractions and ecological implications. *Oikos* **27**, 64-70.

Allirand, J. M. and Gosse, G. (1995) An above-ground biomass production model for a common reed (*Phragmites communis* Trin.) stand. *Biomass and Bioenergy* **9:** 441 – 448

Amblard, C., Boisson, J. C., Bourdier, G., Fontvieille, D., Gayte, X. and Sime-Ngando, T. (1998) Microbial ecology in aquatic systems: a review from viruses to protozoa. *Journal of Water Science* **11:** 145 - 162

Amon, R. M. W. and Benner, R. (1996) Bacterial utilisation of different size classes of dissolved organic matter. *Limnology and Oceanography* **41:** 41 – 51

Amy, P.S., Haldeman, D.L., Ringelberg, D., Hall, D.H. and Russell, C. (1992) Comparison of identification systems for classification of bacteria isolated from water and endolithic habitats within the deep subsurface. *Applied Environmental Microbiology* **58**, 3367-3373.

Andersen, F.O. (1978) Effects of nutrient level on decomposition of *Phragmites communis* Trin. *Arch. Hydrobiol.* **84**, 42-54.

Andersen, P and Fenchel, T (1985) Bacterivory by microheterotrophic flagellates in seawater samples. *Limnology and Oceanography* **30:** 198 – 202

Anesio, A. M., Theil-Nielsen, J. and Graneli, W. (2000) Bacterial growth on photochemicaly transformed leachates from aquatic and terrestrial primary producers. *Microbial Ecology* **40:** 200 – 208

Asaeda, T. and Karunaratne, S. (2000) Dynamic modelling of the growth of *Phragmites australis*: model description. *Aquatic Botany* **67:** 301 – 318

Asaeda, T., Trung, V. K. and Manatunge, J. (2000) Modeling the effects of macrophyte growth and decomposition on the nutrient budget in shallow lakes. *Aquatic Botany* **68:** 217 – 237

Asaeda, Takashi; Nam, Le Hung; Hietz, Peter; Tanaka, Norio, and Karunaratne, Shiromi (2002). Seasonal fluctuations in live and dead biomass of *Phragmites australis* as described by a growth and decomposition model: implications of duration of aerobic conditions for litter mineralization and sedimentation. *Aquatic Botany* **73:** 223-239

Asaeda, Takashi; Manatunge, Jagath; Fujino, Takeshi, and Sovira, Dessy (2003). Effects of salinity and cutting on the development of *Phragmites australis*. *Wetlands Ecology and Management* **11:** 127 – 140

Asaeda, T., Hai, D. N., Manatunge, J., Williams, D. and Roberts, J. (2005) Latitudinal characteristics of below- and above-ground biomass of *Typha*: a modelling approach. *Annals of Botany* **96:** 299 – 312

Atkinson, R. B. and Cairns, J. Jr. (2001) Plant decomposition and litter accumulation in depressional wetlands: functional performance of two wetland age classes that were created via excavation. Wetlands. **21:** 354 - 362

AWRC 1987. 1985 *Review of Australia's Water Resources and Water Use*. Australian Water Resources Council, Department of Primary Industries and Energy, AGPS, Canberra.

Azam, F., Fenchel, T., Gray, J.S., Meyer-Reil, L.-A. and Thingstad, F. (1983) The ecological role of water-column microbes in the sea. *Marine Ecology Progress Series* **10** , 257-263.

Bacic, A., Harris, P. J. and Stone, B. A. (1988) Structure and function of plant cell walls. In *The Biochemistry of Plants, A Comprehensive Treatise* ed. Priess, J. New York: Academic Press.

Baker, A. (2001) Fluorescence Excitation - Emission Matrix Characterization of Some Sewage-Impacted Rivers. *Environmental Science & Technology* **35:** 948-953

Baker, A. (2002a) Spectrophotometric discrimination of river dissolved organic matter. *Hydrological Processes* **16:** 3203-3213

Baker, A. (2002b) Fluorescence properties of some farm wastes: implications for water quality monitoring. *Water Research* **36:** 189-195

Baker, A. and Genty, D. (1999) Fluorescence wavelength and intensity variations of cave waters. *Journal of Hydrology* **217:** 19 – 34

Baldy, V., Gessner, M.O. and Chauvet, E. (1995) Bacteria, fungi and the breakdown of leaf litter in a large river. *Oikos* **74**, 93-102.

Barlocher, F. (1992) Effects of Drying and Freezing Autumn Leaves on Leaching and Colonization by Aquatic Hyphomycetes. *Freshwater Biology* **28:** 1 – 7

Barlocher, F. (1999) Pitfalls of traditional techniques when studying decomposition of vascular plant remains in aquatic habitats. *Limnetica* **13**, 1-11.

Barlocher, F. and Biddiscombe, N.R. (1996) Geratology and decomposition of *Typha latifolia* and *Lythrum salicaria* in a freshwater marsh. *Arch. Hydrobiol.* **136**, 309-325.

Barnes, J. M. (2005) Personal communication. I like horses.

Barrat-Segretain, M-H, (2001) Biomass allocation in three macrophyte species in relation to the disturbance level of their habitat. *Freshwater Biology* **46:** 935-945

Bastardo, H. (1979) Laboratory studies on decomposition of littoral plants. *Pol. Arch. Hydrobiol* **26**, 267-299.

Battle, J. M. and Mihuc, T. B. (2000) Decomposition dynamics of aquatic macrophytes in the lower Atchafalaya, a large floodplain river. *Hydrobiologia* **418:** 123 – 136

Bauerfeind, S. (1985) Degradation of phytoplankton detritus by bacteria: Estimation of bacterial consumption and respiration in an oxygen chamber. *Marine Ecology Progress Series* **21:** 27-36

Bell, R. T., Ahlgren, G. M. and Ahlgren, I. (1983) Estimating bacterioplankton production by measuring (^{3}H)Thymidine incorporation in a eutrophic Swedish lake. *Applied and Environmental Microbiology* **45:** 1709 – 1721

Benke, A.C., Hall, C.A.S., Hawkins, C.P., Lowe-McConnell, R.H., Stanford, J.A., Suberkropp, K. and Ward, J.V. (1988) Bioenergetic considerations in the analysis of stream ecosystems. *Journal of the North American Benthological Society* **7**, 480-502.

Benner, R., Newell, S.Y., Maccubbin, A.E. and Hodson, R.E. (1984) Relative contributions of bacteria and fungi to rates of degradation of lignocellulosic detritus in salt-marsh sediments. *Applied and Environmental Microbiology* **48:** 36 – 40

Benner, R., Moran, M.A. and Hodson, R.E. (1986) Biochemical cycling of lignocellulosic carbon in marine and freshwater ecosystems: relative contributions of prokaryotes and eukaryotes. *Limnology and Oceanography* **21**, 89-100.

Berg, B., Karenlampi, L. and Veum, A. K. (1975) Comparisons of decomposition rates measured by means of cellulose. In Wielgolaski, F.E (Ed) *Fennoscandian Tundra Ecosystems Part 1. Plants and Microorganisms*. Springer-Verlag, New York

Bergbauer, M., Moran, M. A. and Hodson, R. E. (1992) Decomposition of lignocellulose from a freshwater macrophyte by aero-aquatic fungi. *Microbial Ecology* **23:** 159 - 167

Billen, G., Joiris, C., Wijnant, J. and Gillain, G. (1980) Concentration and microbiological utilization of small organic molecules in the Scheldt estuary, the Belgian coastal zone of the North Sea and the English Channel. *Estuarine and Coastal Marine Science* **11:** 279-294

Blanch, S. J., Ganf, G. G. and Walker, K. F. (1998) Growth and recruitment in *Vallisneria americana* as related to average irradiance in the water column. *Aquatic Botany* **61:** 181 - 205

Blanch, S. J., Ganf, G. G. and Walker, K. F (1999a) Growth and resource allocation in response to flooding in the emergent sedge *Bolboschoenus medianus*. *Aquatic Botany* **63:** 145 – 160

Blanch, S. J., Ganf, G. G. and Walker, K. F. (1999b) Tolerance of riverine plants to flooding and exposure indicated by water regime. *Regulated Rivers: Research and Management* **15:** 43 – 62

Blomqvist, P., Jansson, M., Drakare, S., Bergstrom, A-K. and Brydsten, L. (2001) Effects of additions of DOC on pelagic biota in a Clearwater system: results from a whole lake experiment in northern Sweden. *Microbial Ecology* **42:** 383 – 394

Blum, L. K. and Mills, A. L. (1991) Microbial growth and activity during the initial stages of seagrass decomposition. *Marine Ecology Progress Series* **70:** 73 - 82

Boar, Rosalind R (1996) Temporal variations in the nitrogen content of Phragites australis (Cav.) Trin. ex Steud. from a shallow fertile lake. *Aquatic Botany* **55:** 171-181

Bochner, B. (1989) Breathprints at the microbial level. *ASM News* **55**, 536-539.

Bocock, K.L. and Gilbert, O.J.W. (1957) The disappearance of leaf litter under different woodland conditions. *Plant and Soil* **9**, 179-185.

Bohman, I. M. and Tranvik, L. J. (2001) The effects of shredding invertebrates on the transfer of organic carbon from littoral leaf litter to water-column bacteria. *Aquatic Ecology* **35:** 43 - 50

Boon, P.I. (1990) Organic matter degradation and nutrient regeneration in Australian freshwaters: II. Spatial and temporal variation, and relation with environmental conditions. *Arch. Hydrobiol.* **117**, 405-436.

Boschker, H.T.S. and Cappenberg, T.E. (1998) Patterns of extracellular enzyme activities in littoral sediments of Lake Gooimeer, The Netherlands. *FEMS Microbiology Ecology* **25**, 79-86.

Bossio, D.A. and Skow, K.M. (1998) Impacts of carbon and flooding on soil microbial communities: phospholipid fatty acid profiles and substrate utilization patterns. *Microbial Ecology* **35**, 265-278.

Bouchard, V. and Lefeuvre, J-C. (2000) Primary production and macro-detritus dynamics in a European salt marsh: carbon and nitrogen budgets. *Aquatic Botany* **67:** 23 – 42

Bouchard, V., Creach, V., Lefeuvre, J. C., Bertru, G. and Mariotti, A. (1998) Fate of plant detritus in a European salt marsh dominated by *Atriplex portulacoides* (l.) Aellen. *Hydrobiologia* **373/374:** 75 – 87

Boulton, A.J. and Boon, P.I. (1991) A review of methodology used to measure leaf litter decomposition in lotic environments: time to turn over an old leaf? *Australian Journal of Marine and Freshwater Research* **42**, 1-43.

Boulton, A. J. and Brock, M. A. (1999) *Australian Freshwater Ecology: Processes and Management.* Gleneagles Publishing, Glen Osmond, South Australia

Boyd, C. E. (1970) The dynamics of dry matter and chemical substances in a *Juncus effusus* population. *American Midland Naturalist* **86:** 28 - 45

Briggs, S. V., Maher, M. T. and Tongway, D. J. (1985) Dry matter and nutrient loss from decomposing *Vallisneria spiralis* L. *Aquatic Botany* **22:** 387 - 392

Brookshire, E. N. J., Kauffman, J. B., Lytjen, D. and Otting, N. (2002) Cumulative effects of wild ungulate and livestock herbivory on riparian willows. *Oecologia* **132:** 559 – 566

Bruquetas de Zozaya, I.Y. and Neiff, J.J. (1991) Decomposition and colonization by invertebrates of *Typha latifolia* L. litter in Chaco cattail swamp (Argentina). *Aquatic Botany* **40**, 185-193.

Bunn, S. E., Davies, P. M. and Winning, M. (2003) Sources of organic carbon supporting the food web of an arid zone floodplain river. Freshwater Biology 48: 619 - 635

Buesing, N. and Gessner, M. O. (2006) Benthic bacterial and fungal productivity and carbon turnover in a freshwater marsh. *Applied and Environmental Microbiology* **72:** 596 - 605

Cahoon, D.R. and Stevenson, J.C. (1986) Production, predation, and decomposition in a low-salinity *Hibiscus* marsh. *Ecology* **67**, 1341-1350.

Caraco, N.G., Cole, J.J., Raymond, P.A., Strayer, D.L., Pace, M.L., Findlay, S.E.G. and Fischer, D.T. (1997) Zebra mussel invasion in a large, turbid river: phytoplankton response to increased grazing. *Ecology* **78**, 588-602.

Carpenter, S.R. and Adams, M.S. (1979) Effects of nutrients and temperature on decomposition of *Myriophyllum spicatum* L. in a hard-water eutrophic lake. *Limnology and Oceanography* **24:** 520-528

Carpenter, S. R. and Lodge, D. M. (1986) Effects of submersed macrophytes on ecosystem processes. *Aquatic Botany* **26:** 341 – 370

Carr, G.M., Duthie, H.C. and Taylor, W.D. (1997) Models of aquatic plant productivity: A review of the factors that influence growth. *Aquatic Botany* **59:** 195-215

Carreiro, M.M., Sinsabaugh, R.L., Repert, D.A. and Parkhurst, D.F. (2000) Microbial enzyme shifts explain litter decay responses to simulated nitrogen deposition. *Ecology* **81**, 2359-2365.

Cattaneo, A; Galanti, G; Gentinetta, S; Romo, S, (1998) Epiphytic algae and macroinvertebrates on submerged and floating-leaved macrophytes in an Italian lake *Freshwater Biology* **39:** 725-740

Christian, R. R., Bryant, W. L. and Brinson, M. M. (1990) *Juncus roemerianus* production and decomposition along gradients of salinity and hydroperiod. *Marine Ecology Progress Series* **68:** 137 - 145

Chrost, R.J. (1989) Characterization and significance of B-glucosidase activity in lake water. *Limnology and Oceanography* **34**, 660-682.

Chrost, R. J. (1990) Microbial ectoenzymes in aquatic environments. In Chrost, R. J. (Ed) *Aquatic microbial ecology: biochemical and molecular approaches.* Springer-Verlag, New York

Chrost, R.J. (1992) Significance of bacterial ectoenzymes in aquatic environments. *Hydrobiologia* **243/244**, 61-70.

Chrost, R.J. and Faust, M.A. (1983) Organic carbon release by phytoplankton: its composition and utilization by bacterioplankton . *Journal of Plankton Research* **5**, 477-493.

Clevering, OA; Hundscheid, MPJ, (1998) Plastic and non-plastic variation in growth of newly established clones of *Scirpus* (*Bolboschoenus*) *maritimus* L. grown at different water depths. *Aquatic Botany* **62:** 1-17

Cole, J.J. (1982) Interactions between bacteria and algae in aquatic ecosystems. *Anual ReviewAnnual Review of Ecology and Systematics* **13**, 291-314.

Cole, J.J., Findlay, S. and Pace, M. (1988) Bacterial production in fresh and saltwater ecosystems: a cross-system overview. *Marine Ecology Progress Series* **43**, 1-10.

Coops, H., van den Brink, F. W. B., van der Velde, G. (1996) Growth and morphological responses of four helophyte species in an experimental water-depth gradient. *Aquatic Botany* **54:** 11-24

Cota, G.F., Kottmeier, S.T., Robinson, D.H., Smith, W.O. and Sullivan, C.W. (1990) Bacterioplankton in the marginal ice zone of the Weddell **Sea:** biomass, production and metabolic activities during austral autumn. *Deep-Sea Research* **37**, 1145-1167.

Cowie, G.L. and Hedges, J.K. (1984) Carbohydrate sources in a coastal marine environment. *Geochim. Cosmochim. Acta* **48**, 2075-2087.

Crabb, P. (1997) *Murray-Darling Basin Resources*. The Murray-Darling Basin Commission, Canberra

Crawford, R. and Braendle, R. (1996) Oxygen deprivation stress in a changing environment. *Journal of Experimental Botany* **47:** 145 – 159

Crossley, MN; Dennison, WC; Williams, RR; Wearing, AH, (2002) The interaction of water flow and nutrients on aquatic plant growth *Hydrobiologia* **489:** 63-70

Cummins, K.W. (1974) Structure and function of stream ecosystems. *Bioscience* **24**, 631-641.

Cyr, H. and Downing, J. A. (1988) Empirical relationships of phytomacrofaunal abundance to plant biomass and macrophyte bed characteristics. *Canadian Journal of Fisheries and Aquatic Sciences* **45:** 976 - 984

Dagley, S. (1971) Catabolism of aromatic compounds by micro-organisms. *Advances in Microbial Physiology* **6**, 1-46.

Dagley, S. (1975) Microbial degradation of organic compounds in the biosphere. *American Scientist* **63**, 681-689.

Dale, N.G. (1973) Bacteria in intertidal sediments: factors related to their distribution. *Limnology and Oceanography* **19**, 509-518.

Davis, P.G. and Sieburth, J.M. (1984) Estuarine and oceanic microflagellate predation of actively growing bacteria: estimation by frequency of dividing-divided bacteria. *Marine Ecology Progress Series* **19:** 237-246

Davis, C. B. and van der Valk, A. G. (1978) Litter decomposition in prairie glacial marshes. In Good, R. E., Whigham, D. F. and Simpson, R. L. (Eds) *Freshwater Wetlands. Ecological Processes and Management Potential*. Academic Press, New York.

Davis, C.B. and van der Valk, A.G. (1978) The decomposition of standing and fallen litter of *Typha glauca* and *Scirpus fluviatilis*. *Canadian Journal of Botany* **56:** 662-675.

Dawes, CJ; Lawrence, JM (1989) Allocation of energy resources in the freshwater angiosperms *Vallisneria americana* Michx. and *Potamogeton pectinatus* L. in Florida. *Florida Scientist* **52:** 58-63

de Kroon, H.; Hutchings, M.J. (1995) Morphological plasticity in clonal plants: the foraging concept reconsidered. *Journal of Ecology* **43:** 143-152.

de la Cruz, A.A. (1975) Proximate nutritive value changes during decomposition of salt marsh plants. *Hydrobiologia* **47:** 475-480.

de la Cruz, A.A. and Gabriel, B.C. (1974) Caloric, elemental, and nutritive changes in decomposing *Juncus roemerianus* leaves. *Ecology* **55:** 882-886.

Degobbis, D., Homme-Masloska, E., Orio, A.A., Donazzolo, R. and Pavoni, B. (1986) The role of alkaline phosphatase in the sediments of Venice Lagoon on nutrient regeneration. *Estuarine and Coastal Shelf Science* **22:** 425-437.

del Giorgio, P. A. and Cole, J. J. (1998) Bacterial growth efficiency in natural aquatic systems. *Annual Review of Ecology and Systematics* **29:** 503 – 541

Delong, M. D. and Thorp, J. H. (2006) Significance of instream autotrophs in trophic dynamics of the Upper Mississippi River. *Oecologia* **147:** 76 - 85

Dennison, WC; Alberte, RS (1982) Photosynthetic responses of *Zostera marina* L. (eelgrass) to in situ manipulations of light intensity. *Oecologia* **55:** 137-144

Dennison, WC and Alberte, RS (1986) Photoadaptation and growth of *Zostera marina* L. (eelgrass) transplants along a depth gradient. *Journal of Experimental Marine Biology and Ecology* **98:** 265-282

Denno, R. F. and Roderick, G. K. (1991) Influence of patch size, vegetation texture, and host plant architecture on the diversity, abundance, and life history styles of sap-feeding herbivores. In Bell, S. S., McCoy, E. D. and Mushinsky, H. R. (Eds) *Habitat Structure: The physical arrangement of objects in space*. Chapman and Hall, London

Department of Water Resources (1989) *Water Victoria: a Resource Handbook*. Dept. Water Resources, Victoria.

Dickerman, J.A. and Wetzel, R.G. (1985) Clonal growth in *Typha latifolia*: Population dynamics and demography of the ramets. *Journal of Ecology* **73:** 535-552.

Dinka, M.; Agoston-Szabo, E., and Toth, I (2004) Changes in nutrient and fibre content of decomposing *Phragmites australis* litter. *International Review of Hydrobiology* **89:** 519-535

Douglas, M. and Lake, P. S. (1994) Species richness of stream stones: an investigation of the mechanisms generating the species-area relationship. *Oikos* **69:** 387 - 396

Ducklow, H. W. and Carlson, C. A. (1992) Oceanic bacterial production. In Marshall, K.C. (Ed) *Advances in microbial Ecology.* Plenum Press, New York.

Ducklow, H.W. and Kirchman, D.L. (1983) Bacterial dynamics and distribution during a spring diatom blood in the Hudson River Plume. *Journal of Plankton Research* **5:** 333-355.

Elwood, J. W.; Newbold, J. D.; Trimble, A. F., and Stark, R. W. (1981) The limiting role of phosphorus in a woodland stream ecosystem: effects of P enrichment on leaf decomposition and primary producers. *Ecology* **62:** 146-158

Emery, S.L. and Perry, J.A. (1996) Decomposition rates and phosphorus concentrations of purple loosestrife (*Lythrum salicaria*) and cattail (*Typha* spp.) in fourteen Minnesota wetlands. *Hydrobiologia* **323:** 129-138.

Ennabili, Abdeslam; Ater, Mohammed, and Radoux, Michel (1998) Biomass production and NPK retention in macrophytes from wetlands of the Tingitan Peninsula. *Aquatic Botany* **62:** 45-56

Felip, M., Pace, M. L. and Cole, J. J. (1996) Regulation of planktonic bacterial growth rates: the effects of temperature and resources. *Microbial Ecology* **31:** 15 – 28

Fenchel, T. (1982) Ecology of heterotrophic microflagellates. 3. Adaptations to heterogeneous environments. *Marine Ecology Progress Series* **9:** 25-33.

Fenchel, T. (1988) Marine plankton food chains. *Annual Review of Ecology and Systematics* **19:** 19-38.

Findlay, S. E. G. and Arsuffi, T. L. (1989) Microbial growth and detritus transformations during decomposition of leaf litter in a stream. *Freshwater Biology* **21:** 261-269

Findlay, S. and Sinsabaugh, R.L. (1999) Unravelling the sources and bioavailability of dissolved organic matter in lotic aquatic ecosystems. *Marine and Freshwater Research* **50:** 781-790.

Findlay, S., Carlough, L., Crocker, M.T., Gill, H.K., Meyer, J.L. and Smith, P.J. (1986) Bacterial growth on macrophyte leachate and fate of bacterial production. *Limnology and Oceanography* **31:** 1335-1341.

Findlay, S., Howe, K. and Austin, H.K. (1990) Comparison of detritus dynamics in two tidal freshwater wetlands. *Ecology* **71:** 288-295.

Findlay, S., Pace, M.L., Lints, D. and Howe, K. (1992) Bacterial metabolism of organic carbon in the tidal freshwater Hudson Estuary. *Marine Ecology Progress Series* **89:** 147-153.

Findlay, S., Hickey, C. and Quinn, J. (1998a) Microbial enzymatic response to catchment-scale variations in supply of dissolved organic carbon. *New Zealand Journal of Marine and Freshwater Research* **31:** 701-706.

Findlay, S., Sinsabaugh, R.L., Fischer, D.T. and Franchini, P. (1998b) Sources of dissolved organic carbon supporting planktonic bacterial production in the tidal freshwater Hudson River. *Ecosystems* **1:** 227-239.

Fisher, S.G. and Carpenter, S.R. (1976) Ecosystem and macrophyte primary production of the Fort River, Massachusetts. *Hydrobiologia* **47:** 175-187.

Fleishman, E., Ray, C., Sjogren-Gulve, P., Boggs, C.L. and Murphy, D.D. (2002) Assessing the roles of patch quality, area, and isolation in predicting metapopulation dynamics. *Conservation Biology* **16:** 706 – 716

Flint, R. W. and Goldman, C. R. (1975) The effects of a benthos grazer on the primary productivity of the littoral zone of Lake Tahoe. *Limnology and Oceanography* **20:** 935 – 944

Fog, K. (1988) The effect of added nitrogen on the rate of decomposition of organic matter. *Biological Review* **63:** 433-462.

Foreman, C.M., Franchini, P. and Sinsabaugh, R.L. (1998) The trophic dynamics of riverine bacterioplankton: relationships among substrate availability, ectoenzyme kinetics and growth. *Limnology and Oceanography* **43:** 1344-1352.

Franken, R.J. and Hik, D.S. (2004) Influence of habitat quality, patch size and connectivity on colonization and extinction dynamics of collared pikas *Ochotona collaris*. *Journal of Animal Ecology* **73:** 889 – 896

Frankland, J.C. (1966) Succession of fungi on decaying petioles of *Pteridium aquilinum*. *Journal of Ecology* **54:** 41-63.

Fred, M.S. and Brommer, J.E. (2003) Influence of habitat quality and patch size on occupancy and persistence in two populations of the Apollo butterfly (*Parnassius apollo*). *Journal of Insect Conservation* **7:** 85 - 98

Froend, R. H. and McComb, A. J. (1994) Distribution, productivity and reproductive phenology of emergent macrophytes in relation to water regimes at wetlands of south-western Australia. *Australian Journal of Marine and Freshwater Research* **45:** 1491 – 1508

Fuhrman, J.A., Ammerman, J.W. and Azam, F. (1980) Bacterioplankton in the coastal euphotic zone: distribution, activity and possible relationships with phytoplankton. *Marine Biology* **60:** 201-207.

Gajewski, A.J. and Chrost, R.J. (1995) Microbial enzyme activities and phytoplankton and bacterial production in the pelagial of the Great Mazurian Lakes (north-eastern Poland) during summer stratification. *Ekologia Polska* **43:** 245-265.

Gallardo, A. and Merino, J. (1993) Leaf decomposition in two Mediterranean ecosystems of Southwest Spain: influence of substrate quality. *Ecology* **74:** 152-161.

Garbey, C; Thiebaut, G; Muller, S, (2004) Morphological plasticity of a spreading aquatic macrophyte, *Ranunculus peltatus*, in response to environmental variables. *Plant Ecology* **173:** 125-137

Garland, J.L. and Mills, A.L. (1991) Classification and characterization of heterotrophic microbial communities on the basis of patterns of community-level sole-carbon-source utilization. *Applied Environmental Microbiology* **57:** 2351-2359.

Gawne, B., Baldwin, D. S., Beattie, G., Bowen, P. M., Ellis, I., Frankenberg, J., Lorenz, Z., Merrick, C. J., Oliver, R. L., Rees, G., Treadwell, S. and Williams, D. (2002) *Ecological functioning of the Murray River ecosystem*. Final Report for CRCFE Project A500.

Gawne, B., Merrick, C., Williams, D. G., Rees, G. N., Oliver, R. L., Bowen, P. M., Treadwell, S., Beattie, G., Ellis, I., Frankenberg, J. and Lorenz, Z. (submitted) Patterns of primary and heterotrophic productivity in an arid lowland river. *Regulated Rivers: Research and Management*

Gawne, B., Hawking, J., Nielsen, D., Oliver, R. L., Rees, G. N., Williams, D. G., Bowen, P. M., Gigney, H., Lorenz, Z., Watson, G. and Whiterod, N. (in prep) Patterns of productivity and sources of organic matter in the food webs of the Australian lowland rivers.

Gessner, M. O. (2000) Breakdown and nutrient dynamics of submerged *Phragmites* shoots in the littoral zone of a temperate hardwater lake. *Aquatic Botany* **66:** 9 – 20

Gessner, M. O. (2001) Mass loss, fungal colonisation and nutrient dynamics of *Phragmites australis* leaves during senescence and early aerial decay. *Aquatic Botany* **69:** 325 - 339

Gessner, M.O. and Chauvet, E. (1994) Importance of stream microfungi in controlling breakdown rates of leaf litter. *Ecology* **75**, 1807-1817.

Gessner, M. O. and Newell, S. Y. (1997) Bulk quantitative methods for the examination of eukaryotic organoosmotrophs in plant litter. In Hurst, C.J., Knudsen, G., McInerney, M., Stetzenbach, L.D. and Walter, M.V. (Eds) *Manual of environmental microbiology.* American Society for Microbiology, Washington DC**.**

Gessner, M. O., Schieferstein, B., Muller, U., Barkmann, S. and Lenfers, U. (1996) A partial budget of primary organic carbon flows in the littoral zone of a hardwater lake. *Aquatic Botany* **55:** 93 – 105

Gilbert J.J. (1989) The Effect of Daphnia interference on a natural rotifer and Ciliate community short-term bottle experiments. *Limnology and Oceanography* **34:** 606–617

Giovannoni, S.J., Britschgi, T.B., Moyer, C.L. and Field, K.G. (1990) Genetic diversity in Sargasso sea bacterioplankton. *Nature* **345:** 60-63.

Glazebrook, H. S. and Robertson, A. I. (1999) The effect of flooding and flood timing on leaf litter breakdown rates and nutrient dynamics in a river red gum (*Eucalyptus camaldulensis*) forest. *Australian Journal of Ecology* **24:** 625 - 635

Godshalk, G.L. and Wetzel, R.G. (1978a) Decomposition of aquatic angiosperms. I. Dissolved components. *Aquatic Botany* **5:** 281-300.

Godshalk, G.L. and Wetzel, R.G. (1978b) Decomposition of aquatic angiosperms. II. Particulate components. *Aquatic Botany* **5:** 301-327.

Goncalves, J. F.; Santos, A. M., and Esteves, F. A. (2004) The Influence of the Chemical Composition of *Typha Domingensis* and *Nymphaea Ampla* Detritus on Invertebrate Colonization During Decomposition in a Brazilian Coastal Lagoon. *Hydrobiologia* **527:** 125-137

Goldman, J. C., Caron, D. A. and Dennett, M. R. (1987) Regulation of gross growth efficiency and ammonium regeneration in bacteria by substrate C:N ratio. *Limnology and Oceanography* **32:** 1239 – 1252

Graça, M.A.S., S.Y. Newell, and R.T. Kneib. 2000. Grazing rates of organic matter and living fungal biomass of decaying *Spartina alterniflora* by three species of saltmarsh invertebrates. *Mar. Biol.* **136:** 281-289

Grace, J. B. (1989) Effects of water depth on *Typha latifolia* and *Typha deomingensis*. *American Journal of Botany* **76:** 762-768

Grace, J.B.; Wetzel, R.G. (1981) Phenotypic and genotypic components of growth and reproduction in *Typha latifolia*: experimental studies in marshes of differing successional maturity. *Ecology* **62:** 789-801

Hahn, Martin W. and Höfle, Manfred G. (2001) Grazing of protozoa and its effect on populations of aquatic bacteria. *FEMS Microbiology Ecology* **35:** 113-121

Halemejko, G.Z. and Chrost, R.J. (1986) Enzymatic hydrolysis of proteinaceous particulate and dissolved material in an eutrophic lake. *Arch. Hydrobiol.* **107:** 1-21.

Halupa, P. J. and Howes, B. L. (1995) Effects of tidally mediated litter moisture content on decomposition of *Spartina alterniflora* and *S. patens*. *Marine Biology* **123:** 379 - 391

Hanson, R.B., Alvarez-Ossorio, M.T., Cal, R., Campos, M.J., Roman, M., Santiago, G. and Varela, M.Y.J.A. (1986) Plankton response following a spring upwelling event in the Ria de Arosa, Spain. *Marine Ecology Progress Series* **32:** 101-113.

Harden, Gwen J. (1990-) *Flora of New South Wales*. Vol.1-4. NSW University Press, Kensington, N.S.W.

Harrison, P.G. and Mann, K.H. (1975) Detritus formation from eelgrass (*Zostera marina* **L.):** the relative effects of fragmentation, leaching and decay. *Limnology and Oceanography* **20:** 924-934.

Hart, D. D. and Horwitz, R. J. (1991) Habitat diversity and the species-area relationship: alternative models and tests. In Bell, S. S., McCoy, E. D. and Mushinsky, H. R. (Eds) *Habitat Structure: The physical arrangement of objects in space*. Chapman and Hall, London

Haslam, S. M. (1978) River Plants. *The Macrophyte Vegetation of Watercourses*. Cambridge University Press, Cambridge.

Haslam, S. M. (1989) Early decay of *Phragmites* thatch: An outline of the problem. *Aquatic Botany* **35:** 129-132

Hawking, J. H. and Smith, F, J. (1997) *Colour Guide to Invertebrates of Australian Inland Waters*. Co-operative Research Centre for Freshwater *Ecology* and Murray-Darling Freshwater Research Centre, Albury.

Heck, K. L. and Crowder, L. B. (1991) Habitat structure and predator-prey interactions in vegetated aquatic systems. In (Bell, S. S., McCoy, E. D. and Mushinsky, H. R. (Eds) *Habitat Structure: The physical arrangement of objects in space*. Chapman and Hall, London

Hessen, D. (1992) Dissolved organic carbon in a humic lake: effects on bacterial production and respiration. *Hydrobiologia* **229:** 115 – 123

Hietz, P. (1992) Decomposition and nutrient dynamics of reed (*Phragmites australis* (Cav.) Trin. ex Steud.) litter in Lake Neusiedl, Austria. *Aquatic Botany* **43:** 211 - 230

Hill, B. H. (1987) *Typha* productivity in a Texas pond: implications for energy and nutrient dynamics in freshwater wetlands. *Aquatic Botany* **27:** 385 – 394

Hillman, T. J. (1995) Billabongs, floodplains and the health of rivers. *Water* **22:** 6 – 19

Hocking, P. J. (1989) Seasonal dynamics of production, and nutrient accumulation and cycling by *Phragmites australis* (Cav) Trin. Ex Stuedel in a nutrient-enriched swamp in inland Australia. I. Whole plants. *Australian Journal of Marine and Freshwater Research* **40:** 445 – 464

Hocking, P.J.; Finlayson, C.M. and Chick, A.J. (1983) The biology of Australian weeds. 12. *Phragmites australis* (Cav.) Trin. ex Steud.. *Journal of the Australian Institute of Agricultural Science* **49:** 123-132

Hodkinson, I.D. (1975) Dry weight loss and chemical changes in vascular plant litter of terrestrial origin, occurring in a beaver pond ecosystem. *Journal of Ecology* **63:** 131-142.

Hopkinson, C., Buffam, I., Hobbie, J., Vallino, J., Hodson, R., Moran, M.A., Covert, J., Smith, E., Baross, J., Crump, B., Eversmeyer, B., Prahl, F., Perdue, M., Findlay, S. and Foreman, K. (1998) Terrestrial inputs of organic matter to coastal ecosystems: an intercomparison of chemical characteristics and bioavailability. *Biogeochemistry* **43:** 211-234.

Hoppe, H.G. (1983) Significance of exoenzymatic activities in the *Ecology* of brackish water: measurements by means of methylumbelliferyl-substrates. *Marine Ecology Progress Series* **11:** 299-308.

Hoppe, H-G. (1993) Use of fluorogenic model substrates for extracellular enzyme activity (EEA) measurement of bacteria. In Kemp, P.F., Sherr, B. F., Sherr, E. B. and Cole, J. J. (Eds) *Handbook of Methods in Aquatic Microbial Ecology*. Lewis Publishers, Boca Raton.

Hosomi, M. and Sudo, R. (1986) Simultaneous determination of total nitrogen and total phosphorus in freshwater samples using persulfate digestion. *International Journal of Environmental Studies* **27:** 267-275

Howard-Williams, C. and Lenton, G.M. (1975) The role of the littoral zone in the functioning of a shallow tropical lake ecosystem. *Freshwater Biology* **5:** 445-459.

Howard-Williams, C. and Davies, B.R. (1979) The rates of dry matter and nutrient loss from decomposing *Potamogeton pectinatus* in a brackish south-temperate coastal lake. *Freshwater Biology* **9:** 13-21.

Howarth, R.W. and Fisher, S.G. (1976) Carbon, nitrogen, and phosphorus dynamics during leaf decay in nutrient-enriched steam microecosystems. *Freshwater Biology* **6:** 221 - 228

Howarth, R.W., Schneider, R. and Swaney, D. (1996) Metabolism and organic carbon fluxes in the tidal freshwater Hudson River. *Estuaries* **19**, 848-865.

Howitt, J. A. (2003) Photochemical Degradation of Aquatic Dissolved Organic matter: the Role of Suspended Iron Oxides. PhD Thesis, Monash University, Victoria, Australia.

Howitt, J., Baldwin, D., Rees, G. (2005) Blackwater Model – A revised computer model to predict dissolved oxygen and dissolved carbon downstream of Barmah-Millewa Forest following a flood. Report prepared for the Barmah-Millewa Forest Forum by the Murray-Darling Freshwater Research Centre

Hulot, F.D., Morin, P.J. and Loreau, M. (2001) Interactions between algae and the microbial loop in experimental microcosms. *OIKOS* **95:** 231-238.

Ibarra-Obando, S. E., Boudouresque, C-F. and Roux, M. (1997) Leaf dynamics and production of a *Zostera marina* bed near its southern distributional limit. *Aquatic Botany* **58:** 99 – 112

Invers, O., Zimmerman, R. C., Alberte, R. S., Perez, M. and Romero, J. (2001) Inorganic carbon sources for seagrass photosynthesis: an experimental evaluation of bicarbonate use in species inhabiting temperate waters. *Journal of Experimental Marine Biology and Ecology* **265:** 203 – 217

Jackson, C.R., Foreman, C.M. and Sinsabaugh, R.L. (1995) Microbial enzyme activities as indicators of organic matter processing rates in a Lake Erie coastal wetland. *Freshwater Biology* **34:** 329-342.

Jacobsen, D. Sand-Jensen, K. (1992) Herbivory of invertebrates on submerged macrophytes from Danish freshwaters. *Freshwater Biology* **28:**301–308

Jacobsen, T.R. and Rai, H. (1988) Determination of aminopeptidase activity in lake water by short term kinetic assay and its application in two lakes of differing eutrophication. *Arch. Hydrobiol.* **113:** 359-370.

Johnson, R. L., Gross, E. M. and Hairston, N. G. Jr (1998) Decline of the invasive submersed macrophyte *Myriophyllum spicatum* (Haloragaceae) associated with herbivory by larvae of *Acentria ephemerella* (Lepidoptera). *Aquatic Ecology* **31:**273–282

Joint, I.R. and Pomeroy, A.J. (1987) Activity of heterotrophic bacteria in eutrophic zone of the Celtic Sea. *Marine Ecology Progress Series* **41:** 1155-1165.

Jones, J.G. and Simon, B.M. (1975) An investigation of errors in direct counts of aquatic bacteria by epifluorescence microscopy, with reference to a new method for dyeing membrane filters. *Journal of Applied Bacteriology* **39:** 317-329.

Jones, S.E. and Lock, M.A. (1989) Hydrolytic extracellular enzyme activity in heterotrophic biofilms from two contrasting streams. *Freshwater Biology* **22:** 289-296.

Jones, S. E. and Lock, M. A. (1991) Peptidase activity in river biofilms by product analysis. In Chrost, R. J. (Ed) *Microbial enzymes in aquatic environments.* Springer, New York.

Junk, W. J., Bayley, P. B. and Sparks, R. E. (1989) The flood pulse concept in river-floodplain systems. Proceedings of the international large river symposium. *Can. Sp. Publ. Fish. Aquat. Sci.* **1989:** 110-127

Kaplan, L.A., Larson, R.A. and Bott, T.L. (1980) Patterns of dissolved organic carbon in transport. *Limnology and Oceanography* **25:** 1034-1043.

Karunaratne, S., Asaeda, T. and Yutani, K. (2004) Age-specific seasonal storage dynamics of *Phragmites australis* rhizomes: a preliminary study. *Wetlands Ecology and Management* **12:** 343 – 351

Kaushik, NK; Hynes, HBN (1971) The fate of the dead leaves that fall into streams. *Archiv Fur Hydrobiologie* **68:** 465 - 515

Keefe, C.W. (1972) Marsh production: a summary of the literature. *Contributions to Marine Science* **16:** 163 – 181

Kemp, W.M., Smith, E.M., Marvin-DiPasquale, M. and Boynton, W.R. (1997) Organic carbon balance and net ecosystem metabolism in Chesapeake Bay. *Marine Ecology Progress Series* **150:** 229-248.

Keyser, P., Kirk, T.K. and Zeikus, G. (1978) Ligninolytic enzyme system of *Phanerochaete chrysosporium*: synthesized in the absence of lignin in response to nitrogen starvation. *Journal of Bacteriology* **135:** 790-797.

Kirk, T.K. (1987) Enzymatic "combustion": the microbial degradation of lignin. *Annual Review of Microbiology* **41:** 465-505.

Kirkman, L. K. and Sharitz, R. R. (1993) Growth in controlled water regimes of three grasses common in freshwater wetlands of the southeastern USA. *Aquatic Botany* **44:** 345 - 359

Klimes, L., Klimesova, J. and Cizkova, H. (1999) Carbohydrate storage in rhizomes of *Phragmites australis*: the effects of altitude and rhizome age. *Aquatic Botany* **64:** 105 – 110

Kneib, R.T., S.Y. Newell, and E.T. Hermeno. 1997. Survival, growth and reproduction of the salt marsh amphipod *Uhlorchestia spartinophila* reared on natural diets of senescent and dead Spartina alterniflora leaves. *Mar. Biol*. **128:** 423- 431

Kohl, J-G.; Woitke, P.; Kühl, H.; Dewender, M., and König, G. (1998) Seasonal changes in dissolved amino acids and sugars in basal culm internodes as physiological indicators of the C/N balance of *Phragmites australis* at littoral sites of different trophic status. *Aquatic Botany* **60:** 221-240

Kominkova, D., Keuhn, K.A., Busing, N., Steiner, D. and Gessner, M.O. (2000) Microbial biomass, growth, and respiration associated with submerged litter of *Phragmites australis* decomposing in a littoral reed stand of a large lake. *Aquatic Microbial Ecology* **22:** 271-282.

Konopka, A., Oliver, L. and Turco, R.F. (1998) The use of carbon substrate utilization patterns in environmental and ecological microbiology. *Microbial Ecology* **35:** 103-115.

Kornijow, R. (1996) Cumulative consumption of the lake macrophyte *Elodea* by abundant generalist invertebrate herbivores. *Hydrobiologia* **319:** 185 – 190

Kornijow, R., Gulati, R. D. and Ozimek, T. (1995) Food preference of some freshwater macroinvertebrates: comparing fresh and decomposed vascular plants and a filamentous alga. *Freshwater Biology* **33:** 205 – 212

Kuehn, K. A. and Suberkropp, K. (1998a) Decomposition of standing litter of the freshwater emergent macrophyte *Juncus effusus*. *Freshwater Biology* **40:** 717 - 727

Kuehn, K.A. and Suberkropp, K. (1998b) Diel fluctuations in microbial activity associated with standing dead leaf litter of the meergent macrophyte *Juncus effusus*. *Aquatic Microbial Ecology* **14:** 171-182.

Kuehn, K.A., Churchill, P.F. and Suberkropp, K. (1998) Osmoregulatory responses of fungi inhabiting standing-dead litter of the freshwater emergent macrophyte *Juncus effusus*. *Applied Environmental Microbiology* **64:** 607-612.

Kuehn, K.A., Gessner, M.O., Wetzel, R.G. and Suberkropp, K. (1999) Decomposition and CO_2 evolution from standing litter of the emergent macrophyte *Erianthus giganteus*. *Microbial Ecology* **38:** 50-57.

Kuehn, K.A., Lemke, M.J., Wetzel, R.G. and Suberkropp, K. (2000) Microbial biomass and production associated with decaying leaf litter of the emergent macrophyte *Juncus effusus*. *Limnology and Oceanography* **45:** 862-870.

Kvet, J., Svoboda, J. and Fiala, K. (1969) Canopy development in stands of *Typha latifolia* L. and *Phragmites communis* Trin. in South Moravia. *Hydrobiologia* **10:** 63 – 75

Lee, A. A. and Bukaveckas, P. A. (2002) Surface water nutrient concentrations and litter decomposition rates in wetlands impacted by agriculture and mining activities. *Aquatic Botany* **74:** 273 – 285

Lee, S.Y. (1990) Net aerial primary productivity, litter production and decomposition of the reed *Phragmites communis* in a nature reserve in Hong Kong: Management implications. *Marine Ecology Progress Series* **66:** 161-173.

Leff, L. G. and Meyer, J. L. (1991) Biological availability of dissolved organic carbon along the Ogeechee River. *Limnology and Oceanography* **36:** 315 – 323

Lehman, J. T. (1978) Enhanced transport of inorganic carbon into algal cells and its implications for the biological fixation of carbon. *Journal of Phycology* **14:** 33 – 42

Lennon, J. T. and Pfaff, L. E. (2005) Source and supply of terrestrial organic matter affects aquatic microbial metabolism. *Aquatic Microbial Ecology* **39:** 107 - 119

Leslie, D. J. (2001) Effect of river management on colonially-nesting waterbirds in the Barmah-Millewa Forest, south-eastern Australia. *Regulated Rivers: Research and Management* **17:** 21 - 36

Levesque, M. (1972) Fluorescence and gel filtration of humic compounds. *Soil Science* **113:** 346-353.

Lillie, R.A. and Budd, J. (1992) Habitat architecture of *Myriophyllum spicatum* L. as an index to habitat quality for fish and macroinvertebrates. *Journal of Freshwater Ecology* **7:** 113 - 125

Linkins, A. E., Melillo, J. M. and Sinsabaugh, R. L. (1984) Factors affecting cellulase activity in terrestrial and aquatic ecosystems. In Klug, M.H. and Reddy, C.A. (Eds) *Current Perspectives In Microbial Ecology.* American Society of Microbiology.

Linley, EAS; Newell, RC (1984) Estimates of bacterial growth yields based on plant detritus. *Bulletin of Marine Science*

Lodge, D. M. (1991) Herbivory on fresh-water macrophytes. *Aquatic Botany* **41:**195–224

Lombardo, P. (1997) Predation by *Enallagma* nymphs (Odonata, Zygoptera) under different conditions of spatial heterogeneity. *Hydrobiologia* **356:** 1 – 9

Lush, D.L. and Hynes, H.B.N. (1973) Formation of particles in freshwater leachates of dead leaves. *Limnology and Oceanography* **18:** 968-977.

Madsen, J. D. (1991) Resource allocation at the individual plant level. *Aquatic Botany* **41:** 67-86

Madsen, J. D. and Adams, M. S. (1988) The seasonal biomass and productivity of the submerged macrophytes in a polluted Wisconsin stream. *Freshwater Biology* **20:** 41 – 50

Madsen, T. V. and Sand-Jensen, K. (1991) Photosynthetic carbon assimilation in aquatic macrophytes. *Aquatic Botany* **41:** 5 – 40

Maheshwari, B. L., Walker, K. F. and McMahon, T. A. (1995) Effects of regulation on the flow regime of the River Murray, Australia. *Regulated Rivers: Research and Management* **10:** 15 - 38

Major, R. E., Christie, F. J., Gowing, F., Cassis, G. and Reid, C. A. M. (2003) The effect of habitat configuration on arboreal insects in fragmented woodlands of south-eastern Australia. *Biol. Cons*. **113:** 35 – 48

Mallory, L.M. and Sayler, G.S. (1984) Application of FAME (fatty acid methyl ester) analysis in the numberical taxonomic determination of bacterial guild structure. *Microbial Ecology* **10:** 283-296.

Malone, T.C. and Ducklow, H.W. (1990) Microbial biomass in thecoastal plume of Chesapeake **Bay:** phytoplankton-bacterioplankton relationships. *Limnology and Oceanography* **35:** 296-312.

Mann, K. H. (1988) Production and use of detritus in various freshwater, estuarine and coastal marine ecosystems. *Limnology and Oceanography* **33:** 910 - 930

Mann, C.J. and Wetzel, R.G. (1996) Loading and utilization of dissolved organic carbon from emergent macrophytes. *Aquatic Botany* **53:** 61-72.

Mann, K.H. (1991) Production and use of detritus in various freshwater, estuarine and coastal marine ecosystems. *Limnology and Oceanography* **33:** 910-930.

Mason, C.F. and Bryant, R.J. (1975) Production, nutrient content and decomposition of *Phragmites communis* Trin. & *Typha angustifolia* L. *Journal of Ecology* **63:** 71-95.

Mayer, L.M. (1989) Extracellular proteolytic enzyme activity in sediments of an intertidal mudflat. *Limnology and Oceanography* **34:** 973-981.

McCarthy, M., Pratum, T., Hedges, J. and Benner, R. (1997) Chemical composition of dissolved organic nitrogen in the ocean. *Nature* **390:** 150-154.

McKnight, DM; Boyer, EW; Westerhoff, PK; Doran, PT; Kulbe, T; Andersen, DT (2001) Spectrofluorometric characterization of dissolved organic matter for indication of precursor organic material and aromaticity. *Limnology and Oceanography* **46:** 38-48

Melillo, J.M., Aber, J.D. and Muratore, J.F. (1982) Nitrogen and lignin control of hardwood leaf litter decomposition dynamics. *Ecology* **63:** 621-626.

Melillo, J.M., Naiman, R.J., Aber, J.D. and Linkins, A.E. (1984) Factors controlling mass loss and nitrogen dynamics of plant litter decaying in northern streams. *Bull. Mar. Sci.* **35:** 341-356.

Meyer, J. L. (1994) The microbial loop in flowing waters. Microbial *Ecology* **28:** 195 - 199

Meyer, J.L. and Edwards, R.T. (1990) Ecosystem metabolism and turnover of organic carbon along a blackwater river continuum. *Ecology* **71**: 668-677

Meyer, J.L., Edwards, R.T. and Risley, R. (1987) Bacterial growth on dissolved organic carbon from a blackwater river. *Microbial Ecology* **13:** 13-29.

Meyer, J.L., McDowell, W.H., Bott, T.L., Elwood, J.W., Ishizaki, C., Melack, J.M., Peckarsky, B.L., Petersen, B.J. and Rublee, P.A. (1988) Elemental dynamics in streams. *Journal of the North American Benthological Society* **7:** 410-432.

Meyer-Reil, L. A. (1991) Ecological aspects of enzymatic activity in marine sediments. In Chrost, R. J. (Eds) *Microbial enzymes in aquatic environments.* Springer, New York.

Miao, S. L.; and Sklar, F. H. (1997) Biomass and nutrient allocation of sawgrass and cattail along a nutrient gradient in the Florida Everglades. *Wetlands Ecology and Management* **5:** 245-263

Mills, A.L. and Wassel, R.A. (1980) Aspects of diversity measurement of microbial communities. *Applied and Environmental Microbiology* **40:** 578-586.

Minshall, G. W., Petersen, R. C., Bott, T. L. (1992). Stream ecosystem dynamics of the Salmon River, Idaho: an 8th-order system. *Journal of the North American Benthological Society* **11:** 111–137.

Mobed, J.J.; Hemmingsen, S.L.; Autry, J.L.; McGown, L.B. (1996) Fluorescence characterization of IHSS humic substances: total luminescence spectra with absorbance correction. *Environmental Science and Technology* **30:** 3061-3065

Moorhead, D.L. and Sinsabaugh, R.L. (2000) Simulated patterns of litter decay predict patterns of extracellular enzyme activities. *Applied Soil Ecology* **14:** 71-79.

Moran, M. A. and Hodson, R. E. (1989) Bacterial secondary production on vascular plant detritus: relationships to detritus composition and degradation rate. *Applied Environmental Microbiology* **55:** 2178 - 2189

Moran, M.A., Legovic, T., Benner, R. and Hodson, R.E. (1988) Carbon flow from lignocellulose: A simulation analysis of a detritus-based ecosystem. *Ecology* **69:** 1525-1536.

Moran, M.A., Benner, R. and Hodson, R.E. (1989) Kinetics of microbial degradation of vascular plant material in two wetland ecosystems. *Oecologia* **79:** 158-167

Morgan, J.A.W. and Pickup, R.W. (1993) Activity of microbial peptidases, oxidases, and esterases in lake waters of varying trophic status. *Canadian Journal of Microbiology* **39:** 795-803.

Munster, U. and Chrost, R. J. (1990) Origin, composition, and microbial utilization of dissolved organic matter. In Overbeck, J. and Chrost, R.J. (Eds) *Aquatic microbial ecology: biochemical and molecular approaches.* Springer-Verlag, New York.

Murcia, C. (1995) Edge effects in fragmented forests: implications for conservation. *Trends in Ecology and Evolution* **10:** 58 – 62

Naiman, R. J. and Rogers, K. H (1997) Large animals and system-level characteristics in river corriders. *Bioscience* **47:** 521 – 529

Newell, S.Y. (1993) Decomposition of shoots of a saltmarsh grass: methodology and dynamics of microbial assemblages. *Advances in Microbial Ecology* **13:** 301-326.

Newell, S. Y. (2001a) Fungal biomass and productivity in standing-decaying leaves of black needlerush (*Juncus roemerianus*). *Marine and Freshwater Research* **52:** 249 - 255

Newell, S. Y. (2001b) Multiyear patterns of fungal crop dynamics and fungal productivity within naturally decaying smooth-cordgrass shoots. *Limnology and Oceanography* **46:** 573-583

Newell, S. Y. and Barlocher, F. (1993) Removal of fungal and total organic matter from decaying cordgrass leaves by shredder snails. *Journal of Experimental Marine Biology and Ecology* **171:** 39 - 49

Newell, S.Y. and Fallon, R.D. (1989) Litterbags, leaf tags, and decay of nonabscised intertidal leaves. *Canadian Journal of Botany* **67:** 2324-2327.

Newell, S.Y. and Fallon, R.D. (1991) Toward a method for measuring instantaneous fungal growth rates in field samples. *Ecology* **72:** 1547-1559.

Newell, S.Y., Fallon, R.D. and Miller, J.D. (1989) Decomposition and microbial dynamics for standing, naturally positioned leaves of the salt marsh grass *Spartina alterniflora*. *Marine Biology* **101**: 471 - 481

Newell, S.Y., Moran, M.A., Wicks, R. and Hodson, R.E. (1995) Productivities of microbial decomposers during early stages of decomposition of leaves of a freshwater sedge. *Freshwater Biology* **34:** 135-148.

Newell, S. Y., Moran, M. A., Wicks, R. and Hodson, R. E. (1995) Productivities of microbial decomposers during early stages of decomposition of leaves of a freshwater sedge. *Freshwater Biology* **34:** 135 - 148

Newell, S. Y., Arsuffi, T. L. and Palm, L. A. (1996) Misting and nitrogen fertilisation of shoots of a saltmarsh grass: effects upon fungal decay of leaf blades. *Oecologia* **108:** 495 - 502

Newman, R. M. (1991) Herbivory and detritivory on fresh-water macrophytes by invertebrates: a review. *Journal of the North American Benthological Society* **10:**89–114

O'Connell, M., Baldwin, D. S., Robertson, A. I. and Rees, G. (2000) Release and bioavailability of dissolved organic matter from floodplain litter: influence of origin and oxygen levels. *Freshwater Biology* **45:** 333 – 342

Ohno, T. (2002) Fluorescence inner-filtering correction for determining the humification index of dissolved organic matter. *Environmental Science & Technology* **36:** 742-746

Olden, J. D. and Poff, N. L. (2003) Redundancy and the choice of hydrologic indices for characterizing streamflow regimes. *River Res. Applic*. **19:** 101 - 121

Olesen, B; Sand-Jensen, K. (1994) Biomass-density patterns in the temperate seagrass Zostera marina. *Marine Ecology Progress Series* **109:** 283-291

Olsen, G.J., Lane, D.J., Giovannoni, S.J. and Pace, N.R. (1986) Microbial *Ecology* and evolution: a ribosomal RNA approach. *Annual Review of Microbiology* **40:** 337-365.

Otsuki, A. and Wetzel, R.G. (1974) Release of dissolved organic matter by autolysis of a submersed macrophyte *Scirpus subterminalis*. *Limnology and Oceanography* **19:** 842-845.

Pace, M. L. and Funke, E. (1991) Regulation of planktonic microbial communities by nutrients and herbivores. *Ecology* **72:** 904–914

Palumbo, AV; Mulholland, PJ; Elwood, JW (1987) Microbial Communities on Leaf Material Protected from Macroinvertebrate Grazing in Acidic and Circumneutral Streams. *Canadian Journal of Fisheries and Aquatic Sciences* **44:** 1064-1070

Palumbo, AV; Bogle, MA; Turner, RR; Elwood, JW; Mulholland, PJ (1987) Bacterial Communities in Acidic and Circumneutral Streams. *Applied and Environmental Microbiology* **53:** 337-344

Parkinson, A., Mac Nally, R. and Quinn, G. P. (2002) Differential macrohabitat use by birds on the unregulated Ovens River floodplain of southeastern Australia. *River Res. Applic*. **18:** 495 - 506

Parnas, H. (1975) Model for decomposition of organic material by microorganisms. *Soil Biology and Biochemistry* **7:** 161 – 169

Paul, J.H., deFlaun, M.F., Jeffrey, W.H. and David, A.W. (1988) Seasonal and diel variability in dissolved DNA and in microbial biomass and activity in a subtropical estuary. *Applied Environmental Microbiology* **54:** 718-727.

Pengerud, B., Skjoldal, E.G. and Thingstad, T.F. (1987) The reciprocal interaction between degradation of glucose and ecosystem structure. Studies in mixed chemostat cultures of marine bacteria, algae, and bacterivorous nanoflagellates. *Marine Ecology Progress Series* **35:** 111-117.

Perez, M; Duarte, CM; Romero, J; Sand-Jensen, K; Alcoverro, T (1994) Growth plasticity in *Cymodocea nodosa* stands: The importance of nutrient supply. *Aquatic Botany*: **47:** 249-264

Pergent, G., Rico-Raimondino, V. and Pergent-Martini, C. (1997) Fate of primary production in *Posidonia oceanica* meadows of the Mediterranean. *Aquatic Botany* **59:** 307 – 321

Petersen, R.C. and Cummins, K.W. (1974) Leaf processing in a woodland stream. *Freshwater Biology* **4:** 343-368.

Picek, T., Lusby, F., Cizkova, H., Santruckova, H., Simek, M., Kvet, J. and Pechar, L. (2000) Microbial activities in soild of a healthy and a declining reed stand. *Hydrobiologia* **418:** 45-55.

Pinney, M. L., Westerhoff, P. K. and Baker, L. (1999) Transformations in dissolved organic carbon through constructed wetlands. *Water Research* **34:** 1897 – 1911

Pip, E. and Stewart, J. M. (1976) The dynamics of two aquatic plant-snail associations. *Canadian Journal of Zoology* **54:** 1192 – 1205

Poff, NL; Allan, JD; Bain, MB; Karr, JR; Prestegaard, KL; Richter, BD; Sparks, RE; Stromberg, JC, (1997) The natural flow regime. A paradigm for river conservation and restoration. *Bioscience* **47:** 769-784

Polisini, J.M. and Boyd, C.E. (1972) Relationships between cell-wall fractions, nitrogen, and standing crop in aquatic macrophytes. *Ecology* **53:** 484-488.

Polunin, N.V.C. (1982) Processes contributing to the decay of reed (*Phragmites australis*) litter in fresh water. *Arch. Hydrobiol.* **94:** 182-209.

Polunin, N.V.C. (1984) The decomposition of emergent macrophytes in fresh water. *Advances in Ecological Research* **14:** 115-166.

Pomeroy, L.R. and Wiebe, W.J. (1988) Energetics of microbial food webs. *Hydrobiologia* **159:** 7-18.

Porter, K.G. and Feig, Y.S. (1980) The use of DAPI for identifying and counting aquatic microflora. *Limnology and Oceanography* **25:** 943-948.

Poulin, B., Lefebvre, G. and Mauchamp, A. (2002) Habitat requirements of passerines and reedbed management in southern France *Biol. Cons*. **107:** 315 - 325

Puckeridge, J. T., Sheldon, F., Walker, K. F. and Boulton, A. J. (1998) Flow variability and the *Ecology* of large rivers. *Marine and Freshwater Research* **49:** 55 – 72

Pusey, B. J., Arthington, A. H. and Read, M. G (1993) Spatial and temporal variation in fish assemblage structure in the Mary River, south-eastern Queensland: the influence of habitat structure. *Environmental Biology of Fishes* **37:** 355 - 380

Pusey, B. J., Arthington, A. H. and Read, M. G (1998) Freshwater fishes of the Burdekin River, Australia: biogeography, history and spatial variation in community structure. *Environmental Biology of Fishes* **53:** 303 - 318

Qiu, S., McComb, A. J., Bell, R. W. and Davis, J. A. (2005) Estimating production o f gilvin from catchment leaf litter during seasonal rains. *Marine and Freshwater Research* **56:** 843 - 849

Rea, N., Dostine, P. L., Cook, S., Webster, I. & Williams, D. (2002) *Environmental water requirements of Vallisneria nana in the Daly River, Northern Territory*. Report No. 35/2002. Department of Infrastructure, Planning and Environment, Darwin, NT.

Rees, G. N., Beattie, G., Bowen, P. M. and Hart, B. T. (2005) Heterotrophic bacterial production in the lower Murray River, south-eastern Australia. *Marine and Freshwater Research* **56:** 835 - 841

Rees, G. N., Bowen, P. M. and Watson, G. O. (2005) Variability in benthic respiration in three southeastern Australian lowland rivers. *River Research and Applications* **21:** 1147 - 1156

Rickett, H. W. (1922) A quantitative study of the larger aquatic plants of Lake Mendota. *Transactions of the Wisconsin Academy of Sciences* **20:** 501 – 527

Riemann, B. (1985) Potential importance of fish predation and zooplankton grazing on natural populations of freshwater bacteria. *Applied and Environmental Microbiology* **50:** 187-193

Roberts, J. (2000) Changes in the distribution of *Phragmites australis* in eastern Australia: a habitat approach. *Folia Geobotanica and Phytotaxonomica* **35:** 353-362

Roberts, J. and Ganf, G.G. (1986) Annual production of *Typha orientalis* Presl. in inland Australia. *Australian Journal of Marine and Freshwater Research* **37:** 659 – 668

Roberts, J. and Marston, F. (2000) *Water regime of wetland and floodplain plants in the Murray-Darling Basin: A source book of ecological knowledge*. CSIRO Land and Water Technical Report 30/00. October 2000, Canberra.

Roberts, J. and Sainty, G. (1966). *Listening to the Lachlan*. Sainty & Associates: Sydney

Robertson, A. I., Bunn, S. E., Boon, P. I. and Walker, K. F. (1999) Sources, sinks and transformations of organic carbon in Australian floodplain rivers. *Marine and Freshwater Research* **50:** 813 – 829

Rogers, K. H. and Breen, C. M. (1980) Growth and reproduction of *Potamogeton crispus* in a South African lake. *Journal of Ecology* **68:** 561 – 571

Rogers, K.H. and Breen, C.M. (1982) Decomposition of *Potamogeton crispus* L.: the effects of drying on the pattern of mass and nutrient loss. *Aquatic Botany* **12:** 1-12.

Rolletschek, H., Rolletschek, A., Kuhl, H. and Kohl, J-G. (1999) Clone specific differences in a *Phragmites australis* stand II. Seasonal development of morphological and physiological characteristics at the natural site and after transplantation. *Aquatic Botany* **64:** 247 – 260

Rothhaupt, K.O. (1992) Stimulation of phosphorus-limited phytoplankton by bacterivorous flagellates in laboratory experiments. *Limnology and Oceanography* **37:** 750-759.

Sainty, G R, Jacobs, S.W.L. (1981) *Water Plants of New South Wales*. Water Resources, NSW. Sydney.

Sainty, G. R. and Jacobs, S. W. L. (1994). *Water Plants in Australia* (third ed.). Sainty and Associates: Sydney.

Samiaji, J. and Barlocher, F. (1996) Geratology and decomposition of *Spartina alterniflora* Loisel. in a New Brunswick saltmarsh. *Journal of Experimental Marine Biology and Ecology* **201:** 233 - 252

Sand-Jensen, K. M., Foldager Petersen, M., Laurentius, S. (1992) Photosynthetic use of inorganic carbon among primary and secondary water plants in streams. *Freshwater Biol*ogy **27:** 283 - 293

Schindler, D.W. and Holmgren, S.K. (1971) Primary production and phytoplankton in the Experimental Lakes Area, Northwestern Ontario, and other low-carbonate waters, and a liquid scintillation method for determing ^{14}C activity in photosynthesis. *Journal of the Fisheries Research Board of Canada* **28:** 189-399.

Scholz, O. and Boon, P.I. (1993) Alkaline phosphatase, aminopeptidase and β-D glucosidase activities associated with billabong periphyton. *Archiv fuer Hydrobiologie* **126:** 429-443.

Schubert, W. J. (1965) *Lignin Biochemistry*. New York: Academic Press.

Serrano, L. and Boon, P. I. (1991) Effect of polyphenolic compounds on alkaline phosphatase activity: its implication for phosphorus regeneration in Australian freshwaters. *Archiv fuer Hydrobiologie* **123:** 1 – 19

Servais, P; Billen, G; Rego, JV (1985) Rate of Bacterial Mortality in Aquatic Environments. *Applied and Environmental Microbiology* **49:** 1448-1454

Shaver, G. R. and Melillo, J. M. (1984) Nutrient budgets of marsh plants: efficiency concepts and relation to availability. *Ecology* **65:** 1491-1510

Sherr, BF; Sherr, EB; Berman, T (1983) Grazing, growth, and ammonium excretion rates of a heterotrophic microflagellate fed with four species of bacteria. *Applied and Environmental Microbiology* **45:** 1196-1201

Silliman, B. R. and Zieman, J. C. 2001. Top-down control of *Spartina alterniflora* production by periwinkle grazing in a Virginia marsh. *Ecology* **82:** 2830–2843

Silliman, B.R. and S.Y. Newell. 2004. Fungal farming in a snail. *Proc. Natl. Acad. Sci*. **100:** 15643-15648

Sinclair Knight Merz (2001) *Burnett River Dam EIS Report. Section 11. Aquatic Flora and Fauna.* Burnett Water, Pty Ltd.

Sinsabaugh, R.L. and Findlay, S. (1995) Microbial production, enzyme activity and carbon turnover in surface sediments of the Hudson River Estuary. *Microbial Ecology* **30:** 127-141.

Sinsabaugh, R.L. and Linkins, A.E. (1988) Exoenzyme activity associated with lotic epilithon. *Freshwater Biology* **20:** 249-261.

Sinsabaugh, R.L. and Linkins, A.E. (1990) Enzymic and chemical analysis of particulate organic matter from a boreal river. *Freshwater Biology* **23:** 301-309.

Sinsabaugh, R.L. and Linkins, A.E. (1993) Statistical modelling of litter decomposition from integrated cellulase activity. *Ecology* **74:** 1594-1597.

Sinsabaugh, R.L., Antibus, R.K., Linkins, A.E., McClaugherty, C.A., Rayburn, L., Repert, D. and Weiland, T. (1992) Wood decomposition over a first-order watershed: mass loss as a function of lignocellulase activity. *Soil Biology and Biochemistry* **24:** 743-749.

Sinsabaugh, R.L., Moorhead, D.L. and Linkins, A.E. (1994a) The enzymic basis of plant litter decomposition: emergence of an ecological process. *Applied Soil Ecology* **1:** 97-111.

Sinsabaugh, R.L., Osgood, M.P. and Findlay, S. (1994b) Enzymatic models for estimating decomposition rates of particulate detritus. *Journal of the North American Benthological Society* **13:** 160-169.

Smalla, K., Wachtendorf, U., Heuer, H., Liu, W.-T. and Forney, L. (1998) Analysis of BIOLOG GN substrate utilization patterns by microbial communities. *Applied Environmental Microbiology* **64:** 1220-1225.

Smith, D.C., Steward, G.F., Long, R.A. and Azam, F. (1995) Bacterial mediation of carbon fluxes during a diatom bloom in a mesocosm. *Deep-Sea Research* **42:** 75-97.

Soetaert, Karline; Hoffmann, Maurice; Meire, Patrick; Starink, Mathieu; Oevelen, Dick van; Regenmortel, Sabine Van, and Cox, Tom. (2004) Modeling growth and carbon allocation in two reed beds (*Phragmites australis*) in the Scheldt estuary. *Aquatic Botany* **79:** 211-234

Squires, L. and Van der Valk, A. G. (1992) Water-depth tolerances of the dominant emergent macrophytes of the Delta Marsh, Manitoba. *Canadian Journal of Botany* **70:** 1860-1867

Stahl, D.A., Lane, D.J., Olsen, G.J. and Pace, N.R. (1985) Characterisation of a Yellowstone hot spring microbial community by 5S rRNA sequences. *Applied and Environmental Microbiology* **49:** 1379-1384.

Stepanauskas, R., Farjalla, V. F., Tranvik, L. J., Svensson, J. M., Esteves, F. A. and Graneli, W. (2000) Bioavailability and sources of DOC and DON in macrophyte stands of a tropical coastal lake. *Hydrobiologia* **436:** 241 – 248

Stevenson, J. C. (1988) Comparative *Ecology* of submersed grass beds in freshwater, estuarine, and marine environments. *Limnology and Oceanography* **33:** 867 – 893

Suberkropp, K. and Klug, M. J. (1976) Fungi and bacteria associated with leaves during processing in a woodland stream. *Ecology* **57:** 707 - 719

Sun, L., Perdue, E.M., Meyer, J.L. and Weis, J. (1996) Using elemental composition to predict bio-availability of dissolved organic matter in a Georgia River. *Limnology and Oceanography* **42:** 714-721.

Suren, A. M. and Lake, P. S. (1989) Edibility of fresh and decomposing macrophytes to three species of freshwater invertebrate herbivores. *Hydrobiologia* **178:** 165-178

Talbot, V. and Bianchi, M. (1997) Bacterial proteolytic activity in sediments of the Subantarctic Indian Ocean sector. *Deep-Sea Research* **44:** 1069-1084.

Taniguchi, H. Nakano, S. and Tokeshi, M (2003) Influences of habitat complexity on the diversity and abundance of epiphytic invertebrates on plants. *Freshwater Biology* **48:** 718 – 728

Thingstad, T.F., Hagstrom, A. and Rassoulzadegan, F. (1997) Accumulation of degradable DOC in surface waters: is it caused by a malfunctioning microbial loop? *Limnology and Oceanography* **42:** 398-404.

Thorp, J. H. and DeLong, M. D. (1994) The riverine productivity model: an heuristic view of carbon sources and organic processing in large river ecosystems. *Oikos* **70:** 305-308

Thorp, J.H. and Delong, M.D. (2002) Dominance of autochthonous autotrophic carbon in food webs of heterotrophic rivers. *Oikos* **96:** 543-550.

Thorp, J.H., Delong, M.D., Greenwood, K.S. and Casper, A.F. (1998) Isotopic analysis of three food web theories in constricted and floodplain regions of a large river. *Oecologia* **117:** 551-563.

Titus, J. E. and Pagano, A. M. (2002) Decomposition of litter from submersed macrophytes: the indirect effects of high CO_2. *Freshwater Biology* **47:** 1367–1375.

Tonn, W.M. and Magnuson, J.J. (1982) Patterns in the species composition and richness of fish assemblages in northern Wisconsin lakes. *Ecology* **63:** 1149 – 1166

Tranvik, L. J. (1988) Availability of dissolved organic carbon for planktonic bacteria in oligotrophic lakes of differing humic content. *Microbial Ecology* **16:** 311 – 322

Tranvik, L. (1992) Allochthonous dissolved organic matter as an energy source for pelagic bacteria and the concept of the microbial loop. *Hydrobiologia* **229:** 107-114.

Valérie, David, Benoît Sautour, Robert Galois and Pierre Chardy (2006) The paradox high zooplankton biomass–low vegetal particulate organic matter in high turbidity zones: What way for energy transfer? *Journal of Experimental Marine Biology and Ecology* **333:** 202–218

van den Brink, F. W. B., van der Velde, G., Bosman, W. W. and Coops, H. (1995) Effects of substrate parameters on growth responses of eight helophyte species in relation to flooding. *Aquatic Botany* **50:** 79 – 97

van den Wyngaert, I. J. J.; Wienk, L. D.; Sollie, S.; Bobbink, R., and Verhoeven, J. T. A. (2003) Long-term effects of yearly grazing by moulting Greylag geese (*Anser anser*) on reed (*Phragmites australis*) growth and nutrient dynamics. *Aquatic Botany* **75:** 229-248

van Geest, G. J., Roozen, F. C. J. M., Coops, H., Roijackers, R. M. M., Buijse, A. D., Peeters, E. T. H. M. and Scheffer, M. (2003) Vegetation abundances in lowland flood plain lakes determined by surface area, age and connectivity. *Freshwater Biology* **48:** 440 – 454

Vannote, R.L., Minshall, G.W., Cummins, K.W., Sedell, J.R. and Cushing, C.E. (1980) The river continuum concept. *Canadian Journal of Fisheries and Aquatic Sciences* **37:** 130-137.

Vretare, V., Weisner, S. E. B., Strand, J. A., Graneli, W. (2001) Phenotypic plasticity in *Phragmites australis* as a functional response to water depth. *Aquatic Botany* **69:** 127-145

Vretare-Strand, V. and Weisner, S. E. B. (2002) Interactive effects of pressurized ventilation, water depth and substrate conditions on *Phragmites australis*. *Oecologia* **131:** 490-497

Wahbeh, MI (1984) The growth and production of the leaves of the seagrass *Halophila stipulacea* (Forsk.) Aschers. from Aqaba, Jordan. *Aquatic Botany* **20:** 33-41

Walker, K.F. (1992) A semi-arid lowland river: the River Murray, Australia. In Calow, P.A. and Petts, G.E. (Eds) *The Rivers Handbook*. Vol 1. Blackwell Scientific, Oxford.

Walker, K.F. and Thoms, M.C. (1993) Environmental effects of flow regulation on the River Murray, Australia. *Regulated Rivers: Research and Management* **8:** 103 – 119

Walker, K.F., Boulton, A.J., Thoms, M.C. and Sheldon, F. (1994) Effects of water-level changes induced by weirs on the distribution of littoral plants along the River Murray, South Australia. *Australian Journal of Marine and Freshwater Research* **45:** 1421 – 1438

Ward, G.M. (1986) Lignin and cellulose content of benthic fine particulate organic matter (FPOM) in Oregon Cascade Mountain streams. *Journal of the North American Benthological Society* **5:** 127-139.

Weaver, M. J., Magnuson, J. J. and Clayton, M. K. (1997) Distribution of littoral fishes in structurally complex macrophytes. *Canadian Journal of Fisheries and Aquatic Sciences* **54:** 2277 – 2289

Weber, J. A., Tenhunen, J. D., Westrin, S. S., Yocum, C. S. and Gates, D. M. (1981) An analytical model of photosynthetic response of aquatic plants to inorganic carbon and pH. *Ecology* **62:** 697 – 705

Webster, J.R. and Benfield, E.F. (1986) Vascular plant breakdown in freshwater ecosystems. *Annual Review of Ecology and Systematics* **17:** 567-594.

Wehr, J.D., Petersen, J. and Findlay, S. (1999) Influence of three contrasting detrital carbon sources on planktonic bacterial metabolism in a mesotrophic lake. *Microbial Ecology* **37:** 23-35.

Weisner, E. B. (1988) Factors affecting the internal oxygen supply of *Phragmites australis* (Cav.) trin. ex Steudel in situ. *Aquatic Botany* **31:** 329-335

Weisner, Stefan E. B. and Miao, Shi Li (2004) Use of morphological variability in *Cladium jamaicense* and *Typha domingensis* to understand vegetation changes in an Everglades marsh. *Aquatic Botany* **78:** 319-335

Welsch, M. and Yavitt, J. B. (2003) Early stages of decay of *Lythrum salicaria* L. and *Typha latifolia* L. in a standing-dead position. *Aquatic Botany* **75:** 45 – 57

West, R.J.; Larkum, A.W.D. (1979) Leaf productivity of the seagrass, *Posidonia australis*, in eastern Australian waters. *Aquatic Botany* **7:** 57-65

Westerhoff, P; Chen, W; Esparza, M (2001) Organic Compounds in the Environment: Fluorescence Analysis of a Standard Fulvic Acid and Tertiary Treated Wastewater. *Journal of Environmental Quality* **30:** 2037-2046

Westlake, D.F. (1963) Comparisons of plant productivity. *Biol. Rev.* **38:** 385-425.

Westlake, D.F. (1975) Primary production of freshwater macrophytes. In Cooper, J.P (Ed) *Photosynthesis and Productivity in Different Environments*. Cambridge University Press, London

Wetzel, R.G. (1969) Factors influencing photosynthesis and excretion of dissolved organic matter by aquatic macrophytes in hard-water lakes. *Verh. Int. Verein. Limnol.* **17:** 72-85.

Wetzel, R. G. (1975) *Limnology*. Philadelphia: Saunders.

Wetzel, R.G. (1990) Land-water interfaces: metabolic and limnological regulators. *Verh. Int. Verein. Limnol.* **24:** 6-24.

Wetzel, R. G. (2001) *Limnology: lake and river ecosystems*. Academic Press.

Wetzel, R.G. and Howe, M.J. (1999) High production in a herbaceous perennial plant achieved by continuous growth and synchronized population dynamics. *Aquatic Botany* **64:** 111-129

Wetzel, R.G. and Manny, B.A. (1972a) Decomposition of dissolved organic carbon and nitrogen compounds from leaves in an experimental hard-water stream. *Limnology and Oceanography* **17:** 927-931.

Wetzel, R.G. and Manny, B.A. (1972b) Secretion of dissolved organic carbon and nitrogen by aquatic macrophytes. *Verh. Int. Verein. Limnol.* **18:** 162-170.

Weyers, H.S. and Suberkropp, K. (1996) Fungal and bacterial production during the breakdown of yellow poplar leaves in two streams . *Journal of the North American Benthological Society* **15:** 408-420.

Wheeler, J.R. (1976) Fractionation by molecular weight of organic substances in Georgia coastal water. *Limnology and Oceanography* **21:** 846-852.

Wickham S.A. (1995) Trophic relations between cyclopoid copepods and ciliated protists: complex interactions link the microbial and classic food webs. *Limnology and Oceanography* **40:** 1173–1181

Wickham S.A. & Gilbert J.J. (1991) Relative vulnerabilities of natural rotifer and ciliate communities to cladocerans laboratory and field experiments. *Freshwater Biology* **26:** 77–86

Williamson C.E. (1983) Invertebrate predation on planktonic rotifers. *Hydrobiologia* **104:** 385–396

Wohler, J.R., Robertson, D.B. and Laube, H.R. (1975) Studies on the decomposition of *Potamogeton diversifolius*. *Bulletin of the Torrey Botanical Club* **102:** 76-78.

Wright, R.T.; Coffin, R.B. (1984) Measuring microzooplankton grazing on planktonic marine bacteria by its impact on bacterial production. *Microbial Ecology* **10:** 137-149

Wrubleski, D.A., Murkin, H.R., Van der Valk, A.G. and Nelson, J.W. (1997) Decomposition of emergent macrophyte roots and rhizomes in a northern prairie marsh. *Aquatic Botany* **58:** 121-134.

Xie, Yonghong; Yu, Dan, and Ren, Bo (2004) Effects of nitrogen and phosphorus availability on the decomposition of aquatic plants. *Aquatic Botany* **80:** 29 - 37

Xie, Yonghong; An, Shuqing, and Wu, Bofeng (2005) Resource allocation in the submerged plant *Vallisneria natans* related to sediment type, rather than water-column nutrients. *Freshwater Biology* **50:** 391-402

Yamashita, Y and Tanoue, E (2003) Chemical characterization of protein-like fluorophores in DOM in relation to aromatic amino acids. *Marine Chemistry* **82:** 255-271